Canadian
Journal of Chemistry

Canadian Journal of Chemistry

Under the authority of the Chairman of the Committee of the Privy Council on Scientific and Industrial Research, the National Research Council issues THE CANADIAN JOURNAL OF CHEMISTRY and five other journals devoted to the publication, in English or French, of the results of original scientific research. Matters of general policy concerning these journals are the responsibility of a joint Editorial Board consisting of: members representing the National Research Council of Canada; the Editors of the Journals, and members representing the Royal Society of Canada and four other scientific societies.

The Chemical Institute of Canada has chosen the Canadian Journal of Chemistry as its medium of publication for scientific papers.

CORRECTIONS

Volume 37, 1959

Page 2093, line 7. The statement that "unsubstituted $\Delta^{\alpha\beta}$-butenalide (I, R = H) has not been previously synthesized" should be deleted.

Volume 38, 1960

Pages 128, 129. The illustration that appears above the caption for Figure 1 on p. 128 is in fact Figure 2 and should be inserted on p. 129. Likewise the illustration above the caption for Figure 2 on p. 129 is Figure 1 and should appear on p. 128.

Pages 308, 309. The authors of the paper "The reaction of sodium metaperiodate with some nitrogen derivatives of carbohydrate" have submitted the following erratum. "The authors regret that in their note no reference was made to the important work of J. C. Bevington, E. J. Bourne, and C. N. Turton. Chemistry and Industry, 1390 (1953). This publication anticipated some of the work described by Abercrombie and Jones (loc. cit.)."

Page 310. In line 18, "2.209" should read "2.029".

Page 323. In line 5 of the Introduction, "The hydrocarbons studied are compounds" should read "The hydrocarbon studied is one of the compounds".

Page 380. In line 3, "the ratio F" should read "the ratio F^{-1}".

Page 724. In the fifth line from the bottom of the page, "(3)" should read "(6)".

Page 726. In the last line of the third paragraph, "(2)" should read "(5)". In Table II, column 1, first ine, "DPPH–CCl" should read "DPPH–KCl".

Page 1158. In line 6 of the second paragraph, "3,3$^{\iota}$5,5$^{\iota}$-tetramethyl-" should read "3,3$^{\iota}$,5,5$^{\iota}$-tetramethoxy".

Page 1170. In Table I, column 3, last line, "1/2" should read "1.2".

Page 1175. In line 3, "$\alpha_0 = \alpha_0 + \beta_{CO}$" should read "$\alpha_0 = \alpha + \beta_{CO}$ and $\beta_{CO} = \beta$". In line 13, "square" should read "squares".

Page 1208. Reference 2 should read "R. Deghenghi and Ch. R. Engel. J. Am. Chem. Soc. **82**, 3201 (1960)".

Page 1630. In line 1, "10^{-4} to 10^{-2} gram moles per liter" should read "10^{-4} to 10^{-2} millimoles per liter".

Page 1664. In Tables VI and VII, column 3, "(μmolecules sec^{-1})" should read "(μmoles sec^{-1})".

Page 1797. In line 3 of the fourth paragraph, "$w^* \rightarrow w + h$" should read "$w^* \rightarrow w + h\nu$".

Page 1798. In the third line from the bottom of the page, "$w^* \rightarrow w + h$" should read "$w^* \rightarrow w + h\nu$".

Page 1971. In line 6,
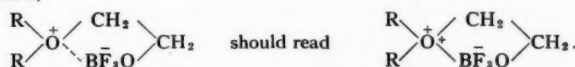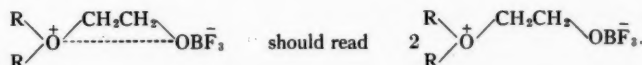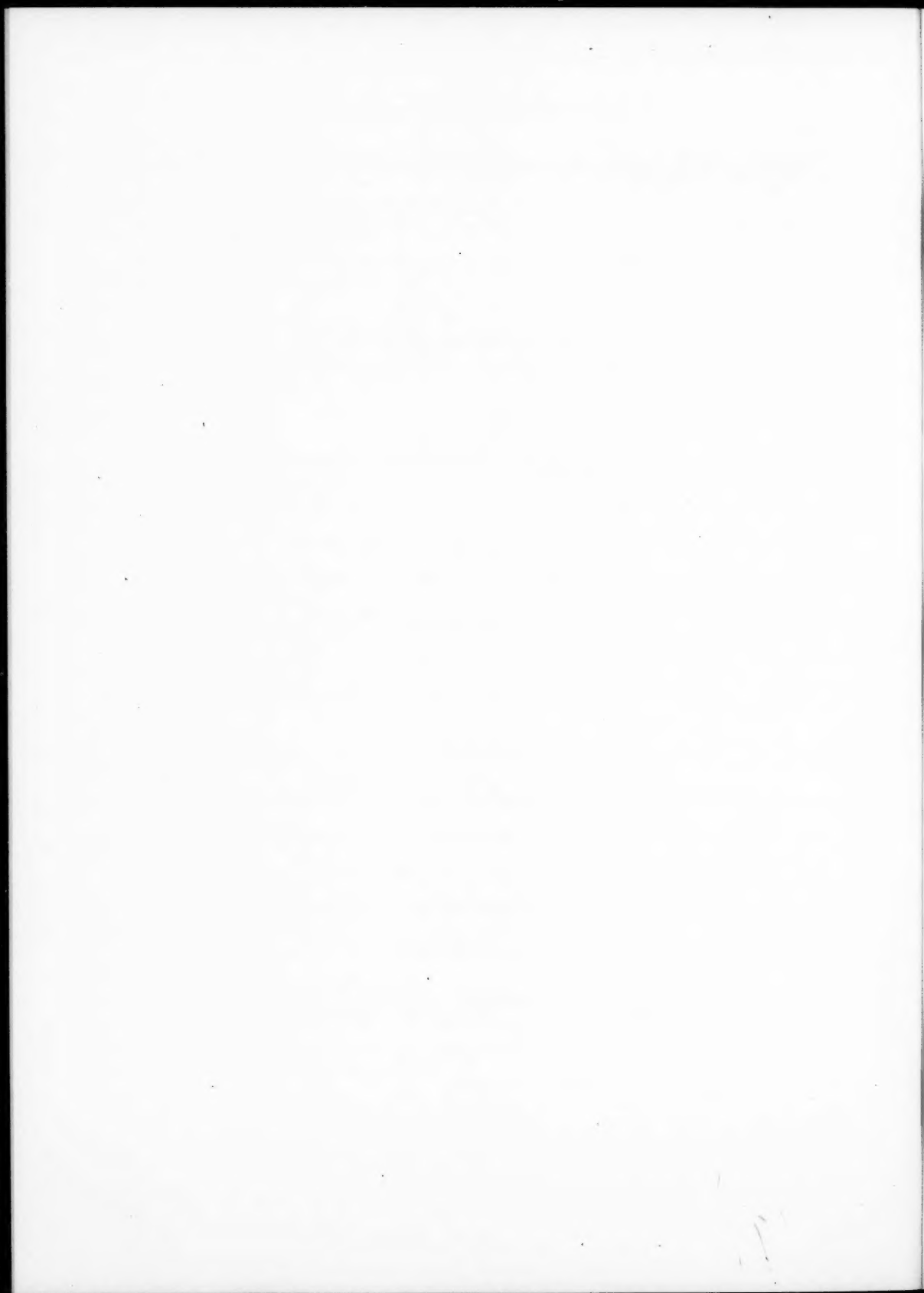
 should read

In line 7,

 should read

i

Canadian Journal of Chemistry

THE SEPARATION OF SUGARS ON ION-EXCHANGE RESINS

PART I. SEPARATION OF OLIGOSACCHARIDES[1]

J. K. N. JONES, R. A. WALL, AND (*in part*) A. O. PITTET[2]

ABSTRACT

Fractionation according to molecular size has been achieved by development of oligo-saccharide mixtures with water on columns of neutral salt forms of sulphonic acid type ion-exchange resins. The method was used to separate a synthetic mixture of raffinose, sucrose, and glucose and a number of hydrolyzates of polysaccharides to give clean, salt-free fractions of high purity. The procedure is rapid and economical and provides a useful extension of older methods of separating such mixtures.

INTRODUCTION

One of the major problems of carbohydrate chemistry is the separation of mixtures of sugars from hydrolyzates and synthetic reactions. Resolution is commonly achieved by using variations of the charcoal–celite columns of Whistler and Durso (1) or partition chromatography on cellulose columns (2). These procedures are usually very efficient and several grams of material can be separated per run, but the time required for fractionation may be of the order of weeks or even months. Moreover, the larger fragments are usually eluted at the end of the process, a reversal of the most desirable order.

The work of Wheaton and Bauman (3) and Samuelson *et al.* (4, 5, 6) on equilibria between aqueous solutions of polyhydroxy organic compounds and ion-exchange resins pointed the way to a new method of fractionation according to molecular bonding or size. It could be inferred from these data that small molecules are much more strongly attracted to the resin than are large molecules, and that column development of a mixture should result in the largest molecules appearing first in the eluate. Any further speculations had to be based on extrapolation, as no data were available for compounds of more than six carbon atoms (although Moore and Stein (7) were able to separate peptides by a similar process), but it seemed clear that bonding could vary greatly with the cross-linkage and salt form of the resin.

This extension of the data of Samuelson and Wheaton and Bauman was shown to be correct and separation of oligosaccharides and monosaccharides according to molecular size has been achieved on Dowex 50W (2% DVB, 200–400 mesh, Li$^+$ form). Many other types of ion exchangers with different degrees of cross-linking and in different salt forms were tried but were less satisfactory.

Synthetic mixtures of mono-, di-, and tri-saccharides and various polysaccharide hydrolyzates have been separated on the resin columns. Surprisingly, the same 2% DVB resin columns also gave some resolution of mixtures of *O*-alkylated monosaccharides,

an interesting point being that the size order was reversed with these derivatives so that the most highly substituted molecules were eluted last.

The developing solvent was distilled water for most of the separations on the 2% DVB Dowex 50W columns, although 50% aqueous ethanol was used for some preliminary experiments. As predicted by theory the material of highest molecular weight was eluted first followed by lower oligosaccharides and continuing the order down to glycerol and ethylene glycol, which were partially separable. Fractionations were rapid (24–48 hours for complete elution) and the method is economical since the columns could be used many times and water was the only solvent used. The sugars were eluted in relatively concentrated aqueous solution such that direct spotting for paper chromatography was possible without evaporation of the eluate fractions.

EXPERIMENTAL

General Methods

Aqueous solutions were evaporated under reduced pressure at ca. 40° C. All melting points are uncorrected and were measured on a Kofler hot stage.
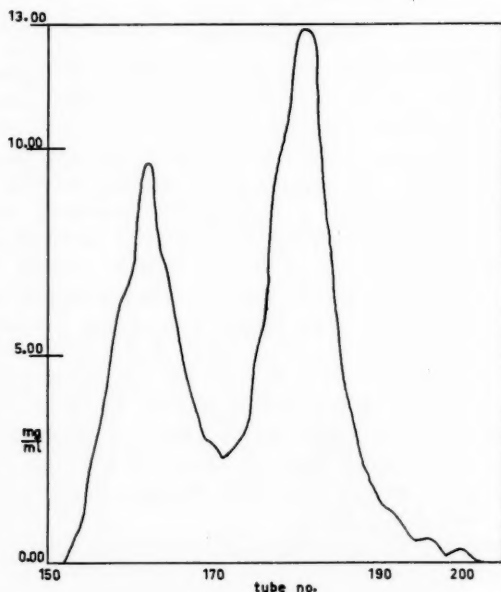
FIG. 1. Separation of raffinose (91 mg) and melibiose (130 mg); flow rate was 1.0 ml per 15-minute fraction. Recoveries calculated from the colorimetric analysis (9) were: raffinose 102% and melibiose 99%. Tubes 154–167 were concentrated to a syrup, and trituration with alcohol–acetone induced crystallization of prisms, m.p. 127–130° and mixed m.p. 131–135°, with authentic recrystallized raffinose of melting point 132–135° (seeded with the 127–130° material). The recovered compound had $[\alpha]_D^{23°}$ +115° (c, 1.2 in water) and an infrared spectrum (potassium bromide pellet) identical with that of authentic raffinose pentahydrate in the 700–1500 cm^{-1} region. Trituration with alcohol of the syrup from the contents of tubes 176–189 gave prisms which had a melting point of 181–184°, which was not depressed on admixture with authentic anhydrous melibiose.
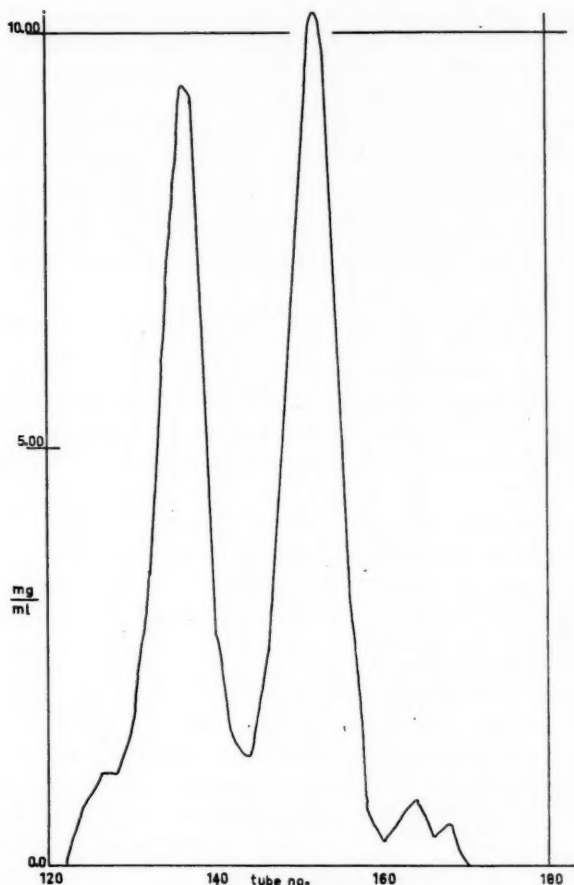
FIG. 2.   Separation of D-glucose (115 mg) and maltose (115 mg) at a flow rate of 1.45 ml per 15-minute fraction. Calculated recoveries were: glucose 99% and maltose 97%. Treatment of the contents of tubes 131–140 as before gave prisms which had a melting point of 125–129° and an infrared spectrum (potassium bromide pellet) identical with that of authentic β-maltose hydrate. These crystals had $[\alpha]_D^{22°}$ +118° (10 minutes) → +131° (24 hours) (c, 1.1 in water) and gave on acetylation a crystalline acetate of melting point 161–163°, which did not depress the melting point of authentic α-maltose octaacetate. Crystalline D-glucose was obtained in a similar manner from the contents of tubes 148–160 and had a melting point and mixed melting point of 142–145°.

Preparation of Columns

Columns were sealed at the bottom with plugs of $\frac{1}{2}$-in. thick polyurethane foam held in place with a tightly fitting rubber stopper with a short piece of glass capillary tubing through it. The capillary outlet was attached to a 4-ft length of 0.022 by 0.042 in. teflon tubing with a No. 24 syringe needle. This procedure allowed regulation of the rate of flow by changing the hydraulic head and gave very even flow.

A slurry of the resin (Dowex 50W X2, 200–400 mesh, Li+ for oligosaccharides and O-alkylated monosaccharides) in water was poured into a glass tube of the desired size
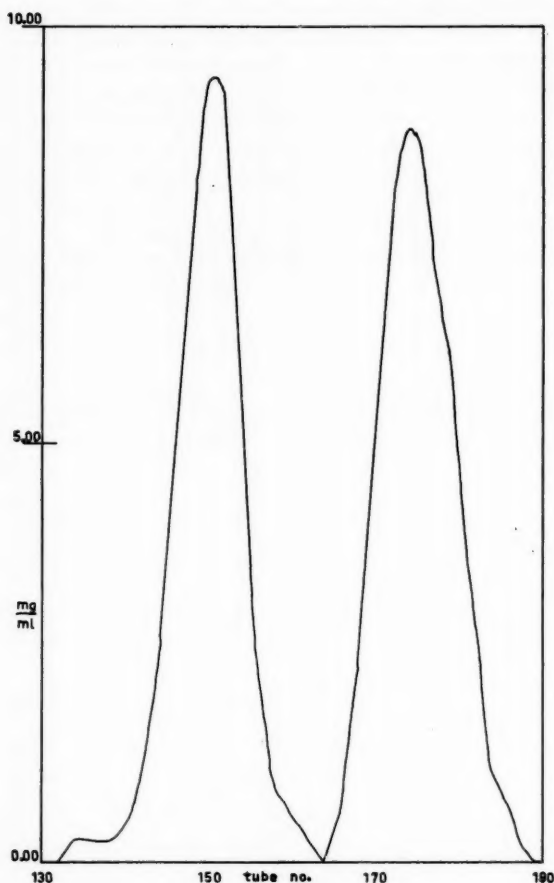
FIG. 3.   Separation of lactose (94 mg) and D-galactose (108 mg) at a flow rate of 1.10 ml per 15-minute fraction. Calculated recoveries were: galactose 100% and lactose 105%. Treatment as before of the contents of tubes 141–160 gave crystalline α-lactose, m.p. and mixed m.p. 210–214° and $[\alpha]_D^{21°}$ +81.9° (9 minutes) → +60.6° (2 hours) → +56° (45 hours) (c, 2.4 in water). Crystalline α-D-galactose, m.p. and mixed m.p. 164–168°, was similarly obtained from the contents of tubes 165–180.

and backwashed for several hours at a rate sufficient to expand the bed to twice its final dimensions. After the fines, air bubbles, etc. had been removed, the backwashing was stopped and the resin was allowed to settle overnight by gravity. This slow settling is essential and should not be hastened by packing under pressure.

Different batches of both the Dowex 50W X2 used in the experiments detailed in this paper and the Dowex 50W X8 used in Part II were utilized at various times. No variation in separating power was ever found.

Oligosaccharide Separations

The first successful experiments with the new method were done by Dr. Pittet, who used Amberlite CG-120 (type 1, H⁺) with 50% aqueous ethanol as the developing

solvent. Using this procedure he was able to separate completely glucose and maltose and to resolve partially the higher oligosaccharides from an enzymatic starch digest (335 mg on a 90×1 cm column). A larger column was used to fractionate a mixture (750 mg) of L-arabinose and an arabinosyl-arabinose obtained from partial hydrolysis of cherry gum. Crystalline L-arabinose (187 mg), m.p. 156° and mixed m.p. 159°, and a syrup (225 mg) having $[\alpha]_D^{21°}$ +165° (water) were isolated in this manner. The syrup gave a crystalline osazone, m.p. 238–241° (decomp.), which had an infrared spectrum identical with that of authentic 3-O-β-L-arabopyranosyl-L-arabinose phenylosazone. Unfortunately, use of the resin in the acid form gave rise to partial hydrolysis of labile oligosaccharides such as sucrose and raffinose, and modifications to reduce this difficulty were sought.

The most satisfactory resin was found to be Dowex 50W X2 (200–400 mesh, Li⁺), and it was possible to separate in 48 hours raffinose, sucrose, and glucose (200 mg each) on a column (95×1.8 cm) with water as the sole developing solvent.

Elution diagrams of separations achieved in this manner are given in Figs. 1–3; the fractionations were followed with a modification of the orcinol reaction (9) and were all done on a column (112×1.8 cm) with flow rates of 1 to 2 ml per 15-minute fraction.

Separation of O-Alkylated Sugars

A hydrolyzate of fully methylated starch (1.0 g) was separated on a column (100 ×2.2 cm) of Dowex 50W X2 (200–400 mesh, Li⁺) with water as sole developing solvent. The first run gave two fractions: the first contained mono-, di-, and tri-O-methyl-glucoses and the second apparently equal quantities of tri- and tetra-O-methyl-glucoses. This second fraction was refractionated on the same column and in this manner a syrup was obtained from which crystalline 2,3,4,6-tetra-O-methyl-D-glucose (60 mg) was isolated. Sublimation at room temperature and pressure of this material gave colorless needles of 2,3,4,6-tetra-O-methyl-α-D-glucose, m.p. and mixed m.p. 89–91°. The main fraction was stored as a viscous syrup and over a period of some months a tri-O-methyl-glucose of melting point 108–110° was obtained; presumably this was the expected 2,3,6-tri-O-methyl-D-glucose, but the melting point could not be raised to the literature (10) value of 121 to 123° by recrystallization.

REFERENCES

1. R. F. WHISTLER and D. F. DURSO. J. Am. Chem. Soc. **72**, 677 (1950).
2. L. HOUGH, J. K. N. JONES, and W. H. WADMAN. J. Chem. Soc. 2511 (1949).
3. R. M. WHEATON and W. C. BAUMAN. Ann. N.Y. Acad. Sci. **57**, 159 (1953).
4. H. RÜCKERT and O. SAMUELSON. Svensk Kem. Tidskr. **66**, 12 (1954).
5. M. MATISSON and O. SAMUELSON. Acta. Chem. Scand. **12**, 1386 (1958).
6. M. MATISSON and O. SAMUELSON. Acta. Chem. Scand. **12**, 1404 (1958).
7. C. H. W. HIRS, W. H. STEIN, and S. MOORE. J. Biol. Chem. **219**, 623 (1956).
8. F. SMITH and A. M. UNRAU. Chem. & Ind. (London), 881 (1959).
9. R. J. WINZLER. *In* Methods of biochemical analysis. Vol. 2. Interscience, New York. 1955. p. 290.
10. W. N. HAWORTH, E. L. HIRST, and J. I. WEBB. J. Chem. Soc. 2681 (1928).

THE SEPARATION OF SUGARS ON ION-EXCHANGE RESINS
PART II. SEPARATION OF MONOSACCHARIDES[1]

J. K. N. JONES AND R. A. WALL

ABSTRACT

Columns of neutral salt forms of sulphonic acid type ion-exchange resins have been shown to be useful in separations of monosaccharide mixtures with water as the developing solvent. A number of synthetic mixtures and a series of plant extracts have been resolved into clean, salt-free fractions by use of the new technique. The procedure is analogous to column partition chromatography, but in many cases it is more rapid and gives a useful extension of separability.

INTRODUCTION

During the initial investigations of the separation of oligosaccharides on acidic ion-exchange resin columns (1a, 1b) it was observed that the fructose produced by partial hydrolysis of the sucrose and raffinose standards was always partially separated from the glucose also present in the standard mixture. This observation was confirmed by examination of the behavior of a series of monosaccharides and by the publication of Felicetta and co-workers (2) of a successful separation of D-xylose and L-arabinose on columns of Dowex 50W X8 (50–100 mesh, Ca++) with water as the development solvent. This article prompted study of the separation of a series of monosaccharides using columns of a slightly more efficient resin, Dowex 50W X8 (200–400 mesh, Ba++).

Table I gives the effluent volume at which maximum concentration of the given sugar is reached on a column (70×2.2 cm) of the above resin with water as the sole developing solvent. Experience has shown that if the difference between two effluent volumes is more than 25 ml, it can be predicted that the corresponding sugars are readily separable, e.g. D-ribose and D-xylose are completely separable, but L-arabinose and D-xylose are not.

TABLE I

Sugar	Volume (ml)	Sugar	Volume (ml)
D-Glucose	157	D-Lyxose	188
N-Acetyl-D-glucosamine	160	D-Mannitol	198
D-Sorbose	164	D-Fructose	200
D-Galactose	170	D-Glycero-D-galacto-heptitol (perseitol)	238
D-Xylose	171	Dulcitol	241
D-Manno-heptulose	176	D-Sorbitol	252
D-Mannose	181	D-Xylitol	257
D-Altro-heptulose (sedoheptulose)	183	D-Ribose	342
L-Arabinose	188	D-Galacturonic acid	350

A series of determinations of percentage recoveries of amounts ranging from 50 mg to 1 g per component gave better than 85% recovery and 90–95% was usual. Separation of a mixture of D-sorbitol and N-acetyl-D-glucosamine (1 g each) on the above column gave ca. 90% recovery of each component in a crystalline, chromatographically pure state.

Methods were worked out for the concentration of sedoheptulose from sedum extracts; D-manno-heptulose and perseitol from the avocado pear; and the main products, D-talose and D-tagatose, from the epimerization of D-galactose.

EXPERIMENTAL

General Methods

All columns were made and used as previously described (1) but using the 8% DVB, Ba^{++} resin mentioned before. The values quoted in Table I were obtained by analysis of mixtures of two known components by paper electrophoresis with borate buffers (3) or by use of paper chromatography on Whatman No. 1 paper using the following solvent systems (v/v ratio):

(A) *n*-butanol:ethanol:water, 3:1:1;
(B) *n*-butanol:pyridine:water, 5:3:2;
(C) *t*-butanol:acetic acid:water, 4:1:1;
(D) ethyl acetate:acetic acid:formic acid:water, 18:3:1:4.

Reducing sugars were detected on chromatograms by the *p*-anisidine hydrochloride spray reagent (4). Non-reducing compounds were detected on chromatograms and electrophorograms by silver nitrate:sodium hydroxide (5) and potassium permanganate: sodium metaperiodate (6) sprays. The orcinol:trichloroacetic acid (7) spray was used to detect ketoses on chromatograms. Aqueous solutions were concentrated under reduced pressure at ca. 40° C on a rotary film evaporator. All melting points are uncorrected and were measured on a Kofler hot stage.

Separation of Standard Mixtures

Figure 1 illustrates the complete separation of D-xylose (179 mg) and D-ribose (178 mg) on the resin column (112×1.8 cm) at a flow rate of 4.0 ml per 15-minute fraction. The colorimetric analysis (benzidine – acetic acid reagent (8)) gave calculated recoveries: D-xylose 99% and D-ribose 99%. Trituration of the syrup obtained on evaporation of the tubes corresponding to the first peak with alcohol–acetone gave crystalline D-xylose, m.p. and mixed m.p. 142–145°. The syrup obtained similarly from the tubes corresponding to the second peak crystallized slowly on trituration with *n*-propanol and seeding with authentic D-ribose to give rosettes of needles which had a melting point and mixed melting point of 84–86°.

Figures 2A and 2B demonstrate the partial separation of a mixture of D-glucose (58 mg) and D-galactose (67 mg) on a column (112×1.8 cm) at an elution rate of 1.5 ml per 15-minute fraction. The sugars were determined colorimetrically using the orcinol reagent (9); the chromatogram shows that even with this poor separation ca. 25% of the individual components could be recovered chromatographically pure.

Experiments on the separation of natural and synthetic mixtures were also carried out, using a three-step column (29.5×2.2 cm, 27.5×1.65 cm, and 21.0×1.2 cm) to sharpen the fractionation (cf. Hagdahl (10)).

Fractionation of Sedum Extract

An extract (700 mg) of *Sedum* sp. prepared by the method of Benson (11) was separated on the three-step column to give three main fractions which contained: (A) aldohexose and aldopentose, (B) heptulose, and (C) ketohexose. There was considerable overlap of the components, but a refractionation of the main fraction (B) gave a syrup (400 mg) which contained traces of hexose and pentose; paper chromatography showed it to be ca. 90% heptulose. Treatment of an aliquot of the syrup with acid according to Hudson (12) gave sedoheptulosan, m.p. and mixed m.p. 154–156°, $[\alpha]_D^{25°}$ −138° (*c*, 1.2 in water) after two recrystallizations from *n*-propanol.
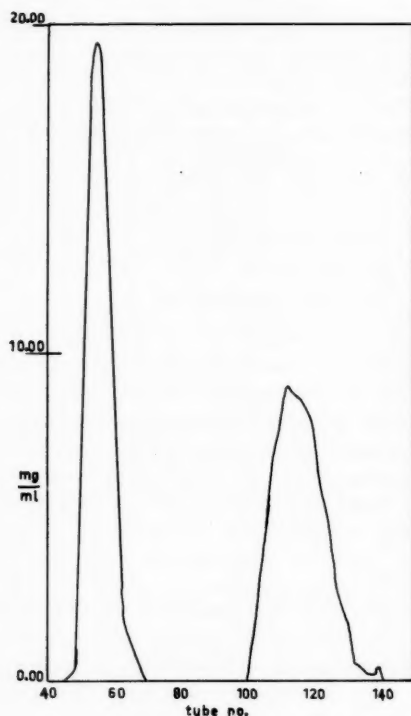
FIG. 1.

Fractionation of Avocado Extract

The acidic components of an alcoholic extract of the flesh of two ripe avocado pears were removed on a column (50×1.4 cm) of Amberlite CG-400 (type I, acetate) and the concentrated neutral effluent was passed down the three-step column to give four main fractions. These had as chief constituents: (A) disaccharide, (B) heptulose and aldo-hexose, (C) heptitol and ketohexose, and (D) ketohexose and unidentified reducing materials. The syrups obtained after several refractionations of mixtures (B) and (C) crystallized on standing overnight. In this manner D-manno-heptulose (2.2 g) was isolated from (B); it had a melting point and mixed melting point of 152–154.5° and $[\alpha]_D^{25°}$ +30° (10 minutes) (c, 2.4 in water) after two recrystallizations from ethanol. Mixture (C) gave rise to D-glycero-D-galacto-heptitol (0.5 g) of melting point 184–185° after two recrystallizations from aqueous methanol. The perseitol isolated in this experiment gave a heptaacetate of melting point 115.5–118.5° and $[\alpha]_D^{22°}$ −13.8° (c, 2.02 in chloroform) on treatment with acetic anhydride and pyridine.

Separation of the Epimerization Products of D-Galactose

D-Galactose (10 g) was epimerized by heating its solution in pyridine (100 ml) according to Karabinos (13). The published method was followed to the stage of removal of D-galactose by dilution with hot ethanol, and the resultant filtrate was evaporated under
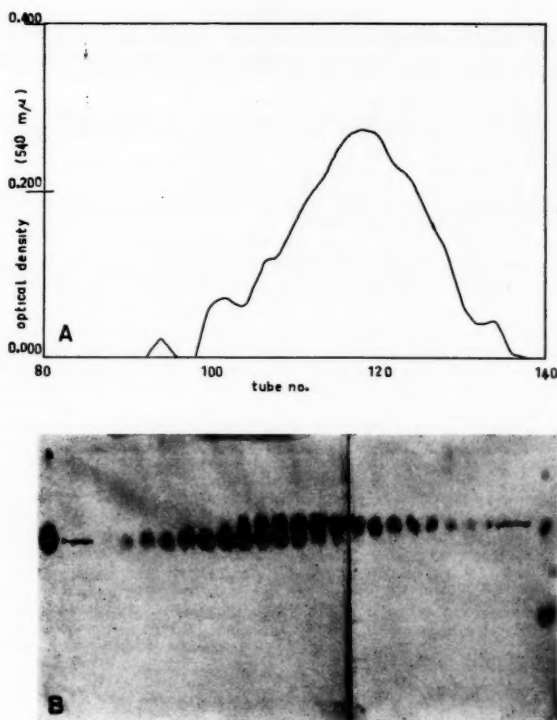
FIG. 2.

reduced pressure to a syrup which was dissolved in water (4 ml) and this solution was fractionated on the three-step column. The first separation gave three main fractions: (A) aldohexose and ketohexose, (B) ketohexose, and (C) aldohexose, of which only (C) was pure enough to crystallize directly from the syrup. Dissolution of (C) in hot ethanol left a small amorphous residue, which was removed by filtration. Colorless prisms (32 mg), which had a melting point and mixed melting point with authentic D-talose of 125.5 to 127.5° and $[\alpha]_D^{20°}$ +25° (10 minutes) (c, 1.0 in water), slowly crystallized from the clear filtrate. Refractionation of (A) and (B) gave syrups which crystallized on standing overnight. The solid from (A) was shown to be D-galactose, m.p. and mixed m.p. 162–166°, and $[\alpha]_D^{24°}$ +81° (10 minutes) (c, 1.2 in water). After two recrystallizations from ethanol the chief component of (B) was found to be D-tagatose (0.68 g), m.p. and mixed m.p. 130–132°, and its infrared spectrum (potassium bromide pellet) was identical with that of authentic D-tagatose; 85% of the initial D-galactose was recovered in a crystalline form.

REFERENCES

1a. J. K. N. JONES, R.A. WALL, and (in part) A. O. PITTET.   This issue.
1b. J. K. N. JONES, R. A. WALL, and (in part) A. O. PITTET.   Chem. & Ind. (London), 1196 (1959).
2. V. F. FELICETTA, M. LUNG, and J. L. MCCARTHY.   Tappi, **42**, 496 (1959).
3. A. B. FOSTER.   Chem. & Ind. (London), 828 (1952).
4. L. HOUGH, J. K. N. JONES, and W. H. WADMAN.   J. Chem. Soc. 1702 (1950).
5. W. E. TREVELYAN, D. P. PROCTOR, and J. S. HARRISON.   Nature, **166**, 444 (1950).
6. R. U. LEMIEUX and H. F. BAUER.   Anal. Chem. **26**, 920 (1954).
7. A. BEVENUE and K. T. WILLIAMS.   Arch. Biochem. Biophys. **34**, 225 (1951).
8. J. K. N. JONES and J. B. PRIDHAM.   Biochem. J. **58**, 288 (1954).
9. R. J. WINZLER.   *In* Methods of biochemical analysis. Vol. 2. Interscience, New York. 1955. p. 290.
10. L. HAGDAHL.   Acta. Chem. Scand. **2**, 574 (1948).
11. A. NORDAL and A. A. BENSON.   J. Am. Chem. Soc. **76**, 5054 (1954).
12. J. W. PRATT, N. K. RICHTMYER, and C. S. HUDSON.   J. Am. Chem. Soc. **74**, 2200 (1952).
13. J. V. KARABINOS.   *In* Advances in carbohydrate chemistry. Vol. 7. Academic Press, New York. 1952. p. 113.

PRIMARY QUANTUM EFFICIENCIES IN THE REACTION
OF CYCLOPENTANE WITH MERCURY 6($^3P_1$) ATOMS[1]

Richard L. Stock and Harry E. Gunning

ABSTRACT

An investigation has been made of the reaction of cyclopentane with Hg 6($^3P_1$) atoms at a substrate pressure of 107 mm, under static conditions at 24° C. Low light intensities were used in order to minimize secondary reactions.

The products of the reaction, for small extents of decomposition, have been shown to be exclusively hydrogen, bicyclopentyl, and cyclopentene. With increasing duration of exposure, the cyclopentene-to-cyclopentane ratio achieves a steady-state value of 5.7×10^{-3}. Furthermore, it has been found that the same ratio is ultimately reached, upon prolonged exposure of a substrate initially containing cyclopentene at a concentration higher than the steady-state value. In the runs with added cyclopentene, a fourth product appeared in measurable quantities. Its molecular weight corresponded to the formula, $C_{10}H_{16}$, and it was assumed to be a cyclopentyl cyclopentene. The same compound appears in extensive decomposition of the pure substrate.

The addition of small amounts of nitric oxide was found to have a marked inhibiting effect on the reaction. Bicyclopentyl formation was completely suppressed when 0.7 mole% of nitric oxide was present; and the cyclopentene yield was reduced to one-fifth of its value for the pure substrate, by adding 0.98 mole% of nitric oxide.

In order to obtain primary quantum yields for the reaction, a series of runs were performed of 1 to 33 minutes in duration, with a cyclopentane which had been purified by gas–liquid chromatography. By a short extrapolation of the mean quantum yields of product formation to zero extent of reaction, it was found that the primary quantum yields for hydrogen, bicyclopentyl, and cyclopentene were respectively 0.8, 0.4, and 0.4.

On the basis of a simple four-step paraffinic mechanism, taken in conjunction with the primary quantum yield data, it is concluded that the reaction has a primary quantum yield of substrate decomposition of 0.8, and that cyclopentyl radicals have the same rates for disproportionation and recombination at 24° C.

INTRODUCTION

In two previous investigations (1, 2) of the reaction of cyclopentane vapor with Hg 6($^3P_1$) atoms, under static conditions, at 30° C, it was shown that the primary process involves scission of the C—H bond with formation of cyclopentyl radicals and H atoms. The products of the reaction were found to be hydrogen, bicyclopentyl, and cyclopentene. In the more recent of the two studies (2), limiting quantum yield values, at high substrate pressures, were used, in conjunction with a simple paraffinic free radical mechanism, to obtain values of 0.49 for the primary quantum yield, and 5.3 for the ratio of the rates of recombination to disproportionation for cyclopentyl radicals. The results reported in this paper represent the first phase in a study of the reaction as a function of temperature. In order to obtain more direct values for the primary quantum yields, the reaction has been studied at small extents of decomposition and low light intensities. The details of the investigation follow.

EXPERIMENTAL

The experiments were performed in cylindrical, fused, quartz reaction cells, 10 cm in length and 5 cm in diameter. For each run a breakseal, product trap, and filling tube were connected to the stem of the reaction cell. The product trap consisted of a short length of 7 mm O.D. tubing, with a constriction to facilitate removal by flame-cutting. In order to introduce the cyclopentane vapor, the cell was connected via the filling tube,

of 3 mm I.D. capillary, to the vacuum manifold, and pumped down to at least 10^{-3} μ. Mercury vapor for the reaction was supplied by placing several drops of mercury in a small depression in the connecting tube of the product trap. In all runs the cell was filled with cyclopentane vapor at a pressure of 107 mm, by placing an ice bath around the reservoir of liquid cyclopentane. After being filled, the cell was flame-cut from the manifold and placed in an oven which was maintained at $24 \pm 0.5°$ C, for the present series of runs.

The 2537-Å resonance radiation was supplied by a Hanovia, Sc-2537 source, which was wound in the form of a five-turn helix. The lamp was rigidly positioned with respect to the cell, in order to assure constant light input. The oven was provided with a filter of Vycor, 7910 glass, to prevent 1849-Å radiation from entering the cell.

At the end of each run, products condensable in liquid nitrogen were frozen into the product trap. In order to assure that high-boiling products were quantitatively transferred to the trap, the remainder of the cell was heated to 250° C during the transfer process. By connecting the cell, via its breakseal, to an analytical system, the noncondensable gases could be transferred, by means of a Toepler pump, to a gas burette. The hydrogen was determined by standard procedures involving combustion over heated copper oxide at 250° C.

The product trap, containing the condensable products, was flame-cut from the cell, and placed in a 4-in. length of 3/8-in. copper tubing, which, in turn fitted into a special sample-insertion device. This device was provided with double-compression fittings, a thumbscrew for shattering the product trap, and a preheater.

The sample-insertion device was placed in series with the hydrogen gas stream to a special gas–liquid chromatographic (G.L.C.) unit. The katharometer was of the Gow-Mac, T/C type, with temperature regulation. Ten-foot chromatographic columns were used, containing 30–60 mesh, silica gel. The analyses were made with the katharometer at 106° C.

The cyclopentane and cyclopentene used were Phillips, Research Grade (P.R.G.). G.L.C. analysis of the cyclopentane showed that the only impurity was 0.051 mole% of cyclopentene. For one series of runs at low conversion, the cyclopentane was further purified by isolating the G.L.C. fraction. This sample showed no detectable impurities. It is estimated that the purity was at least 99.999 mole%. The nitric oxide used was Matheson, C.P. grade, of 99 mole% purity. The gas was further purified by trap-to-trap distillation.

RESULTS

In order to minimize complexities associated with the localized build-up of products in the reaction zone, the runs were carried out at a low absorbed light intensity. By using propane as an actinometer (3), the absorbed light intensity was found to be $3.75 \pm 0.05 \times 10^{-7}$ einstein/minute. All quantum yields reported here are based on this light intensity.

In Fig. 1, the relations are shown between product yield and duration of exposure, for a series of runs with P.R.G. cyclopentane. The cyclopentene yields were corrected for the small amount of cyclopentene present initially in the substrate. From the graph, it is apparent that the rate of bicyclopentyl production is constant throughout the range of duration of exposure studied. For hydrogen production, there is a slight indication of a decreased rate in the runs of long duration. The fact that cyclopentene achieves a steady-state concentration after approximately 120 minutes of exposure is shown clearly in
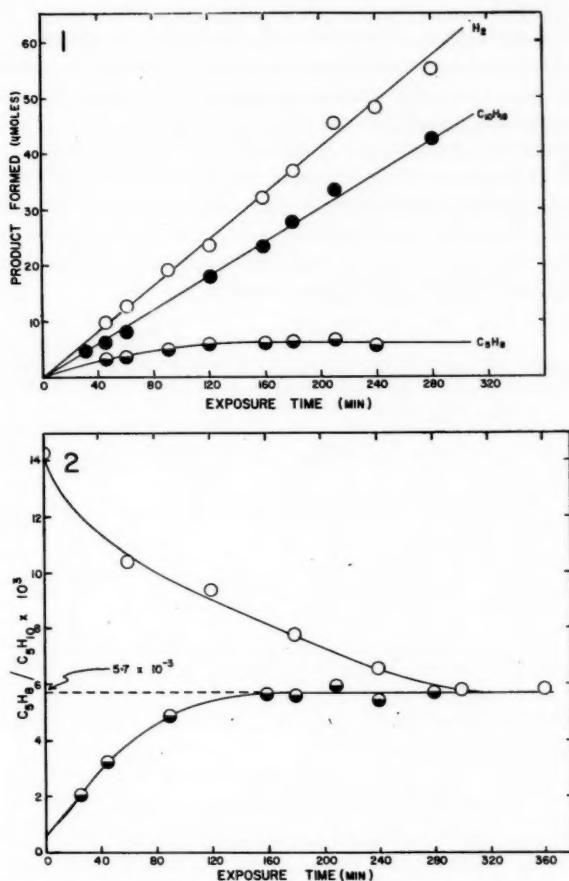
FIG. 1.   Yields, in micromoles, for hydrogen, bicyclopentyl, and cyclopentene vs. exposure time in the mercury-photosensitized decomposition of Phillips, Research Grade (P.R.G.) cyclopentane.

FIG. 2.   The change in the cyclopentene-to-cyclopentane ratio with increasing exposure time in the mercury-photosensitized decomposition of cyclopentane: ◑ P.R.G. cyclopentane, ○ cyclopentane containing 1.43 mole% of cyclopentene.

Fig. 1. In the runs exceeding about 200 minutes in duration, small amounts of a fourth product were detected in the G.L.C. analyses. This product is discussed in more detail below.

The lower curve in Fig. 2 shows the behavior of the cyclopentene-to-cyclopentane ratio, as a function of exposure time, for P.R.G. cyclopentane. The steady-state value for the $(C_5H_8)/(C_5H_{10})$ ratio was found to be $5.7 \pm 0.1 \times 10^{-3}$. In order to determine whether the same steady-state would be achieved with added cyclopentene, a series of runs were done with a sample of cyclopentane for which the $(C_5H_8)/(C_5H_{10})$ ratio was initially 14.3×10^{-3}. It can be seen from the upper curve in Fig. 2 that the same steady-state value is ultimately reached, as with the P.R.G. cyclopentane.

In the runs with added cyclopentene, it was noted that a fourth product appeared in

measurable quantities. In the G.L.C. analysis, the retention time for this product was identical with that of the minor peak obtained in runs of long duration with the P.R.G. substrate. The product was isolated, and a parent-peak determination was made on a mass spectrometer. The molecular weight corresponded to the formula $C_{10}H_{16}$. It was concluded that the product was likely a cyclopentyl cyclopentene. On the assumption that the $C_{10}H_{16}$ product had the same sensitivity as bicyclopentyl (4), the $(C_{10}H_{16})/(C_5H_{10})$ ratio could be estimated. These values, together with the $(C_5H_8)/(C_5H_{10})$ ratios, are given in Table I, for the runs with added cyclopentene. It can be seen from the table that the $(C_{10}H_{16})/(C_5H_{10})$ ratio reaches a steady-state value of $1.6\pm0.1\times10^{-3}$. It should further be noted that the $C_{10}H_{16}$ product and cyclopentene reach their respective steady-state concentrations in essentially the same period of time.

TABLE I

Quantum yields and steady-state concentrations for runs with added cyclopentene*

Exp. time, minutes	Quantum yields			$(C_5H_8)/(C_5H_{10})$ $\times10^3$	$(C_{10}H_{16})/(C_5H_{10})$ $\times10^3$
	C_5H_8	$C_{10}H_{18}$	$C_{10}H_{16}$		
0				14.3	
60	−0.173	0.37	0.016	10.4	0.28
120	−0.116	0.40	—	9.4	—
180	−0.124	0.46	—	7.7	—
240	−0.114	0.35	—	6.5	—
300	−0.090	0.43	0.015	5.8	1.3
360	−0.076	0.40	0.014	5.8	1.6
420	−0.065	0.36	0.013	5.8	1.6
420	—	0.38	0.011	—	1.6

*Initial cyclopentane pressure = 107 mm. Absorbed light intensity = 3.75×10^{-7} einstein/minute.

The data in Table I also show clearly that the quantum yield of bicyclopentyl formation is invariant in exposure time at 0.39 ± 0.03.
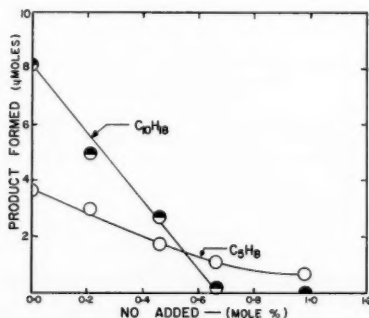
FIG. 3. The effect of added nitric oxide on the yields, in micromoles, of bicyclopentyl, and cyclopentene for 1-hour runs in the mercury-photosensitized decomposition of P.R.G. cyclopentane.

In Fig. 3 the effect is shown of the addition of small amounts of nitric oxide on the yields of cyclopentene and bicyclopentyl. The data are for 1-hour runs. The results demonstrate rather strikingly the free radical nature of the reaction. With 0.7% nitric oxide present, no bicyclopentyl is formed. With 0.98% added nitric oxide, the cyclopentene yield is reduced to 18% of its value for the pure substrate. In the 1-hour run,

with 0.98% nitric oxide, the total yield of cyclopentene was only 0.66 μmole. This small value is liable to considerable error, since correction must be made for the cyclopentene present in the P.R.G. substrate, apart from the inherent error in the determination. It can be concluded that the presence of approximately 1% nitric oxide completely inhibits bicyclopentyl formation, and reduces the cyclopentene yield to a very low value.

In Fig. 4, the mean quantum yields for the formation of hydrogen, bicyclopentyl, and cyclopentene are shown as a function of the exposure time, for P.R.G. cyclopentane. It should first be noted that the quantum yield of bicyclopentyl formation does not change with duration of exposure, maintaining throughout a constant value of 0.40±0.01. Reference to Table I shows that the value is the same as that obtained in the runs with added cyclopentene, within the experimental error. Extrapolation of the mean quantum yields of cyclopentene formation to $t = 0$ suggests a value of 0.4 for $\phi_{C_5H_8}$. From the stoichiometry $\phi_{H_2}^0$ must be 0.8.

In order to obtain more accurate data on the primary quantum yields of the reaction, a special batch of P.R.G. cyclopentane was purified by G.L.C. This ultrapure material showed no detectable impurities, and it was estimated that total impurities could not exceed 0.001 mole%. Runs were made with exposure times from 1.4 to 33 minutes. The

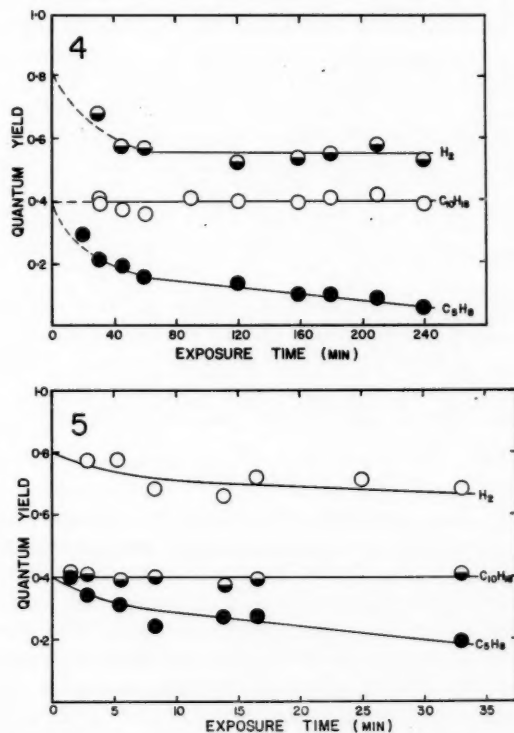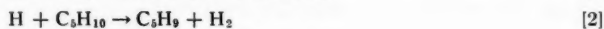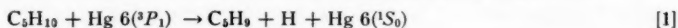FIG. 4. The mean quantum yields of formation for hydrogen, bicyclopentyl, and cyclopentene vs. exposure time in the mercury-photosensitized decomposition of P.R.G. cyclopentane.

FIG. 5. The mean quantum yields of formation of hydrogen, bicyclopentyl, and cyclopentene vs. exposure time in the mercury-photosensitized decomposition of cyclopentane containing less than 0.001 mole% of impurities.

mean quantum yields vs. exposure time are shown in Fig. 5. Again the invariance of the quantum yield of bicyclopentyl formation at 0.40 is to be noted. The extrapolation of $\phi_{C_5H_8}$ to $t = 0$ can now fairly confidently be said to lead to a value of 0.4 for $\phi_{C_5H_8}^0$. Under such conditions, $\phi_{H_2}^0$ must be 0.8, and an inspection of Fig. 5 shows that 0.8 is a reasonable extrapolation of the actual data on the mean quantum yield of hydrogen formation to $t = 0$.

DISCUSSION

As in the previous two studies (1, 2) on the cyclopentane reaction, the mechanism under initial conditions will be represented by the following paraffinic sequence:

$$C_5H_{10} + Hg\,6(^3P_1) \rightarrow C_5H_9 + H + Hg\,6(^1S_0) \tag{1}$$

$$H + C_5H_{10} \rightarrow C_5H_9 + H_2 \tag{2}$$

$$2(C_5H_9) \rightarrow C_5H_8 + C_5H_{10} \tag{3}$$

$$2(C_5H_9) \rightarrow C_{10}H_{18} \tag{4}$$

The above four-step sequence should apply only in the limiting case of zero extent of reaction. A steady-state treatment leads to the following expressions for the primary quantum yields: $\phi_{H_2}^0 = K$, $\phi_{C_5H_8}^0 = K[1/(1+r)]$, $\phi_{C_{10}H_{18}}^0 = K[r/(1+r)]$, and $\phi_{C_5H_{10}}^0 = K[(1+2r)/(1+r)]$. The constant K represents the fraction of the primary quenching collisions which lead to reaction, and r is the ratio k_4/k_3, or the relative rate of recombination to disproportionation for cyclopentyl radicals. Both K and r can now be obtained from the primary quantum yields of formation of hydrogen, cyclopentene, and bicyclopentyl, which, in turn, were derived by short extrapolations of the mean quantum yields of product formation for ultrapure cyclopentane, as shown in Fig. 5. Thus taking $\phi_{H_2}^0 = 0.8$, and $\phi_{C_{10}H_{18}}^0 = \phi_{C_5H_8}^0 = 0.4$, we find that $K = 0.8$ and $r = k_4/k_3 = 1.0$. The data would therefore indicate that the primary chemical efficiency of the reaction is 80%, and that cyclopentyl radicals have the same rates for disproportionation and recombination.

In the earlier study of the cyclopentane reaction at 30° C by Beck, Kniebes, and Gunning (2), the primary quantum yields, and the efficiency constant, K, were calculated from the limiting high-pressure values for the mean quantum yields. Their data were obtained for runs of 60-minute duration, at an absorbed light intensity of 2.5×10^{-6} einstein/minute. It was further assumed that the cyclopentene achieved a steady-state concentration by the reaction

$$C_5H_8 + H \rightarrow C_5H_9. \tag{5}$$

In this study we have measured directly the change in cyclopentene concentration with increasing duration of exposure, at an absorbed light intensity of 3.75×10^{-7} einstein/minute. The data, represented in Fig. 2, as a plot of the ratio $(C_5H_8)/(C_5H_{10})$ vs. the duration of exposure, show unequivocally that a steady-state concentration is indeed achieved, after approximately 160 minutes of irradiation. The steady-state value of $(C_5H_8)/(C_5H_{10})$ was found to be 5.7×10^{-3}. At an absorbed light intensity of 2.5×10^{-6} einstein/minute, with all other reaction parameters remaining constant, we would expect the steady-state to be reached in ca. $160(3.75 \times 10^{-7})/(2.5 \times 10^{-6}) = 24$ minutes. If reaction [5] is assumed to be the only method whereby cyclopentene is consumed, then the conditions in the previous study (2) should indeed represent a steady-state situation for cyclopentene. However, in the present investigation, we have found that

prolonged irradiation leads to the formation of an additional product, $C_{10}H_{16}$, which is assumed to be a cyclopentyl cyclopentene.

This product can be accounted for by the reactions

$$H + C_5H_8 \rightarrow C_5H_7 + H_2,$$ [6]

$$C_5H_7 + C_5H_9 \rightarrow C_{10}H_{16},$$ [7]

where C_5H_7 represents a cyclopentenyl radical. Now, if hydrogen, cyclopentene, and bicyclopentyl are the only products of the reaction, the stoichiometry would demand that the mean quantum yields for hydrogen and bicyclopentyl formation approach each other with increasing exposure. From Fig. 4, it can be seen that the mean quantum yield of hydrogen formation is slightly larger than that calculated from the quantum yields of cyclopentene and bicyclopentyl. The discrepancy, furthermore, becomes greater with increasing duration of exposure. It should also be emphasized that the invariance of the quantum yield of bicyclopentyl formation strongly suggests that the secondary product, $C_{10}H_{16}$, arises by the decomposition of cyclopentene, rather than from bicyclopentyl. The most compelling evidence, however, for ascribing $C_{10}H_{16}$ formation to the secondary decomposition of cyclopentene is presented in Table I, and also in the upper curve of Fig. 2. For the series of runs in which cyclopentene was initially added, the $C_{10}H_{16}$ product becomes considerably more important than in the runs with the P.R.G. cyclopentane.

In comparing the results obtained in the previous investigation (2) with those in the present study, there is another factor which should be considered. In mercury photosensitization, the zone of reaction is concentrated near the window through which the radiation enters the cell. With increasing light intensity, there will be a localized build-up of reaction products near this incident window. Secondary reactions should therefore assume greater importance at higher light intensities. In the previous study (2), the light intensity was 6.7 times higher than in the present work.

Probably the most interesting result of this study is the fact that cyclopentyl radicals, at 24° C, have equal rate constants for recombination and disproportionation. There seems little doubt that the ratio k_3/k_4 is at least 1.0, and by inspection of Fig. 5, it can be seen that the initial rate of cyclopentene formation could conceivably be slightly greater than that for bicyclopentyl. That these rates are essentially identical might suggest that both recombination and disproportionation proceed through the same reaction intermediate.

The results of the runs with added nitric oxide demonstrate rather strikingly the free radical nature of the reaction. From Fig. 3, it can be seen that bicyclopentyl formation is completely suppressed by the addition of 0.7% of nitric oxide. With 1% nitric oxide present in the cyclopentane, there is no bicyclopentyl present after a 1-hour run, and the cyclopentene yield is reduced to about 18% of its value for the pure substrate. Such behavior would indicate that there is a fairly stable compound formed when cyclopentyl radicals interact with nitric oxide. A possible explanation would be that the $C_5H_9 . NO$ intermediate rearranges to the stable cyclopentanone oxime,

$$C_5H_9 . NO \rightarrow C_5H_8 : NOH.$$ [8]

The fact that cyclopentene formation is not completely suppressed would suggest that the intermediate has an alternate mode of decomposition,

$$C_5H_9 . NO \rightarrow C_5H_8 + NOH.$$ [9]

From the data represented in Fig. 2, for the change in the $(C_5H_8)/(C_5H_{10})$ ratio with duration of exposure, it is apparent that the same steady-state concentration of cyclopentene is ultimately achieved, regardless of the initial cyclopentene concentration. If we assume that the over-all reaction in the steady-state region can be described by steps [1] through [7], we find that the steady-state value, $(C_5H_8)/(C_5H_{10})_{SS}$, is related to the rate constants by the equation

$$(C_5H_8)/(C_5H_{10})_{SS} = k_2/(2k_6+k_5).$$

Now k_6, the rate constant for the abstraction reaction, should be considerably smaller than that for the addition reaction, k_5. To a first approximation, therefore,

$$(C_5H_8)/(C_5H_{10})_{SS} = k_2/k_5 = 5.7 \times 10^{-3}.$$

In other words, our results would indicate that reaction [5] is about 175 times faster than reaction [2].

CONCLUSIONS

As a result of this study, it has been shown that the reaction of cyclopentane vapor with Hg $6(^3P_1)$ atoms leads to the formation of cyclopentyl radicals and H atoms with a primary quantum efficiency of at least 80%. The complete free radical nature of the reaction has been demonstrated by showing that as little as 0.7 mole% of added nitric oxide leads to a complete inhibition of bicyclopentyl formation. From the fact that cyclopentene and bicyclopentyl have the same primary quantum yields, it is concluded that cyclopentyl radicals have identical rates for disproportionation and recombination at 24° C. The results of the investigation would further suggest that meaningful values for the ratio of the rates of disproportionation to recombination for free radicals can only be obtained when the reaction in question is studied at low light intensities and at very short durations of exposure.

REFERENCES

1. G. A. ALLEN, D. L. KANTRO, and H. E. GUNNING.   J. Am. Chem. Soc. **72**, 3588 (1950).
2. P. W. BECK, D. V. KNIEBES, and H. E. GUNNING.   J. Chem. Phys. **22**, 678 (1954).
3. S. BYWATER and E. W. R. STEACIE.   J. Chem. Phys. **19**, 319 (1951).
4. A. E. MESSNER, D. M. ROSIE, and P. A. ARGABRIGHT.   Anal. Chem. **31**, 230 (1959).

THE NATURE OF POLYMERIZATION CATALYSTS PREPARED FROM METAL ALKYLS AND TITANIUM HALIDES[1]

M. H. JONES, U. MARTIUS, AND M. P. THORNE

ABSTRACT

A study has been made of the composition and structure of the insoluble complexes formed in the reaction of aluminum triisobutyl or lithium *n*-butyl with titanium tetrachloride or trichloride in heptane at room temperature by chemical and X-ray diffraction analyses. For the tetrachloride systems it has been shown that, with metal alkyl : titanium tetrachloride ratios of 0.5 to 4, at least 50% of the titanium is present in the tetravalent state and that there is considerable loss of chlorine and alkyl groups. The aluminum complexes are amorphous except at component ratios of 0.5 to 1, where the X-ray pattern indicated traces of titanium trichloride.

With the aluminum triisobutyl – titanium trichloride system, X-ray evidence has shown that the titanium trichloride remains essentially unchanged. This result, together with the low aluminum content (less than 0.5%), is consistent with Natta's suggestion that this catalyst for olefine polymerization consists of a trichloride surface on which small quantities of aluminum alkyl are chemisorbed.

The reaction between lithium butyl and titanium trichloride at ratios above unity results in the formation of a new crystalline compound having a sodium chloride type lattice with a lattice spacing of 5.20 Å. The compound is thought to be a double salt of the type $(LiCl)_4$. $TiCl_2$ or $(LiCl)_n$. TiCl. Evidence of a second crystalline component was also noted but it could not be identified.

Tentative reaction schemes are proposed for the formation of the various complexes and their structures are considered in relation to their ability to polymerize 1-butene.

INTRODUCTION

During the past five years widespread interest has been shown in new catalysts available for the polymerization of α-olefines and dienes which are also capable of controlling the orientation of the monomer units entering the polymer chain, so that long sequences of units in a head-to-tail arrangement have the same configuration. One type of such catalysts, first reported by Ziegler (1), is obtained by the interaction in a hydrocarbon solvent of an alkyl of a metal from groups one to three of the periodic table with a halide, or other derivative, of a transition metal from groups four to eight. Although considerable information is available in the literature on the use of different catalyst combinations of this kind for polymerization, and on the nature of the polymers, less attention has been directed towards their composition and structure.

The catalyst system AlR_3–$TiCl_4$ has been studied in most detail and it is considered that complex formation occurs by reduction of the transition metal to a lower valency state by the metal alkyl (2, 3). Chemical analyses of the insoluble complexes (3, 4, 5) have shown that they contain aluminum, titanium, chlorine, and alkyl groups, the composition depending on the starting ratio of aluminum alkyl to titanium tetrachloride and the temperature of preparation. Some doubt exists as to the valency state of the titanium in the complexes and its relationship to catalytic activity both for this system and that in which lithium alkyls are used (2, 6). However, it has been established that catalysts which show the greatest stereospecificity in the polymerization of α-olefines are those derived from lower titanium halides (3).

From these and other considerations several suggestions (3, 7, 8, 9) have been made concerning the nature of the active species and the mechanism by which stereoregular

polymers are formed. In general, for heterogeneous catalysts, the active sites for stereo-specific polymerization are believed to be locations on a reduced titanium halide surface where the metal alkyl is chemisorbed, the resultant complex and the electron character-istics of the adjacent surface providing control of the monomer orientation during the propagation step.

In the present work additional information concerning the nature of complexes pre-pared from aluminum triisobutyl or lithium butyl with titanium tetrachloride or tri-chloride has been obtained from chemical analyses and X-ray diffraction studies, and is considered in relation to their activity as catalysts for the polymerization of 1-butene.

EXPERIMENTAL

Preparation of Reagents

(1) Solvent.—High-purity heptane (Distillation Products Inc.), b.p. 96–97° C, was purified by shaking with concentrated sulphuric acid, washing with 2% sodium hydroxide solution and water, and drying over calcium chloride and metallic sodium. After distilla-tion from a piece of sodium in a nitrogen-flushed apparatus, the heptane was stored over sodium wire.

(2) Nitrogen.—Before use, Linde nitrogen (99.99%) containing a maximum of 15 grains water per 1000 cu. ft, was passed over heated copper and magnesium perchlorate to remove traces of oxygen and moisture.

(3) Aluminum triisobutyl.—A 25% solution in heptane of a mixture of approximately 60% triisobutyl aluminum and 40% diisobutyl aluminum hydride (Hercules Powder Company) was distilled under reduced pressure in a nitrogen atmosphere. The solvent was removed at low temperature and the aluminum triisobutyl distilled as a colorless liquid, b.p. 55° C, at 1.5 mm. The diisobutyl aluminum hydride, having an appreciably lower vapor pressure, remained in the high-boiling residue. The aluminum content of the trialkyl, which was stored as an approximately 45% (w/w) solution, was determined gravimetrically with 8-hydroxyquinoline after hydrolysis in aqueous sulphuric acid (found: Al, 13.4%; calc.: Al, 13.8%).

(4) Lithium butyl.—Lithium butyl was prepared by treating a 20% solution of n-butyl chloride in heptane with lithium wire (15% excess over the theoretical quantity) in an argon atmosphere. Close to 100% yields were obtained if the reaction mixture was cooled to −20° C during the addition of the lithium and allowed to heat up to room temperature slowly. After the solution of lithium alkyl was shaken for 24 hours it was filtered under nitrogen and analyzed by titration of the lithium hydroxide produced on hydrolysis.

(5) Titanium halides.—Fisher C.P. grade titanium tetrachloride was distilled in an inert atmosphere before use. Solutions in heptane were water-white. The violet titanium trichloride obtained from the Stauffer Chemical Company was pumped under vacuum to remove traces of the tetrachloride. Analysis gave a composition of $TiCl_{2.72}$.

Preparation of the Catalysts

Boston round bottles fitted with self-sealing butyl rubber gaskets protected by neoprene were used for preparation of solutions and catalyst suspensions. Particular care was taken to ensure that all the apparatus and solvent was thoroughly flushed with nitrogen before use.

For the titanium tetrachloride catalysts a concentrated solution containing about $1.5.10^{-3}$ moles ml^{-1} was prepared by addition of the pure titanium tetrachloride to a weighed quantity of solvent. The bottle was then flushed with nitrogen, capped, reweighed,

and pressurized with nitrogen. Samples were withdrawn with a hypodermic syringe for use in individual catalyst preparations. These titanium tetrachloride solutions could be used over a period of about 4 days, provided the cap was renewed each time a sample was removed.

For the titanium trichloride catalysts a separate suspension of the solid in heptane was prepared for each catalyst sample. The trichloride (1–2 g) was transferred to weighed bottles in a dry box, which was continuously flushed with nitrogen and gave a maximum dew point of $-40°$ C. After reweighing the bottles, the heptane was added by means of a syringe.

All catalysts were prepared by injection of the metal alkyl solution into the solution or suspension of the halide in heptane. The bottles were shaken by hand during the addition of the alkyl. Concentrations of the catalysts, based on the amount of halide in the solvent, were of the order of 0.2 to 0.3 molar. The catalysts were aged for at least 1 hour before use.

Analysis of the Catalysts

X-Ray diffraction analyses were carried out on suspensions of the complexes in heptane using filtered copper radiation and a powder camera of 114.6 mm diameter. The diffraction patterns were measured and evaluated according to A.S.T.M. procedures. A nitrogen-flushed 0.5 mm bore Lindemann glass capillary tube was filled by lowering it into a sample of the suspension contained in a small tube blanketed by nitrogen. The capillary was sealed in a luminous flame. With careful manipulation no change in the appearance of a catalyst suspension could be detected. Also, once sealed, the complexes were stable over a period of at least several days as indicated by the reproducibility of the diffraction patterns.

For chemical analysis the complexes were isolated by filtration under nitrogen, washed with heptane, and dried under vacuum. About 1 g of dried solid was then hydrolyzed in 50 ml of 2 N sulphuric acid, also in a nitrogen atmosphere, and aliquot samples analyzed for titanium, chlorine, and aluminum or lithium.

Reduced titanium in the trivalent state was determined by running aliquot samples into an excess of ferric ammonium sulphate and estimating the ferrous iron thus produced by titration with 0.3 N potassium permanganate. Oxidation of the chloride ion in the solution was prevented by addition of an excess of a Zimmermann-Reinhardt solution (containing 50 g $MnSO_4.4H_2O$, 100 ml 98% H_2SO_4, and 100 ml 85% H_3PO_4 in 500 ml water). The total titanium was determined by a similar method after passing aliquot samples through a Jones' reductor.

Chlorine was determined by Volhard's method.

The aluminum analyses were carried out spectrographically* on a mixture of titanium and aluminum oxides obtained by precipitation with ammonium hydroxide and subsequent ignition.

Lithium was determined by flame photometry at a wavelength of 671 mμ.

Polymerizations

Butene polymerizations were carried out in a nitrogen atmosphere at 40° C in bottles with self-sealing gaskets. Matheson C.P. grade 1-butene, dried by passage through anhydrous calcium sulphate and phosphorus pentoxide, was condensed in the solvent at $-30°$ C, the excess being allowed to boil off before capping the bottles. The catalyst

---

*Analyses made by Laboratories Branch, Department of Mines, Province of Ontario.

suspensions were added with a syringe at room temperature. In cases where no polymerization occurred at 40° C the temperature was raised to 80° C.

Ethylene polymerizations were carried out at room temperature in a three-necked flask fitted with neoprene rubber stoppers containing inlet tubes for nitrogen and ethylene. The solvent and catalyst components were introduced and the ethylene bubbled in at approximately 50 ml min^{-1}.

At the end of a polymerization reaction the catalyst was killed by the addition of ethanol to the reaction mixture. Decomposition of the catalyst and removal of the solvent were effected by stirring the jelly-like mass in a 10- to 20-fold excess of ethanol in a Waring Blendor. The polymer was filtered and dried under vacuum.

RESULTS

Catalytic Activity of the Complexes

Table I shows the results of a comparative study of the activity of the four catalyst systems towards the polymerization of 1-butene. The aluminum triisobutyl – titanium trichloride complexes are active over the widest range of initial alkyl:halide ratios,

TABLE I

Activity of Ziegler–Natta type complexes towards polymerization of 1-butene, at 40° C

|	Alkyl:halide ratio			
	Below 0.5:1	0.5:1	1:1	Above 1:1
Al(iBu)$_3$–TiCl$_3$		+	+	+
Al(iBu)$_3$–TiCl$_4$	−	−	+	+
LiBu–TiCl$_3$	−	−	−	−
LiBu–TiCl$_4$	−	−	−	+ (if prepared in presence of monomer)

NOTE: Catalyst concentration: 2.10^{-2}–$3.5.10^{-2}$ moles (Ti halide)l^{-1}.

while the lithium systems only give polybutene under special conditions, i.e. with titanium tetrachloride at ratios above 1 provided the complex is prepared in the presence of the monomer. However, under these conditions, polymerization is rapid and almost complete for molar ratios of monomer to titanium up to at least 100. Polyethylene was obtained at ratios of unity and above from LiBu–TiCl$_4$ complexes prepared in the presence or absence of the monomer, but the LiBu–TiCl$_3$ complexes were completely inactive towards both ethylene and 1-butene.

Valency State of Titanium in Complexes

The method employed for the determination of reduced titanium cannot be used to establish the valency state of the metal since, on acid hydrolysis, divalent titanium is rapidly oxidized to the trivalent form (10), viz.

$$2Ti^{2+} + 2H_2O \rightarrow 2Ti^{3+} + 2OH^- + H_2.$$
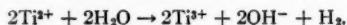
However, from the two titanium analyses, an estimate of the residual tetravalent titanium can be made. These values for the insoluble products obtained from the reaction of lithium butyl or aluminum triisobutyl with titanium tetrachloride are plotted in Fig. 1 as a function of the initial component ratio. It is apparent that for both systems the titanium is present largely in the tetravalent state. With the LiBu–TiCl$_4$ complexes there is a trend to higher percentages of Ti^{4+} as the component ratio increases, while for the Al(iBu)$_3$–TiCl$_4$ complexes the percentage of Ti^{4+} remains essentially constant.
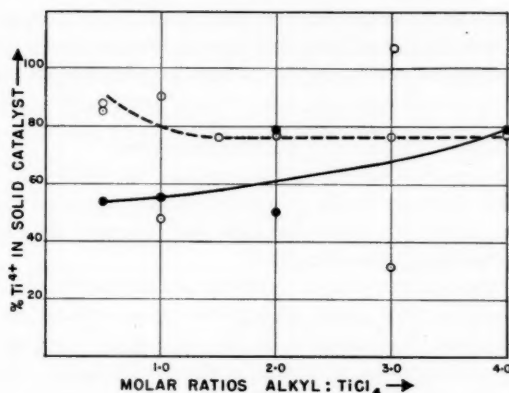
FIG. 1.   Percentage of titanium in tetravalent state as function of component ratio. ○ Al(*i*Bu)₃–TiCl₄, ● LiBu–TiCl₄.

Similar results for the lithium system have been reported by Friedlander and Oita (2) but with aluminum triisobutyl they found almost complete reduction of the titanium at component ratios above unity. In early experiments, where no special precautions were taken to ensure rapid dispersion of the metal alkyl during addition to the titanium tetrachloride solution, considerable reduction of titanium was noted (low values of Ti⁴⁺ at Al(*i*Bu)₃:TiCl₄ ratios of 1 and 3). This may be one of the factors accounting for the discrepancy between the two results. Recently, it has been found that 90% of the titanium in the soluble complexes formed from these components at −78° C is in the tetravalent state (11).

Titanium, chlorine, and aluminum or lithium were found in all the solids analyzed. In calculating the elemental ratios in the insoluble reaction products, the alkyl content was taken as the difference between the weight of complex hydrolyzed and the total analysis of the other elements.

The Aluminum Triisobutyl – Titanium Trichloride System

Addition of the aluminum triisobutyl solution to a suspension of titanium trichloride in heptane resulted in the formation of a brown mixture which, on standing, settled into two layers consisting of a violet precipitate and a dark brown supernatant liquid. No marked difference in appearance was observed at Al(*i*Bu)₃:TiCl₃ ratios in the range of 1 to 5. The dried solids were violet color and gave violet solutions on hydrolysis.

The chemical analyses for a series of the reaction products are recorded in Table II.

TABLE II

Analysis of aluminum triisobutyl – titanium trichloride complexes

Al(*i*Bu)₃:TiCl₃	% Ti total	% Cl	% Al	% R	Atomic ratios			
					Al:Ti	Cl:Ti	R:Ti	R:Al
0.5	33.7	65.3	0.24	0.8	0.012	2.62	0.02	1.5
1.0	31.7	64.6	0.26	3.4	0.014	2.75	0.09	6.3
2.0	31.8	65.9	0.42	1.9	0.023	2.80	0.05	2.1
5.7	31.5	65.5	0.51	2.5	0.029	2.81	0.07	2.3

The results show that the products consist principally of TiCl$_3$, independent of the initial Al(iBu)$_3$:TiCl$_3$ ratio, the aluminum content always being less than 0.5%. Similarly, the X-ray diffraction patterns of the various samples gave only lines of the violet form of titanium trichloride.

The Aluminum Triisobutyl – Titanium Tetrachloride System

The reaction of aluminum triisobutyl with titanium tetrachloride in heptane yields a precipitate whose color changes from a light reddish-brown to dark brown as the Al(iBu)$_3$:TiCl$_4$ ratio is increased. After filtration and vacuum drying, the color of the solid varies from light brown to purplish-black.

X-Ray analysis of suspensions of the complexes showed traces of titanium trichloride at initial component ratios of 0.5 and 1, but there was no indication of crystallinity at ratios below 0.5. Above the equimolar ratio the complexes were entirely amorphous. Natta *et al.* (12) have also reported that the complexes from the Al(Et)$_3$–TiCl$_4$ system are amorphous at component ratios above 0.7.

The results of the chemical analyses of a number of solids prepared at Al(iBu)$_3$:TiCl$_4$ ratios of 0.5 to 4 are given in Table III. The values for the atomic ratios are based on the

TABLE III

Analysis of aluminum triisobutyl – titanium tetrachloride complexes

Al(iBu)$_3$:TiCl$_4$	% Ti		% Cl	% Al	% R	Atomic ratios			
	Red.	Total				Al:Ti	Cl:Ti	R:Ti	R:Al
0.5	5.4	30.6	49.0	7.86	12.4	0.46	2.16	0.34	0.75
0.5	3.2	23.0	39.1	—	—	—	2.30	—	—
1.0	—	26.5	46.4	6.10	21.0	0.41	2.37	0.67	1.63
1.0	14.5	27.9	42.8	—	—	—	2.07	—	—
1.5	6.4	27.6	48.2	7.14	17.1	0.46	2.36	0.52	1.13
2.0	6.5	28.0	31.9	7.94	32.1	0.50	1.54	0.96	1.91
3.0	19.6	28.7	34.8	8.00	28.5	0.49	1.64	0.83	1.69
3.0	6.2	26.3	39.9	—	—	—	2.05	—	—
4.0	6.6	28.0	35.2	11.02	25.7	0.70	1.70	0.77	1.10

analyses for "total" titanium. It is apparent that there is an initial decrease in the Cl:Ti ratio and that the values lie between 2.5 and 1.5 over the whole range of compositions studied. These figures are considerably lower than those reported by Cooper and Rose (5) for similar catalyst systems. The low values for the Al:Ti and R:Ti ratios suggest that only a small proportion of the aluminum triisobutyl or its reaction products takes part in the formation of the precipitate, while the R:Al ratios, lying between 1.2 and 2.0, indicate loss of alkyl groups during the reaction. At least part of this loss is accounted for by the formation of C$_4$ hydrocarbons which were detected in gas chromatographic analysis of a sample of the vapor phase above a reaction mixture. Isobutane and isobutylene or 1-butene were the major constituents. A positive identification of the olefine could not be made, but it is probably isobutylene. Trace amounts of C$_3$ hydrocarbons were also detected.

Analyses of some of the filtrates from the complexes gave Cl:Ti ratios which steadily increased with increasing initial component ratio, having a value of 69 for an Al(iBu)$_3$: TiCl$_4$ ratio of 4. This implies that chlorine compounds soluble in heptane are formed during

the reaction. In addition, the valency state of titanium found in the filtrate was observed to change with component ratio. For an $Al(iBu)_3:TiCl_4$ ratio of 0.5, 98% of the titanium in the filtrate was present as Ti^{4+}, but at a ratio of 3 all the titanium was in the reduced state. At the higher component ratio, the titanium in the filtrate presumably represents soluble titanium compounds or finely divided titanium trichloride which passed through the filter.

The Lithium Butyl – Titanium Trichloride System

The reaction between lithium butyl and titanium trichloride in heptane is highly exothermic and the violet form of the trichloride is converted to an insoluble green complex.

The X-ray diffraction patterns of the complexes were obtained under identical experimental conditions over the whole range of $LiBu:TiCl_3$ ratios from 0.5 to 4. At a ratio of 4 the diffraction pattern could not be identified by comparison with the reference data of the A.S.T.M. index and, consequently, an attempt was made to index the pattern from basic principles. Using the graphic method it was found to consist of two separate compounds, one of them being cubic and having a sodium chloride type lattice with a lattice constant of 5.20 Å. This is appreciably larger than the lattice constant of lithium chloride (5.14 Å), and the compound is considered to be a mixed crystal of lithium and titanium chlorides, probably of composition $(LiCl)_n.TiCl_2$ or $(LiCl)_n.TiCl$. Although alkali metal complexes of both tetravalent and trivalent titanium halides are known, none have been reported in which titanium is in a lower valent state. The pattern of the second component could not be identified, but its higher symmetry suggests that it may be an alkylated compound. Both compounds were also found at component ratios of 2 and 1. At the equimolar ratio the two strongest lines of titanium trichloride were also evident and at ratios of less than one the X-ray diffraction patterns consisted of the trichloride lines only. The d values and approximate line intensities of the patterns obtained at ratios of 2 and 4 are given in Table IV and those for lithium chloride are included for comparison. From the table it is apparent that the relative line intensities of the cubic

TABLE IV

X-Ray diffraction patterns of complexes from $LiBu–TiCl_3$ system

| "d" | Relative intensity of component ratio | | hkl | LiCl* | | hkl |
	2:1	4:1		"d"	Rel. int.	
6.00	80	40				
3.15	40	20				
3.01	60	60	111	2.967	100	111
2.61	100	100	200	2.570	86	200
2.00	10	—				
1.84	90	80	220	1.817	58	220
1.76	10	—				
1.57	10	10	311	1.550	29	311
1.50	30	20	222	1.484	16	222
1.30	10	10	400	1.285	4	400
				1.1791	10	331
1.16	20	10	420	1.1493	12	420
1.06	20	10	422	1.0491	8	422

*A.S.T.M. index (4-0664).

component and lithium chloride differ appreciably. This can be due to the different scattering power of the mixed crystal or to preferred orientation. Comparison of the patterns for the 2:1 and 4:1 complexes indicate that superposition of diffraction lines of the cubic component and the unknown constituent is not an important factor.

Hydrolysis of the dried solids in 2 N sulphuric acid was accompanied by considerable gas evolution, producing violet-colored solutions. In addition, at ratios of unity and above, increasing amounts of an insoluble blue solid were obtained, constituting, at the highest ratio, about 20% of the original weight of the complex. The compound was stable in air and different samples contained 55–61% titanium. Spectrographic analysis showed only traces of lithium. The X-ray diffraction pattern had considerable background scattering and was different from that of the complex before hydrolysis. This hydrolysis product is probably a hydrated form of one of the lower titanium oxides, i.e. of composition between Ti_2O_3 and TiO_2. Stable oxides of a similar color, corresponding to the nominal formulae Ti_3O_5 and Ti_7O_{12}, have been prepared (13) and are also resistant to strong acids except concentrated sulphuric acid.

The results of the chemical analysis of the reaction products for this system are given in Table V. The values for the 2.46 and 4.0 ratios are those for the solution with a correc-

TABLE V

Analysis of lithium butyl – titanium trichloride complexes

LiBu:TiCl₃	% Ti total	% Cl	% Li	% R	Atomic ratios			
					Li:Ti	Cl:Ti	R:Ti	R:Li
0.5	30.9	63.8	3.42	1.9	0.76	2.78	0.05	0.07
0.5	31.5	63.7	2.37	2.4	0.52	2.72	0.06	0.12
1.0	29.5	57.0	5.77	8.7	1.35	2.61	0.25	0.18
1.0	29.5	63.6	4.51	2.4	1.06	2.91	0.07	0.07
2.0	23.6	50.5	—	—	—	2.89	—	—
2.46	23.9	52.5	7.30	16.3	2.11	2.97	0.57	0.25
4.0	23.8	52.4	10.34	12.5	2.99	2.97	0.44	0.15

tion for the titanium present in the insoluble material formed during hydrolysis. It can be seen that the Cl:Ti ratio remains essentially constant while there is a progressive increase in the Li:Ti and R:Ti ratios. It is apparent, also, that there is a considerable loss of alkyl on formation of the complexes. Again, gas chromatographic analysis has shown that, at least in part, this appears as n-butane and 1-butene or isobutylene, probably the former.

The Lithium Butyl – Titanium Tetrachloride System

The reaction between lithium butyl and titanium tetrachloride is exothermic, and brown, jelly-like precipitates are formed, the color darkening as the proportion of lithium butyl is increased.

X-Ray examination did not show the presence of any crystalline component at LiBu:TiCl₄ ratios of less than 1. However, at ratios of 1 and above, a faint diffraction pattern was observed, showing two broad lines in the position of the two main lines of the cubic compound found in the trichloride system.

There appears to be a small decrease in the Cl:Ti ratio with increasing proportion of lithium butyl, but within the range studied it remains above 3. The Li:Ti ratio increases

TABLE VI

Analysis of lithium butyl – titanium tetrachloride complexes

	% Ti					Atomic ratios			
LiBu:TiCl$_4$	Red.	Total	% Cl	% Li	% R	Li:Ti	Cl:Ti	R:Ti	R:Li
0.5	9.82	21.0	53.3	4.07	21.6	1.34	3.43	0.86	0.65
1.0	10.6	23.5	58.5	4.61	13.4	1.35	3.36	0.48	0.35
2.0	10.5	21.1	56.2	6.31	16.4	2.06	3.60	0.65	0.32
2.0	4.57	23.2	48.1	6.41	22.3	1.91	2.80	0.81	0.42
4.0	4.97	23.0	50.6	9.91	14.5	2.97	3.09	0.53	0.18

progressively with the initial component ratio and is at a much higher level than the corresponding relationship for the Al(iBu)$_3$–TiCl$_4$ complexes. It is very similar to that for the LiBu–TiCl$_3$ system. The low R:Li ratios indicate that considerable alkyl is lost in the formation of the complexes. The principal hydrocarbons found in the vapor phase above the reaction mixtures were n-butane and 2-butene (cis and trans). In addition, small amounts of 1-butene or isobutylene, C$_3$, and C$_2$ hydrocarbons were detected.

It was noted that, on hydrolysis of the insoluble complexes in sulphuric acid solution, a greasy deposit formed on the side of the flask. A few milligrams of a white insoluble material recovered from the flask was shown to be a hydrocarbon product, indicating the formation of a small amount of polymer.
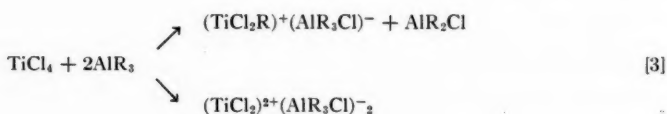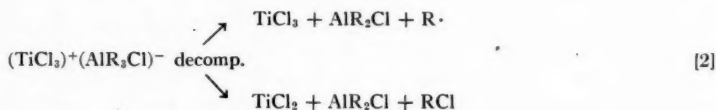
DISCUSSION

The chemical and X-ray diffraction analyses of the Al(iBu)$_3$–TiCl$_3$ catalysts are in agreement with Natta's observations (3, 14) for a similar system in that they consist essentially of unchanged titanium trichloride on which a residual amount of the metal alkyl is chemisorbed. The precision of the aluminum and alkyl contents of the catalysts given in Table II is low because of the small amounts present, but the values are similar to those reported where C^{14}-labelled aluminum triethyl was used (14). This system is one of the simplest in providing a guide to the requirements for catalytic activity and the mechanism by which control of the steric configuration of the monomer units in the polymer chain is achieved. Titanium trichloride has a layered lattice structure and it has been postulated (3) that the active sites are defect locations, or the boundaries of crystal faces, where the metal alkyl can enter into a co-ordination complex with the transition metal atom, the two dissimilar metal atoms being bridged through chlorine or alkyl groups. Polymer growth probably occurs at the aluminum atom although evidence from other catalyst systems (15, 16) suggests that a Ti—C bond may be involved. Steric control during the propagation step is visualized as resulting from the localization of the monomer units in a particular configuration as they enter the complex.

The Al(iBu)$_3$–TiCl$_4$ system is more complex and any mechanism proposed to account for the formation of the complexes must take into consideration the following factors:

(i) the high percentage of Ti^{4+} in the solids,

(ii) the loss of chlorine from the solids,

(iii) the loss of alkyl from the solids.

These factors can be accounted for, in a very general way, by the reaction scheme given below, which is based on suggestions by Natta (3) and Uelzmann (8).
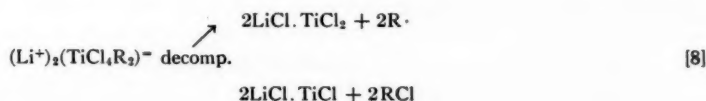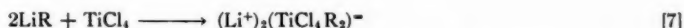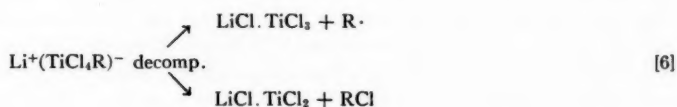
$$TiCl_4 + AlR_3 \longrightarrow (TiCl_3)^+(AlR_3Cl)^- \qquad [1]$$

$$(TiCl_3)^+(AlR_3Cl)^- \text{ decomp.} \quad \nearrow \quad TiCl_3 + AlR_2Cl + R\cdot$$
$$\searrow \quad TiCl_2 + AlR_2Cl + RCl \qquad [2]$$

$$TiCl_4 + 2AlR_3 \quad \nearrow \quad (TiCl_2R)^+(AlR_3Cl)^- + AlR_2Cl$$
$$\searrow \quad (TiCl_2)^{2+}(AlR_3Cl)^-_2 \qquad [3]$$

$$(TiCl_2R)^+(AlR_3Cl)^- \text{ decomp.} \quad \nearrow \quad TiCl_2 + AlR_2Cl + 2R\cdot$$
$$\searrow \quad TiCl + AlR_2Cl + RCl + R\cdot \qquad [4]$$
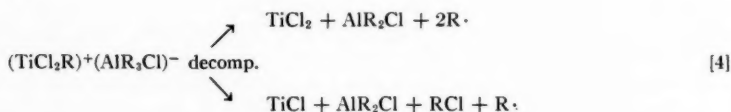
Equations [1] and [3] represent the initial complex-forming reaction with increasing concentration of aluminum alkyl in which the titanium is stabilized in the tetravalent state. Decomposition of the first complex according to reaction [2] would account for the presence of crystalline titanium trichloride at low initial ratios of aluminum alkyl to titanium tetrachloride. Both the decomposition steps [2] and [4] can account for the loss of chlorine and alkyl through the formation of hydrocarbons and soluble halides. The detection in the reaction products of isobutane and a C_4 unsaturate which is probably isobutylene indicates that the isobutyl radicals undergo a disproportionation reaction. Part of the isobutane could also result from a hydrogen abstraction reaction with the solvent or metal alkyl. Also, the presence of alkyl chloride has been reported (17) in the reaction product from the $Al(Et)_3$–$TiCl_4$ system at low component ratios. However, it is obviously difficult to equate the analyses shown in Table III with the above scheme if the high Ti^{4+} content is related solely to this type of complex.

Uelzmann (8, 11) has proposed that the ionic complexes furnish the active polymerization sites but an alternative explanation is that they are formed by adsorption of alkyl upon the lower valent titanium halides formed in the decomposition steps, in analogy with the $Al(iBu)_3$–$TiCl_3$ system.
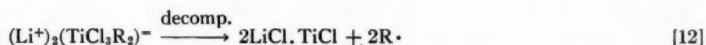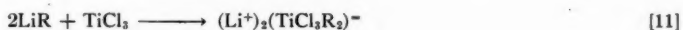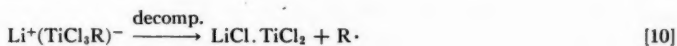
The catalysts from titanium tetrachloride give faster rates for the polymerization of 1-butene than the trichloride catalysts and yield polymers that are less crystalline. They are highly complex mixtures which presumably contain active sites of different configuration. Evidence for this suggestion (18) has come from an extensive study of the molecular weight distribution of polyethylene prepared from similar catalysts. The high degree of polydispersity observed is not compatible with a polymerization mechanism involving a single, well-defined catalyst site.

Since lithium is considerably more electropositive than titanium it is probable that the titanium is bound in complex anions and an acceptable mechanism to account for the

experimental observations on the two lithium systems, which is based on suggestions by Uelzmann, would be as follows:

$$LiR + TiCl_4 \longrightarrow Li^+(TiCl_4R)^- \qquad [5]$$

$$Li^+(TiCl_4R)^- \text{ decomp.} \nearrow \begin{array}{l} LiCl.TiCl_3 + R\cdot \\[1em] LiCl.TiCl_2 + RCl \end{array} \qquad [6]$$

$$2LiR + TiCl_4 \longrightarrow (Li^+)_2(TiCl_4R_2)^- \qquad [7]$$

$$(Li^+)_2(TiCl_4R_2)^- \text{ decomp.} \nearrow \begin{array}{l} 2LiCl.TiCl_2 + 2R\cdot \\[1em] 2LiCl.TiCl + 2RCl \end{array} \qquad [8]$$

or, considering the trichloride complexes:

$$LiR + TiCl_3 \longrightarrow Li^+(TiCl_3R)^- \qquad [9]$$

$$Li^+(TiCl_3R)^- \xrightarrow{\text{decomp.}} LiCl.TiCl_2 + R\cdot \qquad [10]$$

$$2LiR + TiCl_3 \longrightarrow (Li^+)_2(TiCl_3R_2)^- \qquad [11]$$

$$(Li^+)_2(TiCl_3R_2)^- \xrightarrow{\text{decomp.}} 2LiCl.TiCl + 2R\cdot \qquad [12]$$

The complex-forming reactions represented by the steps [5] and [7] would account for the preservation of titanium in the tetravalent state in the $LiBu$–$TiCl_4$ system, while the decomposition reactions [6], [8], [10], and [12] provide an explanation for the loss of alkyl either through the formation of hydrocarbon products or an alkyl chloride. The formation of an alkyl chloride may also account for the loss of chlorine in the tetrachloride complexes. The identification of the C_4 olefine in the tetrachloride catalyst as 2-butene is surprising since in a disproportionation reaction between n-butyl radicals this would involve a hydrogen atom rearrangement. The fact that only traces of 1-butene were detected in this case is consistent with its removal by polymerization.

Again, it is difficult to reconcile the low R:Ti ratio with the high percentage of tetravalent titanium, particularly for complexes with higher initial component ratios. A possible explanation for this inconsistency, which also appears in the $Al(i\text{Bu})_3$–$TiCl_4$ system, is that certain complex anions or cations of titanium in a valency state of less than three may give tetravalent titanium on hydrolysis in acid media, the normal step preceding analysis. The formation of an oxide of probable composition between Ti_2O_3 and TiO_2 on hydrolysis of the $LiBu$–$TiCl_3$ complexes provides evidence for this suggestion since it indicates that oxidation can proceed beyond the trivalent stage. Also, similar behavior has been reported for halides of divalent zirconium and hafnium which are the next elements to titanium in group IVA of the periodic table. The lower valency states of titanium are progressively less stable and the simple monovalent titanium halides have

not been isolated. As these will be odd electron compounds they are likely to exist only in dimeric form and will be extremely reactive.

The inability of the LiBu–TiCl₃ system to initiate polymerization may be attributable to the fact that the well-ordered crystalline compound formed does not provide the type of support on which a catalyst site of suitable configuration can form. It will be noted that this complex has the symmetrical sodium chloride type lattice as opposed to the layered lattice structure of titanium trichloride. Evidence for the formation of the same compound in the LiBu–TiCl₄ system, although to a lesser degree, may also be the explanation of the inactivity of these catalysts for the polymerization of 1-butene if prepared prior to the addition of the monomer. However, they will polymerize ethylene but at a much slower rate than when prepared in its presence. These differences in activity imply that the olefine can take part in complex formation, presumably leading to catalysts of somewhat different structure.

ACKNOWLEDGMENTS

NOTE ADDED

Since this paper was submitted for publication Dr. N. F. H. Bright* and Mr. R. C. Garvie* have completed an examination of one of our X-ray diffraction patterns of the blue solid obtained on hydrolysis in aqueous sulphuric acid of a complex prepared in the reaction of lithium butyl with titanium trichloride. They find that, although the pattern is ill-defined, it indicates that the crystalline constituents of the solid are titanium sesquioxide (Ti₂O₃) and rutile (TiO₂). As the titanium content (55%) of this particular sample is less than that of the higher oxide (TiO₂) they suggest that some amorphous hydrated TiO₂ is probably present. Evidence of an amorphous material was noted in the X-ray pattern.

Dr. Bright and Mr. Garvie also comment on the unusual fact that the TiO₂ content is in the rutile form. Normally, anatase is the crystal form in which TiO₂ is obtained when precipitated chemically.

REFERENCES

1. K. ZIEGLER. Belgium Patent No. 533,362 (Nov. 16, 1954). K. ZEIGLER, E. HOLZCAMP, and H. MARTIN. Angew. Chem. **67**, 541 (1955).
2. H. N. FRIEDLANDER and K. OITA. Ind. Eng. Chem. **49**, 1885 (1957).
3. G. NATTA. J. Inorg. & Nuclear Chem. **8**, 589 (1958).
4. W. M. SALTMAN, W. E. GIBBS, and J. LAL. J. Am. Chem. Soc. **80**, 5616 (1958).
5. M. L. COOPER and J. B. ROSE. J. Chem. Soc. 795 (1959).
6. D. B. LUDLUM, A. W. ANDERSON, and C. E. ASHBY. J. Am. Chem. Soc. **80**, 1380 (1958).
7. F. EIRICH and H. MARK. J. Colloid Sci. **11**, 748 (1956).
8. H. UELZMANN. J. Polymer Sci. **32**, 457 (1958).
9. A. GILCHRIST. J. Polymer Sci. **34**, 49 (1959).
10. G. PATSCHEKE and W. SCHALLER. Z. anorg. Chem. **235**, 257 (1938).
11. H. UELZMANN. J. Polymer Sci. **37**, 561 (1959).
12. G. NATTA, L. PORRI, A. MAZZEI, and D. MORERO. Chim. e. ind. **41**, 398 (1959).
13. GMELINS HANDBUCH. Vol. 8. System No. 41 (Titan). 1951. p. 212.
14. G. NATTA. J. Polymer Sci. **34**, 21 (1959).
15. C. VAN HEERDEN. J. Polymer Sci. **34**, 46 (1959).
16. W. L. CARRICK, F. J. KAROL, G. L. KARAPINKA, and J. J. SMITH. J. Am. Chem. Soc. **82**, 1503 (1960).
17. A. MALATESTA. Can. J. Chem. **37**, 1176 (1959).
18. H. WESSLAU. Makromol. Chem. **26**, 102 (1958).

*Mineral Sciences Division, Mines Branch, Department of Mines and Technical Surveys, Ottawa, Ontario.

REARRANGEMENT STUDIES WITH C^{14}

X. ETHANOL-2-C^{14} FROM THE IRRADIATION OF ETHANOL-1-C^{14} WITH Co^{60} GAMMA RAYS[1]

C. C. LEE AND D. G. LEE[2]

ABSTRACT

The irradiation of aqueous solutions of ethanol-1-C^{14}, containing about 2% ethanol by weight, with up to 58.0 million rads of Co^{60} γ-rays led to the formation of up to 0.49% ethanol-2-C^{14} in the alcohol recovered after irradiation. The G value of this isotope position rearrangement was about 0.04 and amounted to approximately 2% of the G value for the total amount of ethanol decomposed. Possible mechanisms for the rearrangement are discussed.

In a review in 1956, Collinson and Swallow (1) pointed out that radiolysis of alcohols follows the general pattern of a fission of an α-carbon – hydrogen bond to give an α-hydroxyalkyl radical which can either dimerize to a glycol or be further oxidized to a carbonyl compound. In the case of ethanol, this generalization can be applied to account satisfactorily for the formation of the chief products derived from the ethanol, namely, acetaldehyde and 2,3-butanediol (2–6).

While a number of minor products have been quantitatively estimated for the radiolysis of pure ethanol with α-particles (3), the irradiation of dilute aqueous solutions of ethanol with X or Co^{60} γ-rays was reported to give, besides hydrogen and hydrogen peroxide, only acetaldehyde in the presence of oxygen and acetaldehyde and 2,3-butanediol in deaerated solutions (2, 5, 6). The organic products can, therefore, be regarded as being formed from the α-hydroxyethyl radical. The most recently suggested mechanism for the radiolysis of aqueous solutions of ethanol postulated reactions of H or OH radicals with the solute to give α-hydroxyethyl from the breaking of an α-carbon – hydrogen bond (6). No rupture of the carbon–oxygen bond was envisaged. In the present study, dilute aqueous solutions of ethanol-1-C^{14} was irradiated with Co^{60} γ-rays to ascertain whether any isotope position rearrangement to ethanol-2-C^{14} would result. Detection of such a rearrangement could possibly be regarded as indicating some rupture of the carbon–oxygen bond to give an ethyl radical followed by a 1,2-hydrogen shift in the radical analogous to 1,2-hydride shifts observed in certain reactions involving the ethyl cation (7, 8, 9).

A stock solution containing 2.02% ethanol by weight was made up with distilled water and ethanol-1-C^{14}.* Its C^{14} content was about 10 μc/ml. Three-milliliter aliquots were placed in 4-ml glass vials, stoppered and sealed with wax, and then irradiated at room temperature in fixed positions near a 90-curie Co^{60} source. The dose rates were measured by determining the ferric ions formed upon irradiating solutions of ferrous ammonium sulphate (10). Under the conditions of the present experiments, the dose rates were of the order of 1200 rads/minute.

After irradiation, the samples were analyzed for total decomposition of ethanol and for the presence of isotopically rearranged ethanol-2-C^{14} in the recovered alcohol. Before and after irradiation, equal aliquots of the solution were diluted with exactly the same amounts of absolute ethanol as a carrier. The diluted solutions were converted to ethyl

3,5-dinitrobenzoate and to iodoform. The decrease in activity in the ethyl 3,5-dinitro-benzoate after irradiation represented the ethanol decomposed during the irradiation. The ethanol so decomposed most likely was chiefly converted to the known products, acetaldehyde and 2,3-butanediol. The activity in the iodoform corresponded to the C^{14} in the C-2 position of ethanol and thus would be a measure of the rearrangement to ethanol-2-C^{14}. The results are summarized in Table I.

TABLE I

Decomposition and rearrangement in the irradiation of ethanol-1-C^{14}

Dose (10^6 rads)	Derivative counted[a]	Activity[b] ($m\mu c$/mmole)	Decomposition of EtOH		Rearrangement to EtOH-2-C^{14c}	
			%	G_d	%	G_r
0	Benzoate	690				
	CHI_3	0.15				
41.8	Benzoate	572	17.1	1.7		
	CHI_3	2.98			0.41	0.04
44.1	Benzoate	562	18.5	1.8		
	CHI_3	2.60			0.39	0.04
52.0	Benzoate	516	25.2	2.0		
	CHI_3	3.56			0.49	0.04
58.0	Benzoate	517	25.1	1.8		
	CHI_3	3.18			0.44	0.03

[a]Benzoate designates ethyl 3,5-dinitrobenzoate.
[b]C^{14} activity in millimicrocuries per millimole of sample was assayed as CO_2 gas with a vibrating reed electrometer.
[c]Corrected for the activity of iodoform from the ethanol before irradiation.

It may be noted that the iodoform obtained from degradation of the commercial ethanol-1-C^{14} before irradiation showed a small amount of radioactivity (Table I). This was subtracted from the activity of iodoform derived from the irradiated ethanol before rearrangement to ethanol-2-C^{14} was calculated.

In some preliminary experiments with radiation dosages of up to 7 million rads, only about 0.1% rearrangement to ethanol-2-C^{14} was indicated. With higher radiation doses as tabulated in Table I, more significant amounts of rearrangement were observed. The activities of iodoform from these experiments were quite large, being some 20 to 30 times that of background depending on the size of sample counted. Moreover, all iodoform samples were shown to have practically constant specific activity on repeated recrystallization, indicating that the iodoform activity was not due to contamination. It is, therefore, reasonable to conclude that rearrangement of ethanol-1-C^{14} to ethanol-2-C^{14} actually occurred during the irradiation. The G_r value, designating the number of molecules of ethanol-1-C^{14} rearranged to ethanol-2-C^{14} per 100 electron volts of energy absorbed, was calculated to be about 0.04. The ratio of G_r to G_d was of the order of 0.02, indicating that rearrangement to ethanol-2-C^{14} occurred only to about 2% of the extent of total decomposition.

Two possible explanations for the observed formation of ethanol-2-C^{14} from ethanol-1-C^{14} may be suggested. Firstly, minute amounts of ethylene could be produced during irradiation which remained in solution and subsequently reacted with water to give ethanol-1-C^{14} and ethanol-2-C^{14}.

$$CH_3C^*H_2OH \xrightarrow{\quad\quad} CH_2 = C^*H_2 \xrightarrow{H_2O} CH_3C^*H_2OH + C^*H_3CH_2OH \qquad [1]$$
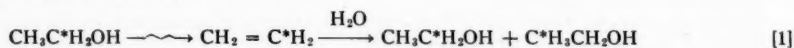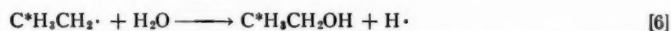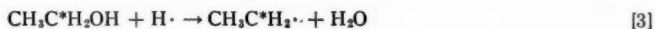
The presence of some ethylene after radiolysis of pure ethanol has been reported (3),

though no attempts have been made to detect or estimate ethylene in studies with aqueous ethanol (5, 6). The formation of some alcohol, assumed to be ethanol, upon gamma irradiation of mixtures of ethylene and oxygen in water under pressure has been reported by Henley and co-workers (11, 12). However, similar studies by Clay, Johnson, and Weiss (13) on the action of Co^{60} γ-radiation on aqueous solution of ethylene at different pressures did not report ethanol as a product. Considering this somewhat conflicting evidence from the literature, it is reasonable to conclude that upon irradiation of a dilute aqueous solution of ethanol, formation of ethylene followed by rehydration back to ethanol does not occur extensively. Nevertheless, it is possible that such a process may take place to a minor extent during irradiation. Reaction sequence [1] given above is, therefore, a plausible explanation for the formation of the small amount of ethanol-2-C^{14} from the irradiation of ethanol-1-C^{14}.

A second explanation for the observed isotope position rearrangement involves the postulation of a 1,2-hydrogen shift in an ethyl radical. The chemical effects of ionizing radiation in dilute aqueous solutions are generally considered to be due primarily to the action of H and OH radicals from the net process

$$H_2O \longrightarrow\!\!\sim\!\!\longrightarrow H\cdot + OH\cdot.$$ [2]

A mechanism for the rearrangement of ethanol-1-C^{14} to ethanol-2-C^{14} may then be postulated as follows:

$$CH_3C^*H_2OH + H\cdot \rightarrow CH_3C^*H_2\cdot + H_2O$$ [3]

$$CH_3C^*H_2OH + OH\cdot \rightarrow CH_3C^*H_2\cdot + H_2O_2$$ [4]

$$CH_3C^*H_2\cdot \xrightarrow[\text{shift}]{\text{1,2-H}} \cdot CH_2C^*H_3$$ [5]

$$C^*H_3CH_2\cdot + H_2O \longrightarrow C^*H_3CH_2OH + H\cdot$$ [6]

The G_r value for the rearrangement is low because the chief effects in the radiolysis of dilute aqueous ethanol result from the breaking of the α-carbon – hydrogen bond rather than the carbon–oxygen bond. Moreover, the H produced in reaction [6] does not necessarily have to propagate a chain leading to a high yield of ethanol-2-C^{14} because the H atoms can enter into other processes such as its reaction with ethanol to give the α-hydroxyethyl radical (6).

The 1,2-shift depicted in reaction [5] is not unreasonable as a number of reported isomerizations induced by irradiation have been explained in a similar way. The formation of isopropyl chloride from irradiation of n-propyl chloride (14) and of t-butyl chloride and bromide from isobutyl chloride and bromide, respectively (15, 16), were postulated to take place through rearrangement of the n-propyl to isopropyl and isobutyl to t-butyl radicals, processes which involve 1,2-hydrogen shifts.

In conclusion, the present work has shown that Co^{60} γ-irradiation of a 2.02% aqueous solution of ethanol-1-C^{14} led to the formation of some ethanol-2-C^{14}, the G value for this isotope position rearrangement being about 0.04. Two plausible explanations for the rearrangement have been suggested. From the present data, however, it is not possible to decide whether only one or both of the suggested mechanisms actually accounted for the observed formation of ethanol-2-C^{14} from ethanol-1-C^{14}.

REFERENCES

1. E. COLLINSON and A. J. SWALLOW.   Chem. Revs. 56, 471 (1956).
2. A. J. SWALLOW.   Biochem. J. 54, 253 (1953).
3. W. R. McDONELL and A. S. NEWTON.   J. Am. Chem. Soc. 76, 4651 (1954).
4. J. G. BURR.   J. Phys. Chem. 61, 1477 (1957).
5. G. G. JAYSON, G. SCHOLES, and J. WEISS.   J. Chem. Soc. 1358 (1957).
6. J. T. ALLAN, E. M. HAYON, and J. WEISS.   J. Chem. Soc. 3913 (1959).
7. J. D. ROBERTS and J. A. YANCEY.   J. Am. Chem. Soc. 74, 5943 (1952).
8. R. M. ROBERTS, G. A. ROPP, and O. K. NEVILLE.   J. Am. Chem. Soc. 77, 1764 (1955).
9. C. C. LEE, M. C. HAMBLIN, and N. JAMES.   Can. J. Chem. 36, 1597 (1958).
10. J. WEISS, A. O. ALLEN, and H. A. SCHWARZ.   Proc. Intern. Congr. Peaceful Uses Atomic Energy, 14, 179 (1956).
11. E. J. HENLEY and J. P. SCHWARTZ.   J. Am. Chem. Soc. 77, 3167 (1955).
12. E. J. HENLEY, W. P. SCHIFFRIES, and N. F. BARR.   A.I.Ch.E. Journal, 2, 211 (1956).
13. P. G. CLAY, G. R. A. JOHNSON, and J. WEISS.   J. Chem. Soc. 2175 (1958).
14. R. H. WILEY, C. H. JARBOE, J. R. HARRELL, and D. J. PARISH.   Proc. Chem. Soc. 347 (1957).
15. W. S. WILCOX.   Radiation Research, 10, 112 (1959).
16. E. B. DISMUKES and W. S. WILCOX.   Radiation Research, 11, 754 (1959).

ELECTRONIC STATES OF HYDRATED VANADIUM (II) ION[1]

RUTH M. BENNETT AND O. G. HOLMES

ABSTRACT

The optical absorption of a single crystal of $VSO_4.7H_2O$ was measured in the range 9000–35,000 cm^{-1}. The three observed bands were assigned to transitions between the four orbital levels resulting from cubic electrostatic perturbation of the spherical terms of configuration $3d^3$. Values of $Dq = 1200$ cm^{-1} and $E = 10,000$ cm^{-1} were derived from the spectral analysis.

INTRODUCTION

Ligand field theory has been applied with success to the hydrates and other complexes of ions of the first transition group metals. Several reviews of this work are available (1, 2, 3). The usual procedure is to consider the effect of the electrostatic potential generated by the ligands upon the electronic states of the central ion. Energy levels, magnetic and optical properties, etc. can then be evaluated for the perturbed ion. Some authors (4, 5, 6) have allowed for the possibility of covalent bonding by constructing appropriate molecular orbitals.

Inadequate optical data for hydrated V^{++} ion has led to some confusion about its electronic levels. We have therefore prepared $VSO_4.7H_2O$ crystals of sufficient size and purity for the accurate measurement of its optical absorption spectrum in the region 9000–35000 cm^{-1}. The observed bands have been assigned to transitions between levels derived from configuration $3d^3$ by a perturbing electrostatic field of cubic symmetry. Since both the "weak field" and "strong field" formalisms have become popular, we shall present both, even though they lead to identical results.

EXPERIMENTAL WORK

(a) Preparation of Hydrated Vanadium (II) Ion

The method of Jones and Colvin (7) was used for the preparation of $VSO_4.7H_2O$. Fisher reagent vanadium pentoxide was suspended in a sulphuric acid solution. Sulphur dioxide was bubbled through to reduce the vanadium to the plus four state (vanadyl). The filtered vanadium (IV) solution was reduced electrolytically at a mercury cathode to V^{++}. This solution was transferred to a flask under an atmosphere of nitrogen and ethyl alcohol poured over the surface. Over a period of several hours large well-formed violet crystals of $VSO_4.7H_2O$ deposited.

The total reducing power of the vanadium in the crystal was determined by titration to the plus five state with standard $KMnO_4$ (titer A). The vanadium concentration was found by reducing back to vanadium (IV) with sulphur dioxide and reoxidizing with $KMnO_4$ (titer B). The concentrations of V^{++} and V^{+++} were then calculated from titers A and B. The titration procedure was that suggested by Treadwell (8).

(b) Absorption Spectrum of Hydrated Vanadium (II) Ion

Figure 1 shows the optical absorption spectrum of a single crystal of $VSO_4.7H_2O$. These data were obtained with a Beckman DU spectrophotometer. Salient features of the spectrum are summarized in Table I.
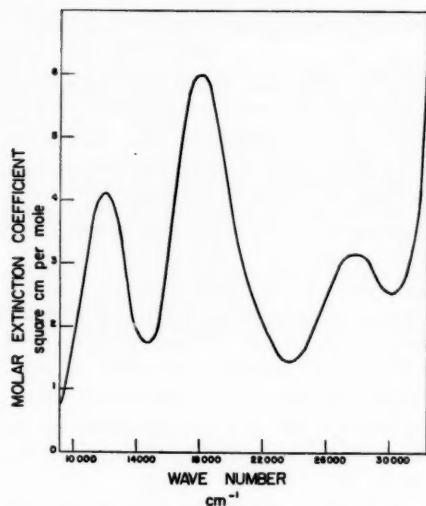
FIG. 1.   Absorption spectrum of $VSO_4.7H_2O$.

TABLE I

Electronic transitions of hydrated V^{++}

Band peak, cm^{-1}	Peak extinction coefficient	f-Number	Transition	Calculated energy levels	
				$E = 11,320$ cm^{-1}	$E = 10,000$ cm^{-1}
12000	4.1	0.5×10^{-4}	$^4A_2\text{-}^4T_2$	12000	12000
18200	6.0	0.9×10^{-4}	$^4A_2\text{-}^4T_1$	18400	18000
27800	3.1	0.3×10^{-4}	$^4A_2\text{-}^4T_1$	28900	28000

The principal difficulty in measuring this absorption spectrum lies in the inevitable presence of V^{+++} generated by the very powerful reducing agent V^{++}. Since hydrated V^{+++} exhibits absorption bands at 17,800 and 25,700 cm^{-1}, respectively, with maximum extinction coefficients of 3.5 and 6.6 cm^2 per mole, as reported by Hartman and Schlafer (9), it interferes seriously with the spectral measurements.

For the spectrum in Fig. 1, a crystal of $VSO_4.7H_2O$ was chosen in which $97 \pm 1\%$ of the vanadium was present as V^{++} with the V^{+++} concentration then being spectroscopically negligible.

ASSIGNMENT OF ABSORPTION BANDS

(a) Weak Field Treatment

Configuration $3d^3$ of V^{++} yields several terms which are separated by Coulombic electron interactions. However, only the ground state term ^4F and an upper ^4P term have the maximum spin multiplicity of four. If intercombination transitions are unimportant, all the other terms from $3d^3$ can be ignored.

In the heptahydrates of the transition ions for which the crystal structures are known, the central ion is surrounded by six water molecules at the corners of a regular octahedron,

with the seventh water molecule occupying a distant interstitial site. The electrostatic potential which perturbs the central ion has cubic symmetry and is of the form

[1] $$V = D(x^4 + y^4 + z^4 - \tfrac{3}{5}\bar{r}^4).$$

Such a field splits the ground term ^4F of V^{++} into three terms belonging to the cubic representations $^4A_2$, $^4T_2$, and $^4T_1$. The $^4A_2$ term is orbitally non-degenerate, the $^4T_2$ and $^4T_1$ terms threefold degenerate. The higher ^4P term is not split by V, but follows the representation $^4T_1$.

Thus a field with cubic symmetry produces four energy levels from the spin quartet terms. The three observed bands are then due to transitions between the $^4A_2$ ground level and the other three levels.

The matrix elements of V for the cubic orbitals are given in Table II, where D is the

TABLE II

Energy matrices for $3d^3$ in cubic field

	Weak field			
	$^4A_2$	$^4T_2$	$^4T_1(^4F)$	$^4T_1(^4P)$
$^4A_2$	$-12\,Dq$			
$^4T_2$		$-2\,Dq$		
$^4T_1(^4F)$			$6\,Dq$	$4\,Dq$
$^4T_1(^4P)$			$4\,Dq$	E

	Strong field			
	$^4A_2(t_2^3)$	$^4T_2(t_2^2e)$	$^4T_1(t_2^2e)$	$^4T_1(t_2e^2)$
$^4A_2(t_2^3)$	$-12\,Dq$			
$^4T_2(t_2^2e)$		$-2\,Dq$		
$^4T_1(t_2^2e)$			$-2\,Dq+12\,B$	$6\,B$
$^4T_1(t_2e^2)$			$6\,B$	$-8\,Dq+3\,B$

field parameter and $q = (2/105)\bar{r}^4$. Details of this treatment are given by Finkelstein and Van Vleck (10). The term separation matrix has been added to that for V, and appears as E, which is the $^4F - ^4P$ energy in the absence of the cubic field.

Table III shows the cubic energy level diagram which results from the solution of the

TABLE III

Energy levels of hydrated V^{++}

Weak field origin	Cubic field	Strong field origin
^4P and ^4F	$^4T_1$	$3dt_2\ 3de^2$
	$\left.\begin{array}{c}^4T_1\\^4T_2\end{array}\right\}$	$3dt_2^2\ 3de$
^4F	$^4A_2$	$3dt_2^3$

secular determinant. The $^4A_2$ level is located at $-12\,Dq$, with respect to the free ion ^4F energy, and the $^4T_2$ level at $-2\,Dq$. The first observed transition energy 12,000 cm^{-1} is then 10 Dq, fixing Dq at 1200 cm^{-1}. The two $^4T_1$ levels depend upon the value of E. Table I shows the calculated positions of these levels with $E = 11,320$ cm^{-1}, which is the free ion value, and with $E = 10,000$ cm^{-1}, which gives the least difference between calculated and observed $^4T_1$ levels.

(b) Strong Field Treatment

In a cubic field the five $3d$ orbitals convert into an orbital triplet t_2 and an orbital doublet e at energy higher by 10 Dq. The ground state of V^{++} then is the term of highest multiplicity from $3dt_2^3$, which is $^4A_2$. Configuration $3dt_2^23de$ gives rise to $^4T_2$ and $^4T_1$ cubic terms, while $3dt_23de^2$ yields a $^4T_1$ term. No other spin quartet terms are possible.

The observed absorption bands are then allotted to transitions between the ground state $^4A_2$ and the three higher levels, these transitions involving the promotion of one or two t_2 electrons to e orbitals.

Tanabe and Sugano (11) have given the matrix elements for V between the strong field states. These elements have been added to the Coulombic repulsion elements in Table II, where $B = F_2-5F_4$, the F_n being Slater–Condon integrals. The identity of the roots of the strong field and weak field secular equations is apparent since $^4F-{^4P} = E = 15B$.

DISCUSSION

The dearth of optical data on the complexes of V^{++} has resulted in differing interpretations of their electronic states. Owen (4) assumed that the absorption bands of aqueous V^{++} reported by Dreisch and Kallscheuer (12) at 12,200 and 18,200 cm^{-1} corresponded to the two $^4A_2-{^4T_1}$ transitions and that another band should lie in the infrared region. This led to values for the parameters $Dq = 760$ cm^{-1} and $E = 9000$ cm^{-1}.

On the other hand Jörgenson (2) used the band energies of 12,600, 18,200, and 26,500 cm^{-1} with the same assignment as presented here to calculate $Dq = 1260$ cm^{-1} (13).

On the basis of the spectrum of spectroscopically pure $VSO_4 \cdot 7H_2O$, the "best values" we propose are $Dq = 1200$ cm^{-1} and $E = 10,000$ cm^{-1}, which gives Racah's parameter $B = 670$ cm^{-1}.

The decrease in E upon hydrating an ion such as V^{++} has been attributed by Owen (4) to covalent bonding between the central ion and the ligands. This would require that a small contribution from ligand orbitals be added to the $3d$ orbitals of the central ion to give the appropriate molecular orbitals. Then the distance between electrons would be increased and Coulombic interaction decreased, thus reducing term separations. Our results indicate that this effect is not so great for V^{++} as estimated by Owen.

The f-numbers for the three bands are listed in Table I. The value for the transition at 27,800 is not very reliable because the band is a shoulder on the strong charge transfer absorption and its area must be estimated. The relative intensities of the transitions are roughly 0.5:0.9:0.3. The higher T_1 band would be expected to have the lowest intensity since it requires that two $3dt_2$ electrons be promoted while the other transitions require only one promotion.

Nickel (II) with configuration $3d^8$ in $NiSO_4 \cdot 7H_2O$ has the same energy level pattern as V^{++} and its three observed bands have f-numbers in order of increasing energy, 0.45×10^{-4}, 0.35×10^{-4}, and 0.6×10^{-4} (14). In this case contrary to expectations the higher transition $^3A_2-{^3T_1}$ has the greatest intensity. Several authors (see, for example, McClure (15)) have shown that this band includes transitions from the $^3A_2$ to $^1A_1$, $^1T_1$, and $^1T_2$ as well as $^3T_1$. However, Ballhausen and Liehr (16) have calculated recently that the intercombination transitions have negligible intensity for Ni^{++}, and that the intensity ratios can be explained with fair agreement by $d-p$ mixing introduced through vibrational–electronic interaction. Calculations are under way to see if a similar mechanism applies to V^{++}.

REFERENCES

1. W. Low. Ann. N. Y. Acad. Sci. **72**, 69 (1958).
2. C. K. Jörgenson. Report to the Tenth Solvay Council, Brussels. 1956.
3. P. George and D. S. McClure. Progress in inorganic chemistry. Vol. 1. Interscience Publishers, Inc., New York. 1959.
4. J. Owen. Proc. Roy. Soc. (London), A, **227**, 183 (1955).
5. J. S. Griffiths. J. Inorg. & Nuclear Chem. **2**, 1 (1956).
6. T. M. Dunn. J. Chem. Soc. 623 (1959).
7. G. Jones and J. H. Colvin. J. Am. Chem. Soc. **66**, 1563 (1944).
8. F. P. Treadwell. Analytical chemistry. Vol. 2. John Wiley & Sons, Inc., New York. 1935. p. 575.
9. H. Hartman and H. L. Schlafer. Z. Naturforsch. Pt. a, **6**, 760 (1951).
10. R. Finkelstein and J. H. Van Vleck. J. Chem. Phys. **8**, 790 (1940).
11. Y. Tanabe and S. Sugano. J. Phys. Soc. Japan, **9**, 753 (1954).
12. T. Dreisch and O. Kallscheuer. Z. physik. Chem. (Leipzig), B, **45**, 19 (1939).
13. L. E. Orgel. J. Chem. Phys. **23**, 1004 (1955).
14. O. G. Holmes and D. S. McClure. J. Chem. Phys. **26**, 1686 (1957).
15. D. S. McClure. J. Phys. and Chem. Solids, **3**, 311 (1957).
16. C. J. Ballhausen and A. D. Liehr. Mol. Phys. **2**, 123 (1959).

CELLULOSE COLUMN CHROMATOGRAPHIC SEPARATION
OF LIGNIN OXIDATION PRODUCTS[1]

J. M. PEPPER AND M. SIDDIQUEULLAH[2]

ABSTRACT

A brief review is presented of the chemical nature and the methods of separation of those lignin derivatives obtained by the oxidation and/or alkaline hydrolysis of woody plants and isolated lignin or lignosulphonates. Nine such closely related derivatives, vanillin, syringaldehyde, *p*-hydroxybenzaldehyde, acetovanillone, acetosyringone, *p*-hydroxyacetophenone, vanillic acid, syringic acid, and *p*-hydroxybenzoic acid, were selected for a detailed study of their separation by cellulose column chromatography. Methods are presented whereby, by either a one- or two-stage process, a mixture of from any two to all nine of these compounds may be separated and the components recovered, using solvent systems which are suitable for subsequent quantitative spectrophotometric analysis. The application to a study of lignin chemistry is discussed.

INTRODUCTION

In recent years considerable attention has been given to the chromatographic separation of the products of oxidation and/or alkaline hydrolysis of the lignin component of woody plants and cereal straws. From the earlier work the characterization of these various lignin derivatives has contributed substantially to the present knowledge regarding the aromatic nature of lignin. More recently this phase of lignin research has been stimulated by an increased study of the fate of various C^{14}-labelled compounds which have been introduced into growing plants in a study of the biosynthetic pathway leading to lignin. The only reliable method whereby proof is obtained that the C^{14} has been incorporated into the lignin has been to obtain, from this fraction, purified degradation products whose specific activity may be measured. The larger the isolated lignin fragment the greater the structural significance that may be given to it and the more valuable the information that may be obtained from the position of the C^{14}-labelling. To date one of the more fruitful of such degradation studies has been the oxidation of lignin and, in particular, that using alkaline nitrobenzene as the oxidant system (1). By such means substantial yields of vanillin and a mixture of vanillin and syringaldehyde have been obtained from gymnosperms and angiosperms respectively. Along with both these compounds much smaller yields of *p*-hydroxybenzaldehyde have been found in the oxidation products of monocotyledons. This technique has been used by several workers interested in lignin chemistry and from various lignified materials the following other derivatives have been isolated and characterized (2, 3, 4): vanillic acid, syringic acid, *p*-hydroxybenzoic acid, acetovanillone, acetosyringone, 5-carboxyvanillin, 5-carboxy-vanillic acid, 5-formylvanillin, 5-formylvanillic acid, dehydrodivanillin, and dehydro-divanillic acid.

In a series of investigations by both Pearl and McCarthy and their co-workers (5, 6, 7, 8, 9) using the alkaline cupric oxide, silver oxide, and mercuric oxide oxidations of lignosulphonates, many lignin degradation products have been obtained. These include

vanillin, syringaldehyde, vanillic acid, syringic acid, p-hydroxybenzoic acid, acetovanillone, acetosyringone, ferulic acid, p-coumaric acid, 5-carboxyvanillin, 5-carboxyvanillic acid, dehydrodivanillin, dehydrodivanillic acid, vanillil, 5-formylvanillin, 4,4'-dihydroxy-3,3'-dimethoxychalcone, vanillovanillone, and vanilloyl formic acid.
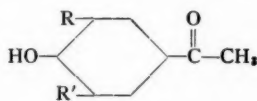
Apart from these lignin fragments that have been obtained from lignin under oxidizing conditions, many of the same compounds have been obtained by alkaline hydrolysis of the whole wood or of an isolated lignin. Hibbert (10, 11) early isolated vanillin and syringaldehyde by the alkaline hydrolysis of the lignin sulphonates from a deciduous wood. Smith (12) has reported the isolation of p-hydroxybenzoic acid from the products of a similar hydrolysis of the "native" lignin of *Populus tremula*. In another extensive investigation of the alkaline hydrolysis of various hardwoods and palms, Pearl and co-workers (13, 14, 15, 16, 17) isolated several phenolic compounds which may have arisen from the lignin fraction. The following such substances were identified: vanillin, syringaldehyde, p-hydroxybenzaldehyde, vanillic acid, syringic acid, p-hydroxybenzoic acid, ferulic acid, p-coumaric acid, acetovanillone, and acetosyringone. Stanek (18) using only an aqueous extraction, at 170°, of pre-extracted aspen wood obtained vanillin, syringaldehyde, coniferyl aldehyde, sinapaldehyde, vanillic acid, syringic acid, and p-hydroxybenzoic acid. Tanaka and Kondo (2) have reported the isolation also of both pyrogallol-1,3-dimethyl ether and 3,3'-dimethoxy-4,4'-dihydroxystilbene from the alkaline hydrolysis products of *Fagus cremata* and of the latter compound from red pine sawdust.

(I) R = H, R' = OCH₃	(IV) R = H, R' = OCH₃	(VII) R = H, R' = OCH₃
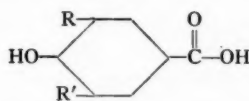
(I)   R = H, R' = OCH₃   (IV)   R = H, R' = OCH₃   (VII)   R = H, R' = OCH₃
(II)   R = R' = OCH₃   (V)   R = R' = OCH₃   (VIII)   R = R' = OCH₃
(III)   R = R' = H   (VI)   R = R' = H   (IX)   R = R' = H

Several methods have been devised for the separation of these compounds. Hibbert (19, 20, 21) reported separations of guaiacyl and syringyl compounds based upon the differential solubilities of their potassium and ammonium salts, upon fractional sublimation in high vacuum, and upon their conversion to the p-nitrobenzoate derivatives. The m-nitrophenylhydrazones of the phenolic aldehydes have been used also to assist in their separation (22). A qualitative paper chromatographic separation of vanillin and syringaldehyde was effected in 1949 by Bland (23). Later in 1951, a similar separation was reported by Pearl and Dickey (24) using a column of acid-washed Magnesol and Celite. Using benzene–ethanol (20:1) as the developer, Pearl and Beyer (25) were able to separate vanillic acid and protocatechuic acid on a similar type column. Stone and Blundell (26) further developed the paper chromatographic separation of the phenolic aldehydes into a quantitative analytical procedure. n-Butyl ether saturated with water separated vanillin and syringaldehyde but if p-hydroxybenzaldehyde were also present a suitable solvent system was petroleum ether (100–120°):n-butyl ether (6:1) saturated with water. These authors were the first to apply this method to the quantitative analyses of the products of the alkaline nitrobenzene oxidation of protolignin. In 1955, Brown and Neish (27) reported a partition chromatographic separation of these three aldehydes on a column of acid-washed Celite 535 using a two-step elution technique, i.e. isooctane

containing 10% benzene and saturated with water to elute vanillin and syringaldehyde, followed by benzene saturated with water for elution of the p-hydroxybenzaldehyde. To separate the various combinations of the alkaline hydrolyses products referred to earlier, the principal method has been paper chromatography with a variety of developers. The following solvent systems have been used: butanol saturated with 2% ammonia (13, 16, 17, 18), butanol:pyridine:water (10:3:3) (13, 16, 17), n-heptane:n-butyl ether: water (6:1:1) (15, 17), benzene saturated with formic acid (11), n-butyl ether saturated with water (18). Stanek (18) also used petroleum ether (65–110°):ethanol (50:1) as the developer for an acid-washed Magnesol column.

In 1953, Newcombe and Reid (28) reported the complete separation of vanillin, acetovanillone, verataldehyde, and acetoveratrone using chromatographic paper that had been sprayed with dilute sodium bisulphite and a solvent system consisting of hexane:chloroform:water (9:1:10). Later Pearl (7) employing a paper that had been sprayed only partially with sodium bisulphite, and developing with n-heptane:n-butyl ether:water (6:1:1) successfully separated vanillin, syringaldehyde, acetovanillone, and acetosyringone. Leopold (3) found that a phosphate-buffered paper (pH 7.5) was advantageous for the separation of acids.

Three other analytical procedures have been applied to the separation of lignin oxidation products. Cellulose column chromatography using butanol – 2% aqueous ammonia as the developer has been used by Pearl and Beyer (5, 29). McCarthy et al. effected a separation using anion exchange resins and also electrophoresis. Recently Kratzl and Puschmann (30) have applied the semimicro thin-layer chromatographic technique, developed by Stahl, to the separation of C^{14}-labelled oxidation products.

It was therefore clear that in an extensive study of the products of lignin oxidation, the large variety of such possible derivatives had to be considered and any quantitative procedure for their estimation must ensure no interference of one with another. Starting with the established method of Stone and Blundell (26) using the solvent system of petroleum ether (100–120°):n-butyl ether:water (6:1:1) (15 hours), the possible interference of vanillic, syringic, p-hydroxybenzoic acids on the separation of vanillin and syringaldehyde was investigated. The vanillin and p-hydroxybenzaldehyde, which moved the farthest, were well resolved but the syringaldehyde, which moved only slightly, was not separated distinctly from the acids which tended to tail from the base line. This may account, in part, for the usually poorer reproducibility of the syringaldehyde analysis by this method if applied to the oxidation of lignin materials. Subsequently, a study of the separation of the three aldehydes (I, II, III) and the three ketones (IV, V, VI) showed that using the same solvent system (16 hours) the aldehyde and its corresponding ketone had similar R_f values. It became clear that the quantitative analysis for vanillin, syringaldehyde, and p-hydroxybenzaldehyde by the Stone and Blundell method would be inaccurate should the conditions of oxidation be such that some of these other substances were also produced.

In an attempt to solve these interference problems and at the same time to devise a system whereby the products of large-scale oxidation may be separated, attention was directed to the use of cellulose column chromatography. Since usually not more than half of the original lignin can be accounted for in the form of the lower molecular weight oxidation products of the types outlined, it was hoped that this method would permit of the removal and separation of these units so that attention could then be directed to the purified lignin residues left on the column. The research reported here was limited to the study of the cellulose column chromatographic separation of the nine related possible

products of lignin oxidation: vanillin (I), syringaldehyde (II), p-hydroxybenzaldehyde (III), acetophenone (IV), acetosyringone (V), p-hydroxyacetophenone (VI), vanillic acid (VII), syringic acid (VIII), and p-hydroxybenzoic acid (IX). The study was conducted in three parts: (*a*) the resolution of a mixture of aldehydes alone, ketones alone, or acids alone; (*b*) the resolution of a mixture of any six components comprising the aldehydes and ketones, aldehydes and acids, or ketones and acids; and (*c*) the resolution of a mixture of all nine compounds. The synthetic mixtures were prepared from highly purified compounds using amounts ranging from 2 to 5 mg. The mixture of pure compounds was charged at the top of columns prepared from partially hydrated cellulose powder and the eluting solvents collected in 5-ml fractions. The presence of the phenolic substances was detected using the method of Barton *et al.* (31). In each case blanks using the individual pure compound were run to determine the order of elution.

Separation of Three-component Mixtures

Using the recommended (26) solvent system for the separation of aldehydes by paper chromatography (petroleum ether (100–120°):n-butyl ether:water (6:1:1) (organic phase)) good resolution was achieved on the cellulose column. A second developing system was found which resulted in an even more efficient separation using a shorter column. By this procedure the column was first eluted with cyclohexane saturated with water to remove and separate the vanillin (I) and syringaldehyde (II), and then with cylohexane: diethyl ether:water (6:1:1) (organic phase) (or an 8:1:1 mixture) to remove the p-hydroxybenzaldehyde (III). It is of interest to note the inversion in the order of elution of II and III using the two different solvents. The three ketones were separated in a similar manner. The elution and separation of the three acids was found to be best accomplished using a cyclohexane:diethyl ether:water (8:1:1) system to remove first the vanillic acid (VII) and then the p-hydroxybenzoic acid (IX). By increasing the solvent power using a similar system but in a 4:1:1 ratio, the syringic acid (VIII) was readily removed.

Separation of Six-component Mixtures

Since it was not possible to separate the aldehydes from the ketones by any of the solvent systems studied, recourse was made to the principle outlined by Newcombe and Reid (28) whereby the movement of aldehydes may be preferentially retarded using a sodium-bisulphite-sprayed paper. It was found that an effective separation may be obtained by using the technique whereby the six components were added to a cellulose column at the top of which was a small section containing cellulose saturated with sodium bisulphite. By first developing with the cyclohexane:water system the acetovanillone (IV) and the acetosyringone (V) were eluted and resolved in that order. The p-hydroxyacetophenone (VI) was then removed by changing to a cyclohexane:diethyl ether:water (8:1:1) system. Under these conditions it was proved, by a series of separate experiments, that no aldehydes were removed from the column nor were any ketones left on the column. To release, recover, and resolve the aldehydes, hydrochloric acid was added, the aldehydes washed through the column using diethyl ether, and then subsequently separated on a second column as described above.

In the case of the mixture of aldehydes and acids or ketones and acids the two-column technique was not necessary. Using the one cellulose column, and the following series of solvent changes, a complete separation and recovery of each compound of either six-component mixture was achieved. This was accomplished by using first the cyclohexane: water system to elute vanillin (I) (or acetovanillone IV), followed by syringaldehyde (II)

(or acetosyringone V), then the cyclohexane:diethyl ether:water (8:1:1) mixture to remove the p-hydroxybenzaldehyde (III) (or p-hydroxyacetophenone (VI)), the vanillic acid (VII), and the p-hydroxybenzoic acid (IX) in that order, and finally using cyclohexane:diethyl ether:water (4:1:1) to elute the syringic acid (VIII).

Separation of the Nine-component Mixture

To separate the components of a mixture of all nine components (I through IX), a two-stage procedure was required. A column of cellulose was used on the top of which was a smaller layer of cellulose saturated with sodium bisulphite. Elution of the ketones was done using cyclohexane–water to resolve the acetovanillone (IV) and acetosyringone (V) followed by cyclohexane:diethyl ether:water (8:1:1) to remove the p-hydroxyacetovanillone (VI). The three acids were then washed through the column with diethyl ether and the aldehydes first released by the addition of hydrochloric acid and then also washed through using ether. The recombined acids and aldehydes were charged to a second column and eluted and separated as described earlier.

This technique has been applied to the analysis of the products of the alkaline nitrobenzene oxidation, at 180°, of aspen wood lignin. Under these conditions no ketones were detected and hence this aspect of the interference objections raised earlier to Stone and Blundell's method is not valid. However, this does not mean that under either milder or stronger conditions of oxidation, the proportions of aldehydes, ketones, and acids may not vary and then this technique for their separation would become of value. This may be important for those studies requiring the isolation of purified C^{14}-labelled compounds especially of the C_6–C–C type. It is becoming evident that the other products of lignin oxidation, formed concurrently with the simple units discussed here, must be studied. It should be possible using this general technique to remove all the smaller molecular weight products from a cellulose column and thus leave behind the larger units which may subsequently be washed through and their structure investigated.

EXPERIMENTAL

Reagents

Genuine Whatman cellulose powder, standard grade, was obtained from W. and R. Balston, Ltd., England.

The syringaldehyde and acetosyringone were synthesized by previously reported methods (32, 33). All other chemicals were obtained from commercial sources and highly purified before use.

General Chromatographic Procedure

Preparation of Columns

The chromatographic columns were made of tubing 18 mm I.D. and 55 cm long, fitted at the lower end with a perforated disk immediately above a stopcock. The preferred method of packing the column was as follows. To each 10 g of cellulose powder was added 2.5 ml water and this mixture was intimately mixed until wetting was uniform and complete. This hydrated cellulose powder was then mulled using cyclohexane saturated with water (10 ml) and any lumps well broken before it was charged into the column using the wet method. Occasional pressing down of the cellulose during addition was beneficial. Each 10 g of cellulose packing was equivalent to about 3 inches in length.

The sodium bisulphite "traps" were prepared as follows. Each 2 g of cellulose powder was thoroughly mixed with a slurry of 1 g of sodium bisulphite in 1 ml of water. This mixture was then added onto the top of a cellulose column as described above for those

separations involving aldehydes and ketones. Such a "trap" was approximately 0.5 inch in length.

Charging of Synthetic Mixtures

The samples were added in concentrated ether solution to 1 g of cellulose powder which had been thoroughly mixed with 0.5 ml water. After the ether had evaporated, the powder was moistened with a few drops of cyclohexane saturated with water before packing onto the top of the column as described above.

Nature of Eluting Solvents

Solvent A = petroleum ether (100–120°):n-butyl ether:water (6:1:1) (organic phase).
Solvent B = cyclohexane saturated with water.
Solvent C = cyclohexane:diethyl ether:water (6:1:1) (organic phase).
Solvent D = solvent C (8:1:1).
Solvent E = solvent C (4:1:1).

Elution Technique

The eluting solvent was allowed to pass through the column while under a slight positive pressure of nitrogen so that the rate of elution varied from approximately 0.5 drop/second for the short columns to 1 drop/second for the longer columns. For those experiments which required changing of the solvent, the first solvent was allowed to flow until its upper level coincided with the top of the packing, before addition of the second solvent system. All eluates were collected in 5-ml fractions and the presence of each phenolic substance was determined using the ferric chloride – potassium ferricyanide spray reagent described by Barton et al. (31).

Chromatographic Separation of Three-component Mixtures

Aldehydes

To a 50-g column a mixture of vanillin (I) (4.48 mg), syringaldehyde (II) (5.48 mg), and p-hydroxybenzaldehyde (III) (4.65 mg) was added. Upon development using solvent A, I appeared in fractions 25–36, III in 45–67, and II in 75–107.

A second resolution of these aldehydes was made using a 20-g column and a mixture of I (4.5 mg), II (4.1 mg), and III (3.8 mg). By eluting first with solvent B, I appeared in fractions 13–23, II in 44–75, but even after a further 150 fractions III did not appear. After changing to solvent C, III was found in fractions 7–12.

Ketones

To a 10-g column a mixture of acetovanillone (IV) (5.6 mg), acetosyringone (V) (5.4 mg), and p-hydroxyacetophenone (VI) (5.0 mg) was added. Using solvent B, IV appeared in fractions 4–12 and V in fractions 21–39. Then solvent C was used whereupon VI appeared in fractions 2–5.

Acids

To a 25-g column a mixture of vanillic acid (VII) (1.1 mg), syringic acid (VIII) (5.1 mg), and p-hydroxybenzoic acid (IX) (2.9 mg) was added. Using solvent D, VII appeared in fractions 58–85 and IX in 90–130. After changing to solvent E, VIII appeared in fractions 21–76.

Chromatographic Separation of Six-component Mixtures

Aldehydes and Ketones

To a 10-g cellulose column on top of which was a 2-g cellulose – sodium bisulphite column, a mixture of vanillin (I) (4.65 mg), syringaldehyde (II) (4.10 mg), p-hydroxy-benzaldehyde (III) (4.18 mg), acetovanillone (IV) (4.34 mg), acetosyringone (V) (4.23

mg), and *p*-hydroxyacetophenone (VI) (4.48 mg) was added. Using solvent B, IV appeared in fractions 5–18 and V in 28–55. After changing to solvent D, VI appeared in fractions 5–11. Excess hydrochloric acid (2 ml conc. in 6 ml water) was then added to the top of the column and forced through by means of nitrogen pressure. The released aldehydes were washed through the column using diethyl ether, the ether solution dried over anhydrous $MgSO_4$ and then concentrated to 1 ml. This sample was then charged to a 10-g column. Using solvent B, I appeared in fractions 3–19, and II in 25–48. After changing to solvent D, III appeared in fractions 4–13.

Aldehydes and Acids

(See procedure below.)

Ketones and Acids

To a 25-g column a mixture of acetovanillone (IV) (4.97 mg), acetosyringone (V) (4.68 mg), *p*-hydroxyacetophenone (VI) (5.06 mg), vanillic acid (VII) (0.9 mg), syringic acid (VIII) (3.29 mg), and *p*-hydroxybenzoic acid (IX) (3.64 mg) was added. Using solvent B, IV appeared in fractions 22–35 and V in 68–110. By changing then to solvent D, VI appeared in fractions 15–23, VII in 70–102, and IX in 115–175. After changing again to solvent E, VIII appeared in fractions 18–76.

Chromatographic Separation of Aldehydes, Ketones, and Acids

To a 10-g column, on top of which was a 2-g cellulose – sodium bisulphite column, a mixture of vanillin (I) (5.00 mg), syringaldehyde (II) (4.89 mg), *p*-hydroxybenzaldehyde (III) (5.62 mg), acetovanillone (IV) (5.42 mg), acetosyringone (V) (5.55 mg), *p*-hydroxy-acetophenone (VI) (5.05 mg), vanillic acid (VII) (1.08 mg), syringic acid (VIII) (3.08 mg), and *p*-hydroxybenzoic acid (IX) (3.32 mg) was added. Using solvent B, IV appeared in fractions 6–20 and V in fractions 26–64. After changing to solvent D, VI appeared in fractions 6–12.

Diethyl ether (200 ml) was passed through the column to wash out the free acids. Excess hydrochloric acid (2 ml conc. HCl in 6 ml water) was added to the top of the column and passed through using slight nitrogen pressure. The released aldehydes were washed from the column using ether. The combined ether extracts were dried over anhydrous magnesium sulphate and concentrated to 1 ml. This sample was charged to a 25-g cellulose column. Using solvent B, I appeared in fractions 18–32 and II in fractions 58–90. After changing to solvent D, III appeared in fractions 14–22, VII in 73–112, and IX in 124–181. After changing again to solvent E, VIII appeared in fractions 23–73.

REFERENCES

1. F. E. BRAUNS. The chemistry of lignin. Academic Press Inc., New York. 1952. Chap. XIX.
2. J. TANAKA and T. KONDO. Mokuzai Gakkaishi, **3**, 28 (1957) (Chem. Abstr. **51**, 11711 (1957)); Mokuzai Gakkaishi, **4**, 34 (1958) (Chem. Abstr. **52**, 11410 (1958)); Mokuzai Gakkaishi, **5**, 105 (1959) (Chem. Abstr. **53**, 22919 (1959)); Parupukami Kogyo Zasshi, **11**, 29 (1957) (Chem. Abstr. **52**, 6784 (1958)).
3. B. LEOPOLD. Acta Chem. Scand. **6**, 38 (1952).
4. J. C. PEW. J. Am. Chem. Soc. **77**, 2831 (1955).

5. I. A. PEARL and D. L. BEYER.   J. Am. Chem. Soc. **76**, 6106 (1954).
6. I. A. PEARL and D. L. BEYER.   Tappi, **39**, 171 (1956).
7. I. A. PEARL and D. L. BEYER.   Tappi, **42**, 800 (1959).
8. D. W. GLENNIE, H. TECHLENBERG, E. T. REAVILLE, and J. L. McCARTHY.   J. Am. Chem. Soc. **77**, 2409 (1955).
9. R. E. DAVIS, E. T. REAVILLE, O. P. PENISTON, and J. L. McCARTHY.   J. Am. Chem. Soc. **77**, 2405 (1955).
10. F. LEGER and H. HIBBERT.   Can. J. Research, B, **16**, 151 (1938).
11. W. L. HASKINS, G. F WRIGHT, and H. HIBBERT.   J. Am. Chem. Soc. **59**, 2447 (1937).
12. D. C. C. SMITH.   J. Chem. Soc. 2347 (1955).
13. I. A. PEARL, D. L. BEYER, B. JOHNSON, and S. WILKINSON.   Tappi, **40**, 374 (1957).
14. I. A. PEARL.   Tappi, **41**, 621 (1958).
15. I. A. PEARL, D. L. BEYER, and B. JOHNSON.   Tappi, **41**, 255 (1958).
16. I. A. PEARL, D. L. BEYER, S. S. LEE, and D. LASKOWSKI.   Tappi, **42**, 61 (1959).
17. I. A. PEARL, D. L. BEYER, and D. LASKOWSKI.   Tappi, **42**, 779 (1959).
18. D. A. STANEK.   Tappi, **41**, 601 (1958).
19. M. J. HUNTER and H. HIBBERT.   J. Am. Chem. Soc. **61**, 2190 (1939).
20. J. J. PYLE, L. BRICKMAN, and H. HIBBERT.   J. Am. Chem. Soc. **61**, 2198 (1939).
21. R. H. J. CREIGHTON, J. L. McCARTHY, and H. HIBBERT.   J. Am. Chem. Soc. **63**, 3049 (1941).
22. K. KRATZL.   Mikrochim. Acta, 159 (1956).
23. D. E. BLAND.   Nature, **164**, 1093 (1949).
24. I. A. PEARL and E. E. DICKEY.   J. Am. Chem. Soc. **73**, 863 (1951).
25. I. A. PEARL and D. L. BEYER.   Anal. Chem. **24**, 1366 (1952).
26. J. E. STONE and M. J. BLUNDELL.   Anal. Chem. **23**, 771 (1951).
27. S. A. BROWN and A. C. NEISH.   Can. J. Biochem. and Physiol. **33**, 948 (1955).
28. A. G. NEWCOMBE and S. G. REID.   Nature, **172**, 455 (1953).
29. I. A. PEARL and D. L. BEYER.   J. Am. Chem. Soc. **76**, 2224 (1954).
30. VON K. KRATZL and G. PUSCHMANN.   Holzforschung, **14**, 1 (1960).
31. G. BARTON, R. S. EVANS, and J. A. F. GARDNER.   Nature, **170**, 249 (1952).
32. J. M. PEPPER and J. A. MACDONALD.   Can. J. Chem. **31**, 476 (1953).
33. L. W. CRAWFORD, E. O. EATON, and J. M. PEPPER.   Can. J. Chem. **34**, 1562 (1956).

PHOTOLYSIS OF AZOISOPROPANE[1]

R. H. RIEM[2] AND K. O. KUTSCHKE

ABSTRACT

The photolysis of azoisopropane has been reinvestigated in an attempt to obtain a better understanding of the discrepancies found between the behavior of *sec*-propyl radicals produced from this source (1) and other sources under similar experimental conditions.

Analytical difficulties encountered in an earlier investigation (1) were avoided through the extensive use of gas chromatography.

It was found necessary to include an internal conversion reaction among the primary processes to explain the observed phenomena. A rough estimate of $E_{internal\ conversion} - E_{dissociation} = (1.99 \pm 0.72)$ kcal/mole has been deduced. This is believed to be the first observation of $E_{internal\ conversion} > E_{dissociation}$. An explanation of this observation remains a matter of conjecture though a tentative suggestion is offered.

The data also leads to results in agreement with those found for other azo compounds and in agreement with the rates of reactions of *sec*-propyl radicals obtained from other sources under similar conditions.

INTRODUCTION

Recent studies of the rates of reactions of *sec*-propyl radicals (2, 3, 4) present a slightly different picture to that obtained by Durham and Steacie (1) in the photolysis of azoisopropane. To some extent these differences can be traced back to the analytical difficulties encountered by Durham and Steacie. Since many of these difficulties can now be avoided, a reinvestigation of the photolysis of azoisopropane, making extensive use of gas chromatography, was undertaken. A further reason for the reinvestigation was the rather poor agreement at lower temperatures between the mechanism proposed and the experimental data obtained by Durham and Steacie (1).

EXPERIMENTAL

The high-vacuum apparatus was in general of the design usually employed in these laboratories; however, stopcocks and oil diffusion pumps were used in order to obtain a mercury-free system. Part of the analytical line, consisting of a simple mercury-containing system used to handle noncondensable reaction products, was connected to the mercury-free system in the manner described by McElcheren, Wijnen, and Steacie (5).

The quartz reaction cell, 10 cm in length with a volume of 180 cc, was enclosed in a thermostatted hot box in which the temperature could be controlled to within $1/2°$ C. A medium pressure Hanovia S500 mercury arc was employed as the light source. This, in conjunction with the filter A described by Kasha (6), supplied incident radiation consisting of the 3662.9 Å and 3663.3 Å lines. The ultraviolet absorption spectrum of azoisopropane shows one large band extending from 2900 Å to 3900 Å with a flat maximum at 3540 Å. A 935 phototube positioned behind the reaction cell and outside the hot box was coupled to a sensitive galvanometer to measure the transmitted intensity. By using azomethane in the reaction cell as an actinometer and making the assumption that, with this compound, $\Phi_{N_2} = 1$ (7), it was possible to correlate directly the difference in galvanometer readings obtained with the empty cell and the filled cell with the number of quanta absorbed per cubic centimeter per second. The error introduced into the actinometer

measurements by any slight deviation from unity in the quantum yield of nitrogen for azomethane is felt to be no larger than the errors involved in the use of an external actinometer. Reproducibility in these measurements was found to be 3%.

A small cold finger attached to the reaction cell protruded slightly beyond the hot box; as this construction entailed a considerable amount of tubing outside the illuminated volume, the reactant was continuously circulated during a run by means of a small impeller. In an actual run the contents of the cell were condensed into the finger prior to opening the cell to the analytical line. By allowing the finger subsequently to warm very slowly, an effective separation of the noncondensables from the rest of the material, which shows a very strong tendency to occlusion, was obtained. In this manner it was found possible to obtain a quantitative separation in a reasonable time (1 hour). The analytical line consisted of two traps and a Ward–Le Roy still after which a two-way stopcock was placed to enable the products to be diverted either into the continuation of the mercury-free system to the introduction trap of a gas chromatography column, or into the small oil diffusion pump forming the first part of the bridge section (5) leading to the mercury system. The mercury system also consisted of a toepler pump, gas burette, and a mass spectrometer take-off.

The following fractions were removed and analyzed:

Noncondensables.—This contained only nitrogen, which was removed at $-198°$ C and measured in the gas burette.

Second fraction $-135°$ *C.*—This fraction consisted of C_3H_6 and C_3H_8. Analysis was done by mass spectrometry after the total pressure had been measured in the gas burette.

Liquid products.—All further material was introduced onto a 15-ft column (8) of 1/4-in. O.D. copper tubing packed with 30% bis-2,2-methoxyethoxyethylether (Eastman Kodak) on 30–60 mesh (Johns-Manville) Chromosorb (temperature, 40° C; flow, 64 ml H_2/minute). The reaction product 2,3-dimethylbutane emerged after 1/2 hour while the excess unreacted azoisopropane was retained for 2 hours. Though it was clearly not necessary to use such a long column for this separation, this length was necessary to obtain a separation between acetone and azoisopropane. This situation arose when purifying the starting material. The azoisopropane employed in this work was shown by gas chromatography to contain trace quantities of amines or hydrazines (mass spectrometric identification), 2,3-dimethylbutane, and approximately 5% acetone. As the separation of acetone from azoisopropane proved impossible by means of a Ward still distillation at $-85°$ C (1) all material used in these experiments was purified by gas chromatography on the column described previously. Azoisopropane purified in this manner showed only a single peak when passed through a 10-ft column, 5 mm internal diameter, containing 25% dinonylphthalate + 5% glycerol on fire brick (temperature, 29° C; flow, 45 ml H_2/minute).

Azoisopropane has been subjected to thermal decomposition at different pressures at 127° C. Within the range of time employed in the photolytic experiments there was no evidence of thermal decomposition of azoisopropane.

RESULTS AND DISCUSSION

The following mechanism is proposed to explain the results obtained in the photolysis of azoisopropane between 34.7° C and 127° C. In the mechanism AIP refers to the normal ground-state molecule of azoisopropane while AIP* refers to an electronically excited state.

$$AIP \xrightarrow{h\nu} AIP^* \qquad\qquad I_a$$

$$AIP^* \to N_2 + 2sec\text{-}C_3H_7 \qquad k_1 \qquad [1]$$

$$AIP^* + AIP \to 2AIP \qquad\qquad k_2 \qquad [2]$$ Primary processes

$$AIP^* \to AIP \qquad\qquad k_1 \qquad [6]$$

$$2sec\text{-}C_3H_7 \to C_3H_6 + C_3H_8 \qquad k_3 \qquad [3]$$

$$2sec\text{-}C_3H_7 \to C_6H_{14} \qquad\qquad k_4 \qquad [4]$$ Secondary processes

$$sec\text{-}C_3H_7 + C_3H_7NNC_3H_7 \to C_3H_8 + C_3H_6NNC_3H_7 \quad k_5 \quad [5]$$
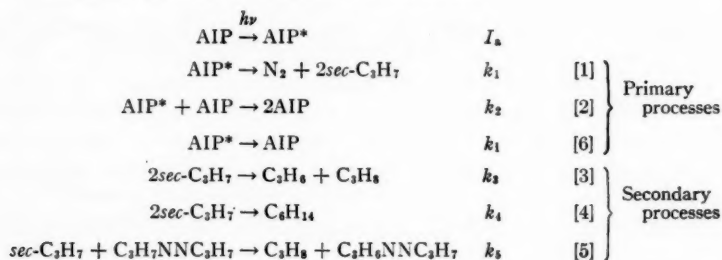
Primary Processes

Assuming a steady-state concentration of AIP^* (10) one arrives at the following expression for the reciprocal quantum yield of nitrogen:

$$[I] \qquad\qquad 1/\Phi_{N_2} = 1 + (k_2/k_1)[AIP] + k_1/k_1.$$

A plot of the reciprocal quantum yield of nitrogen against [AIP], at each temperature measured, should be linear with intercepts of $1 + (k_1/k_1)$. The experimental data from Table I (units employed are quanta, cubic centimeters, seconds, and molecules) plotted in this manner in Fig. 1 do in fact give five lines with intercepts significantly larger than unity. Moreover, the values of these intercepts increase in a continuous manner with increasing temperature, this in contrast to the decreasing intercepts found with azoethane
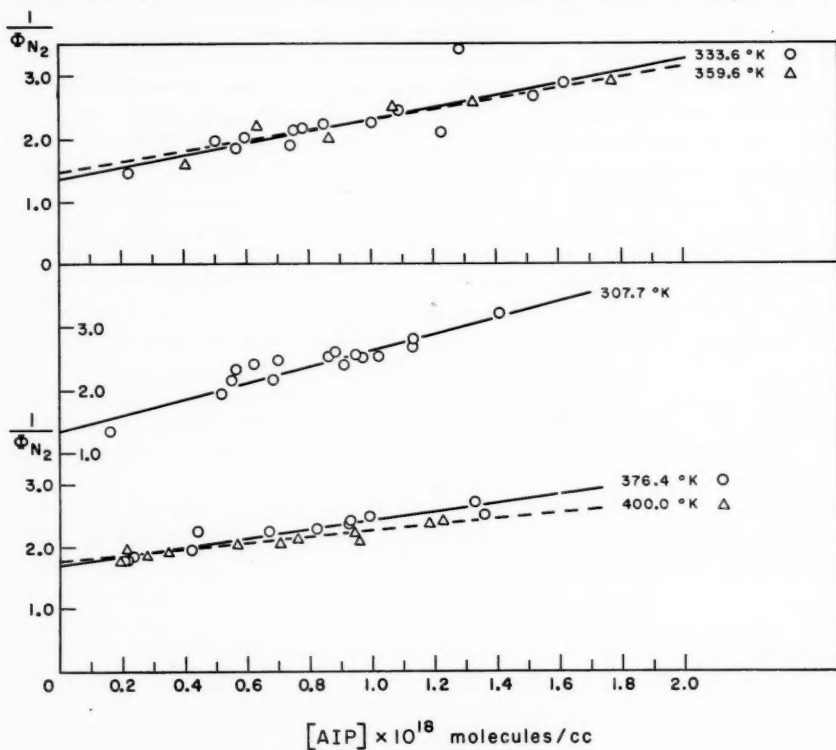
FIG. 1. Plots of expression [I].

TABLE I

[AIP] 10^{-18} molecules per cc per sec	I_a 10^{-12} quanta per cc per sec	Φ_{N_2}	$R_{C_6H_{14}}$ 10^{-12} molecules per cc per sec	$R_{C_3H_6}/R_{C_6H_{14}}$	$R_{C_3}/R_{C_6H_{14}}$
Temp. 307.7° K (hydrocarbons not determined)					
0.166	1.78	0.733			
0.521	6.75	0.508			
0.557	10.36	0.459			
0.566	11.65	0.427			
0.625	8.18	0.361			
0.687	8.66	0.328			
0.706	12.49	0.488			
0.866	15.80	0.394			
0.882	12.67	0.385			
0.913	15.85	0.416			
0.953	16.88	0.391			
0.976	16.27	0.392			
1.033	16.81	0.392			
1.132	15.20	0.371			
1.136	15.56	0.354			
1.411	20.09	0.312			
Temp. 333.6° K					
0.225	3.85	0.679	1.671	0.515	1.121
0.501	9.28	0.510	—	—	—
0.569	10.35	0.537	3.497	0.536	1.175
0.597	11.75	0.491	—	—	—
0.743	15.25	0.524	—	—	—
0.756	13.46	0.467	—	—	—
0.783	14.54	0.459	—	—	—
0.850	15.90	0.446	4.400	0.531	1.198
1.006	18.37	0.443	—	—	—
1.090	19.67	0.403	—	—	—
1.228	20.81	0.473	—	—	—
1.285	23.25	0.329	5.098	0.560	1.279
1.522	24.20	0.374	—	—	—
1.619	27.76	0.345	5.957	0.557	1.357
Temp. 359.6° K					
0.405	8.19	0.592	2.869	0.534	1.240
0.636	12.98	0.453	3.348	0.548	1.329
0.865	15.86	0.499	4.560	0.539	1.308
1.072	20.06	0.399	4.281	0.557	1.443
1.324	22.94	0.384	4.582	0.553	1.497
1.773	26.07	0.341	—	—	—
Temp. 376.4° K					
0.210	3.72	0.560	1.153	0.530	1.266
0.216	3.84	0.557	—	—	—
0.239	4.14	0.543	—	—	—
0.423	8.02	0.512	2.310	0.598	1.373
0.443	8.97	0.445	2.046	0.595	1.481
0.454	—	—	2.123	0.589	1.462
0.674	12.46	0.445	—	—	—
0.827	15.38	0.436	3.436	0.541	1.467
0.924	16.27	0.424	3.238	0.572	1.711
0.936	17.05	0.414	—	—	—
0.995	18.65	0.402	—	—	—
1.331	22.68	0.369	3.634	0.595	1.901
1.363	22.54	0.399	4.114	0.581	1.736
Temp. 400.0° K					
0.193	4.07	0.557	1.272	0.545	1.325
0.214	4.84	0.512	—	—	—
0.280	7.16	0.534	2.072	0.509	1.375
0.348	7.07	0.518	1.890	0.552	1.464
0.569	10.86	0.488	—	—	—
0.706	13.41	0.480	2.882	0.604	1.800
0.760	15.58	0.466	3.236	0.534	1.838
0.946	17.66	0.443	3.404	0.531	1.936
0.959	18.47	0.475	4.022	0.508	1.810
1.185	21.42	0.421	—	—	—
1.224	21.79	0.415	—	—	—

.(9). Values for k_2/k_1 were obtained from the slopes of the lines in Fig. 1, and are given in Table II. The related Arrhenius plot, Fig. 3, indicates that $E_1 - E_2 = (2.28 \pm 0.35)$ kcal/

TABLE II

T, °K	$(k_2/k_1)\ 10^{18}$	S.D.	Inter.	S.D.	(k_i/k_1)
307.2	1.28	0.13	1.35	0.11	0.35
333.6	0.93	0.14	1.38	0.14	0.38
359.6	0.86	0.15	1.46	0.17	0.46
376.4	0.707	0.075	1.715	0.061	0.715
400.0	0.500	0.050	1.753	0.031	0.753

mole and $A_2/A_1 = (3.2 \pm 1.9)\ 10^{-20}$ (molecule/cc)$^{-1}$.

The mechanism proposed above differs from that of Durham and Steacie (1) in the inclusion of reaction [6]. Neglecting this reaction leads to

[II] $$1/\Phi_{N_2} = 1 + (k_2/k_1)\ [AIP],$$

a relation which is not supported by the experimental data.

There is the possibility of a reduction in the quantum yield of nitrogen through an activated molecule of sufficient complexity, such as the AIP* molecule, whose large number of internal degrees of freedom would be able to contain the activating energy for a considerable time. Thus a certain portion of these activated molecules could reach the walls of the reaction vessel and there be deactivated. This process would entail including the following reaction in the mechanism:

$$AIP^* + wall \rightarrow AIP, \qquad k_w \qquad \qquad [7]$$

which in turn would lead to

[III] $$1/\Phi_{N_2} = 1 + (k_2/k_1)[AIP] + k_1/k_1 + k_w/k_1\ [AIP],$$

where [AIP] is included in the denominator of the last term to take into account the variation of diffusion with pressure. Including this reaction, therefore, would require non-linearity in Fig. 1, the deviation from linearity depending on the ratio k_w/k_1, but in any case being most pronounced at low [AIP]. It is just in this region that the measurements become less accurate due to the small amount of light absorption. However, from [III] it can be shown that

[IV] $$[AIP]/\Phi_{N_2} = k_2/k_1\ [AIP]^2 + (1 + k_1/k_1)[AIP] + k_w/k_1.$$

A plot of $[AIP]/\Phi_{N_2}$ against [AIP] should therefore be parabolic with an intercept equal to k_w/k_1. The experimental data has been treated statistically using the least squares method for a quadratic parabola (11). For example, the data at 400° K (Fig. 2) are best described by the following expression:

$$[AIP]/\Phi_{N_2} = (0.66 \pm 0.12)\ 10^{-18}[AIP]^2 + (1.549 \pm 0.058)[AIP] + (0.045 \pm 0.70)\ 10^{-18}.$$

The uncertainties given are the statistical probable errors (12). Both from this and from the calculation of correlation coefficients it is clear that the data are best represented when wall deactivation is excluded. Under the present experimental conditions of pressure range and surface-to-volume ratio, wall deactivation may, therefore, be neglected.

As the amounts by which the intercepts in Fig. 1 are in excess of unity equals k_1/k_1 it is possible to obtain $E_1 - E_1$ by the usual Arrhenius plot. Considering the standard deviation of these intercepts as given in Table II, it is obvious that this determination will not be highly accurate (Fig. 3). The best line calculated by weighing each point according
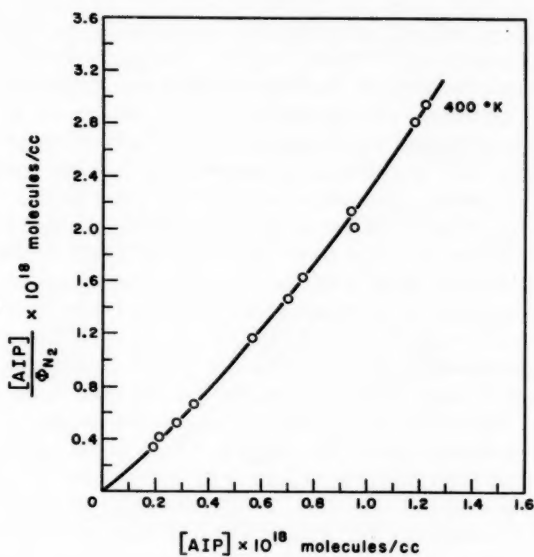
FIG. 2. Test for wall deactivation, expression [III].
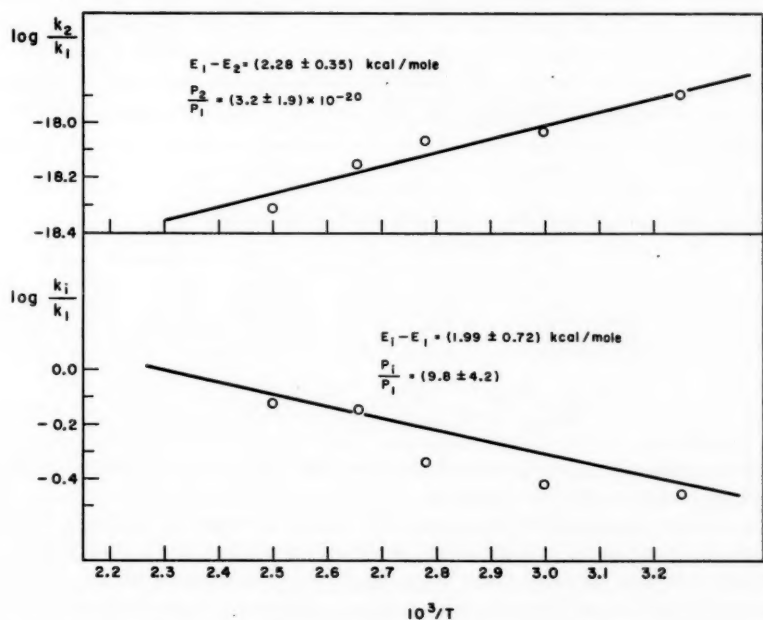
FIG. 3. Arrhenius plots of the ratio of rates of deactivation to decomposition and internal conversion to decomposition.

to its standard deviation (12) gives the values $E_1 - E_1 = (1.99 \pm 0.72)$ kcal/mole and $P_1/P_1 = (9.8 \pm 4.2)$. This is believed to be the first case reported in which $E_1 > E_{decomp}$.

In an attempt to specify further the physical nature of the internal conversion reaction, luminescence measurements were made. No luminescence was discernible with 3660 Å incident radiation when a sensitive photomultiplier (IP 21) instrument normally used in studying the fluorescence of ketones was employed. As a logical extension of the theory of Franck and Livingston (13) it might be suggested that internal conversion of the excitation energy in the case of azoisopropane occurs through isomerization to a cis ground state when starting from trans ground state molecules. Fischer (14) has shown that *trans*-azobenzene in toluene solution, when irradiated with 3650 Å light until equilibrium has been obtained, consists of 91% of the cis form. The activation energy of this isomerization in various solvents, as determined by Hartley (15) and by Halpern, Brady, and Winkler (16), lies in the range 28.8 to 24.7 kcal/mole. As in the cis–trans isomerization of azobenzene, considerable resonance stabilization is possible of the unpaired electrons in the activated complex, a situation which does not exist in the case of azoisopropane, the activation energy for the cis–trans isomerization of the latter compound will undoubtedly be even higher. Since the energy supplied in the form of radiation is equivalent to only 78 kcal the resultant cis form will not contain sufficient energy to decompose unless it absorbs another quantum. If this were the only route to decomposition the quantum yield of nitrogen would be 0.5. The fact that this is not the case, both higher and lower values being observed, justifies the inclusion of the other steps in the primary process.

The large radical created in reaction [5] through abstraction from the parent compound was also generated in darkness through the thermal decomposition of di-*tertiary*-butyl peroxide at 127° C (17) in the presence of azoisopropane. Though methane was formed in the required manner, no nitrogen could be detected. Thus a chain reaction is not anticipated in the photolysis and the quantum yields discussed in the section on primary processes are not subject to correction for the possible further decomposition of the azoalkyl radical.

Secondary Processes

The preceding mechanism also leads to the following relations:

[V] $$R_{C_3H_6}/R_{C_6H_{14}} = k_3/k_4,$$

[VI] $$\frac{R_{C_3H_8} + R_{C_3H_6}}{R_{C_6H_{14}}} = \frac{R_{C_3}}{R_{C_6H_{14}}} = \frac{2k_3}{k_4} + \frac{k_5}{k_4^{\frac{1}{2}}} \frac{[AIP]}{R^{\frac{1}{2}}_{C_6H_{14}}},$$

[VII] $$\frac{R_{C_3H_8} - R_{C_3H_6}}{R_{C_6H_{14}}} = \frac{\Delta R_{C_3}}{R_{C_6H_{14}}} = \frac{k_5}{k_4^{\frac{1}{2}}} \frac{[AIP]}{R^{\frac{1}{2}}_{C_6H_{14}}}.$$

The various quantities necessary to test these expressions have been calculated from the experimental data and are given in Table I.

The ratio of k_3/k_4, as calculated for each individual run, is given in Table I. These values are compared with the values obtained from expression [VI] using Fig. 4 and Table III. From Table I it is seen that $R_{C_3H_6}/R_{C_6H_{14}}$ has a slight tendency to increase with increasing [AIP]. This tendency is, however, not very pronounced and seems in fact to have disappeared at the highest temperature employed. Further though there would
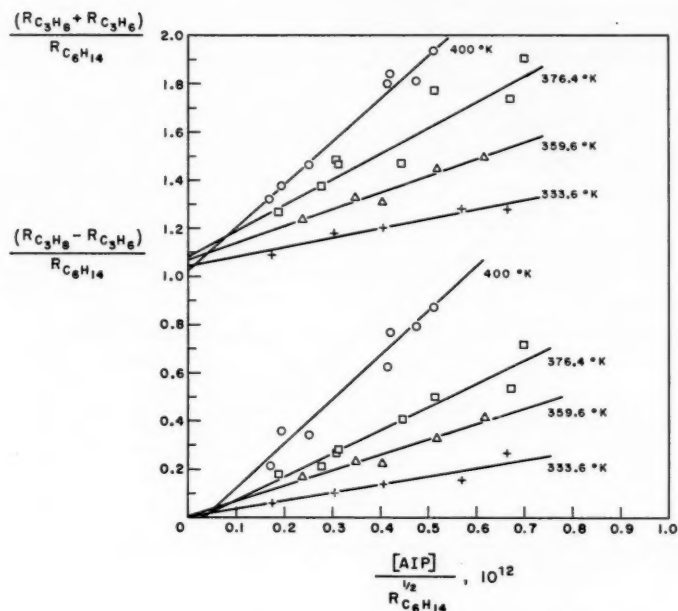
FIG. 4. Plots of the expressions [VI] and [VII].

TABLE III

Rate constants of secondary processes
(Units entering constants are molecules, cc, and sec)

T, °K	Equation [VII]				Equation [VI]				Average $\dfrac{R_{C_3H_6}}{R_{C_6H_{14}}}$	S.D.
	$(k_5/k_4^{\frac{1}{2}})\,10^{12}$	S.D. $\times$ 10^{12}	Inter.	S.D.	$(k_5/k_4^{\frac{1}{2}})\,10^{12}$	S.D. $\times$ 10^{12}	k_3/k_4	S.D.		
333.6	0.335	0.032	−0.0020	0.015	0.389	0.054	0.520	0.013	0.532	0.018
359.6	0.633	0.053	−0.0052	0.035	0.690	0.095	0.535	0.021	0.546	0.010
376.4	0.950	0.046	−0.0220	0.046	1.07	0.14	0.540	0.033	0.575	0.026
400.0	1.82	0.057	−0.069	0.057	1.78	0.12	0.511	0.022	0.540	0.033

at first seem to be an increase of $R_{C_3H_6}/R_{C_6H_{14}}$ with temperature, this is invalidated by the results at 127° C. Therefore within experimental error it is considered that k_3/k_4 is constant. Identical conclusions must be drawn from the results obtained using equation [VI]. It may be noted that constancy has also been found for this ratio of rates in the case of azoethane to 150° C (9) and in the case of diisopropyl ketone to 192° C (2). Since k_3/k_4 is independent of temperature, $E_3 - E_4 = 0$. The actual numerical value of k_3/k_4 agrees well with the data of Heller and Gordon (2) and Robb and Boddy (4). The value reported by Kerr and Trotman-Dickenson (3) for this ratio of rates is, however, slightly higher.
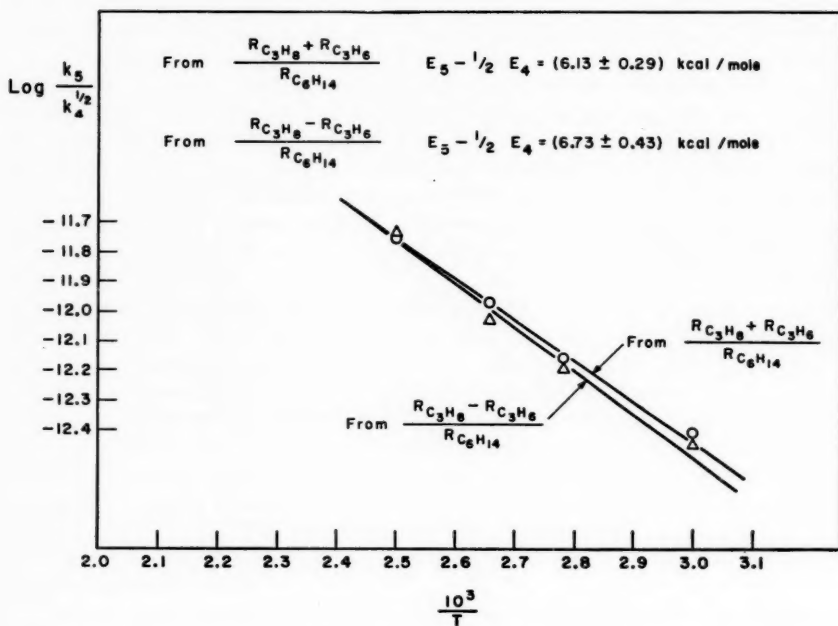
FIG. 5. Arrhenius plots relevant to the expressions [VI] and [VII]. $\bigcirc$ from expression [VI] and $\triangle$ from expression [VII].

The ratio $k_5/k_4^{\frac{1}{2}}$ has also been obtained from both [VI] and [VII] (Table III). The Arrhenius plot for both cases is given in Fig. 5 and leads to

$$E_5 - \tfrac{1}{2} E_4 = (6.12 \pm 0.29) \text{ kcal/mole},$$

$$P_5\sigma_5^2/P_4^{\frac{1}{2}}\sigma_4 = 0.369 \; 10^{-10}.$$

Assuming (10) that $\sigma_5 = 3$ Å and $\sigma_4 = 2.1$ Å leads to

$$P_5/P_4^{\frac{1}{2}} = 0.85 \; 10^{-3}$$

when equation [VI] is used. If equation [VII] is employed it is found that

$$E_5 - \tfrac{1}{2}E_4 = (6.73 \pm 0.43) \text{ kcal/mole},$$

$$P_5\sigma_5^2/P_4^{\frac{1}{2}}\sigma_4 = 0.774 \; 10^{-10} \rightarrow P_5/P_4^{\frac{1}{2}} = 1.8 \; 10^{-3}.$$

These results are in good agreement with those of Heller and Gordon (2).

The experimental data in Table I show a decrease in the mass balance, i.e. $\{\tfrac{1}{2}(C_3H_6 + C_3H_8) + C_6H_{14}\}/N_2$, with increasing temperature. As no new compounds are found in the first two fractions removed in the runs at higher temperature it must be concluded that these new compounds are of high molecular weight and constitute part of the "liquid products". No positive identification of these new products could be made by mass spectrometry though it was noted that $(sec\text{-}Pr)_2NN(sec\text{-}Pr)_2$ would, among other compounds, be consistent with the observed spectrum.

ACKNOWLEDGMENT

REFERENCES

1. R. W. DURHAM and E. W. R. STEACIE. Can. J. Chem. **31**, 377 (1953).
2. C. A. HELLER and A. S. GORDON. J. Phys. Chem. **60**, 1315 (1956).
3. J. A. KERR and A. F. TROTMAN-DICKENSON. Trans. Faraday Soc. **55**, 921 (1959).
4. P. J. BODDY and J. C. ROBB. Proc. Roy. Soc. (London), A, **249**, 547 (1959).
5. D. E. MCELCHEREN, M. H. J. WIJNEN, and E. W. R. STEACIE. Can. J. Chem. **36**, 321 (1958).
6. H. KASHA. J. Opt. Soc. Am. **38**, 929 (1948).
7. M. H. JONES and E. W. R. STEACIE. J. Chem. Phys. **21**, 1018 (1953).
8. C. R. YOKLEY and R. E. FERGUSON. Combustion and Flame, **2**, 117 (1958).
9. H. CERFONTAIN and K. O. KUTSCHKE. Can. J. Chem. **36**, 344 (1958).
10. J. L. WEINIGER and O. K. RICE. J. Am. Chem. Soc. **74**, 6216 (1952).
11. A. G. WORTHING and J. GEFFNER. Treatment of experimental data. John Wiley & Sons, Inc., New York. 1943.
12. D. BRUNT. The combination of observations. 2nd ed. Cambridge University Press. Cambridge, England. 1931.
13. J. FRANCK and R. LIVINGSTON. J. Chem. Phys. **9**, 184 (1941).
14. E. FISCHER. J. Chem. Phys. **23**, 1369 (1955).
15. G. S. HARTLEY. Nature, **140**, 281 (1937).
16. J. HALPERN, G. W. BRADY, and C. A. WINKLER. Can. J. Research, B, **28**, 140 (1950).
17. A. R. BLAKE and K. O. KUTSCHKE. Can. J. Chem. **37**, 1462 (1959).

THE OXIDATION OF MANGANATE BY PERIODATE[1]

M. W. Lister and Y. Yoshino

ABSTRACT

The reaction between periodate and manganate ions in alkaline solution has been examined, and at 35° C the rate is given by the equation, time being measured in minutes,

$$\text{rate} = 107[\text{MnO}_4^{--}]^2(1+167[\text{H}_3\text{IO}_6^{--}])(1+0.111[\text{OH}^-]^{-1}).$$

It is proposed that the main reaction mechanism is

$$2\text{MnO}_4^{--} \underset{k_2}{\overset{k_1}{\rightleftharpoons}} \text{MnO}_4^- + \text{MnO}_4^{-3}, \tag{i}$$

$$\text{MnO}_4^{-3} + \text{H}_3\text{IO}_6^{--} \overset{k_3}{\rightarrow} \text{MnO}_4^- + \text{IO}_3^- + 3\text{OH}^-. \tag{ii}$$
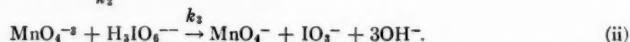
Hence $k_1 = 107$ (g-molecule/l.)$^{-1}$ min^{-1} at 35° C, and it was found that the activation energy is about 13.9 kcal/g-molecule. Data of Carrington and Symonds (2), combined with the value for k_1, make $k_2 = 2.8\times10^6$ (g-molecule/l.)$^{-1}$ min^{-1}. Added permanganate ions slow up the reaction; this is ascribed to the reverse of reaction (i) competing with reaction (ii). This gives a value for k_3 of 2×10^7 (g-molecule/l.)$^{-1}$ min^{-1}; this is so large a rate constant as to make it probable that the hypomanganate ions are hydrolyzed. The effect of hydroxide concentration on the rate is ascribed to partial hydrolysis of manganate ions. The observed results would require the ionization constant of HMnO$_4^-$ to be 7×10^{-11}.

In a recent paper (1) the present writers prepared several complex manganese periodates, such as Na$_7$H$_4$Mn(IO$_6$)$_3$.17H$_2$O, containing tetravalent manganese. These were shown to decompose in solution to give manganate ions as the first product, and finally permanganate ions. The mechanism of the decomposition of the complex salt was investigated, and shown to go through a partial breaking up of the complex to simpler ions. The present paper reports an examination of the second stage of this reaction, that is, the oxidation of manganate to permanganate. Apart from its connection with the behavior of manganato-periodates, this reaction is of interest because it involves a change of two in the oxidation state of the iodine, and of one in the oxidation state of the manganese. Thus we might expect either a termolecular reaction, or a mechanism which avoided this. In the latter case, the reaction would have to go through an intermediate containing either iodine or manganese in a usual valency. As it turned out, the main route seemed to be through hypomanganate ions, containing the relatively rare pentavalent manganese. There is also evidence for a termolecular reaction.

The over-all reaction is

$$2\text{MnO}_4^{--} + \text{H}_3\text{IO}_6^{--} \rightarrow 2\text{MnO}_4^- + \text{IO}_3^- + 3\text{OH}^-.$$
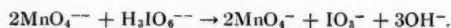
EXPERIMENTAL METHOD

The reaction was followed by mixing known amounts of stock solutions of sodium manganate, sodium periodate, and sodium hydroxide, previously brought to the required temperature. The mixture was kept in a thermostat, and the extent of reaction was found by measuring the optical density of a sample.

The sodium manganate was prepared by boiling sodium permanganate in concentrated sodium hydroxide solution, as described by Carrington and Symonds (2). Sodium periodate was prepared by oxidation of a weakly alkaline sodium iodate solution by means of sodium hypochlorite at about 80° C; the fairly insoluble sodium periodate,

$Na_3H_2IO_6$, crystallized out, and was filtered off and thoroughly washed with distilled water.

The initial concentration of manganate in the runs was between 1.6×10^{-4} M and 6×10^{-4} M, and the initial concentration of periodate between 3×10^{-4} M and 13×10^{-4} M. Sodium hydroxide was present in sufficient excess for its concentration not to change appreciably during the runs; many runs were in 0.1 M sodium hydroxide.

The optical density was measured on a Beckmann DU spectrophotometer, with a 1-cm cell. The wavelength used was 610 mμ, which is at the absorption maximum for manganate ions. Measurements on several solutions gave a value of 1530 for the extinction coefficient of sodium manganate, and 207 for sodium permanganate (2, 3). The concentrations of the solutions were calculated assuming that only these two ions contributed to the optical density, and that all the manganese was present as one or other ion. This was supported by the fact that the solutions showed no signs of any precipitate of manganese dioxide. It was checked that the total oxidizing power of the solutions, as measured by the amount of iodine liberated by adding potassium iodide and sulphuric acid, did not change during the reaction; and finally it was checked that iodate caused no oxidation of manganate. Thus there is no evidence of any side reactions.

RESULTS

It was found that for all runs a plot of the inverse of the manganate concentration against time was linear, as in a second-order reaction. Accordingly the results are shown in the figures as graphs of this sort. The initial concentrations and temperatures are given in Table I. The ionic strengths of the solutions were close to 0.1, except for the

TABLE I

Initial concentrations

Run	Temp., °C	$[MnO_4^{--}] \times 10^{-4}$ M	$[H_3IO_6^{--}] \times 10^{-4}$ M	$[OH^-]$, M	$d[MnO_4^{--}]^{-1}/dt$, (g-molecule/l.)$^{-1}$ min^{-1}
2	35	2.83	7.85	0.099	277
3	35	1.69	7.85	0.100	280
4	35	3.38	12.56	0.0985	290
5	35	3.38	3.14	0.0965	254
6	35	3.38	7.85	0.100	271
7	35	3.38	7.85	0.100	284
8	40	3.38	7.85	0.100	383
9	45	3.38	7.85	0.100	520
10	25	3.38	7.85	0.100	118
11	35	3.38	12.56	0.100	294
12	35	3.38	3.14	0.100	254
13	35	3.38	3.14	0.022	729
14	35	3.38	3.14	0.049	394
15	35	3.38	0	0.049	9
16	35	3.38	3.14	0.0091	1485
17	35	3.38	0	0.050	7
18	35	3.45	7.85	0.050	465
19	25	3.45	7.85	0.050	209
20	45	3.45	7.85	0.050	1010
21	45	3.45	7.85	0.100	535
22	25	3.45	7.85	0.100	125
23	25	3.34	7.85	0.200	113
24	35	3.34	7.85	0.200	224
25	45	3.34	7.85	0.200	435
26*	35	3.34	7.85	0.100	222
27*	35	3.34	7.85	0.100	137

*Potassium permanganate was added to these solutions. In run 26 $[KMnO_4] = 10.8 \times 10^{-4}$ M, in run 27 $[KMnO_4] = 54.0 \times 10^{-4}$ M initially.
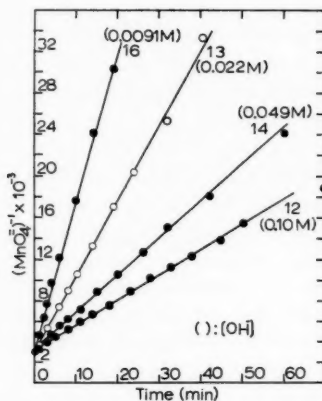
FIG. 1. Effect of hydroxide concentration on rate.
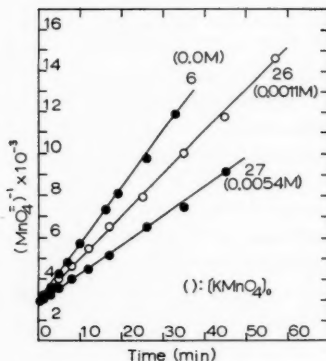
FIG. 2. Effect of permanganate
concentration on rate.
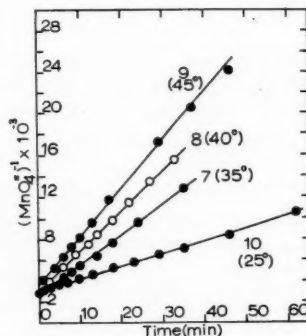
FIG. 3. Effect of temperature on rate.

three runs in 0.2 M sodium hydroxide, where the ionic strength was slightly above 0.2.

There are two comments to make on these graphs. Firstly the points at the time of mixing were calculated from the volumes of stock solution put in, the stock solution being standardized by adding potassium iodide and acid, and titrating with thiosulphate. These are plotted at $t = 0$, and the next point, usually at $t = 1$ minute, represents the first measurement of optical density. These first two points were always in reasonable agreement. The second comment is that the final points fall off somewhat from a second-order plot, though by this time the manganate concentration was usually less than 25% of its initial value. The best straight lines were drawn through the experimental points obtained before this falling off became apparent, and the slopes of these lines are given in the last column of Table I, headed "$d[MnO_4{}^{--}]^{-1}/dt$". Time is measured in minutes.

DISCUSSION OF RESULTS

Attention may first be drawn to runs 15 and 17 in which no periodate was present. These runs show that the disproportionation of manganate is much slower than the

oxidation by periodate. In these runs a precipitate of manganese dioxide appeared, while in no run with periodate present was any precipitate observed. Although the rate of disproportionation is about 5% of the rate in the slowest runs with periodate, no correction was made for this in the calculations, because the absence of any sign of manganese dioxide made it doubtful if the disproportionation to manganese dioxide and permanganate was in fact occurring. The reason for this will appear later when the mechanism of the reaction with periodate is discussed.

Turning now to the main series of runs, the first point, of course, is that the rate is proportional to $[MnO_4{}^{--}]^2$. Secondly, when rates at different periodate concentrations are compared, it is seen that this has only a moderate effect on the rate. In runs at 35° C and 0.1 M sodium hydroxide, the average values of $d[MnO_4{}^{--}]^{-1}/dt$ at various periodate concentrations were:

$$\begin{cases} [H_3IO_6{}^{--}] & 12.56 \quad 7.85 \quad 3.14 \times 10^{-4}\ M \\ d[MnO_4{}^{--}]^{-1}/dt & 292 \quad\ \ 278 \quad\ 254 \end{cases}$$

Over this range, the results approximately follow the equation

$$\text{rate} = [MnO_4{}^{--}]^2(241 + 4.0 \times 10^4 [H_3IO_6{}^{--}]).$$

Although the term in periodate looks large, its contribution was fairly small.

The effect of hydroxide concentration can be seen from the runs at 35° C and $7.85 \times 10^{-4}\ M$ periodate, and an ionic strength of 0.1.

$$\begin{cases} [OH^-] & 0.100 \quad 0.049 \quad 0.022 \quad 0.0091\ M \\ d[MnO_4{}^{--}]^{-1}/dt & 254 \quad\ \ 394 \quad\ \ 729 \quad\ \ 1485 \end{cases}$$

If $[OH^-]^{-1}$ is plotted against $d[MnO_4{}^{--}]^{-1}/dt$, the first three results fall on a straight line, and the fourth is near the line, but a little low. The straight line has the equation

$$d[MnO_4{}^{--}]^{-1}/dt = 121 + 13.4[OH^-]^{-1}.$$

Combining these two equations, the total equation is

(A) $$\text{rate} = 107[MnO_4{}^{--}]^2(1 + 167[H_3IO_6{}^{--}])(1 + 0.111[OH^-]^{-1}).$$

This is for 35° C. It is evident that this could be written in terms of hydrogen ions,

$$\text{rate} = 107[MnO_4{}^{--}]^2(1 + 167[H_3IO_6{}^{--}])(1 + 4.83 \times 10^{12}[H^+]).$$

The mechanism which could give this equation must involve more than one reaction. However, at high hydroxide concentrations, the main part of the reaction is simply a second-order reaction in manganate ions. The most obvious suggestion is that the reaction goes through hypomanganate ions:

$$2MnO_4{}^{--} \underset{k_2}{\overset{k_1}{\rightleftharpoons}} MnO_4{}^- + MnO_4{}^{---}, \tag{i}$$

$$MnO_4{}^{---} + H_3IO_6{}^{--} \overset{k_3}{\to} MnO_4{}^- + IO_3{}^- + 3OH^-. \tag{ii}$$
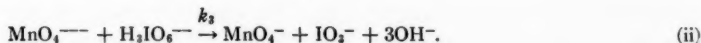
The scheme has the advantage that each stage is a simple bimolecular reaction. For the reaction to depend on the manganate concentration alone, it would be necessary for reaction (ii) to go much faster than the reverse of (i), so that all hypomanganate is oxidized to permanganate. Otherwise the permanganate formed during the run would cause a continuous extra decrease in the rate, which is not found until the reaction is

nearly over. If this is the correct mechanism, then k_1, the rate constant of reaction (i) going to the right, is 107 (g-molecule/l.)$^{-1}$ min^{-1} at 35° C, from equation (A) above.

Carrington and Symonds (2) calculate that ΔF^0 for reaction (i) is 6.2 kcal at 25° C. This makes the equilibrium constant of reaction (i) 2.85×10^{-5} at 25° C. ΔH^0 is 5.5 kcal, so the equilibrium constant is 3.85×10^{-5} at 35° C. Hence k_2, the rate constant of reaction (i) going to the left, is 2.8×10^6 (g-molecule/l.)$^{-1}$ min^{-1} at 35° C.

The dependence on [OH$^-$] or [H$^+$] probably means that the sodium manganate is partially hydrolyzed. One might expect this to give $Mn_2O_7{}^{--}$ ions, by analogy with the behavior of chromate, but this would require a dependence on the square of [H$^+$]; the first power of [H$^+$] in the equation shows that the hydrolyzed species is HMnO$_4{}^-$, which then must react thus:

$$HMnO_4{}^- + MnO_4{}^{--} \overset{k_4}{\rightleftharpoons} MnO_4{}^- + HMnO_4{}^{--}. \tag{iii}$$

On this hypothesis, if k_a is the ionization constant of HMnO$_4{}^-$ (to give H$^+$ and MnO$_4{}^{--}$), and k_4 is the rate constant of reaction (iii) going to the right, then it is easily found that the contribution of reaction (iii) to the rate is

$$k_4[MnO_4{}^{--}]^2 \left\{ \frac{[H^+]k_a}{(k_a + [H^+])^2} \right\}$$

where [MnO$_4{}^{--}$] here means the total manganate present. The contribution of reaction (i) becomes

$$k_1[MnO_4{}^{--}]^2 \left\{ \frac{k_a{}^2}{(k_a + [H^+])^2} \right\};$$

so that the total equation is

$$\text{rate} = [MnO_4{}^{--}]^2 \left\{ \frac{k_1 + k_4[H^+]/k_a}{(1 + [H^+]/k_a)^2} \right\}.$$

Evidently if [H$^+$] is low, and k_4 not too small, this will give an equation for the rate of the type actually found: by comparison, $k_4/k_1 \cdot k_a = 4.83 \times 10^{12}$. The slight decrease of the rate in 0.0091 M sodium hydroxide below what is calculated is presumably due to the term $(1 + [H^+]/k_a)^2$; this explanation would require k_a to be 7×10^{-11}. This is perhaps a somewhat small value for k_a; for instance, the bichromate ion, HCrO$_4{}^-$, has an ionization constant of 3.2×10^{-7} (4). This value of k_a gives 340 for the ratio k_4/k_1, so that k_4 is 3.6×10^4 (g-molecule/l.)$^{-1}$ min^{-1} at 35° C. This ratio is not unreasonable as MnO$_4{}^{--}$ and HMnO$_4{}^-$ will repel each other less than two MnO$_4{}^{--}$ ions.

The graphs of [MnO$_4{}^{--}$]$^{-1}$ against time cease to be linear towards the end of the reaction. It can be calculated that this is not due to the decrease in periodate concentration, which would cause only a very small decrease in the rate. Another possible explanation is that reaction (ii) is reversible, and that the equilibrium lies far from complete conversion to permanganate. Latimer (4) gives -0.564 volt for the standard potential of the half reaction: $MnO_4{}^{--} \rightarrow MnO_4{}^- + e^-$, and a rather doubtful -0.7 volt for $IO_3{}^- + 3OH^- \rightarrow H_3IO_6{}^{--} + 2e^-$. If this value of -0.7 volt is right, then the equilibrium lies at almost complete conversion to permanganate. A check on this was made by mixing potassium permanganate with a relatively large concentration of sodium iodate (and sodium hydroxide) and examining the spectrum of the mixture to see whether any manganate ions were formed. A small concentration of manganate ions did appear,

and a rough measurement showed that the equilibrium constant of reaction (ii) is at least 25 or larger (this is with the permanganate on top). Hence in concentrations of sodium hydroxide below 0.1 M, the equilibrium mixture will be almost entirely permanganate. It was calculated that, in a typical run such as run 6, at equilibrium 0.4% or less of the manganese would be present as manganate.

A more plausible explanation is that as the permanganate increases in concentration and periodate decreases, the reverse of reaction (i) starts to compete with reaction (ii). This suggestion was tested in runs 26 and 27, when appreciable amounts of permanganate were added initially, and it was found that the permanganate reduced the rate of reaction. If ordinary kinetic considerations are applied to these reactions, it is found that the concentration should follow the equation

$$\text{(B)} \qquad k_1 t - (\theta - \theta_0) = a\left[\frac{(2+2y_0\theta_0)(\theta-\theta_0)}{2b-1} - \frac{2\theta_0(2b+y_0\theta_0)}{(2b-1)^2} \ln \frac{\theta(2b-1)+\theta_0}{2b\theta_0} \right]$$

where $\theta = [\text{MnO}_4^{--}]^{-1}$, initially θ_0,
$a = k_2/k_3$,
b = initial value of the ratio $[\text{H}_3\text{IO}_6^{--}]/[\text{MnO}_4^{--}]$,
y_0 = initial $[\text{MnO}_4^{-}]$.

In the earlier runs, $y_0 = 0$. If k_2 is zero, this equation reduces to the usual second-order equation; and it is found that for moderate values of a, a plot of θ against t only deviates to any great extent from a straight line when the reaction is nearly over. This is in agreement with experiment, as the experimental points followed a second-order equation for a considerable time. The above equation gives

$$\left(\frac{d\theta}{dt}\right)_0 = \frac{k_1}{1 + ay_0/[\text{H}_3\text{IO}_6^{--}]_0}$$

where $(d\theta/dt)_0$ is the initial value of $d\theta/dt$, and $[\text{H}_3\text{IO}_6^{--}]_0$ is the initial periodate concentration. Hence with no added permanganate, $(d\theta/dt)_0 = k_1$, as was assumed above. The value of a can be found (i) from the initial slopes, $(d\theta/dt)_0$, in runs 26 or 27, or (ii) by applying the full equation to the later points in runs with no added permanganate. The first method is obviously more accurate, but the values of a found by the second are in rough agreement.

For run 26, the initial $d\theta/dt$ is about 222, for conditions where $d\theta/dt$ without added permanganate is 278. The ratio $[\text{MnO}_4^{-}]/[\text{H}_3\text{IO}_6^{--}]$ is initially 1.38. This makes $a = 0.18$. In run 27, the initial $d\theta/dt$ is 137, with $[\text{MnO}_4^{-}]/[\text{H}_3\text{IO}_6^{--}]$ initially 6.88. This makes $a = 0.15$. Applying the second method above to the earlier runs gives slightly smaller values of a, mostly between 0.1 and 0.15. Hence the value of k_2/k_3 at 35° C is evidently about 0.15. From the value of k_2 obtained above, it follows that k_3 is about 2×10^7 (g-molecule/l.)$^{-1}$ min^{-1} at 35° C. This is a relatively large rate constant, and is surprisingly large if the reaction is one between MnO_4^{--} and $\text{H}_3\text{IO}_6^{--}$, because of the electrostatic repulsion of the ions. There seems to be no doubt that the periodate is mainly $\text{H}_3\text{IO}_6^{--}$ in these solutions, as Crouthamel, Hayes, and Martin (5) find pk_2 to be 8.36 and $pk_3 = 15$, for periodic acid. Hence at the concentrations of sodium hydroxide used in these experiments the periodate must be predominantly $\text{H}_3\text{IO}_6^{--}$. This is in agreement with the phase diagram for sodium hydroxide, periodic acid, and water, as determined by Hill (6). However, although the periodate ion is $\text{H}_3\text{IO}_6^{--}$, it is possible that the hypomanganate is hydrolyzed to ions of lower charge, HMnO_4^{--} or $\text{H}_2\text{MnO}_4^{-}$.

There are no values for the ionization constants of hypomanganic acid, and the most that can be said is that the present results provide some evidence for partial hydrolysis of hypomanganate ions in $0.1\ M$ sodium hydroxide. The reaction might consist of hydrogen atom transfer from $H_2MnO_4^-$ to $H_3IO_6^{--}$.

The experimental rate equation (A) above contained a term in $[H_3IO_6^{--}]$, which suggests that part of the reaction is termolecular. However, it is necessary to be sure that this is not an indirect result of the varying success of the competition between the k_2 and k_3 reactions. Obviously a high periodate concentration will favor reaction (ii), with rate constant k_3. This will not affect the initial slope for $[MnO_4^{--}]^{-1}$ plotted against t, but as in practice the slope has to be obtained over a number of points, the periodate concentration may alter the slope in effect; in equation (B) this would be due to different values of b. It is found that if equation (B) is plotted, it gives very nearly a straight line for a considerable distance, after which the values of θ fall below the straight line. Over the range of θ used in the experiments (about 3,000 to 15,000) the curvature is slight, but the mean slope is altered by the value of b. If the slope is taken as unity for $b = 1$, it is 1.05 for $b = 2$, and 1.07 for $b = 4$. However, over this range of b (or periodate concentration) the relative observed slopes are about 1.067 for $b = 2$ and 1.16 for $b = 4$. The conclusion must therefore be that there is a direct effect due to periodate, apart from its alteration of the relative rates of the k_2 and k_3 reactions, that is, that there is a termolecular reaction, at least to a small extent.

The temperature dependence of the slope, $d[MnO_4^{--}]^{-1}/dt$, needs some comment. For the same values of $[OH^-]$ and $[H_3IO_6^{--}]$, the usual plot of $\log(d[MnO_4^{--}]^{-1}/dt)$ against $1/T$ gives nearly straight lines. The activation energies so obtained are: $[OH^-] = 0.05\ M$, $E = 14.8$ kcal/g-molecule; $[OH^-] = 0.1\ M$, $E = 13.9$ kcal/g-molecule; and $[OH^-] = 0.2$ M, $E = 12.7$ kcal/g-molecule. If the value of 13.9 kcal/g-molecule is taken to apply to k_1 deduced above, and if $k_1 = Ae^{-E/RT}$, then $\log A = 11.9$ (time measured in minutes). This is an unremarkable value. This activation energy may also be compared with that obtained (7) for the interchange of radioactive manganese between manganate and permanganate ions: here $E = 10.5$ kcal. As might be expected, this is somewhat less than the value for the reaction between two manganates, which involves the transfer of an electron between two doubly charged ions. If ΔH^0 is 5.5 kcal, then the activation energy for $MnO_4^{-3} + MnO_4^- \rightarrow 2MnO_4^{--}$ is only 8.4 kcal; however, the hypomanganate ion may be partially hydrolyzed, which would vitiate any arguments concerned with the size of the charges on the ions. The activation energy found above drifts to slightly lower values as the hydroxide concentration increases. The difference is not large, but the cause is at present obscure, as the change is in the opposite direction from what would be expected from the rate constants. The change is too large, and the rate constants too consistent, to ascribe this to experimental error.

REFERENCES

1. M. W. LISTER and Y. YOSHINO. Can. J. Chem. **38**, 1291 (1960).
2. A. CARRINGTON and M. C. R. SYMONDS. J. Chem. Soc. 3373 (1956).
3. G. ZIMMERMAN. J. Chem. Phys. **23**, 825 (1955).
4. W. M. LATIMER. Oxidation potentials. 2nd ed. Prentice Hall, New York. 1952. p. 249.
5. C. E. CROUTHAMEL, A. M. HAYES, and D. S. MARTIN. J. Am. Chem. Soc. **73**, 81 (1951).
6. A. E. HILL. J. Am. Chem. Soc. **50**, 2678 (1928).
7. J. C. SHEPHERD and A. C. WAHL. J. Am. Chem. Soc. **79**, 1020 (1957).

SOME OBSERVATIONS ON THE STRUCTURE OF
ETHYLENETHIURAM MONOSULPHIDE[1]

G. D. Thorn

ABSTRACT

An attempt has been made to answer several apparent objections to the structure ethylene-
thiuram monosulphide assigned to the monomeric material of formula $C_4H_6N_2S_3$ obtained by
air oxidation of disodium ethylenebisdithiocarbamate. Comparison of the ultraviolet and
infrared absorption spectra, potentiometric titrations, and biological assays of the compound
and several heterocyclic and other compounds containing the N–C–S grouping has eliminated
two possible alternative structures containing thiadiazolidine and dithiazolidine ring systems
and has led to the conclusion that the original assignment of structure was correct.

Vigorous aeration of dilute aqueous solutions of disodium ethylenebisdithiocarbamate
(nabam) results in the formation of a yellow insoluble fungicidal material consisting
mainly of a polymer $(C_4H_6N_2S_3)_n$, together with up to 20% of the corresponding monomer
and varying amounts of elemental sulphur (1, 2). The compound $C_4H_6N_2S_3$ has been
assigned the structure ethylenethiuram monosulphide (hexahydro-1,3,6-thiadiazepine-
2,7-dithione) (IA), which can be written also as the enethiol (IB). Interpretation of the
infrared spectrum of the compound favored the latter structure. The strong band at
1610 cm^{-1} was taken as indicative of C=N (3); the bands attributable to the thioamide
group (4, 5) are absent, and there is no evidence of absorption in the N—H stretching
region.
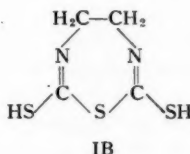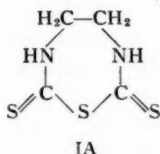
A number of objections can be raised to the formulation of the compound $C_4H_6N_2S_3$
as structure I. From a study of its infrared spectrum, two points can be made. Firstly,
there is the lack of SH absorption in the 2600–2550 cm^{-1} region, and secondly, the
observation that 2,5-di(methylmercapto)-1,3,4-thiadiazole (II, R = CH$_3$) does not
display the "C=N absorption" in the 1650–1500 cm^{-1} region (6). From a chemical
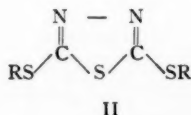
standpoint, the formation of mono-addition products with HCl and HClO$_4$ (2) and with
carbon disulphide* is suggestive of unequivalent nitrogens in the structure. Also, the

---

only other thiuram monosulphide derived from a primary amine which has been reported in the literature is in the recent work by D'Angeli and Iliceto (8), who described N,N'-dimethylthiuram monosulphide. This material is highly unstable either in solution or in the solid form, in contrast with the much more stable material designated ethylene-thiuram monosulphide. Accordingly, further evidence was sought either to support the ethylenethiuram monosulphide structure, or perhaps to suggest that an entirely different structure might well be assigned to fit the data more adequately. The results of these investigations are reported in this paper.

Two compounds of interest in this study which are obtainable by oxidation of sodium methyldithiocarbamate or the intermediate dimethylthiuram disulphide (III) are 4-methyl-5-methylimino-1,2,4-dithiazolidine-3-thione (IV) and 2,4-dimethyl-1,2,4-thia-diazolidine-3,5-dithione (V). These compounds were first prepared by Freund and co-workers (9, 10) and the assignments of structure by Hantzsch and Wolvekamp (11) confirmed by means of infrared absorption spectra by Bradsher et al. (12). Freund and Asbrand (10) had given structure VI to what is now considered to be the thiadiazolidine (V), but Bradsher et al. (12) discounted this assignment because of lack of C=N absorption in the 1660–1610 cm^{-1} region. It might be noted again that the thiadiazole (II) does not exhibit absorption in this region, but this point alone cannot be used as evidence for structure VI, as the compound exhibits "thioureide" absorption in the 1450 cm^{-1} region.
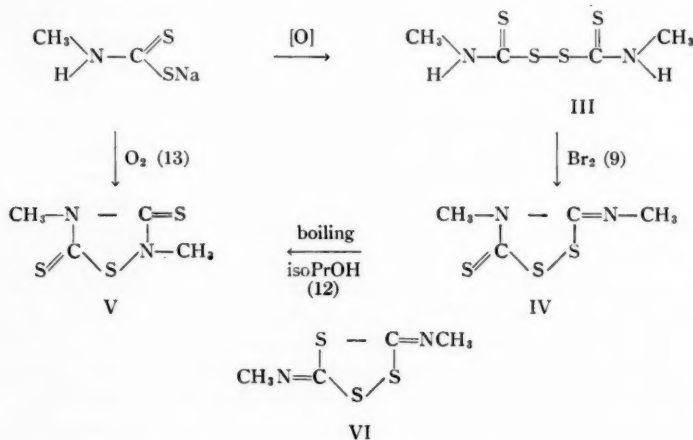
Since Benghiat et al. (13) have shown that the thiadiazolidine (V) can be obtained merely by conveying wet sodium methyldithiocarbamate in air through a pneumatic conveying drier, it is conceivable that disodium ethylenebisdithiocarbamate on aeration might yield, instead of a thiuram monosulphide (I), structures analogous to IV and V, namely VII and VIII, respectively.
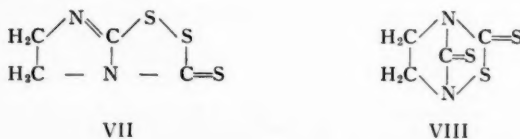
Compound VII especially answers several of the objections raised to the thiuram monosulphide structure designation. It was therefore considered important to make chemical and biological comparisons of ethylenethiuram monosulphide* with 4-methyl-5-methylimino-1,2,4-dithiazolidine-3-thione (IV) and 2,4-dimethyl-1,2,4-thiadiazolidine-3,5-dithione (V).

Ultraviolet Absorption Spectra

The similarity in ultraviolet absorption spectra of ethylenethiuram monosulphide and of tetramethylthiuram monosulphide was used by Thorn and Ludwig (2) as part of the evidence in favor of the thiuram monosulphide structure for the former compound. However, making further comparisons shows a possible fallacy in this argument. Figures 1 and 2 give the ultraviolet absorption spectra (ethanol solution) of several of the compounds in question. For ethylenethiuram monosulphide, the peaks are at 280 mμ, $\epsilon = $ 19,600, and at 227.5 mμ, $\epsilon = 8800$; for tetramethylthiuram monosulphide the maxima are at 280 mμ, $\epsilon = 16,300$, and at 210 mμ, $\epsilon = 17,000$; and for dimethylthiuram monosulphide maximum absorption is at 287 mμ, $\epsilon = 11,300$,† and at 250 mμ, $\epsilon = 8700$.† On the other hand, 4-methyl-5-methylimino-1,2,4-dithiazolidine-3-thione (IV) also shows an ultraviolet absorption spectrum (Fig. 1) very similar to that of ethylenethiuram monosulphide, with peaks at 274 mμ, $\epsilon = 16,000$, and at 223 mμ, $\epsilon = 8250$. Compound V, 2,4-dimethyl-1,2,4-thiadiazolidine-3,5-dithione, displays a different absorption to that of the above compounds (Fig. 2). Thus, on the basis of ultraviolet absorption, no decision can be made between a thiuram monosulphide or a dithiazolidine structure for "ethylenethiuram monosulphide".

Infrared Absorption Spectra

Table I summarizes the important absorption bands in the infrared region 2000–900 cm^{-1} of ethylenethiuram monosulphide and a number of other compounds containing the N–C–S linkage. The ethylenethiuram monosulphide structure is a more plausible assignment than that of a dithiazolidine structure (VII), based on the following observations. Methyl-methylimino-dithiazolidine-thione (IV) shows absorption at 1650 cm^{-1}, assignable to $\nu_{C=N}$ (3), at 1470 cm^{-1}, attributable to $\ce{>N-C<^S}$ (6) and at 1430 cm^{-1}, which Thorn (6) has assigned to the $\ce{-N=C<^{S-}}$ grouping. Ethylenethiuram monosulphide also shows $\nu_{C=N}$ absorption, at 1615 cm^{-1}, and a band at 1410 cm^{-1} ($\ce{-N=C<^{S-}}$) but no thioureide absorption in the region of 1510–1470 cm^{-1} (6). The lack of C=N absorption in the region of 1600 cm^{-1} in the spectrum of 2,5-dimercapto-1,3,4-thiadiazole (II, R = H) can be accounted for by the pseudoaromatic character of the compound (14). Likewise, in 2,5-di(methylmercapto)-1,3,4-thiadiazole (II, R = CH$_3$), this band is missing. (In this latter compound the structure is rigidly held in the enethiol form, whereas in II, R = H, the thione–thiol tautomeric structure has been assigned (6).) On the basis of our interpretation of the infrared spectra, then, the assignment of the ethylenethiuram monosulphide structure originally proposed (2) can be taken as correct, the only unexplainable feature being the lack of SH absorption in the 2600–2550 cm^{-1} region.

*Although the remarks above raise doubt as to the actual structure, the name ethylenethiuram monosulphide will be used throughout this discussion for the sake of convenience.
†These values are approximate, owing to the instability of dimethylthiuram monosulphide.
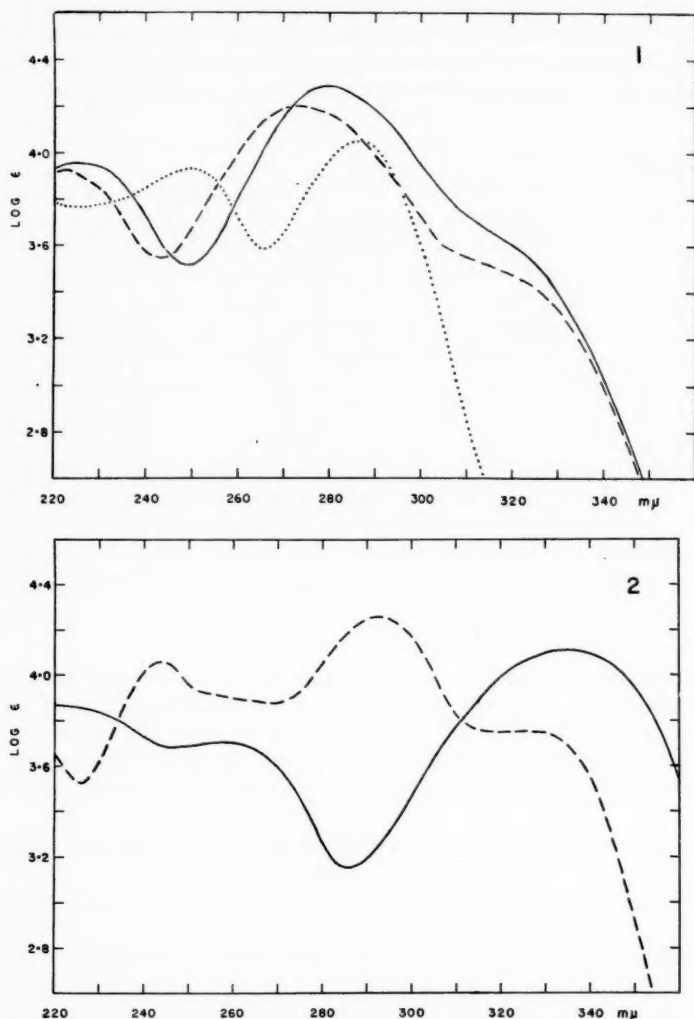
FIG. 1. Ultraviolet absorption spectra. ——— Ethylenethiuram monosulphide. - - - 4-Methyl-5-methylimino-1,2,4-dithiazolidine-3-thione. ····· Dimethylthiuram monosulphide.
FIG. 2. Ultraviolet absorption spectra. ——— 2,5-Dimercapto-1,3,4-thiadiazole. - - - 2,4-Dimethyl-1,2,4-thiadiazolidine-3,5-dithione.

In this connection, thiourea also displays a strong band at 1615 cm^{-1}, assignable to $\nu_{C=N}$ vibration, but shows no absorption band in the region 2600–2550 cm^{-1} given by Bellamy (15) as assignable to ν_{SH} vibration.

Potentiometric Studies

The apparent lack of SH according to the infrared spectrum in ethylenethiuram

TABLE I

Principal absorption bands of several compounds containing the $\big\rangle$N—C$\underset{\diagdown}{\overset{S}{\parallel}}$ grouping, in the region 2000–900 cm^{-1}

Compound	Solvent	Absorption bands, cm^{-1}														
Ethylenethiuram monosulphide	CHCl₃	1615				1410		1325	1300m			1085			980	
Dimethylthiuram monosulphide	Nujol	1572m	1535m	1473	1428w		1385	1350		1155			1045			912
Dimethylthiuram disulphide	CHCl₃		1525		1430m			1360		1165			1040			920
Tetramethylthiuram monosulphide	CHCl₃		1505		1450w		1385		1245w	1150			1050m	1005	965	
4-Methyl-5-methylimino-1,2,4-dithiazolidine-3-thione	CHCl₃	1650		1470	1430	1410	1385		1278	1145w	1112		1057w	1010w	955	
2,4-Dimethyl-1,2,4-thiadiazolidine-3,5-dithione	CHCl₃			1450	1425		1375		1300	1165		1095		1030		
Ethylenethiuram monosulphide - CS₂ complex	KBr	1605m		1485	1435w	1420			1280	1195	1135	1085			970	
Thiourea	Nujol	1615		1475		1415						1085				
N,N-Dimethyl dimethylthiocarbamylsulphenamide	CHCl₃		1500		1445w	1410w	1382		1255	1150			1050m	995	980	

monosulphide prompted potentiometric titrations to determine the presence or absence of weakly acid hydrogen in the compound in question. Harlow *et al.* (16) have shown the feasibility of potentiometric titration of very weak acids using tetrabutylammonium hydroxide as titrant in non-aqueous media. Structurally, 4-methyl-5-methylimino-1,2,4-dithiazolidine-3-thione (IV) and 2,4-dimethyl-1,2,4-thiadiazolidine-3,5-dithione (V) should show no consumption of alkali. The other compounds tested, i.e., ethylenethiuram monosulphide, dimethylthiuram mono- and di-sulphide, and 3,5-dimercapto-1,3,4-thiadiazole (II, R = H) should each show two inflection points in its titration curve. The results of these titrations, using tetrabutylammonium hydroxide in isopropyl alcohol as titrant and acetonitrile as solvent, are given in Figs. 3 and 4. Pyridine was also used as solvent in a parallel series of titrations, but, except in the case of dimercaptothiadiazole, no greater resolution was obtained. Cundiff and Markunas (17) have demonstrated the possibility of titrating potentiometrically organic dibasic acids whose ionization constants (K_1 and K_2) are close together, and of obtaining two sharp inflections in the titration curve. As can be seen in Figs. 3 and 4, two inflections were obtained with
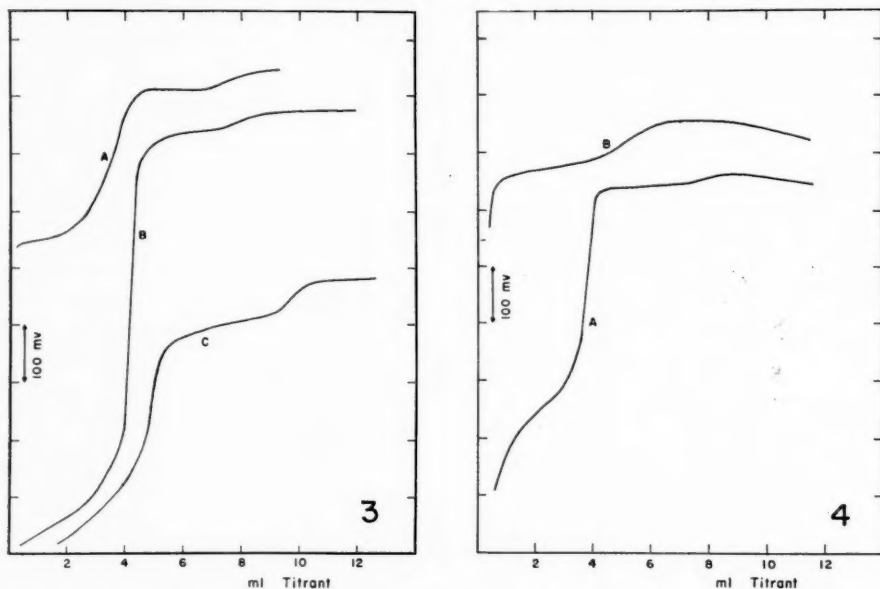
FIG. 3. Potentiometric titration curves. (A) Ethylenethiuram monosulphide. (B) Dimethylthiuram disulphide. (C) 2,5-Dimercapto-1,3,4-thiadiazole.
FIG. 4. Potentiometric titration curves. (A) Dimethylthiuram monosulphide. (B) 2,4-Dimethyl-1,2,4-thiadiazolidine-3,5-dithione.

all the above-mentioned compounds, except for IV and V. With ethylenethiuram mono-sulphide and dimethylthiuram disulphide, the inflections occurred at about 85% of equivalence, and with dimethylthiuram monosulphide, the inflections were at about 60–65% of equivalence. The discrepancy shown by dimethylthiuram monosulphide is not surprising in the light of the work of D'Angeli and Iliceto (8), who showed the instability of this compound in neutral solution and also the formation of molecular amounts

of sodium methyldithiocarbamate and methylisothiocyanate when the thiuram monosulphide was treated with an equivalent of sodium hydroxide. Similar decompositions probably occurred with ethylenethiuram monosulphide and dimethylthiuram disulphide during the titrations. It had been shown in earlier work (18) that ethylenethiuram monosulphide is converted to ethylenethiourea on treatment with alcoholic potassium hydroxide.

One unexpected result arising from these potentiometric titrations was the occurrence of a single weak inflection in the titration curve of dimethylthiadiazolidinedithione (V), at 80% of one equivalent of alkali. As expected, however, methyl-methylimino-dithiazolidine-thione (IV), on the other hand, gave no "titration curve".

Biological Studies

Ethylenethiuram monosulphide, 4-methyl-5-methylimino-1,2,4-dithiazolidine-3-thione (IV), 2,4-dimethyl-1,2,4-thiadiazolidine-3,5-dithione (V), and 2,5-dimercapto-1,3,4-thiadiazole were tested for biological activity by the A.P.S.-recommended spore drop method (19) using *Monilinia fructicola* as test organism. Dimethylthiuram monosulphide was not assayed in view of its instability. The dosage response data are shown in Fig. 5, plotted on logarithmic probability grid. These data were subjected to probit analysis, and $Y = a + bx$, the linear regression equation of toxicity probit values on the dose metameter, determined for each toxicant according to Finney (20). From these equations not only is the median lethal dosage, $m = (5 - a)/b$, obtainable, but also the spread in distribution of tolerance, σ^2, a second expression of the effectiveness of the toxicant. The variance, σ^2, is equal to the reciprocal of the square of the slope, b, of the regression line. Toxicants whose physiological effects are similar often have approximately equal variances for any given organism, even though they may display substantial differences in their median lethal dosages. In other words, the slope of the regression line is considered a criterion of mechanism of fungicidal action (21, 22). If two fungicidal compounds yield different dosage response slopes, a different mechanism of action is inferred. Parallel slopes are given by members of homologous series.

The regression line equations for ethylenethiuram monosulphide (I), 4-methyl-5-methylimino-1,2,4-dithiazolidine-3-thione (IV), and 2,4-dimethyl-1,2,4-thiadiazolidine-3,5-dithione (V) were calculated to be: $Y_I = 4.26 + 8.65 \log \lambda$, $Y_{IV} = 3.45 + 0.12 \lambda$, and $Y_V = 4.78 + 0.024 \lambda$. It will be noted that whereas I gives the more usual linear log–dosage response (20), a linear regression line is given by compounds IV and V according to the Parker–Rhodes equation (21). In most toxicity tests, the logarithm of λ is normally distributed, but occasionally λ itself has been found to be normally distributed. No explanation has as yet been advanced for this variation. The widely different values of b for the three compounds are thus indicative of differing chemical structure. This biological evidence complements the physicochemical evidence, presented above, that the structure of ethylenethiuram monosulphide is *not* given by VII, an analogue of the iminodithiazolidinethione (IV), but is in all likelihood structure (IB) as originally suggested (1, 2). It has been shown earlier (23) that ethylenethiuram monosulphide and 2,5-dimercapto-1,3,4-thiadiazole displayed regression lines of the same slope, differing in position, suggesting a similarity in structure.

Still unexplained is the formation of mono-addition compounds of ethylenethiuram monosulphide with HCl, HClO$_4$, and CS$_2$. The precipitation of these 1:1 compounds from solution as they are formed, together with electromeric influence through the

conjugated system to the second enethiol grouping, may be sufficient explanation for
this apparent anomaly in structure.
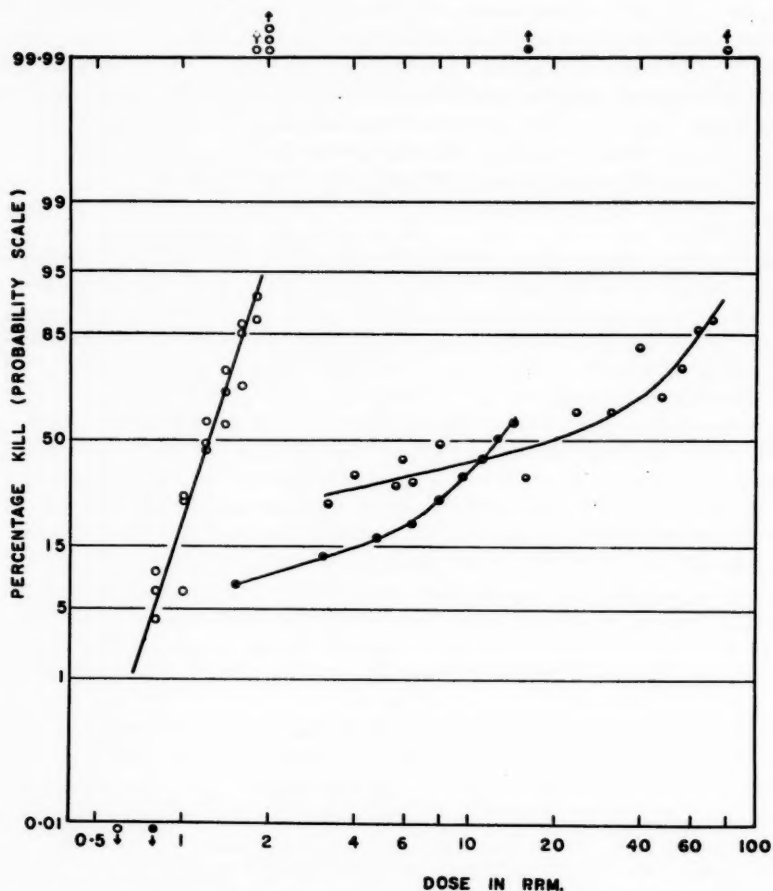
FIG. 5. An in vitro comparison of the fungicidal activities of ethylenethiuram monosulphide (O),
4-methyl-5-methylimino-1,2,4-dithiazolidine-3-thione (●), and 2,4-dimethyl-1,2,4-thiadiazolidine-3,5-
dithione (◗).

EXPERIMENTAL

Ultraviolet absorption spectra were obtained in ethanol solution, using the Beckman
DK-1 spectrophotometer. Infrared spectra were obtained with the Perkin–Elmer model
21, with NaCl optics, in chloroform solution or in Nujol[R] mull. Potentiometric titrations
were performed with the aid of the Radiometer Titrator, type TTT1 with standard
plug-type calomel and glass electrodes. The sample, 0.100 g, dissolved in 50 ml aceto-
nitrile or pyridine, was stirred magnetically under a blanket of nitrogen, and the e.m.f.
measured with increments of titrant. The titrant, approximately 0.2 N tetrabutyl-

ammonium hydroxide in methanol, was prepared according to the method of Harlow *et al.* (16) and standardized potentiometrically against benzoic acid.

Ethylenethiuram monosulphide (I) was isolated from the mixture resulting from air oxidation of disodium ethylenebisdithiocarbamate (24) by extraction with chloroform, addition of concentrated HCl to precipitate the ethylenethiuram monosulphide hydrochloride (2), filtration and suspension of the hydrochloride in chloroform, and addition of sodium hydroxide solution to convert the insoluble salt to ethylenethiuram monosulphide. The yellow chloroform solution was filtered, dried with anhydrous sodium sulphate, and evaporated to dryness to yield the thiuram monosulphide free of elemental sulphur, m.p. 120–123°. Crystallization from chloroform–ethanol gave material of melting point 125–126°.

2,5-Dimercapto- and *2,5-di(methylmercapto)-1,3,4-thiadiazole* (II) were prepared according to Thorn and Ludwig (21) and Thorn (6), respectively.

4-Methyl-5-methylimino-1,2,4-dithiazolidine-3-thione (IV) was obtained according to the method of Freund and Asbrand (10) by the action of bromine on ammonium methyldithiocarbamate. Crystallization from ethanol gave pale yellow material of melting point 84° (lit. (10), m.p. 86°). Calc. for $C_4H_6N_2S_3$: S, 53.9; N, 15.7%. Found: S, 53.7; N, 15.6%. *2,4-Dimethyl-1,2,4-thiadiazolidine-3,5-dithione* (V), obtained by rearrangement of IV with alcoholic ammonia (10), melted at 122–123° (lit. (12) gives 123–124°). Calc. for $C_4H_6N_2S_3$: S, 53.9; N, 15.7%. Found: S, 54.0; N, 15.5%.

Dimethylthiuram monosulphide was prepared by the reaction of equimolar amounts of methyl isothiocyanate and aqueous sodium methyldithiocarbamate (8). Addition of glacial acetic acid yielded colorless crystals of melting point 77–78° (lit. (8), m.p. 78–80°). Calc. for $C_4H_8N_2S_3$: S, 53.3; N, 15.5%. Found: S, 52.9; N, 15.6%.

The *ethylenethiuram monosulphide – carbon disulphide addition complex* was obtained by dissolving ethylenethiuram monosulphide in carbon disulphide. The brick-red complex, which precipitates within a few minutes, loses CS_2 upon heating above 100°, and melts at 125–126°. Calc. for $C_5H_6N_2S_5$: S, 63.0%. Found: S, 62.9%.

ACKNOWLEDGMENTS

REFERENCES

1. R. A. LUDWIG and G. D. THORN. Plant Disease Reptr. **37**, 127 (1953).
2. G. D. THORN and R. A. LUDWIG. Can. J. Chem. **32**, 872 (1954).
3. M. G. ETTLINGER. J. Am. Chem. Soc. **72**, 4699 (1950).
4. H. M. RANDALL, R. G. FOWLER, N. FUSON, and J. R. DANGL. Infrared determination of organic structures. D. Van Nostrand Co. Inc., New York. 1949. p. 66.
5. D. T. ELMORE. J. Chem. Soc. 3489 (1958).
6. G. D. THORN. Can. J. Chem. **38**, 1439 (1960).
7. A. H. M. KIRBY and E. L. FRICK. Ann. Rept. East Malling Res. Station. 1956. p. 146.
8. F. D'ANGELI and A. ILICETO. Gazz. chim. ital. **89**, 2095 (1959).
9. M. FREUND. Ann. **285**, 154 (1895).
10. M. FREUND and E. ASBRAND. Ann. **285**, 166 (1895).
11. A. HANTZSCH and M. WOLVEKAMP. Ann. **331**, 278 (1904).
12. C. K. BRADSHER, F. C. BROWN, E. F. SINCLAIR, and S. T. WEBSTER. J. Am. Chem. Soc. **80**, 414 (1958).
13. I. BENGHIAT, J. B. BOWERS, G. E. LUKES, and S. L. GIOLITO. To Stauffer Chemical Co. U.S. Patent No. 2,863,803 (December 9, 1958).
14. R. ZAHRADNÍK. Collection Czechoslov. Chem. Commun. **24**, 3193 (1959).
15. L. J. BELLAMY. The infrared spectra of complex molecules. Methuen & Co. Ltd., London. 1954.

CANADIAN JOURNAL OF CHEMISTRY. VOL. 38, 1960

16. G. A. Harlow, C. M. Noble, and G. E. A. Wyld. Anal. Chem. **28**, 787 (1956).
17. R. H. Cundiff and P. C. Markunas. Anal. Chem. **28**, 792 (1956).
18. G. D. Thorn and R. A. Ludwig. Unpublished data.
19. The American Phytopathological Society. Committee on Standardization of Fungicidal Tests. Phytopathology, **33**, 627 (1943).
20. D. J. Finney. Probit analysis. Cambridge University Press, Cambridge. 1952.
21. A. F. Parker-Rhodes. Ann. Appl. Biol. **29**, 126 (1942).
22. J. G. Horsfall. Principles of fungicidal action. Chronica Botanica Co., Waltham, Mass. 1956.
23. G. D. Thorn and R. A. Ludwig. Can. J. Botany, **36**, 389 (1958).
24. R. A. Ludwig and G. D. Thorn. Can. J. Botany, **36**, 473 (1958).

EXOTHERMIC REACTIONS DUE TO ANNEALING OF DEFECTS IN OXIDE LATTICES: STUDY OF THE DECOMPOSITION OF CARBONATES[1]

C. N. R. RAO,[2] S. R. YOGANARASIMHAN, AND M. P. LEWIS[3]

ABSTRACT

Small exothermic reaction peaks are observed in the differential thermal curves of carbonates. The heat evolution is probably due to the removal of internal crystal defects in the metastable oxide lattices.

Recently, Rao and Pitzer (1) have reported that when magnesium and calcium hydroxides are heated just beyond their decomposition temperatures, there is some evolution of heat of the order of 300 to 400 calories per mole. This exothermic reaction was explained as due to the removal of internal crystal defects in the metastable oxide lattices formed just after the decomposition of the hydroxides. The possibility that the reduction in surface area of the oxides also contributed to the heat evolution was not excluded. We have now studied the decomposition of a few carbonates to see if similar exothermic reactions are observed in the oxides obtained by their decomposition. Differential thermal analysis and X-ray diffraction analysis have been employed for the study.

EXPERIMENTAL

The differential thermal analysis was carried out using a high-sensitivity apparatus described by Pask and Warner (2). A constant heating rate of 12 degrees per minute was employed in all the runs. The reaction temperatures reported here are constant only for a given set of experimental conditions.

The carbonates studied are $MgCO_3$, $CaCO_3$, $CdCO_3$, $ZnCO_3$, and Ag_2CO_3. All the carbonates were obtained commercially. The X-ray diffraction patterns were taken using a Rich Seifert X-ray unit or a North American Philips diffractometer fitted with a Geiger counter recording device.

RESULTS AND DISCUSSION

Typical differential thermal analysis curves are shown in Fig. 1. All the carbonates first showed large endothermic reaction peaks due to their decomposition to the corresponding oxides and carbon dioxide; immediately following these were observed small exothermic reaction peaks. The exothermic reactions were irreversible and occurred at temperatures usually 40–80° higher than the decomposition temperatures of the carbonates (Table I). It was made certain by X-ray analysis that the carbonates had completely decomposed to the oxides before the exothermic reaction. There was no change in crystal structure or parameters of the oxides after the exothermic reaction. Thus, the heat evolution could not have resulted from a crystal structure transformation. However, marked decrease in X-ray line widths were noticed in samples heated just past the exothermic reaction temperature indicating greater crystallinity in the samples. The
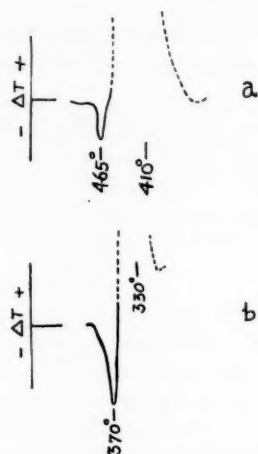
FIG. 1. Differential thermal analysis curves. (a) $MgCO_3$, (b) $ZnCO_3$. The dotted peaks correspond to the decomposition of the carbonates.

results reported in this communication on carbonates are similar to those observed in the decomposition of magnesium and calcium hydroxides (1).

The heats of the exothermic reactions were estimated by comparing the peak areas with the peak area for the α–β inversion of quartz (4.3 calories per gram). The heats thus estimated and the reaction temperatures for the different oxides are given in Table I. The values of ΔH are good to within ±25%.

TABLE I

Carbonate	Endothermic reaction (decomposition) peak temperature, °C	Exothermic reaction peak temperature, °C	Estimated ΔH of the exothermic reaction, cal/mole of oxide
$MgCO_3$	410	465	360
$CaCO_3$	1015	1090	230
$ZnCO_3$	330	370	1000
$CdCO_3$	510	570	640
Ag_2CO_3	180	210	200

It is interesting to note that the heat evolution is very sharp and occurs over a short range of temperature in all the cases. It is known that the surface areas of oxides decrease with increase in temperature (3); but there is no reason why reduction in surface should result in a sharp evolution of heat over a short temperature range. When differential thermal analysis of oxides was extended to high temperatures where considerable reduction in surface area occurred, sharp exothermic reaction peaks were not noticed. The more important contribution to the heat evolution may be from the removal of internal crystal defects in the metastable oxide lattices. It is understandable that when a compound, say a hydroxide or carbonate, decomposes, it first gives a metastable or active oxide associated with a high degree of lattice disorder. This metastable oxide, when heated to a slightly higher temperature, goes into an ordered lattice. The decrease in the X-ray line widths apparently results from the annealing of these defects in the metastable oxide lattices. Such an interpretation of the decrease in X-ray line widths

is by no means new. It is therefore suggested that the observed evolution of heat mainly results from the disorder → order reaction (metastable oxide* → crystalline oxide) in the oxide lattice.

Exothermic reactions associated with large heats have been observed in the differential thermal analysis of hydrates of chromic and ferric hydroxides (4, 5) and titanium peroxide gel (6). The exothermic reactions are found just after the endothermic peaks due to the decomposition of the hydrate or the peroxide. It has been shown that the exothermic reactions in these cases result from the crystallization of the oxides from the amorphous state. The small exothermic reactions reported in this communication and elsewhere (1) may be similar to these crystallization reactions differing only in the magnitude of heat evolution. One may thus visualize the so-called disorder → order reaction in metastable oxide lattices as a crystallization process.

The formation of a metastable or active calcium oxide (CaO*) during decomposition of calcium carbonate has been proposed by Hyatt *et al.* (7) on the basis of their kinetic studies. These active CaO* groups are supposed to act as bridges between layers of well-crystallized cubic CaO and the decomposing $CaCO_3$. Razouk and Mikhail (8) have observed that the rate of crystallization of magnesium oxide obtained from the decomposition of magnesium hydroxide or carbonate at 500° is rather slow. This is probably reasonable. If the initial formation of a metastable MgO* similar to the CaO* proposed by Hyatt *et al.* (7) is postulated, the results of Razouk and Mikhail can be explained. Razouk and Mikhail have reported that some of the lines of the parent compound persist in the X-ray pattern of the oxides obtained by decomposition at 500° C. However, when the oxide was hydrated and then dehydrated at the same temperature only the pattern of the oxide was obtained. This indicates that Razouk and Mikhail have affected the crystallization of magnesium oxide by prolonged heating at 500° C, which would naturally render the process of rehydration difficult. If they had carried out their experiments at a slightly higher temperature, i.e. a temperature high enough for the exothermic disorder → order reaction of the metastable oxide, they would have probably obtained highly crystalline magnesium oxide in the first instance itself.

The crystalline and finely divided samples of magnesium oxide (9) and calcium oxide (10) have been reported to show large differences in their heat contents (~900 and 500 calories per mole respectively). The heat capacity of finely divided magnesium oxide is also found to be higher than that of crystalline magnesium oxide (9). The crystalline oxides were inevitably prepared by the decomposition of the hydroxides at high temperatures whereas the finely divided samples were prepared by decomposition at relatively low temperatures. On the basis of the investigations on the decomposition of carbonates and hydroxides (1), it is suggested that at least the major part of these heat content differences may be explained on the basis of the disorder → order reaction in oxides. A small irreversible exothermic reaction peak (ca. $\Delta H \sim -100$ calories per mole) has been noticed around 200° in the differential thermal analysis curve of silver oxide prepared by the dehydration of the freshly precipitated oxide (11). It is interesting to note that the oxide obtained by the decomposition of silver carbonate* also exhibits an irreversible exothermic reaction of the same magnitude (Table I). An irreversible heat evolution of about 300 calories per mole has been observed by Kobayashi (12) in the range 100–200° C during his measurements of the heat capacity of silver oxide. Kobayashi suggested

*The differential thermal analysis of curve Ag_2CO_3 first shows an endothermic peak due to decomposition of the carbonate to the oxide (Ag_2O^*) and CO_2 and then a small exothermic reaction peak around 210° C ($Ag_2O^* \rightarrow Ag_2O$, cryst.) followed by another endothermic peak due to the dissociation of Ag_2O.

that the heat "originates in the melting of the *freezing in* of the crystal imperfections". Such "stabilization" of the silver oxide lattice at higher temperatures has successfully explained the discrepancies in the thermodynamics of the dissociation of silver carbonate (13). It therefore appears likely that the evolution of heat in the differential thermal analysis curves of silver oxide arises from the annealing of crystal defects.

ACKNOWLEDGMENTS

REFERENCES

1. C. N. R. Rao and K. S. Pitzer. J. Phys. Chem. 64, 282 (1960).
2. J. A. Pask and M. F. Warner. Am. Ceram. Soc. Bull. 33, 168 (1954).
3. R. I. Razouk and R. Sh. Mikhail. J. Phys. Chem. 63, 1050 (1959).
4. S. K. Bhattacharya, V. S. Ramachandran, and J. C. Ghosh. Advances in Catalysis, 9, 114 (1957).
5. C. N. R. Rao and A. Mountwala. Unpublished results.
6. C. N. R. Rao and S. R. Yoganarasimhan. Unpublished results.
7. E. P. Hyatt, I. B. Cutler, and M. E. Wadsworth. J. Am. Ceram. Soc. 41, 70 (1958).
8. R. I. Razouk and R. Sh. Mikhail. J. Phys. Chem. 62, 920 (1958).
9. W. F. Giauque. J. Am. Chem. Soc. 71, 3192 (1949).
10. K. Kobayashi. Sci. Repts. Tôhoku Univ. 34, 153 (1950).
11. K. S. Pitzer, R. E. Gerkin, L. V. Gregor, and C. N. R. Rao. Symposium on Chem. Thermodynamics. Intern. Union of Pure and Appl. Chem. Wattens, Austria. 1959.
12. K. Kobayashi. Sci. Repts. Tôhoku Univ. 35, 173 (1951).
13. K. Kobayashi. Sci. Repts. Tôhoku Univ. 35, 283 (1951).

REDUCTION OF MONOHALOGENATED NITROBENZENES WITH HYDRAZINE AND RANEY NICKEL

A CONVENIENT PREPARATION OF HALOGENATED ANILINES[1]

B. E. Leggetter and R. K. Brown

ABSTRACT

The isomeric fluoro-, chloro-, bromo-, and iodo-nitrobenzenes can be converted to the corresponding halogenated anilines in good yield by refluxing methanolic hydrazine hydrate in the presence of Raney nickel.

INTRODUCTION

The reduction of alcoholic solutions of substituted nitrobenzenes with hydrazine hydrate in the presence of Raney nickel provides a facile and convenient method for the preparation of aromatic amines. This method has in recent years been applied successfully not only to the reduction of nitro compounds directly to amines without affecting most functional groups (1, 2) or destroying heat sensitive amines (3) but also to the conversion of nitro compounds to intermediate azoxy and hydrazo derivatives (4, 5, 6) and of nitriles to the hydrazones of the corresponding aldehydes (7). Palladized charcoal (8–12), ruthenium on charcoal (11, 12), and platinum (8) have been used in place of Raney nickel quite successfully in hydrazine reductions. Copper and iron powder have also been employed though with inferior results (13).

The present work was undertaken in order to provide a convenient method for the preparation of halogenated anilines, particularly the iodo derivatives, via reduction of the corresponding nitro compounds.

Whilst previous methods of preparation of halogenated anilines by reduction of the nitro precursors with reagents such as stannous chloride and hydrochloric acid (14, 15), tin and hydrochloric acid (16), iron and hydrochloric acid (15, 17, 18), or hydrogen and a nickel catalyst (19, 20, 21) and rhodium on alumina (22) have given fair to good yields in the case of fluoro-, chloro-, and bromonitro-benzenes, the same methods applied to the iodonitrobenzenes caused considerable displacement of the iodine atom and generally gave very low yields of the halogenated amines. Baeyer (14), however, has reported good yields of *o*-iodoaniline from the low-temperature reduction of *o*-iodonitrobenzene with stannous chloride and hydrochloric acid. The same reagents were used to prepare the para and meta isomers from their nitro precursors but no yields were given although it was stated that because increased temperatures were necessary to effect reduction of the *p*-iodonitrobenzene the yield of the *p*-iodoaniline was low (14). We have found that when *m*-bromonitrobenzene was reduced with Raney nickel and hydrogen at low pressure and at room temperature much aniline was produced (23).

RESULTS AND DISCUSSION

A summary of the results of this work is presented in the accompanying table. The melting points and boiling points are recorded for convenience along with reported constants.

The reduction of methanolic solutions of iodonitrobenzenes to iodoanilines with freshly prepared Raney nickel and hydrazine hydrate proceeds smoothly in reasonably good yields (64 to 87%) with little or no displacement of the iodine atom. The results are even better when the fluoro (80 to 90%), chloro (95%), and bromo (80 to 90%) analogues are involved. A study of the reaction conditions showed that the reduction is best accom-

TABLE I

Reduction of halogenated nitrobenzenes with Raney nickel and hydrazine
$(R = C_6H_4NO_2)$

Compound	% yield of halogenated amine	Reduction method	Melting point or boiling point	
			Observed	Literature
o-F-R	80	A	45°/2 mm	58°/11 mm (15)
m-F-R	90	A	50°/2 mm	187°/760 mm (25)
p-F-R	86	A	50°/2 mm	187°/767 mm (15)
o-Cl-R	95	A	201°/700 mm	207°/760 mm (26)
m-Cl-R	96	A	224°/700 mm	230°/760 mm (26)
p-Cl-R	95	A	70–71°	69–70° (26)
o-Br-R	90	A	27–28° (88°/8 mm)	32° (229°/760) (27)
m-Br-R	82	A	14–15° (124°/12 mm)	17° (130°/12 mm) (16)
p-Br-R	80	A	65–66°	66° (27)
o-I-R	64	B	57–59°	60–61° (14)
m-I-R	73	B	22–24° (128°/8 mm)	25° (145°/15 mm) (27)
p-I-R	87	B	64–65°	67–68° (14)

plished at elevated temperatures. Complete reduction of the nitro group to the amine occurs at the temperature of boiling methanol whereas reduction in methanolic solution at 25° was found to give in some cases only partially reduced products such as the azoxy or hydrazobenzene even though excess reducing agent is present. Furthermore, unless a large ratio of solvent to nitro compound is used, some products tend to precipitate as the less soluble intermediate compound. Furst and Moore (6) have also reported the formation of intermediate reduction products, the azoxybenzene and hydrazobenzene (but no azobenzene) particularly when a lower proportion of hydrazine to nitro compound is used, or when small volumes of solvent are employed. In addition, the quality of the Raney nickel catalyst has been shown by these authors to influence the extent of reduction (4).

In our work gradual addition of the hydrazine hydrate to a refluxing methanolic solution of the nitro compound to which Raney nickel had been added approximated the conditions of limited amount of reducing agent reported by Furst and Moore (6) and, especially when smaller amounts of solvent were employed, tended to produce intermediate reduction products as contaminants. Generally, best results were obtained when an excess of solvent was involved (solvent:solute ≈ 10:1 by weight) and the reducing agent (hydrazine:nitro compound ≈ 2:1) was always kept in excess by slow addition of the nitro compound to the refluxing alcoholic solution of hydrazine hydrate containing a small amount of Raney nickel. This modified procedure (method A in the experimental section) was found to be superior for the fluoro, chloro, and bromo analogues but gave somewhat lower yields than did the original method (method B in the experimental section) in the case of the iodo compounds. Attempts to reduce m-iodonitrobenzene to m-iodoaniline at 25° gave 3,3'-diiodoazobenzene rather than the expected m-iodoaniline.

EXPERIMENTAL

The methods of reduction employed for these experiments are shown in the following two examples. Commercially available reagent grade samples of the halogenated nitrobenzenes were used while the Raney nickel catalyst was prepared by published directions (24).

o-Bromoaniline by Method A

A methanolic solution of o-bromonitrobenzene (20.2 g, 0.1 mole) was added dropwise to a refluxing solution of hydrazine hydrate (64% hydrazine in water) (15.0 g, 0.3 mole) in methanol (70 ml) to which about 1 gram of Raney nickel had been added. The rate of addition of the o-bromonitrobenzene solution was such that the evolution of gases from the reaction mixture did not become too vigorous; generally about 10–15 minutes were required for this step. At the end of the addition, the solution was refluxed for 10 minutes by which time the characteristic yellow color of the nitro compound had disappeared. The Raney nickel was then separated by filtration. Evaporation of the solvent and purification of the product by steam distillation gave 15.5 g of material boiling at 88°/8 mm.

The following anilines were also prepared by this method, the percentage yields obtained being reported in the table: o-, m-, and p-fluoroaniline, o-, m-, and p-chloro-aniline, and o-, m-, and p-bromoaniline.

m-Iodoaniline by Method B

A solution of m-iodonitrobenzene (13.0 g, 0.052 mole) in methanol (150 ml), containing 1 g of Raney nickel catalyst, was refluxed while hydrazine hydrate was added dropwise at such a rate that the evolution of gas did not become too vigorous. The addition of the hydrazine was discontinued when the reaction solution became colorless indicating complete reduction. Steam distillation of the residual oil obtained after removal of the solvent gave the required product, which was further purified by distillation under reduced pressure, b.p. 128°/5 mm, m.p. 22–24°; yield, 8.3 g (73%).

o-Iodo- and p-iodo-aniline were prepared by the above methods. Yields and physical constants are reported in the table.

REFERENCES

1. D. BALCOM and A. FURST. J. Am. Chem. Soc. **75**, 4334 (1953).
2. L. M. LITVNENKO and A. P. GREKOV. Zhur. Obshcheĭ Khim. **27**, 234 (1957); Chem. Abstr. **51**, 12866 (1957).
3. R. K. BROWN and N. A. NELSON. J. Am. Chem. Soc. **76**, 5149 (1954).
4. R. E. MOORE and A. FURST. J. Org. Chem. **23**, 1504 (1958).
5. P. M. G. BAVIN. Can. J. Chem. **36**, 238 (1958).
6. A. FURST and R. E. MOORE. J. Am. Chem. Soc. **79**, 5492 (1957).
7. S. PIETRA and C. TRINCHERA. Gazz. chim. ital. **86**, 1045 (1956); Chem. Abstr. **52**, 3721 (1958).
8. L. P. KUHN. J. Am. Chem. Soc. **73**, 1510 (1951).
9. S. PIETRA. Ann. chim. (Rome), **45**, 850 (1955); Chem. Abstr. **50**, 10668 (1956).
10. M. J. S. DEWAR and T. MOLE. J. Chem. Soc. 2556 (1956).
11. S. PIETRA. Ann. chim. (Rome), **47**, 410 (1957); Chem. Abstr. **51**, 15438 (1957).
12. S. PIETRA and M. RIS. Ann. chim. (Rome), **48**, 299 (1958); Chem. Abstr. **52**, 18277 (1958).
13. S. KUBOTA, K. NARA, and S. ONISHI. J. Pharm. Soc. Japan, **76**, 801 (1956); Chem. Abstr. **51**, 1086 (1957).
14. A. BAEYER. Ber. **38**, 2760 (1905).

15. G. SHIEMAN and R. PILLARSKY.   Ber. **62**, 3035 (1929).
16. S. NATELSON and S. P. GOTTFRIED.   J. Am. Chem. Soc. **61**, 1001 (1939).
17. S. E. HAZLET and C. A. DORNFELD.   J. Am. Chem. Soc. **66**, 1781 (1944).
18. D. W. MATHIESON and G. NEWBURY.   J. Chem. Soc. 1133 (1949).
19. C. F. WINANS.   J. Am. Chem. Soc. **61**, 3564 (1939).
20. F. BENINGTON, E. V. SHOOP, and R. H. POIRIER.   J. Org. Chem. **18**, 1506 (1953).
21. N. M. LÖFGREN, B. J. LUNDQUIST, and S. LINDSTRÖM.   Acta Chem. Scand. **9**, 1079 (1955).
22. Unpublished results.
23. U.S.P. 2,772,313; Chem. Abstr. **51**, 10570 (1957).
24. ORGANIC SYNTHESES.   Coll. Vol. III. John Wiley and Sons, Inc., New York, 1955. p. 181.
25. C. K. INGOLD and C. C. N. VASS.   J. Chem. Soc. 421 (1928).
26. F. BEILSTEIN and A. KURBATOW.   Ann. **176**, 27 (1875).
27. J. M. HEILBRON.   Dictionary of organic compounds. Eyre and Spottiswoode, London. 1934.

A SYSTEM OF MOLECULAR THERMOCHEMISTRY FOR ORGANIC GASES AND LIQUIDS

PART II. EXTENSION TO COMPOUNDS CONTAINING SULPHUR AND OXYGEN[1]

Edward G. Lovering and Keith J. Laidler

ABSTRACT

The system of bond and group energies described in Part I has been extended and applied to certain compounds containing sulphur and oxygen. The substances treated are the alkanethiols, the thiaalkanes, and the dithiaalkanes. The bond additivity scheme enables reliable values for heats of formation, combustion, atomization, and vaporization to be calculated for these compounds.

A similar treatment has been applied to the data for alcohols, ethers, and alkyl peroxides.

INTRODUCTION

In Part I of this series (1) a scheme of bond and group energies, suitable for the reliable calculation of heats of formation, combustion, and atomization of organic compounds, was developed. The method was applied in some detail to the paraffins, olefins, and acetylenes. For other compounds adequate data for homologous series were not available, and only approximate group contributions could be obtained. A method whereby the scheme could be extended to substituted homologous series, when sufficient reliable data became available, was also given. During the past few years excellent data have become available for alkanethiols (R—S—H), thiaalkanes (R—S—R), and dithiaalkanes (R—S—S—R), and in the present paper the scheme is applied to these. A few recent data are also available for certain alcohols, ethers, and peroxides, and the scheme has been extended to cover these compounds also.

The previous paper also provided a scheme for the calculation of heats of vaporization, and it is applied in the present work to the sulphur compounds mentioned above.

HEATS OF FORMATION, COMBUSTION, AND ATOMIZATION

The heat of atomization is the energy required to dissociate 1 mole of a compound, in the gaseous state, into its constituent atoms in their ground states. The heats of atomization given in this paper are calculated with the aid of the following relationships, which apply at $25.0°$ C:

$$C \text{ (graphite)} = C(g, {}^3P) -171.7 \text{ kcal,}$$
$$\tfrac{1}{2}H_2 \text{ (g)} = H(g) -52.09 \text{ kcal,}$$
$$\tfrac{1}{2}O_2 \text{ (g)} = O(g) -59.16 \text{ kcal,}$$
$$S \text{ (rhombic)} = S(g, {}^3P) -57 \text{ kcal.}$$
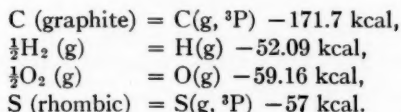
The choice of the first three values was discussed in Part I. The value for the heat of sublimation of rhombic sulphur has not been firmly established. Cottrell (2) has recently reviewed the chemical and spectroscopic evidence, on the basis of which he favors the value of 57 kcal. We have chosen to use this value in the present paper.

Based upon the above relations, the heat of atomization, Q_a, of compounds containing carbon, hydrogen, sulphur, and oxygen is obtained through the equation

[1]
$$Q_a = Q_f + 171.7\, n_C + 52.09\, n_H + 57\, n_S + 59.16\, n_O.$$

Here Q_t $(= -\Delta H_t)$ is the heat (evolved) of formation of the gaseous compound at 25° C and n_C, n_H, n_S, and n_O are the numbers of carbon, hydrogen, sulphur, and oxygen atoms, respectively.

The relationship between Q_a and the heat of combustion, Q_c, depends upon the combustion products. If these are carbon dioxide, water, and rhombic sulphur, then

[2] $$Q_a = -Q_c + 265.75\ n_C + 86.25\ n_H + 57\ n_S + 59.16\ n_O.$$

This equation is based upon heat of formation values for carbon dioxide and liquid water of 94.05 and 68.32 kilocalories per mole, respectively (3).

In view of the relationships between heats of combustion, formation, and atomization it is necessary to obtain a scheme for only one of them. In the following section this is done for heats of atomization.

EMPIRICAL SCHEMES FOR SULPHUR-CONTAINING COMPOUNDS

Heats of Atomization

The strength of all C—C bonds, denoted by c_1, and of the primary (p), secondary (s), and tertiary (t) C—H bonds is assumed to be the same as given in Part I, except in the case of C—H bonds when there is a sulphur atom bound to the carbon. These bonds, the bond symbol, and the bond strength are given in Table I.

TABLE I

Paraffin bond strengths

Bond	Symbol	Bond energy, kcal
C—C	c_1	85.40
C—H (primary)	p	98.47
C—H (secondary)	s	97.65
C—H (tertiary)	t	96.80

It is assumed that the presence of a C—S bond will affect the bond strength of hydrogen atoms bound to that carbon atom. These C—H bonds can be primary, secondary, or tertiary, and their strengths are denoted by p_s, s_s, or t_s respectively. It is further assumed that the S—C bond does not affect any other C—H bonds. Three types of bond directly involving sulphur atoms are considered. These are the S—H bond, of energy sh, the S—C bond, of energy sc, and the S—S bond, of energy ss. It is assumed that these bonds have the same energy in each of the three classes of sulphur compounds considered (alkanethiols, thiaalkanes, and dithiaalkanes).

Six quantities, sh, sc, ss, p_s, s_s, and t_s, must be determined from the experimental data. This has been done by a standard least-squares procedure, carried out on the IBM 650 computer through the courtesy of the staff of the Computing Center of the University of Ottawa. In this way the values given in Table II were obtained.

TABLE II

The bond strengths for sulphur compounds

$sh = 81.90$	$p_s = 98.14$
$sc = 66.36$	$s_s = 97.63$
$ss = 54.46$	$t_s = 97.14$

Heats of atomization calculated from these values, together with those in Table I, are compared with the experimental heats of atomization for various compounds in Table III. The heats of formation of the gaseous compounds at 25° C are also given in Table III.

TABLE III

Sulphur compounds: heats of atomization

Compound	Bonds	Q_f(obs.), kcal/mole	Q_a(obs.), kcal/mole	Q_a(calc.), kcal/mole	Q(obs.) − Q(calc.)	Ref.
Ethanethiol C_2H_6S	$sh+sc+2s_a+3p+c_1$	11.03	724.0	724.3	−0.3	4
2-Thiapropane C_2H_6S	$2sc+6p_a$	8.98	721.9	721.6	0.3	4
2,3-Dithiabutane $C_2H_6S_2$	$2sc+ss+6p_a$	5.75	775.7	776.0	−0.3	14
1-Propanethiol C_3H_8S	$sh+sc+2s_a+3p+2s+2c_1$	16.04	1004.9	1005.0	−0.1	12
2-Propanethiol C_3H_8S	$sh+sc+t_a+6p+2c_1$	18.04	1006.9	1007.0	−0.1	13
2-Thiabutane C_3H_8S	$2sc+3p_a+2s_a+3p+c_1$	14.07	1002.9	1003.2	−0.3	17
1-Butanethiol $C_4H_{10}S$	$sh+sc+2s_a+3p+4s+3c_1$	20.87	1285.6	1285.7	−0.1	5, 6
2-Butanethiol $C_4H_{10}S$	$sh+sc+t_a+6p+2s+3c_1$	22.97	1287.7	1287.7	0	5, 7
2-Methyl-1-propanethiol $C_4H_{10}S$	$sh+sc+2s_a+6p+t+3c_1$	23.06	1287.8	1287.7	0.1	5, 8
2-Methyl-2-propanethiol $C_4H_{10}S$	$sh+sc+9p+3c_1$	25.99	1290.7	1290.7	0	9
3-Thiapentane $C_4H_{10}S$	$2sc+4s_a+6p+2c_1$	19.77	1284.5	1284.9	−0.4	5, 15
2-Thiapentane $C_4H_{10}S$	$2sc+3p_a+2s_a+3p+2s+2c_1$	19.36	1284.1	1283.9	0.2	5, 6
3-Methyl-2-thiabutane $C_4H_{10}S$	$2sc+3p_a+t_a+6p+2c_1$	21.43	1286.1	1285.9	0.2	5, 16
3,4-Dithiahexane $C_4H_{10}S_2$	$2sc+ss+4s_a+6p+2c_1$	17.42	1339.1	1339.3	−0.2	14
1-Pentanethiol $C_5H_{12}S$	$sh+sc+2s_a+3p+6s+4c_1$	26.29	1566.9	1566.4	0.5	10, 11
4,5-Dithiaoctane $C_6H_{14}S_2$	$2sc+ss+4s_a+6p+4s+4c_1$	27.77	1901.2	1900.7	0.5	14
5-Thiononane $C_8H_{18}S$	$2sc+4s_a+6p+8s+6c_1$	40.3*	2408.5	2407.7	0.8	11

*T = 20° C; this compound was not included in the least-squares calculation.

The S—H, S—C, and S—S bond energies have also been given by Sunner (11). Since these are based upon heats of sublimation of graphite and rhombic sulphur of 138 and 66.3 kilocalories per mole, respectively, they are not directly comparable to the bond energies derived in this paper.

Heats of Vaporization

In Part I a scheme was developed which related the heat of vaporization (ΔH_v) to bond contributions. This scheme may now be extended to the sulphur compounds. The bond terms are the same as those used for the heats of atomization; they were evaluated by the least-squares procedure in the computer, and are given in Table IV. As in the

TABLE IV

Bond contributions to the heat of vaporization of sulphur compounds

$sh = 2.209$	$p_a = 0.877$
$sc = 0.735$	$s_a = 1.002$
$ss = 2.349$	$t_a = 1.117$

previous treatment, all C—C bonds are assumed to make a contribution of zero. The C—H contributions when there is no sulphur atom bound to the carbon are, as given in Part I,

$$p = 0.494 \text{ kcal/mole,}$$
$$s = 0.579 \text{ kcal/mole,}$$
$$t = 0.518 \text{ kcal/mole.}$$

Table V gives the experimental and calculated heats of vaporization, and the difference between them for each compound. The source of the heat of vaporization data is given in Table III.

TABLE V

Heats of vaporization of sulphur compounds

Compound	ΔH_v(obs.), kcal/mole	ΔH_v(calc.), kcal/mole	ΔH_v(obs.) − ΔH_v(calc.)
Ethanethiol	6.58	6.68	−0.10
2-Thiapropane	6.66	6.73	−0.07
2,3-Dithiabutane	9.18	9.08	0.10
1-Propanethiol	7.65	7.59	0.06
2-Propanethiol	7.08	7.03	0.05
2-Thiabutane	7.61	7.59	0.02
1-Butanethiol	8.74	8.75	−0.01
2-Butanethiol	8.13	8.18	−0.05
2-Methyl-1-propanethiol	8.30	8.43	−0.13
2-Methyl-2-propanethiol	7.39	7.39	0.00
3-Thiapentane	8.57	8.44	0.13
2-Thiapentane	8.67	8.74	−0.07
3-Methyl-2-thiabutane	8.18	8.18	0.00
3,4-Dithiahexane	10.86	10.79	0.07
1-Pentanethiol	9.83	9.90	−0.07
4,5-Dithiaoctane	12.94	13.11	−0.17
5-Thianonane	12.4	13.1	−0.7

HEAT OF ATOMIZATION CONTRIBUTIONS FOR COMPOUNDS CONTAINING OXYGEN

The data available for the oxygen analogues of the above sulphur compounds are not as plentiful, and in most cases they are not as reliable. The manner of treatment is the same as for the sulphur compounds: thus C—H bonds are assumed to be affected by the presence of oxygen only when the oxygen is attached to the same carbon atom, and all other interactions are neglected. The C—H bonds evaluated, with an oxygen bound to the carbon, and the symbols used to denote their energies are: the C—H primary, p_o; the C—H secondary, s_o; and the C—H tertiary, t_o. The bonds involving oxygen directly are the O—H bond, oh; the O—C bond, oc; and the O—O bond, oo. The bond energy terms were evaluated by putting the least-squares method in the computer. The bond energies are given in Table VI. The bonds involved, the heats of formation, and the experimental and calculated heats of atomization are given in Table VII.

TABLE VI

The bond strengths for oxygen compounds

$oh = 109.79$	$p_o = 96.24$
$oc = 90.99$	$s_o = 95.42$
$oo = 47.72$	$t_o = 94.54$

TABLE VII

Oxygen compounds: heats of atomization

Compound	Bonds	Q_f(obs.) (g, 25° C), kcal/mole	Q_a(obs.), kcal/mole	Q_a(calc.), kcal/mole	Q_a(obs.) − Q_a(calc.)	Ref.
Ethanol C_2H_6O	$oh+oc+2s_o+3p+c_1$	56.24	771.3	772.4	−1.1	3
Methyl ether C_2H_6O	$2oc+6p_o$	44.3	759.4	759.4	0.0	3
2-Propanol C_3H_8O	$oh+oc+t_o+6p+2c_1$	65.96*	1056.9	1056.9	0.0	19
1-Butanol $C_4H_{10}O$	$oh+oc+2s_o+3p+4s+3c_1$	67.84†	1334.7	1333.8	0.9	20
2-Methyl-2-propanol $C_4H_{10}O$	$oh+oc+9p+3c_1$	77.0	1343.9	1343.2	0.7	21
Diethyl peroxide $C_4H_{10}O_2$	$2oc+oo+4s_o+6sp+2c_1$	47.3	1373.3	1373.0	0.3	22
Diisopropyl ether $C_6H_{14}O$	$2oc+2t_o+12p+4c_1$	75.68†	1894.3	1894.3	0.0	19
2-Ethyl-1-hexanol $C_8H_{18}O$	$oh+oc+2s_o+6p+8s+t+7c_1$	87.43†	2457.8	2458.2	−0.4	20
Di(tert-butyl) peroxide $C_8H_{18}O_2$	$2oc+oo+18p+6c_1$	84.7	2514.2	2514.6	−0.4	21

*ΔH_f (l, 25° C) was given in the reference; ΔH_f (g, 25° C) was calculated from ΔH_f (1) and vapor pressure data (19).

†ΔH_f (l, 25° C) was given in the reference; ΔH_f (g, 25° C) was calculated from ΔH_f (1) and ΔH_v as calculated by the method given in Part I.

HEATS OF FORMATION AND COMBUSTION

Using the method described in Part I, bond contributions have been evaluated for the heats of formation and combustion of the gaseous and liquid compounds: these are given in Table VIII. For sulphur compounds, the products of combustion are taken to be water,

TABLE VIII

Bond contributions to heats of atomization, formation, and combustion of sulphur- and oxygen-containing liquids and gases

Bond	Symbol	Q_a		Q_f		Q_c	
		Gas	Liquid	Gas	Liquid	Gas	Liquid
C—C	c_1	85.40	85.40	−0.45	−0.45	47.48	47.48
C—H	p	98.47	98.96	3.45	3.94	54.22	53.73
C—H	s	97.65	98.23	2.63	3.21	55.04	54.46
C—H	t	96.80	97.32	1.78	2.30	55.89	55.37
S—H	sh	81.90	84.11	1.31	3.52	32.85	30.64
S—C	sc	66.36	67.10	−5.07	−4.33	28.58	27.84
S—S	ss	54.46	56.81	−2.34	0.01	2.34	0
C—H	p_s	98.14	99.02	3.12	4.00	54.55	53.67
C—H	s_s	97.63	98.63	2.61	3.61	55.06	54.06
C—H	t_s	97.14	98.26	2.12	3.24	55.55	54.43
O—H	oh	109.79		28.12		6.04	
O—C	oc	90.99		18.48		5.03	
O—O	oo	47.72		−11.44		11.44	
C—H	p_o	96.24		1.22		56.45	
C—H	s_o	95.42		0.40		57.27	
C—H	t_o	94.54		−0.48		58.15	

carbon dioxide, and rhombic sulphur. In practice the combustion products are carbon dioxide, and an aqueous sulphuric acid solution.

DISCUSSION

The differences between the experimental and calculated heats of formation indicate that the scheme is more successful with the sulphur compounds than with the oxygen compounds. This is probably because the experimental data are more accurate in the case of the former than the latter. The authors feel that the relatively poor agreement between the experimental and calculated heats of atomization of the oxygen compounds points out the need for more accurate heat of formation data on the various homologous series.

ACKNOWLEDGMENT

REFERENCES

1. K. J. LAIDLER. Can. J. Chem. 34, 626 (1956).
2. T. L. COTTRELL. The strengths of chemical bonds. Butterworths Scientific Publications, London. 1958.
3. U.S. NATIONAL BUREAU OF STANDARDS. Selected values of chemical thermodynamic properties. Ser. I. Washington. 1952.
4. J. P. MCCULLOUGH, W. N. HUBBARD, F. R. FROW, I. A. HOSSENLOPP, and G. WADDINGTON. J. Am. Chem. Soc. 79, 561 (1957).
5. W. N. HUBBARD, W. D. GOOD, and G. WADDINGTON. J. Phys. Chem. 62, 614 (1958).
6. D. W. SCOTT, H. L. FINKE, W. N. HUBBARD, J. P. MCCULLOUGH, G. D. OLIVER, M. E. GROSS, C. KATZ, K. D. WILLIAMSON, G. WADDINGTON, and H. M. HUFFMAN. J. Am. Chem. Soc. 79, 1062 (1957).
7. J. P. MCCULLOUGH, H. L. FINKE, D. W. SCOTT, R. E. PENNINGTON, M. E. GROSS, J. F. MESSERLY, and G. WADDINGTON. J. Am. Chem. Soc. 80, 4786 (1958).
8. D. W. SCOTT, J. P. MCCULLOUGH, J. F. MESSERLY, R. E. PENNINGTON, I. A. HOSSENLOPP, H. L. FINKE, and G. WADDINGTON. J. Am. Chem. Soc. 80, 55 (1958).

9. J. P. McCullough, D. W. Scott, H. L. Finke, W. N. Hubbard, M. E. Gross, C. Katz, R. E. Pennington, J. F. Messerly, and G. Waddington. J. Am. Chem. Soc. **75**, 1818 (1953).
10. W. N. Hubbard, C. Katz, and G. Waddington. J. Phys. Chem. **58**, 142 (1954).
11. S. Sunner. Acta Chem. Scand. **9**, 837 (1955).
12. R. E. Pennington, D. W. Scott, H. L. Finke, J. P. McCullough, J. F. Messerly, I. A. Hossenlopp, and G. Waddington. J. Am. Chem. Soc. **78**, 3266 (1956).
13. J. P. McCullough, H. L. Finke, D. W. Scott, M. E. Gross, J. F. Messerly, R. E. Pennington, and G. Waddington. J. Am. Chem. Soc. **76**, 4796 (1954).
14. W. D. Scott and J. P. McCullough. J. Am. Chem. Soc. **80**, 3547 (1958).
15. W. D. Scott, H. L. Finke, W. N. Hubbard, J. P. McCullough, G. D. Oliver, M. E. Gross, C. Katz, K. D. Williamson, G. Waddington, and H. M. Huffman. J. Am. Chem. Soc. **74**, 4656 (1952).
16. J. P. McCullough, H. L. Finke, J. F. Messerly, R. E. Pennington, I. A. Hossenlopp, and G. Waddington. J. Am. Chem. Soc. **77**, 6119 (1955).
17. D. W. Scott, G. B. Guthrie, J. P. McCullough, and G. Waddington. J. Chem. & Eng. Data Ser. **4**, No. 3, 246 (1958).
18. K. D. Williamson and R. H. Harrison. J. Chem. Phys. **26**, 1409 (1957).
19. G. S. Parks and K. E. Manchester. I.U.P.A.C. Sub-Commission on Experimental Thermochemistry. Thermochemical Bull. No. 2, March, 1956; the value is quoted with the kind permission of Professor G. S. Parks.
20. J. Tjebbes. Acta Chem. Scand. **14**, 180 (1960).
21. J. H. Raley, F. F. Rust, and W. E. Vaughan. J. Am. Chem. Soc. **70**, 88 (1948).
22. R. E. Rebbert and K. J. Laidler. J. Chem. Phys. **20**, 574 (1952).

ABOUT THE PRIMARY ACT OF PHOTOCHEMICAL DECOMPOSITION REACTIONS OF MONOSUBSTITUTED COBALTIHEXAMINE IONS[1]

Z. SIMON

ABSTRACT

We will discuss the primary act of photochemical decomposition of $Co(NH_3)_5X^{n+}$ ions in aqueous solution. The potential energy surfaces are plotted correlating the complex ion's energy levels with those of the decomposition products. For this purpose spectral and kinetic data are used, as well as Wigner–Witmer correlation rules. The potential energy surfaces and certain rules regarding the radiationless transitions between them permit us to draw certain qualitative conclusions concerning these decompositions. Our conclusions seem to be confirmed by available experimental data.

INTRODUCTION

In order to describe the primary act of photochemical reactions, the potential energy surfaces of the molecules in their ground states and in electronically excited states, as well as the transition rates between the surfaces, should be known. Shuler (1) and Higuki (2) have discussed the photochemical decompositions of certain relatively simple molecules. They obtained the necessary surfaces by correlating the energy levels of the molecule and of the decomposition products, using the Wigner–Witmer correlation rules (3, 4). Linhard and Weigel (4a) have discussed the photochemical decomposition of the $Co(NH_3)_5X^{n+}$ ions based on ideas similar to those expressed in this article, without, however, taking into consideration the symmetry properties of the ions and the radiationless transitions.

In our paper we apply these correlation rules to more complicated molecules, namely to $Co(NH_3)_5X^{++}$ ions. We attach greater importance to the radiationless transitions than other authors and we use symmetry properties of the wave functions and the nuclear vibration co-ordinates. We proceed in the following manner: the decomposition of the molecule excited by light takes place following one of these processes:

1. The potential-energy surface for the excited state is unstable with respect to a vibrational co-ordinate along which the molecule is dissociated.

2. The electronic excitation energy is converted into vibrational energy of the ground state.

(a) If the vibration of a single valence bond is strongly enough excited, the molecule will immediately dissociate (predissociation).

(b) If a vibration which does not lead to direct dissociation is excited, the molecule will become vibrationally "overheated" and will either dissociate thermally or cool down without dissociation.

Should process 1 or 2 (a) take place, the quantum yield of the decomposition is about 1. Should process 2(b) take place, the quantum yield is small (ϕ smaller than about 0.01) for complex molecules as shown by Zimmermann (5) for the MnO_4^- ion. The correlation rules show whether process 1 or 2 takes place and indicate the decomposition products. If process 2 takes place, considerations regarding the radiationless transitions show whether it is a direct decomposition ($\phi \cong 1$) or a decomposition by the mechanism of the "hot" (i.e. containing excess vibrational energy) molecule ($\phi \gtrsim 0.01$).

Experimentally, it has been established that $Co(NH_3)_5X^{++}$ ions irradiated in aqueous solution undergo aquation and oxidation–reduction decomposition. Photochemical and thermal aquation reactions follow, according to Adamson and Sporer (6), Basolo and Pearson (7), an S_N1 mechanism with the primary act,

$$Co(NH_3)_5X^{++}\,(aq.) \rightarrow Co(NH_3)_5^{+++}\,(aq.) + X^-\,(aq.). \qquad [1]$$
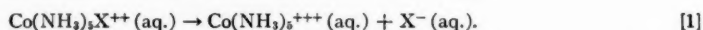
The primary act of the oxidation–reduction decomposition is also a unimolecular decomposition (6),

$$Co(NH_3)_5X^{++}\,(aq.) \rightarrow Co(NH_3)_5^{++}\,(aq.) + X\,(aq.). \qquad [2]$$
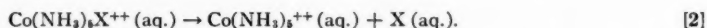
The quantum yields ϕ for irradiation with $\lambda = 370$ mμ and $\lambda = 550$ mμ, according to Adamson (6a), are given in Table I.

TABLE I

Experimental photochemical data (aqueous solutions $0.01\,M$; $25°$ C) (6a)

| Ion | ϕ and the nature of the reaction | | | | | | Thermal aquation rate, k, min^{-1} |
	370 mμ			550 mμ			
$Co(NH_3)_6^{+++}$	$<2\times10^{-3}$			$<2\times10^{-3}$			
$Co(NH_3)_5SO_4^+$		About 10^{-3}					7×10^{-5}
$Co(NH_3)_5F^{++}$		Small					4×10^{-6}
$Co(NH_3)_5Cl^{++}$	0.011	100% Tr	A R	1.5×10^{-3}	100% Tr	A R	1×10^{-4}
$Co(NH_3)_5Br^{++}$	0.21	50% 50%	A R	1.3×10^{-3}	100% Tr	A R	4×10^{-4}
$Co(NH_3)_5NO_2^{++}$	1.0	35% 65%	A R				$<1\times10^{-6}$
$Co(NH_3)_5SCN^{++}$	0.045	30% 70%	A R	6.7×10^{-4}	80% 20%	A R	2×10^{-7}
$Co(NH_3)_5N_3^{++}$	0.44	<1% 100%	A R	0.011	<1% 100%	A R	$<1\times10^{-6}$
$Co(NH_3)_5J^{++}$	0.66	<1% 100%	A R	0.10	<1% 100%	A R	5×10^{-4}

NOTE: A = aquation decomposition. R = oxidation–reduction decomposition. Tr = traces.

CORRELATION DIAGRAMS AND DECOMPOSITION PRODUCTS

The energy levels of $Co(NH_3)_5X^{++}$ ions were determined by using the spectral data of Nakamoto *et al.* (8) (and from tables (13)). The small differences of energy between the levels corresponding to the same spectral band are those calculated by Nakamoto *et al.* according to the simple molecular orbital method.

The energies for the ground states of the aquation reaction products (the right-hand equation [1] have been assumed equal to the activation energies for the thermal aquation reactions, that is about 1.1 ev (25 kcal/mole) for $X^{-1} = Cl^-$, Br^-, SCN^-, J^- and 1.5 ev (34 kcal/mole) for the aquation of the $Co(NH_3)_6^{+++}$ ion (7).

In order to calculate the energies of the ground states of oxidation–reduction decomposition products (the right-hand equation [2]), as sufficient data are not available to us, we will proceed as follows, based upon the observation of oxidation–reduction reaction traces at 370 mμ. We assume the energy of the ground state of $Co(NH_3)_5^{++}$ (aq.) + Cl (aq.) products should be 3.5 ev (a little more than the energy corresponding to 370 mμ), the corresponding energy of the $Co(NH_3)_5^{++}$ (aq.) + X (aq.) products being 3.5 ev plus the difference of energy ΔE_x between the process Cl^- (aq.) $\rightarrow$ Cl (aq.) + e and the processes:

$$\text{Br}^- \text{ (aq.)} \rightarrow \text{Br (aq.)} + e \qquad\qquad \Delta E_{\text{Br}} = -0.5 \text{ ev}$$

$$\text{J}^- \text{ (aq.)} \rightarrow \text{J (aq.)} + e \qquad\qquad \Delta E_{\text{J}} = -1.0 \text{ ev}$$

$$\text{NH}_3 \text{ (aq.)} \rightarrow \text{NH}_3{}^+\text{(aq.)} + e \qquad\qquad \Delta E_{\text{NH}_3} = +1.5 \text{ ev}$$
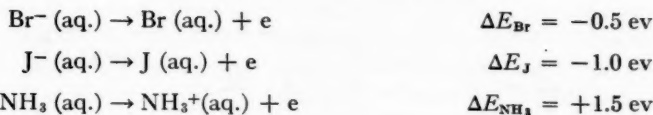
The values for ΔE_x were taken from (8) and thermochemical data (9).

A not very reliable, approximate, estimate of the difference between the energies of the products $\text{Co(NH}_3)_5{}^{++} + \text{Cl}$ and $\text{Co(NH}_3)_5{}^{+++} + \text{Cl}^-$ can be obtained identifying this difference with the enthalpy $\Delta H = \Delta H_2 - \Delta H_1 + \Delta H_3$ of the reactions:

$$\text{Co(NH}_3)_6{}^{++} \text{ (aq.)} \rightleftarrows \text{Co(NH}_3)_6{}^{+++} \text{ (aq.)} + e \quad \Delta H_1$$

$$\text{Cl}^- \text{ (aq.)} \rightleftarrows \tfrac{1}{2}\text{Cl}_2\text{(g.)} + e \quad \Delta H_2$$

$$\tfrac{1}{2}\text{Cl}_2\text{(g.)} \rightleftarrows \text{Cl (aq.)} \quad \Delta H_3$$
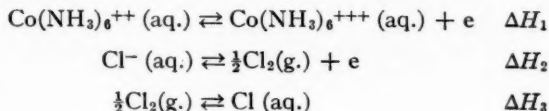
$\Delta H_2 - \Delta H_1 = 1.36 - 0.16 = 1.2$ ev (9) respectively Lamb and Larson (14), $\Delta H_3 \cong 1.2$ ev (9).

Thus $\Delta H \cong 2.4$ ev and the energy of the $\text{Co(NH}_3)_5{}^{++} + \text{Cl}$ products would be approximately $2.4 + 1.1 = 3.5$ ev. The value is perhaps an upper limit, as $\text{Co(NH}_3)_6{}^{+++}$ is more stable than $\text{Co(NH}_3)_6{}^{++}$ towards the dissociation of a NH_3 group.

We supposed that the energies of the first excited states of the $\text{Co(NH}_3)_5{}^{+++}$ are approximately equal to the excitation energies corresponding to the crystalline field bands in the $\text{Co(NH}_3)_5\text{X}^{n+}$ ions. This hypothesis appears plausible from the point of view of the crystalline field theory and from the fact that the position of the ligand field bands is approximately the same in the $\text{Co(NH}_3)_6{}^{+++}$, $\text{Co(NH}_3)_5\text{Cl}^{++}$, etc. ions (about 2.5 ev and 3.3 ev (8)). It also agrees with the result of the calculation based on the simple molecular orbital method (used for the excited energy levels of the aquation and oxidation–reduction decomposition products). The excited states of the halogen ions and of the NH_3 groups have not been taken into consideration because they have a very high energy. The position of the excited levels of the oxidation–reduction decomposition is less important (at least for not too short wave lengths) for the interpretation of the correlation diagrams because the energy of the ground state is high enough.

In Figs. 1, 2, 3, and 4 the energy levels of some complex ions have been listed on the left and the levels of the decomposition products on the right. The capital letters beside the energy levels represent electronic states having energy equal or approximately equal to that indicated by the level. The identification of the electronic states of complex ions with the energy levels observed spectroscopically was performed by taking into account the order of the molecular orbital energy levels calculated by Nakamoto et al. (8) and the degree of their occupation. The states of the oxidation–reduction decomposition products are starred. The capital letters show the species of the C_{4v} point group to which the respective electronic states belong. The states of the $\text{Co(NH}_3)_6{}^{+++}$ ion are recorded considering the resolution of the species belonging to the O_h point group to those of the C_{4v} point group. According to Nakamoto (8), the states marked in $E(\text{I})$, $E(\text{II})$, B_2, and A_2 which derive from the electronic configuration $(1e_g)^4(1a_{1g})^2(1f_{1u})^6(2f_{2g})^5$ $(2e_g)$ belong to the two energy levels which correspond to the first two absorption bands of the $\text{Co(NH}_3)_6{}^{+++}$ ion. The attribution of these two states to the two energy levels is arbitrary. This does not affect the interpretation of the correlation diagrams, if the states of the dissociation products with which these states can be correlated are higher than the two first levels of the $\text{Co(NH}_3)_6{}^{+++}$ ion. This is the case if the first excited
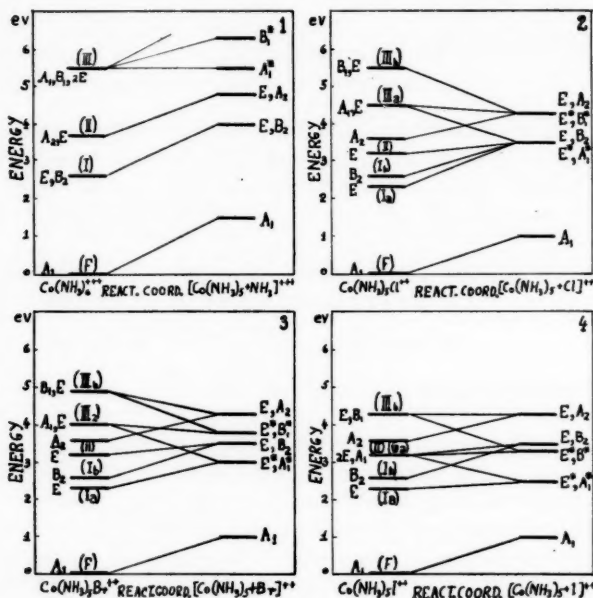
FIGS. 1–4.   Correlation diagrams for the $Co(NH_3)_6^{+++}$, $Co(NH_3)_5Cl^{++}$, $Co(NH_3)_5Br^{++}$, and $Co(NH_3)_5J^{++}$ ions.

state of the $Co(NH_3)_5^{+++}$ ion has approximately the same energy as in the $Co(NH_3)_6^{+++}$ ion; the reasons for this situation were discussed above.

In every case the energy of the complex ion's ground state was taken as origin in the scale of energies.

The energy levels of the complex ions are correlated with those of the aquation reaction products and of the oxidation–reduction decomposition products using the Wigner–Witmer correlation rules (3, 4). In the course of the decomposition (the elimination of X or X$^-$), the symmetry of the system remains C_{4v}. Although we are concerned with polyatomic molecules, we shall assume that only one vibrational co-ordinate varies. Thus, only the surfaces of different species of the molecular point group can intersect each other. In the case of the decomposition of the $Co(NH_3)_5X^{++}$ ions, no new valence bonds are formed, so that we assume that the electronic energy of different states changes continuously with respect to the reaction co-ordinate.*

Levels III from ultraviolet ($\lambda \gtrsim 300$ mμ) correlate with lower levels of the ionic and oxidation–reduction decomposition products. That is why in ultraviolet the quantum yield for the redox and aquation reactions should approach 1 (or be even greater if

If the energy levels were known more exactly, it would be useful to correlate first the "crystalline field (the Co^{+3}) states" of the reactants with those of the ionic decomposition products and the "charge transfer (the Co^{+2}) states" with those of the redox decomposition products. Afterwards, taking into account the configuration interaction which appears between some Co^{+3} and Co^{+2} states, a correlation diagram would be obtained which respects the Wigner–Witmer non-crossing rules and also indicates intermediate maxima on potential-energy curves. For example, the E(II) state of $Co(NH_3)_5Cl^{++}$ would correlate with the state E at about 4.3 ev of the ionic decomposition products; configuration interaction with the E(IIIa) (which without Cl correlates with the E level at 3.5 ev) state would produce the correlation with an E* level at about 3.5 ev, producing also a maxima on the E(II)−E* potential curve.

chain reactions are involved). The decomposition should take place by process 1. The I and II levels of the near ultraviolet and visible spectrum usually correlate with higher states of the decomposition products. For this reason, the decomposition at 370 mμ and 550 mμ for which ϕ was measured will take place via process 2. Figures 1, 2, 3, 4 show that the oxidation–reduction decomposition is favored by the increase in oxidizability of X$^-$ in the series NH$_3$, Cl$^-$, Br$^-$, J$^-$. For instance, the level I (corresponding to the first crystalline field band) of Co(NH$_3$)$_5$Cl^{++} correlate with higher levels of the decomposition products. For Co(NH$_3$)$_5$J^{++} the first excited level $E(I)$ already correlates with level E^* of the oxidation–reduction decomposition products which is approximately isoenergetic. The correlation diagrams show that the complex ions in their ground state may only undergo aquation reaction. The data in Table I confirm the favoring of the oxidation–reduction decomposition passing from Co(NH$_3$)$_6$$^{+++}$ to Co(NH$_3$)$_5$J^{++}. The complex ions in Table I are placed, according to Adamson, approximately in the ascending order of oxidizability of X$^-$.

RADIATIONLESS TRANSITIONS. QUANTUM YIELDS

When we plotted the correlation diagrams we considered the singlet states alone. The neglect of the triplet states is justified by the following three circumstances: Nakamoto (8) succeeded in interpreting the absorption spectra of these complexes on the ground of only their singlet states. According to Kasha (10) the radiationless transitions between excited singlet states are much more rapid than those between singlet and triplet states. In some previous papers (11), we have shown that radiationless singlet–singlet transitions can occur with a high probability (corresponding to a rate of approximately 10^{10} sec^{-1}) if the interaction between the movement of the electrons and that of the nuclei is strong enough and the anharmonicity of the nuclear movement great enough. The interaction energy W_{AB}, which produces the transition between the potential-energy surfaces A and B, is equal to

$$[3] \qquad W_{AB} = \frac{h^2}{2\pi^2 M} \int \phi_A^* \frac{\partial \phi_B}{\partial r}\, dr \int X_A^* \frac{\partial X_B}{\partial r}\, dx.$$

X_A and X_B are electronic wave functions; ϕ_A and ϕ_B are vibrational wave functions in the Born–Oppenheimer approximation; x stands for electronic co-ordinates, r the vibrational (nuclear) ones, and M is the corresponding reduced nuclear mass. Formula [3] is obtained by a method of first approximation in relation to the Born–Oppenheimer approximation (11) (see likewise Hellmann (12)). In our case we have diluted aqueous non-fluorescent solutions (7). That is why we do not consider the possibility of intermolecular energy transfer between the complex ions and we shall assume that the radiationless transitions have a high rate ($> 10^{10}$ sec^{-1}) unless they are forbidden by symmetry considerations.

In this way, we can explain the low quantum yields for the aquations at $\lambda = 550$ mμ (see Table I) and also at 370 mμ for Co(NH$_3$)$_5$Cl^{++} and the preceding ions. The correlation diagrams show that the decomposition in this case will take place according to process 2. Let us show that process 2(a) is prevented for reasons of symmetry, so that the decomposition actually takes place according to process 2(b), for which we must expect $\phi \gtrsim 0.01$. The dissociation of particle X in Co(NH$_3$)$_5$X^{++} does not change the symmetry of the system, therefore the vibrational co-ordinate r and also $\partial/\partial r$ belong to the A_1 species. The electronic function of the ground state also belongs to A_1 species. In order that integral $\int X_A^*(\partial X_B/\partial r)dx$ should not vanish, the electronic wave function

X_B of the excited state must also belong to the A_1 species (independent of the vibrational wave functions ϕ_A and ϕ_B, which are not implied in this integral). As may be seen in Nakamoto's work (8), it is only by absorption in the relative distant ultraviolet that such a state can be obtained.

It remains to be explained why aquation is not produced by the elimination of the NH_3 molecule. The activation energy for the elimination of NH_3, at least from $Co(NH_3)_6{}^{+++}$, is greater than for the elimination of halogen (1.5 ev instead of 1.1 ev (7)). According to Zimmermann's arguments, this fact explains why NH_3 is eliminated with greater difficulty than X^- in the case of process 2(b). But process 2(a) is no longer prevented for reasons of symmetry, because the elimination of NH_3 considerably modifies the symmetry of the complex. For the ions under consideration, however, the five or six Co–NH_3 valency vibrations interact strongly. That is why the elimination of NH_3 can only be achieved by the simultaneous excitation of the five or six corresponding normal vibrations. The interaction energy W_{AB} (formula [3]) is also proportional to the integral $\int \phi_A^* (\partial \phi_B / \partial r) dr$. In this integral the derivative is only once performed with respect to a single normal vibrational co-ordinate. There remain as factors four or five overlap integrals amid a vibration function corresponding to a low vibrational quantum number (from ϕ_A) and a function for a high quantum number (from ϕ_B). We have shown that such overlap integrals are small (11). Therefore, the electronic excitation energy will be converted into the energy of a vibration that leads to the formation of a "hot" molecule (process 2(b)).

CONCLUSIONS

We applied the Wigner–Witmer correlation rules to discuss the photochemical decomposition of certain molecules more complex than those to which these rules have so far been applied. We discussed in greater detail than in other papers of this kind the radiationless transitions between different potential-energy surfaces. Theoretical considerations suggest the following mechanism for the photochemical decomposition of the $Co(NH_3)_5X^{++}$ ions:

(a) Through excitation with fairly short wave-length light ($\lambda \gtrsim 220$ mμ for $Co(NH_3)_6{}^{+++}$, $\lambda \gtrsim 350$ mμ for $Co(NH_3)_5Br^{++}$) unstable states with respect to the dissociation of atom X or of ion X^- (or rather $NH_3{}^+$ and NH_3) are obtained. Both aquation and oxidation–reduction decomposition should take place with a large total quantum yield ($\phi \cong 1$).

(b) Through excitation with longer wave-length light only ionic dissociation (followed by aquation) occurs according to the "hot" molecule mechanism. Hence the quantum yield is low. As we indicated above, the most stable of the ions is $Co(NH_3)_6{}^{+++}$.

The experimental data of Adamson (6a) (Table I) agree with this mechanism, which, however, differs from that suggested by Adamson and Sporer (6). They assume the same initial stage for all the wave lengths—an internal oxidation–reduction reaction—the final transformation of the ion depending on the subsequent stages.

Their mechanism also explains the photochemical decomposition characteristics of the complex ions, but according to the correlation diagrams by the excitation with $\lambda = 550$ mμ the energy is in many cases insufficient for redox decomposition. It is true that the value assumed for the ground state of the $Co(NH_3)_5{}^{++} + Cl$ (and therefore also for $Co(NH_3)_5{}^{++} + X$) is not too reliable. If, however, the redox decomposition products separate with an energy excess of 0.5 ev or more, considering the activation energy of

diffusion in water (which is about 0.15 ev) it seems improbable that the cage effect of the solvent should be capable of providing the recombination of the dissociated particles, as stated by Adamson and Sporer (6).

ACKNOWLEDGMENTS

We are indebted to Dr. Léo Marion, who was so kind to give us the opportunity of seeing the preprint of a paper by Adamson (6a) (from the Discussion meeting of the Faraday Society, April 1960).

REFERENCES

1. K. E. SHULER. J. Chem. Phys. **21**, 624 (1953).
2. K. HIGUKI. Bull. Chem. Soc. Japan, **30**, 382 (1957).
3. J. NEUMANN and E. WIGNER. Physik. Z. **30**, 467 (1929).
4. K. J. LAIDLER. The chemical kinetics of excited states. Oxford at the Clarendon Press. 1955. p. 21.
4a. M. LINHARD and M. WEIGEL. Z. anorg. Chem. **266**, 49 (1951).
5. G. ZIMMERMANN. J. Chem. Phys. **23**, 825 (1955).
6. A. ADAMSON and A. SPORER. J. Am. Chem. Soc. **80**, 3865 (1958).
6a. A. W. ADAMSON. Discussions Faraday Soc. (1960).
7. F. BASOLO and R. G. PEARSON. Mechanisms of inorganic reactions. John Wiley & Sons, Inc., New York. 1958. Chap. 3.
8. K. NAKAMOTO, J. FUJITA, M. KOBAYASHI, and R. TSUCHIDA. J. Chem. Phys. **27**, 439 (1957).
9. A. F. KAPUSTINSSKI. Termiceskie Konstanty neorganiceskich beskestv. izd. Akad. Nauk S.S.S.R. Moskov, Leningrad. 1949. Tables.
10. M. KASHA. Discussions Faraday Soc. **9**, 14 (1950).
11. Z. SIMON. Studii si cercetări de fizică, **9**, 469 (1958); **10**, 291, 317 (1959).
12. H. HELLMANN. Einführung in die Quantenchemie Deuticke, Leipzig, Wien. 1937. Chap. VIII.
13. LANDOLT-BÖRNSTEIN. Tabellen Bd. 1. 3 Teil: Molekeln 2. Springer-Verlag, Berlin. 1951.
14. A. B. LAMB and A. T. LARSON. J. Am. Chem. Soc. **42**, 2024 (1920).

CONSTITUTION OF AN ARABINOGALACTAN FROM MAPLE SAP[1]

G. A. Adams and C. T. Bishop

ABSTRACT

An arabinogalactan ($[\alpha]_D^{25}$ −41°) has been isolated from maple sap in yields varying between 7.5 and 17.0 mg per 100 ml of sap. The polysaccharide was electrophoretically homogeneous and contained D-galactose, L-arabinose, and rhamnose in a molar ratio of 51:44:5. Methylation and hydrolysis of the polysaccharide yielded the following O-methyl ethers which were analyzed by gas–liquid partition chromatography: 2,3,5-tri-O-methyl-L-arabinose (4 moles); 2,5-di-O-methyl-L-arabinose (2 moles); 2,4-di-O-methyl-D-galactose (4 moles); 2,4,6-tri-O-methyl-D-galactose (7 moles); 2,3,4-tri-O-methyl-L-rhamnose (1 mole). A possible structure for the polysaccharide is proposed and discussed in relation to other arabinogalactans.

One of the reasons for studying non-cellulosic wood polysaccharides is that a knowledge of their structures may help in elucidating the modes of formation and the physiological roles of these materials in the plant. In recent years there have been reports of the synthesis of polymeric carbohydrates by transglycosidation reactions catalyzed by enzymes extracted from plants (1, 2, 3). It seemed possible that a physiologically active material like wood sap might be rich in products of transglycosidation reactions and that it would be interesting to see, by correlation of structures, if such products bore any significance as precursors in the formation of non-cellulosic wood polysaccharides. Maple wood was chosen for this study because of its high production of sap and because the non-cellulosic polysaccharides of this wood had already been examined (4, 5).

A previous publication (6) described the isolation of a polysaccharide from maple sap, some of its properties, identification of the component monosaccharides, and showed that it was a true sap constituent and not of bacterial or fungal origin. The present report describes methylation studies on the maple sap polysaccharide and compares the main structural features with those of other arabinogalactans.

The polysaccharide, isolated from the non-dialyzable sap constituents by precipitation with ethanol, contained D-galactose, L-arabinose, and rhamnose and showed one large pand one small component on electrophoresis (6). One repetition of the fractional precipitation with ethanol (7) yielded the larger component in a form which gave a single sharp peak ($\mu = 9.36 \times 10^{-5}$ cm² volt⁻¹ sec⁻¹) on free-boundary electrophoresis in borate buffer (8). The relative amounts of constituent monosaccharides reported previously (6) were found to be inaccurate because of variations in reactivity of the different sugars with silver nitrate in the method used (9). The monosaccharide composition was therefore redetermined by a new method: the polysaccharide was hydrolyzed and the reducing sugars were converted to their glycosides which were then methylated completely by the Kuhn (10) procedure. The resulting mixture of fully methylated methyl glycosides was then analyzed by gas–liquid partition chromatography (11, 12) giving the separation shown in Fig. 1. Areas under the six peaks were measured and those arising from a single monosaccharide were totalled giving a molar ratio of galactose:arabinose:rhamnose of 51:44:5. It was possible to use this method here because each of the fully methylated monosaccharides was completely separated in both furanoside and pyranoside ring forms. It is interesting to note that considerable amounts of the furanoside forms of D-galactose and L-arabinose were present although the methanolysis was carried out under conditions that are generally considered to yield primarily pyranosides.

The polysaccharide was methylated to completion and hydrolyzed by formic acid (13). Paper chromatographic examination of this hydrolyzate revealed the presence of three components having the same mobilities as 2,3,5-tri-O-methyl arabinose; 2,4,6-tri-O-methyl galactose; and 2,4-di-O-methyl galactose. The mixture of O-methyl ethers was converted to methyl glycosides and examined by gas–liquid partition chromatography to give the separation shown in Fig. 2. Identities of the compounds listed were established by comparison of their retention volumes on the gas–liquid partition chromatogram with authentic samples and by their isolation as crystalline derivatives. The shoulder on peak 2, Fig. 2, was identified as methyl 2,3,4-tri-O-methyl α-L-(?)-rhamnopyranoside

FIG. 1. Separation of fully methylated methyl glycosides of sugars present in maple sap arabinogalactan. Conditions: butanediol succinate polyester liquid phase, 150° C, 150 ml argon/minute.

(I)   Methyl 2,3,4-tri-O-methyl-α-L-rhamnopyranoside.
(II) and (III) Methyl 2,3,5-tri-O-methyl-α-β-L-arabofuranoside.
(IV) Methyl 2,3,4-tri-O-methyl-α-β-L-arabopyranoside.
(V)   Methyl 2,3,5,6-tetra-O-methyl-α-β-D-galactofuranoside.
(VI) Methyl 2,3,4,6-tetra-O-methyl-α-β-D-galactopyranoside.

FIG. 2. Separation of methanolysis products from fully methylated maple sap arabinogalactan. Conditions: Apiezon M liquid phase, 150° C, 170 ml argon/minute.

(1)   Methyl 2,3,5-tri-O-methyl-α-β-L-arabofuranoside.
(2)   Methyl 2,5-di-O-methyl-α-β-L-arabofuranoside.
(3), (4), (5), and (6)   Not identified positively.
(7)   Methyl 2,4,6-tri-O-methyl-β-D-galactopyranoside.
(8)   Methyl 2,4,6-tri-O-methyl-α-D-galactopyranoside.
(9)   Methyl 2,4,-di-O-methyl-β-D-galactopyranoside.
(10) Methyl 2,4-di-O-methyl-α-D-galactopyranoside.

by separation of the mixture on butanediol succinate polyester liquid phase (see, for example, Fig. 1). This procedure also permitted the quantitative estimation of the rhamnose component. The amounts of the rhamnose moiety obtained here and in the preliminary study (6) were not sufficient for measurement of specific rotation. Its assignment as the normally occurring L-enantiomorph must therefore be regarded as tentative, although probably correct.

The components giving peaks 3, 4, 5, and 6 could not be identified positively. Peaks 3 and 4 (together, about 7% of the total mixture) had retention volumes in the range predicted for di-O-methyl pentoses but were different from glycosides of 2,3-, 2,4-, and 2,5-di-O-methyl-L-arabinose on the gas–liquid chromatogram. These peaks could represent glycosides of 3,4- and 3,5-di-O-methyl-L-arabinose or could be the separated anomeric glycosides of one of these isomers; however, lack of authentic samples prevented further investigation of these components. The component represented by peak 5 constituted less than 1% of the total mixture and was therefore regarded as of doubtful structural significance. Component 6 was different, on the gas–liquid chromatogram, from glycosides of all available O-methyl ethers of L-arabinose and D-galactose. When the mixture was run on a polar liquid phase (butanediol succinate polyester) component 6 had a much higher retention volume indicative of the presence of hydroxyl or other polar groups (12). In an attempt to isolate component 6 the mixture of glycosides was hydrolyzed by aqueous hydrochloric acid and separated into three fractions by preparative paper chromatography. These three fractions were then methanolyzed and examined by gas–liquid partition chromatography. No trace of component 6 could be found in these fractions or in methanolyzates of eluates from blank areas of the paper chromatograms. It must therefore be concluded that component 6 was an acid-labile artifact produced during the formic acid hydrolysis of the methylated polysaccharide. Such an artifact could be either a formate ester or an anhydro sugar and the former is favored because of the polar characteristics mentioned above. Quantitative estimation of those components in Fig. 2 that were identified gave a molar ratio of galactose:arabinose:rhamnose of 61:33:6 (see Fig. 3). This is low in arabinose when compared with the composition of the original polysaccharide (galactose:arabinose:rhamnose 51:44:5) and indicated that component 6 was probably an arabinose derivative. When the disappearance of component 6 after acid hydrolysis was observed some of the other components had already been isolated as crystalline compounds and it was not possible to reconstitute the mixture to see which component had increased at the expense of component 6. No new compounds were found after the disappearance of component 6 so it must have been a derivative of one of the other compounds in the mixture. It should be mentioned that components 3–6 inclusive were not detectable by paper chromatography and, indeed, the 2,5-di-O-methyl-L-arabinose may have been missed because of the difficulty in separating it from tri-O-methyl-D-galactose by that technique. The detection of unknown components is to be expected in the application of gas–liquid partition chromatography to this field; their identification will depend on the accumulation of pure standards and on improved gas–liquid chromatographic procedures that will permit their isolation.

Despite the presence of some unidentified methyl ethers the identification and estimation of the major components in the methanolysis products revealed the gross structural features of the polysaccharide. Figure 3 shows the molar ratio of the methyl ethers that were identified and a structure that would give those results. This structure is not proposed as unique or complete for the arabinogalactan from maple sap but simply serves

to illustrate those structural features that are known. Thus the predominant O-methyl ether was 2,4,6-tri-O-methyl-D-galactose which must have arisen from $1 \rightarrow 3$ linked D-galactose units as illustrated. The 2,4-di-O-methyl-D-galactose represented the only branch points found and originated from D-galactose units substituted in positions 1, 3, and 6. The 2,5-di-O-methyl-L-arabinose arose from chain-forming units joined through positions 1 and 3 and, because arabinose but not galactose was released by partial hydrolysis of the polysaccharide (6), these units could not have been interposed between galactose units but must have been joined to other arabinose residues as shown in Fig. 3. The 2,3,5-tri-O-methyl-L-arabinose and 2,3,4-tri-O-methyl-L-(?)-rhamnose repre-

	Moles
2,3,5-Tri-O-methyl-L-arabinose	4
2,5-Di-O-methyl-L-arabinose	2
2,4-Di-O-methyl-D-galactose	4
2,4,6-Tri-O-methyl-D-galactose	7
2,3,4-Tri-O-methyl-L-rhamnose	1

$$A1 \rightarrow 3G1 \rightarrow \begin{bmatrix} A3 \leftarrow 1A \\ 1 \\ \downarrow \\ 6 \\ 3G1 \end{bmatrix}_2 \rightarrow 3G1 \rightarrow \begin{matrix} A \\ 1 \\ \downarrow \\ 6 \\ 3G1 \end{matrix} \rightarrow \begin{matrix} R \\ 1 \\ \downarrow \\ 6 \\ 3G1 \end{matrix} \rightarrow \begin{bmatrix} 3G1 \end{bmatrix}_4 \rightarrow 3G$$

A = arabofuranose
G = galactopyranose
R = rhamnopyranose
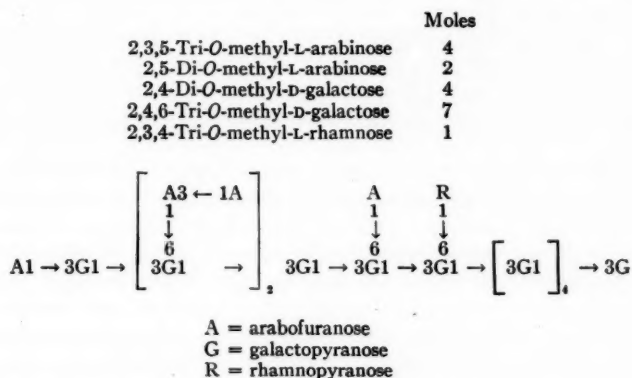
FIG. 3. Molar ratio of methylated sugars and a possible structure for the arabinogalactan.

sented terminal, non-reducing units. Of course, the galactan portion of the molecule need not be straight as shown but could consist of a branch-on-branch structure of $1 \rightarrow 3$ linked chains joined by $1 \rightarrow 6$ linkages.

It is clear from the foregoing evidence that the polysaccharides in maple sap bear no structural relation to the non-cellulosic polysaccharides of the wood which are predominantly acidic xylans (4, 5). The possibility exists that the arabinogalactans found in aqueous extracts of numerous woods (14) might be of sap origin rather than components of the plant tissue. An attempt to obtain further evidence on this point by examination of the sap from a tamarack tree which is rich in arabinogalactan was frustrated by a lack of sap flow. However, an examination of the structures reported for various arabinogalactans reveals some differences in the galactan portions of the molecules. In most of the water-soluble arabinogalactans from woods the *unbranched* portion of the galactan chain is formed by $1 \rightarrow 6$ linkages and gives rise to 2,3,4-tri-O-methyl-D-galactose after methylation and hydrolysis (14). On the other hand, in the more complex group of polysaccharides which form the plant gums, the unbranched portion of the galactan chain is usually formed by $1 \rightarrow 3$ linkages giving rise to 2,4,6-tri-O-methyl-D-galactose after methylation and hydrolysis (15). In this respect, and in having rhamnose as an integral part of its structure, the arabinogalactan from maple sap resembles more closely the plant gums than the water-soluble arabinogalactans of coniferous woods.

EXPERIMENTAL

Paper chromatograms were run by the descending method using the following solvent systems (v/v ratio):

(A) 2-butanone:water, azeotrope;
(B) n-butanol:ethanol:water, 9:3:3;
(C) n-butanol:ethanol:water, 40:11:19.

Reducing sugars were detected on chromatograms by the p-anisidine hydrochloride spray reagent (16). Evaporations were carried out at 35° C or less under diminished pressure and specific rotations are equilibrium values unless stated otherwise. Melting points are corrected.

Gas–liquid partition chromatography was done as previously described (12). The Pye argon chromatograph was used for the qualitative and quantitative estimations. Samples isolated by gas–liquid partition chromatography were collected from the effluent gas stream after separation on a modified (11) Podbielniack "Chromacon" (series 9475-3V).

Isolation of Polysaccharide, Electrophoresis, and Estimation of Constituent Sugars

The isolation and yields of polysaccharide from maple sap were described previously (6). The crude polysaccharide which contained a large and a small component as shown by electrophoresis was refractionated from aqueous solution by gradient addition of ethanol (7). A portion (150 mg) of the main fraction (precipitated at an ethanol concentration of 65%) was dissolved in 0.05 M borate buffer (15 ml) and dialyzed through cellophane against 3 liters of the buffer. The solution of polysaccharide was then subjected to electrophoresis in a Tiselius-type Spinco Model-H apparatus and showed a single, sharp, peak with $\mu = 9.36 \times 10^{-5}$ cm² volt⁻¹ sec⁻¹.

A sample (50 mg) of the polysaccharide was hydrolyzed by N sulphuric acid (2 ml) at 100° C in a sealed tube. Since no uronic acids were found in the previous investigation (6) the acid was neutralized by Amberlite IR-45 (OH) exchange resin and the filtrate was evaporated to dryness. The dried residue was refluxed with 4% methanolic hydrogen chloride for 20 hours, acid was neutralized with silver carbonate, and silver salts were filtered. The mixture of methyl glycosides obtained by evaporation of the filtrate was methylated by being shaken for 20 hours with silver oxide (200 mg) and methyl iodide (2 ml) in dimethylformamide (10 ml) (10). The silver salts were allowed to settle out and the clear supernatant was examined directly by gas–liquid partition chromatography to give the separation shown in Fig. 1. Areas under the peaks originating from a single monosaccharide were added together and the resulting three areas gave a molar ratio of galactose:arabinose:rhamnose of 51:44:5. Methyl α-D-glucopyranoside when methylated under the same conditions showed no partially methylated products detectable by gas–liquid partition chromatography or, after hydrolysis, by paper chromatography.

Methylation of Arabinogalactan

The polysaccharide (3.0 g) was methylated five times with 30% aqueous sodium hydroxide and dimethyl sulphate (17). The reaction mixture was extracted continuously with chloroform for 3 days and the extract was dried (anhydrous sodium sulphate) and evaporated to yield the partially methylated polysaccharide (2.08 g, methoxyl 34.7%; calc. methoxyl 41.3%). This product was methylated twice in tetrahydrofuran with solid sodium hydroxide and dimethyl sulphate (18) to yield a product having no hydroxyl absorption at 3500–3600 cm⁻¹. Precipitation from chloroform by addition of petroleum

ether (b.p. 30-60° C) yielded the fully methylated polysaccharide as a cream-colored powder, 1.47 g, $[\alpha]_D^{25} = -93°$ (c, 2% in chloroform), methoxyl = 40.7%.

Hydrolysis of Methylated Arabinogalactan

The fully methylated polysaccharide was hydrolyzed by formic acid according to the procedure of Jones and Wilkie (13). Paper chromatography of the hydrolyzate revealed three components with the following R_g values in solvents A and B respectively: component 1—1.01, 0.97; component 2—0.54, 0.82; component 3—0.22, 0.61. These values and the color reactions with the p-anisidine spray reagent were the same as those given by authentic samples of 2,3,5-tri-O-methyl-L-arabinose (component 1), 2,4,6-tri-O-methyl-D-galactose (component 2), and 2,4-di-O-methyl-D-galactose (component 3).

To obtain a quantitative estimate of the above components the mixture was refluxed for 20 hours with 4% methanolic hydrogen chloride and the methyl glycosides were analyzed by gas–liquid partition chromatography (11, 12). Figure 2 shows the separation obtained on a liquid phase of Apiezon M; separation on butanediol succinate polyester gave complete resolution of the shoulder on peak 2, which had the same retention volume as methyl-2,3,4-tri-O-methyl α-L-rhamnopyranoside, and permitted its quantitative estimation. The molar ratio of identified components (Fig. 3) was obtained by measurement of areas under the peaks on the gas–liquid partition chromatograms. These separations also provided additional evidence for the identities of the components which had the same retention volumes as authentic specimens.

In an attempt to isolate component 6, Fig. 2, the mixture of glycosides was hydrolyzed by N hydrochloric acid at 97° C for 24 hours. The hydrolyzate was neutralized by Amberlite IR-45 (OH) exchange resin and chromatographed on paper sheets in solvent C to give three fractions which were eluted from the papers and refluxed with 4% methanolic hydrogen chloride for 20 hours. Examination of the methanolyzates by gas–liquid partition chromatography showed that fraction 1 (R_g 0.9) contained only 2,3,5-tri-O-methyl-L-arabinose; fraction 2 (R_g 0.8) contained 2,4,6-tri-O-methyl-D-galactose and 2,5-di-O-methyl-L-arabinose; and fraction 3 (R_g 0.6) contained only 2,4-di-O-methyl-D-galactose. No component corresponding to peak 6, Fig. 2, was found in methanolyzates of eluates from blank areas of these chromatograms.

Identification of O-Methyl Ethers

2,3,5-Tri-O-methyl-L-arabinose

A sample of the mixed anomeric methyl glycosides of this component was collected from the effluent gas stream of the gas–liquid partition chromatogram. Hydrolysis, bromine oxidation, lactonization, and reaction with methanolic ammonia yielded 2,3,5-tri-O-methyl-L-arabonamide (19), which was crystallized from ethyl acetate:petroleum ether (b.p. 30–60° C) to a melting point of 134–136° C, $[\alpha]_D^{27} = +18°$ (c, 0.35% in methanol).

2,4,6-Tri-O-methyl-D-galactose

The anomeric glycosides were collected separately from the gas–liquid partition chromatogram. The faster-moving component (peak 7, Fig. 2) was crystallized from petroleum ether (b.p. 30–60° C) as fine needles, m.p. 108–109° C, $[\alpha]_D^{25} = -44°$ (c, 0.25% in methanol). The slower-moving component (peak 8, Fig. 2) was crystallized from petroleum ether (b.p. 65–110° C) to a melting point of 65–68° C, $[\alpha]_D^{25} = +149°$ (c, 0.45% in methanol). Bell and Williamson (20) report a melting point of 111–112° C, $[\alpha]_D^{25} = -40.9°$ (in chloroform), for methyl 2,4,6-tri-O-methyl-β-D-galactopyranoside and a melting point of 73-74° C, $[\alpha]_D^{25} = +163.9°$ (in chloroform), for the α-anomer.

The two crystalline fractions were combined and hydrolyzed to yield a sirupy reducing sugar which could not be crystallized. The crystalline anilide derivative had a melting point of 160–165° C raised to 178–179° C by recrystallization from methanol:ether, $[\alpha]_D^{25} = +35°$ (c, 1% in methanol). These are in good agreement with the reported values of melting point 179° C, $[\alpha]_D^{25}$ +38° (in acetone) for N-phenyl-2,4,6-tri-O-methyl-D-galactosylamine (21).

2,4-Di-O-methyl-D-galactose

The anomeric glycosides of this component (peaks 9 and 10, Fig. 2) were collected separately from the gas–liquid partition chromatogram. The faster-moving component crystallized in the collecting tube and was found to be methyl 2,4-di-O-methyl-β-D-galactopyranoside, m.p. 168–170° C (22). The slower-moving component was recrystallized twice from petroleum ether (b.p. 30–60° C) to yield methyl 2,4-di-O-methyl-α-D-galactopyranoside, m.p. 106.5–108° C (22).

Another sample of this component was isolated from preparative paper chromatograms as the reducing sugar, m.p. 98–100° C, $[\alpha]_D^{26} = +85°$ (c, 1% in water). These values agree with those reported for 2,4-di-O-methyl-D-galactose monohydrate (22).

2,5-Di-O-methyl-L-arabinose

The fraction from preparative paper chromatograms that contained 2,4,6-tri-O-methyl-D-galactose and 2,5-di-O-methyl-L-arabinose was rechromatographed on paper sheets in solvent A to yield a chromatographically pure sample of 2,5-di-O-methyl-L-arabinose. Bromine oxidation, lactonization, and reaction with methanolic ammonia yielded crystalline 2,5-di-O-methyl-L-arabonamide (23), m.p. and mixed m.p. 132° C.

ACKNOWLEDGMENTS

REFERENCES

1. W. A. M. DUNCAN and D. J. MANNERS. Biochem. J. 69, 343 (1958).
2. F. B. ANDERSON and D. J. MANNERS. Biochem. J. 71, 407 (1959).
3. W. A. M. DUNCAN, D. J. MANNERS, and J. L. THOMPSON. Biochem. J. 73, 295 (1959).
4. L. G. NEUBAUER and C. B. PURVES. Can. J. Chem. 35, 388 (1957).
5. T. E. TIMELL. Can. J. Chem. 37, 893 (1959).
6. G. A. ADAMS, C. T. BISHOP, and I. J. McDONALD. Can. J. Biochem. and Physiol. 37, 507 (1959).
7. R. L. WHISTLER and K. W. KIRBY. J. Am. Chem. Soc. 78, 1755 (1956).
8. D. H. NORTHCOTE. Biochem. J. 58, 353 (1954).
9. S. M. MARTIN. Chem. & Ind. (London), 823 (1957).
10. R. KUHN, H. TRISCHMANN, and I. LÖW. Angew. Chem. 67, 32 (1955).
11. A. G. McINNES, D. H. BALL, F. P. COOPER, and C. T. BISHOP. J. Chromatog. 1, 556 (1958).
12. C. T. BISHOP and F. P. COOPER. Can. J. Chem. 38, 388 (1960).
13. J. K. N. JONES and K. C. B. WILKIE. Can. J. Biochem. and Physiol. 37, 377 (1959).
14. G. O. ASPINALL. Advances in Carbohydrate Chem. 14, 429 (1959).
15. F. SMITH and R. MONTGOMERY. Chemistry of plant gums and mucilages. Reinhold Publishing Corp., New York. 1959.
16. L. HOUGH, J. K. N. JONES, and W. H. WADMAN. J. Chem. Soc. 1702 (1950).
17. W. N. HAWORTH. J. Chem. Soc. 107, 8 (1915).
18. E. L. FALCONER and G. A. ADAMS. Can. J. Chem. 34, 338 (1956).
19. R. W. HUMPHREYS, J. PRYDE, and E. T. WATERS. J. Chem. Soc. 1298 (1931).
20. D. J. BELL and S. WILLIAMSON. J. Chem. Soc. 1196 (1938).
21. E. L. HIRST and J. K. N. JONES. J. Chem. Soc. 1482 (1939).
22. F. SMITH. J. Chem. Soc. 1724 (1939).
23. F. SMITH. J. Chem. Soc. 1035 (1940).

THE POLYOXYPHENOLS OF WESTERN RED CEDAR
(THUJA PLICATA DONN)

II. DEGRADATION STUDIES ON PLICATIC ACID, A POSSIBLE LIGNAN ACID[1]

J. A. F. Gardner, B. F. MacDonald, and Harold MacLean

ABSTRACT

Plicatic acid, $C_{20}H_{22}O_{10}$, a polyoxyphenol from western red cedar heartwood, described in a previous paper, has been further characterized by preparation and analysis of additional crystalline derivatives. Crystalline trimethyl and triethyl ethers have been oxidized by alkaline permanganate. The trimethyl ether yielded 3,4,5-trimethoxybenzioc acid, 4,5-dimethoxyphthalic acid (m-hemipinic acid), a pentamethoxy anthraquinone, and a pentamethoxy o-benzoylbenzoic acid which decarboxylated to 3,4,5,3',4'-pentamethoxy benzophenone. Correspondingly, the triethyl ether gave 3,4-diethoxy-5-methoxybenzoic and 4-ethoxy-5-methoxyphthalic acids, a mixture of pentaalkoxy anthraquinones and a pentaalkoxy o-benzoylbenzoic acid which decarboxylated to 3,3',4-triethoxy-4',5-dimethoxy benzophenone identified by cleavage to 3-ethoxy-4-methoxybenzoic and 3,4-diethoxy-5-methoxybenzoic acids. These results fix the positions of the two methoxyl, three phenolic hydroxyls, and mode of linkage of the two benzene rings. Further evidence is provided indicating plicatic acid is probably a lignan of the 4-aryltetrahydronaphthalene series.

In a previous paper (1), the isolation and properties of plicatic acid, a reactive polyoxyphenolic amorphous acid, occurring in the aqueous extractive of western red cedar, were described. Analysis of crystalline derivatives, methylation results, color tests, and spectra indicated it to be an n-propylphenol dimer, $C_{20}H_{22}O_{10}$, probably a lignan acid, in which one phenyl ring was 4-hydroxy-3-methoxyphenyl and the other was 3,4-dihydroxy-5-methoxyphenyl, but the mode of linkage was unknown. Thus the formula was given provisionally as $C_6H_3(OH)(OCH_3) \cdot C_5H_4(OH)_3(COOH) \cdot C_6H_2(OH)_2(OCH_3)$. This paper describes the alkaline permanganate oxidation of the crystalline trimethyl and triethyl ethers which establishes the aromatic substitution and indicates that plicatic acid is a lignan of the aryltetrahydronaphthalene series.

Alkaline permanganate oxidation of plicatic acid trimethyl ether (IIa) gave a 15% yield of a crystalline colorless pentamethoxy keto-acid, $C_{19}H_{20}O_8$, m.p. 225.5–226°; smaller quantities of a neutral brilliant yellow crystalline substance, $C_{19}H_{18}O_7$, m.p. 209–210°, which gave qualitative tests and had spectral characteristics of an anthraquinone; 3,4,5-trimethoxybenzoic acid (Va); and 4,5-dimethoxyphthalic acid (IVa). The latter two acids were not isolated but their presence in the oxidation mixture was shown by paper chromatographic comparison with synthetic samples.

The pentamethoxy keto-acid decarboxylated to a benzophenone shown to be 3,4,5,3',4'-pentamethoxybenzophenone by comparison with a synthetic sample. With concentrated sulphuric acid, the keto-acid readily gave a yellow anthraquinone. The infrared absorption spectrum of the acid was typical of the lactol form of a γ keto-acid (2) showing an alcoholic, but no acidic, hydroxyl band. These results indicate it to be an o-benzoylbenzoic acid, either 2,3,4-trimethoxy-6-(3',4'-dimethoxybenzoyl)-benzoic acid or 3,4-dimethoxy-6-(3',4',5'-trimethoxybenzoyl)-benzoic acid (IIIa), either of which would give the same benzophenone (VIIIa) on decarboxylation. Since Chatterjee and Chakravarti (3) had reported the isolation of an o-benzoylbenzoic acid of formula IIIa of much lower melting

point, 210–211°, by the permanganate oxidation of the lignan, sikkimotoxin, and since plicatic acid gave some vanillin on alkaline nitrobenzene oxidation, the former was considered first. However, this possibility was eliminated when neither veratric acid nor 3,4,5-trimethoxyphthalic could be detected in the other oxidation products. The presence of 3,4,5-trimethoxybenzoic acid (Va) and 4,5-dimethoxyphthalic acid (IVa) as shown by paper chromatography required formula IIIa. It was concluded that Chatterjee and Chakravarti's compound, m.p. 210–211° from boiling water and dilute ethanol, must have been a mixture of the keto-acid (IIIa) and its lactol form (IIIc).

In the present work, the acid when purified by repeated recrystallization, was obtained in the lactol form (IIIc), m.p. 225.5–226°, as shown by the infrared absorption spectra. However, acidification of a dilute alkaline solution of the lactol gave a crystalline product, m.p. 180–185° depending on the rate of heating, which on the basis of its infrared absorption was the keto-acid (IIIa), i.e., a strong acidic hydroxyl band, no alcoholic hydroxyl band, and a shift of the carbonyl band to the benzoic acid region. This material was rapidly transformed on the melting point stage to the lactol form. The lactol nature was confirmed by the formation of a neutral crystalline acetate whose infrared absorption spectrum was clearly characteristic of a pseudoacetate, showing one broad enhanced carbonyl absorption band at 1758 cm^{-1} (2).

The anthraquinone obtained in nearly quantitative yield from the o-benzoylbenzoic acid by ring closure with concentrated sulphuric acid was found to be identical with that obtained as one of the permanganate oxidation products of plicatic acid trimethyl ether. Inspection of formula IIIa shows that ring closure of this substituted o-benzoylbenzoic acid, at either the 2′ or 6′ position, would give only one anthraquinone, namely, 1,2,3,6,7-pentamethoxy anthraquinone (VI).

Formation of the products IIIa, IVa, and Va proves that the position of aromatic substitutions in plicatic acid is as shown in formula I. To confirm the relative positions of the phenolic hydroxyl and methoxyl groups, which had been indicated by color tests and vanillin formation (1), the permanganate oxidation products at 100° of plicatic acid triethyl ether were examined. A crystalline monomeric acid was obtained which was shown to be 3,4-diethoxy-5-methoxybenzoic acid (Vb) by comparison with a synthetic sample. The presence in the oxidation products of 4-ethoxy-5-methoxyphthalic acid (IVb) was demonstrated by paper chromatography in three solvent systems using a synthetic reference sample.

A neutral brilliant yellow crystalline product, giving qualitative tests for an anthraquinone, was also obtained in small yield. In contrast to the readily purified sharply melting anthraquinone obtained in the oxidation of plicatic acid trimethyl ether, the product in this case appeared to be a mixture since, after repeated recrystallizations, it melted over a wide range. This result was to be expected since, in the case of the ethylated derivatives, two anthraquinones, VIIa and VIIb, should result in approximately equal yield from ortho ring closure of the triethoxy-dimethoxy-o-benzoylbenzoic acid (IIIb).

The formation of 3,4-diethoxy-5-methoxybenzoic proves ring C to be 3,4-dihydroxy-5-methoxyphenyl and the formation of the 4-ethoxy-5-methoxyphthalic acid indicates the substitution pattern on ring A as shown in formula I for plicatic acid. Alkaline permanganate oxidation of the triethyl ether at lower temperature yielded mainly the ethylated keto-acid 4-ethoxy-3-methoxy-6-(3′,4′-diethoxy-5′-methoxybenzoyl)-benzoic acid (IIIb) which underwent conversion from its keto form IIIb to the lactol form IIId near the melting point similar to the methylated derivative previously obtained. Decarboxylation gave the corresponding benzophenone, 3,3′,4-triethoxy-4′,5-dimethoxy benzo-

phenone, which on cleavage with potassium *t*-butoxide yielded 3-ethoxy-4-methoxy-benzoic acid (IX) and 3,4-diethoxy-5-methoxybenzoic acid (V*b*). The formation of these latter products fixes with certainty the position of the hydroxyl group on ring A, as shown in Fig. 1, formula I.
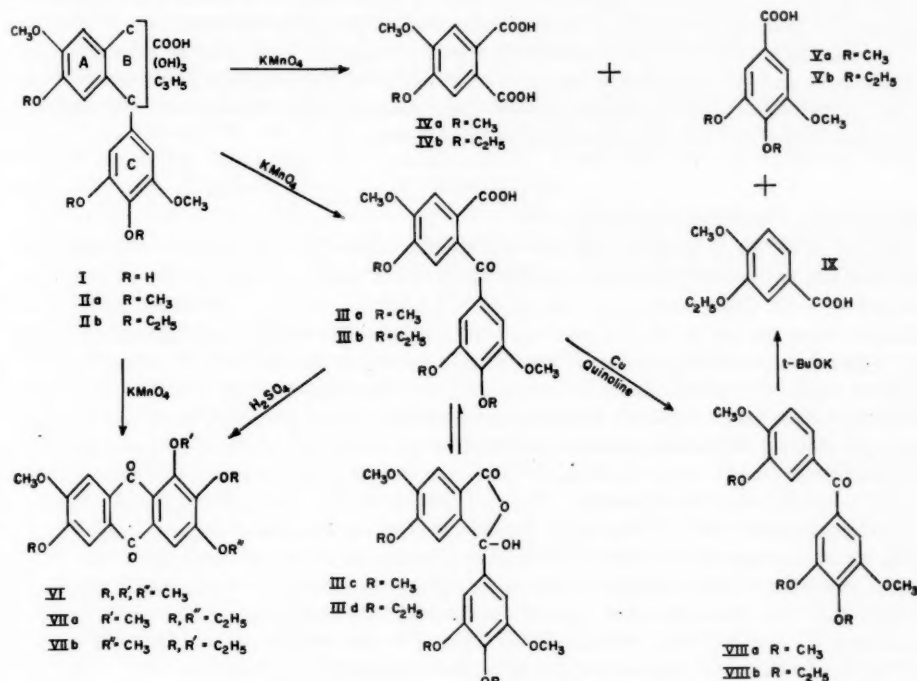
FIG. 1. Oxidation of methyl and ethyl ethers of plicatic acid.

The yield of vanillin (4%) obtained by alkaline nitrobenzene oxidation of plicatic acid (1) is in the same low range as that obtained from two other lignans, conidendrin and iso-olivil, 1 and 3% respectively (4). In the case of plicatic acid, since the C ring is a pyrogallol derivative, the vanillin formed must arise from the A ring via cleavage of an ortho-formylbenzophenone or decarboxylation of 6-carboxyvanillin. The vanillin from conidendrin and iso-olivil is probably derived similarly. This mode of vanillin formation is of interest in connection with alkaline nitrobenzene oxidation studies on lignins since a part of the vanillin formed could be so derived. While there is no evidence for the presence in lignin *in situ* of 3-methoxy-4-hydroxyphenylpropane structural units linked to the next through the 6-position, Richtzenhain (5) suggested the presence of such linkages in lignins isolated by acidic procedures to explain the formation of *m*-hemipinic acid by oxidation after methylation.

The presence of a monomethylated pyrogallol nucleus in plicatic acid explains the positive Mäule test, although this test is usually considered indicative of the dimethylated (syringyl) derivative. In contrast to the dimethylated (syringyl) derivatives, which occur widely in deciduous extractives and lignin, monomethylated derivatives of pyrogallol

are very rare in all plant products, none having been reported in wood components heretofore. It will be of considerable interest to determine whether products of additional methylation, i.e., syringyl derivatives, are also present in the western red cedar phenols.

In view of the easy formation of the tropolone derivative purpurogallin from pyrogallol, the occurrence of pyrogallol derivatives as well as tropolones in western red cedar is of interest in considering possible modes of biogenesis of the latter substances.

The oxidation products obtained herein together with the formation of γ lactones by plicatic acid and its trimethyl ether (1) are consistent with plicatic acid being a lignan of the 4-aryltetrahydronaphthalene series. Experimental proof of this and the pattern of hydroxylation on the saturated ring is in progress.

EXPERIMENTAL

Plicatic Acid Trimethyl Ether (IIa)

Plicatic acid (20 g) in water (40 ml) was treated with dimethyl sulphate (28 ml) and 20% sodium hydroxide dropwise at reflux for 2 hours under nitrogen while maintaining the pH at 9–10. After addition of the dimethyl sulphate, sodium hydroxide (50%) was added to raise the pH to 14. On cooling of the solution, the sodium salt precipitated and was separated on the centrifuge. The precipitated salt was dissolved in a minimum of distilled water, the solution acidified to pH 7 with sulphuric acid, extracted with chloroform to remove tarry residues, filtered, and further acidified to pH 2 to precipitate the free acid product. After filtration an additional crop was obtained by partial evaporation of the filtrate. Crude yield, 14.79 g (74%). The product was recrystallized from boiling water using decolorizing charcoal. Yield, 10.52 g (53%). Anal. Calc. for $C_{23}H_{28}O_{10}$: neutral equivalent, 464; OCH_3, 33.4. Found: neutral equivalent, 467; OCH_3, 32.7.

On rapid heating, the product melted with foaming between 210° and 218° depending on the rate of heating. It slowly recrystallized on the melting point stage and remelted at 253–255°. On slow heating, the product underwent a change in crystal structure between 220° and 245° and melted at 253–255°. The gas evolved during this conversion was shown to be water vapor and the new product proved to be plicatic acid trimethyl ether lactone, previously prepared from plicatic acid trimethyl ether methyl ester through loss of methanol (1), by mixed fusion and comparison of infrared spectra.

3,4-Dimethoxy-6-(3',4',5'-trimethoxybenzoyl)-benzoic Acid (IIIa)

Plicatic acid trimethyl ether (IIa) (4.56 g) was dissolved in 4% sodium hydroxide (100 ml) on a steam bath and 4% potassium permanganate (511 ml) slowly added with stirring in 10-ml portions until 400 ml had been added, and then in smaller portions to a 15-minute end point. The manganese dioxide together with the small yellowish precipitate which floated on the reaction mixture was filtered out (precipitate A) and washed with hot water (200 ml). After the pink filtrate had been decolorized with a few drops of bisulphite solution and acidified to pH 2 with hydrochloric acid, cooling precipitated pale yellow crystals. Filtration (filtrate B) and recrystallization from methanol–water (1:2) gave colorless needles. Yield, 0.679 g (15%). Anal. Calc. for $C_{19}H_{20}O_8$: C, 60.78; H, 5.10; OCH_3, 41.28; neutral equivalent, 375.4; mol. wt., 375.4. Found: C, 60.86; H, 5.09; OCH_3, 41.00; neutral equivalent, 371.3; mol. wt. (isothermal distillation), 388. The product gave a positive test with 2,4-dinitrophenylhydrazine. Heating rapidly gave partial melting at 180–185° followed by recrystallization and remelting at 218–220°, m.p. after five recrystallizations 225.5–226°. Infrared absorption spectrum was characteristic of the lactol of a keto-acid. ν_{max}^{KBr} 3340, 1702, 1668, 1582, 1322, 1128, 997, 765.

Acidification of a dilute alkaline solution and vacuum drying at room temperature produced the pure keto-acid form (IIIa), m.p. 184–185°. ν_{max}^{KBr} no hydroxyl band, 2600, 1668, 1648, 1580, 1502, 1460, 1410, 1322, 1280, 1120, 1003, 772.

When treated with concentrated sulphuric acid, the product gave a brilliant purple color transformed in a few minutes warming to brown. Dilution of the brown mixture with water and neutralization precipitated a bright yellow crystalline substance, m.p. 207–208° from methanol, showing no mixed melting point depression with 1,2,3,6,7-pentamethoxy anthraquinone (VI) (see below).

Treatment with diazomethane in methanol–ether gave a crystalline monomethyl ester, m.p. 147–147.5°, showing no absorption bands for the hydroxyl group in the infrared spectrum. Anal. Calc. for $C_{20}H_{22}O_8$: OCH_3, 47.64; mol. wt., 390. Found: OCH_3, 46.87; mol. wt. (Rast), 390.

Refluxing with acetic anhydride in pyridine gave a crystalline acetate, insoluble in bicarbonate solution, m.p. 118–119° from methanol. The infrared absorption spectrum showed no hydroxyl band and had one broad intense carbonyl band at 1758 cm^{-1} typical of a lactol acetate (2).

1,2,3,6,7-Pentamethoxy Anthraquinone (VI)

"Precipitate A" after drying was triturated with chloroform (4×50 ml). The solution was then dried over sodium sulphate and evaporated to yield a brilliant yellow powder (0.154 g, 3% yield), melting point after two recrystallizations from methanol, 209–210°. This compound when heated with sodium hydrosulphite in alkali gave a red solution which precipitated the yellow starting material on air oxidation. The red solution on further reduction with zinc and alkali gave a pale yellow precipitate. These positive qualitative tests for anthraquinone structure were supported by formation of the same substance by ring closure of the keto-acid (IIIa) and by the absorption spectra. The ultraviolet absorption in methanol exhibited an intense maximum at 285 mμ (log ϵ = 4.81). The infrared absorption (KBr pellet) showed one weak and one very strong band attributable to the carbonyls at 1740 cm^{-1} and 1662 cm^{-1}, respectively, comparable to those of anthraquinone at 1740 cm^{-1} and 1665 cm^{-1}. Anal. Calc. for 1,2,3,6,7-pentamethoxy anthraquinone, $C_{19}H_{18}O_7$: C, 63.67; H, 5.06; OCH_3, 43.24; mol. wt., 358. Found: C, 63.56; H, 4.97; OCH_3, 42.80; mol. wt. (Rast), 360.

Identification of 3,4,5-Trimethoxybenzoic Acid (Va) and 4,5-Dimethoxyphthalic Acid (IVa)

"Filtrate B" was extracted with ether (3×100 ml) and the ether solution extracted with sodium bicarbonate (3×25 ml). The mixed acids were isolated by acidification of the bicarbonate solution, extraction into ether, and solvent removal to yield a light tan solid (135 mg, 3% yield). This material was compared by descending paper chromatography on Whatman No. 1 using two solvents, n-propanol:26% ammonia (3:2) (6) and n-butanol:2% ammonia (1:1) using reference samples of 3,4,5-trimethoxybenzoic acid and 4,5-dimethoxyphthalic acid (7). Spots at R_f's 0.79 and 0.29 and at 0.30 and 0.036 in the two solvents systems respectively, identical with those of the reference samples, were present. Detection was made first with short ultraviolet light which shows the acids as dark spots, then by spraying with universal indicator (B.D.H.). Since 4,5-dimethoxyphthalic acid (m-hemipinic acid) and 3,4-dimethoxyphthalic acid (hemipinic acid) (7) have very similar R_f's in these solvents, the oxidation product was also run in benzene:acetic acid:water (125:72:3) over a period of 16 hours, the solvent being allowed to run off the paper. The synthetic 4,5-dimethoxyphthalic and the oxidation product ran 15¼ inches while the 3,4-dimethoxyphthalic acid ran 17 inches. These acids

were detected with short ultraviolet light as dark spots. No spots corresponding to synthetic veratric and 3,4,5-trimethoxyphthalic acid (8) were detected.

3,4,5,3',4'-Pentamethoxy Benzophenone (VIIIa)

3,4,5,3',4'-Pentamethoxy benzophenone was prepared by dissolving the keto-acid (IIIa) (275 mg) and its copper salt (25 mg) as catalyst (9) in quinoline (7 ml) and refluxing for $\frac{1}{2}$ hour. Metallic copper settled out on cooling. The reaction mixture was diluted with ether (20 ml) and filtered. The filtrate was washed with 2 N hydrochloric acid (5×10 ml) until nearly colorless, then with 5% sodium hydroxide (2×10 ml) to remove the trace yellow color, dried over sodium sulphate, and evaporated to colorless crystals. Yield, 123 mg (45%). Recrystallization from methanol:water gave colorless platelets, m.p. 120.5–121°, oxime, m.p. 149.5–150°. Mixed melting point with synthetic samples (10, 11) 123.5° and 148.5–149.5°, respectively, showed no depression and the infrared absorption spectra of the benzophenones were identical. ν_{max}^{KBr} 1632, 1582, 1518, 1466, 1415, 1326, 1268, 1125, 770.

Plicatic Acid Triethyl Ether (IIb)

Plicatic acid (28.1 g) in water (25 ml) was treated with diethyl sulphate (30 ml) and 20% sodium hydroxide dropwise at reflux for 3 hours under nitrogen while maintaining the pH at 9–10. After addition of the diethyl sulphate, sodium hydroxide (10 ml, 20%) was added and the reaction mixture refluxed for an additional hour. On cooling, the reaction mixture solidified. After stirring and centrifuging several times, the supernatant liquor was decanted, the precipitated sodium salt acidified, and the free acid taken up in chloroform. The chloroform solution was extracted with sodium bicarbonate solution, the bicarbonate solution acidified, and the precipitated product recrystallized from methanol:water (1:1), m.p. 113–114°. Yield, 10.74 g (38%). As this compound lactonized very readily at 140°, excessive heating during recrystallization and drying was avoided. Stable gels were formed by cooling benzene solutions. Calc. for $C_{26}H_{34}O_{10}$: alkoxyl as methoxyl, 30.6%; neutral equivalent, 506. Found: alkoxyl as methoxyl, 30.2%; neutral equivalent, 509.

Permanganate Oxidation of Plicatic Acid Triethyl Ether (IIb) at 100°

Oxidation of this ether (6.2 g) was similar to that of the trimethyl ether with the exception that 5% potassium hydroxide and 5% potassium permanganate were used and the solution kept boiling throughout the addition of the potassium permanganate (864 ml). Due to the more drastic oxidation conditions no ethyl-substituted o-benzoylbenzoic acid was obtained. The monomeric acids were obtained as a yellow plastic solid. Yield, 0.334 g (5.4%).

As in the case of oxidation of the trimethyl ether, brilliant yellow crystals precipitated from the boiling alkaline reaction mixture. Yield, 0.143 g (2%). Qualitative tests for anthraquinone structure were positive. A mixture of anthraquinones was suspected since two recrystallizations gave no change in the melting point range of 150–167°.

Isolation of 3,4-Diethoxy-5-methoxybenzoic Acid (Vb)

A portion of the mixed acids (0.09 g) was fractionated by column chromatography on silicic acid using the technique of Hathaway (6). Evaporation of the first fraction gave a crystalline product, m.p. 112–113°, from ethanol:water (1:1) identical with, by mixed melting point and infrared absorption spectrum, a reference sample synthesized from 5-hydroxy vanillin (12) by ethylation with diethyl sulphate followed by oxidation with cold 1% permanganate (13).

Detection of 4-Ethoxy-5-methoxyphthalic Acid (IVb)

A sample of the mixed acids was examined by descending paper chromatography in three solvent systems, n-propanol:26% ammonia (3:2), n-butanol:2% ammonia (1:1) and benzene:acetic acid:water (125:72:3). In each case, spots at R_f's identical with those of a synthetic sample of 4-ethoxy-5-methoxyphthalic acid were obtained. In the first two, the spots (R_f's 0.51 and 0.045 respectively) were detected first by short ultraviolet light and then by spraying with universal indicator (B.D.H.). In the last, the solvent was allowed to run off the paper to give 14 inches of migration by the acid and detection was by short ultraviolet light.

The reference sample of 4-ethoxy-5-methoxyphthalic acid (melting point of ethyl-imide, 204°) was obtained by the permanganate oxidation (13) of 4-ethoxy-5-methoxy-phthalide synthesized from the ethyl ether of vanillic acid using the method of King and King (14).

4-Ethoxy-3-methoxy-6-(3',4'-diethoxy-5'-methoxybenzoyl)-benzoic Acid (IIIb)

Permanganate oxidation of plicatic acid triethyl ether (IIb) at 50–55° was analogous to the previous oxidation for the trimethyl ether (IIa). At this temperature only a trivial amount of the corresponding anthraquinones (VIIa and VIIb) was obtained. The main product was similarly a keto-acid, 4-ethoxy-3-methoxy-6-(3',4'-diethoxy-5'-methoxy-benzoyl)-benzoic acid (IIIb) (8% yield). Anal. Calc. for $C_{22}H_{26}O_8$: neutral equivalent, 418. Found: 416. Heating rapidly gave a partial melting at 120–124° followed by re-crystallization and remelting at 136–137°. Infrared absorption spectrum of the original material before melting was that of the keto-acid (IIIb). ν_{max}^{KBr} no hydroxyl band, 2600, 1670–1660 (doublet), 1580, 1500, 1418, 1320, 1270. After melting at 136–137° the spectrum was mainly that of the lactol (IIId) contaminated with some of the keto-acid. ν_{max}^{KBr} 3250, 2600, 1705, 1680, 1580, 1500, 1418, 1320, 1270, 1120, 766.

3,3',4-Triethoxy-4',5-dimethoxy Benzophenone (VIIIb)

3,3',4-Triethoxy-4',5-dimethoxy benzophenone was prepared from the keto-acid (IIIb) in an analogous manner to the fully methylated benzophenone (VIIIa). Yield, 68% of theoretical. Recrystallization from methanol:water (2:1) gave colorless needles, m.p. 96–96.5°. The infrared spectrogram was free of acid hydroxyl and acid carbonyl bands showing only the expected diaryl ketone carbonyl. ν_{max}^{KBr} 1640, 1580, 1518, 1420, 1322, 1262, 1122, 1023, 776.

Cleavage of 3,3',4-Triethoxy-4',5-dimethoxy Benzophenone (VIIIb)

In accordance with the procedure of Swan (15), potassium wire (30 mg, 0.00075 mole) was converted to potassium tertiary butoxide. A solution of the benzophenone (90.3 mg, 0.000242 mole) and water (4.8 microliters, 0.000265 mole) in anhydrous dioxane (5 ml) was added and refluxed at 90° for 18 hours under anhydrous conditions. The solvent was evaporated under reduced pressure, the residue dissolved in water, and extracted with ether (2×10 ml) to remove unreacted benzophenone and the neutral products. On acidification with HCl, the acids precipitated as colorless solids (36 mg, 80% yield). The mixed acids (30 mg) were separated by dissolving in acetone and streaking across a 9-in. wide No. 17 Whatman chromatographic paper. Development was with butanol – 2% ammonia (1:1) solvent and detection by short ultraviolet light. The spots were excised and Soxhlet extracted with acetone. After removal of the acetone under reduced pressure, the separated acids were taken up in bicarbonate, filtered, and precipitated with HCl. Yields were 3-ethoxy-4-methoxybenzoic acid (IX), 13 mg, m.p. 167.5–168° ($R_f = 0.32$

in butanol – 2% ammonia), and 3,4-diethoxy-5-methoxybenzoic acid (Vb), 9 mg, m.p. 113–114° (R_f = 0.51 in butanol – 2% ammonia), identical with authentic samples by mixed melting point and infrared spectrogram.

REFERENCES

1. J. A. F. GARDNER, G. M. BARTON, and H. MacLEAN. Can. J. Chem. 37, 1703 (1959).
2. J. F. GROVE and H. A. WILLIS. J. Chem. Soc. 877 (1951).
3. R. CHATTERJEE and S. C. CHAKRAVARTI. J. Am. Pharm. Assoc. Sci. Ed. 41, No. 8, 415 (1952).
4. B. LEOPOLD and I. L. MALMSTROM. Acta Chem. Scand. 5, 936 (1951).
5. H. RICHTZENHAIN. Svensk Papperstidn. 53, 644 (1950).
6. D. E. HATHWAY. J. Chem. Soc. 520 (1958).
7. G. A. EDWARDS, W. H. PERKIN, JR., and F. W. STOYLE. J. Chem. Soc. 127, 195 (1925).
8. R. L. ALIMCHANDANI and A. N. MELDRUM. J. Chem. Soc. 117, 964 (1920).
9. LOUIS F. FIESER. Experiments in organic chemistry. 2nd ed. D. C. Heath & Co., New York. 1941. p. 199.
10. W. H. PERKIN, JR. and CARL WEIZMANN. J. Chem. Soc. 89, 1649 (1906).
11. W. H. PERKIN, JR. and J. NAYLOR. J. Chem. Soc. 89, 1664 (1906).
12. W. BRADLEY, R. ROBINSON, and G. SCHWARZENBACH. J. Chem. Soc. 793 (1930).
13. R. H. F. MANSKE, A. E. LEDINGHAM, and H. L. HOLMES. Can. J. Chem. 23, 100 (1945).
14. F. E. KING and T. J. KING. J. Chem. Soc. 726 (1942).
15. G. A. SWAN. J. Chem. Soc. 1408 (1948).

PROTON MAGNETIC RESONANCE ABSORPTION IN ANHYDROUS SODIUM STEARATE[1]

R. F. GRANT[2] AND B. A. DUNELL

ABSTRACT

The proton magnetic resonance absorption in anhydrous sodium stearate has been investigated over the temperature range −182° C to 200° C. An abrupt change in the line width and the second moment has been observed between 113° C and 114° C, which corresponds to a known phase transition. The results suggest that at temperatures below 114° C the motion of the hydrocarbon-chain portion of the sodium stearate molecule is chiefly one of oscillation or rotation about the chain longitudinal axis. The hydrocarbon chains may be free to move about other axes at temperatures above 114° C, although the molecule as a whole retains a fixed position in the crystal lattice.

INTRODUCTION

The various mesomorphic phase transitions in sodium salts of long-chain fatty acids have been extensively studied by several physical methods (1). X-Ray, infrared, and nuclear magnetic resonance studies have indicated that the lower temperature transitions may represent the onset of rapid reorientation in the paraffin-chain part of the sodium soap molecule (2, 3, 4). Of particular interest are the phase transitions curd–supercurd at 89–92° C, supercurd–subwaxy at 110–117° C, and subwaxy–waxy at 125–135° C (4). The following is a proton magnetic resonance investigation of these transitions in sodium stearate, and is an extension and correction of the work in a previous communication (4).

EXPERIMENTAL

The sodium stearate was prepared from Eastman Kodak white label stearic acid, f.p. 68.1° C, which had been purified by repeated crystallization at −20° in acetone (5). The purified acid, f.p. 69.2° C, was dissolved in hot ethanol and titrated to a phenolphthalein end point with an aqueous ethanol solution of sodium hydroxide. The sodium stearate precipitate was filtered, dried in air, and melted under vacuum to remove residual solvents and to render it anhydrous (6). This compact, fused soap was remelted under vacuum in sample tubes; dry nitrogen was admitted to the system and the tubes were sealed off.

The nuclear magnetic resonance spectrometer and the methods of temperature control have been described previously (7). The temperature of the sample was measured with a thermocouple inserted in a well in the side of the sample tube. The line width was taken as the separation in gauss between points of maximum and minimum slope. The second moments of the resonance lines were obtained from the experimental derivative curves (8) by numerical integration and were corrected for the effects of modulation (9).

RESULTS

The proton magnetic resonance line widths, measured from −68° C to 130° C, are given by the open circles in Fig. 1. The line width was also measured at −182° C where it is 16.1 gauss. Particularly notable is the extensive decrease in the line width at temperatures above 30° C, and the abrupt change from a width of 2.8 gauss at 113° C to a width determined by the field homogeneity at 114° C. This abrupt narrowing coincides with

the supercurd–subwaxy phase transition. In all these measurements it was found necessary to maintain a given temperature for at least 2 hours before the proton magnetic resonance absorption was recorded. In most cases the temperature was maintained for about 4 hours, and above 100° C, in the vicinity of the phase transition, temperatures were held constant for about 12 hours. The filled circles in Fig. 1 represent one continuous experiment in which each temperature was maintained for only 30 minutes before the resonance
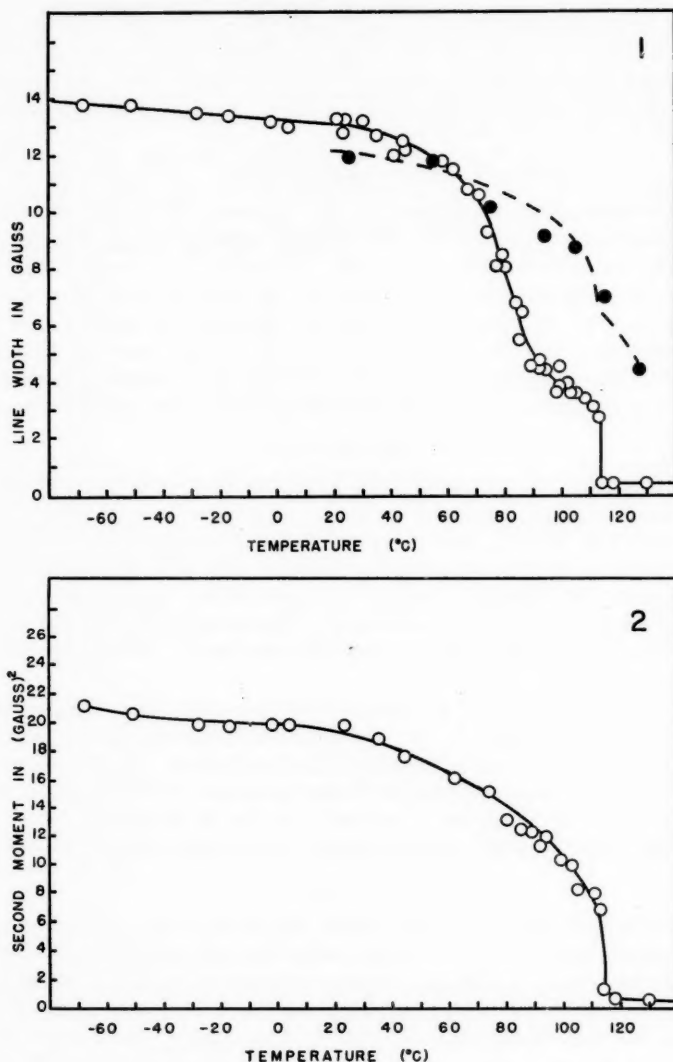
FIG. 1.   Line width of sodium stearate as a function of temperature. Open circles, line width from samples at thermal equilibrium; filled circles, line width from samples not at thermal equilibrium; dashed line, line width from previous study.

FIG. 2.   Second moment of sodium stearate as a function of temperature.

absorption was measured. These points fall closely along the discontinuous line in Fig. 1, which represents the course of the results in the original magnetic resonance studies on sodium stearate (4). It seems evident, therefore, that this previous work (4) reported a situation where thermal equilibrium had not been properly established although the line-width changes were reproducible.

The second moment of the proton magnetic resonance absorption in sodium stearate at $-182°$ C was found to be 28.0 ± 1.5 gauss^2. The behavior of the second moment over the temperature range $-68°$ C to $130°$ C is shown in Fig. 2. Like the line width, the second moment begins to decrease rapidly above about $30°$ C and changes abruptly from 6.7 gauss^2 to 1.2 gauss^2 as the temperature is raised through the supercurd–subwaxy transition. Above $114°$ C the second moment decreases even more: it is 0.6 gauss^2 at $118°$ C and 0.4 gauss^2 at $130°$ C, near the subwaxy–waxy transition temperature. Although the line width is very narrow above $114°$ C, the second moment does not approach zero because of small wings on the resonance absorption line. These wings decrease in amplitude and width as the temperature is raised, and there is some evidence for them up to $200°$ C; however, the amplitude becomes so small that it is difficult to determine a reliable second moment.

DISCUSSION

The X-ray diffraction analysis of most solid fatty acid salts shows that they have a layer structure in which the carboxyl ion ends lie in parallel sheets. Two such sheets form a double layer, and both individual sheets and the double layer are held together by positive ions. The long paraffin chains stick out parallel to each other from both sides of this electrically balanced double layer, with their longitudinal axes slightly inclined to it. Reliable and reproducible results are difficult to obtain from X-ray studies of sodium stearate and details of the molecular arrangement in the unit cell have not been determined (10). However, the unit cell cross section of sodium stearate (11) is almost identical with that of silver stearate (12), whose triclinic structure has been fairly well defined. Infrared studies have suggested that the higher sodium soaps also have a triclinic structure (3). In view of these similarities it seems reasonable to assume that the arrangement of sodium stearate molecules in the crystal lattice is very much the same as the arrangement of the silver stearate molecules. In the paraffin-chain portion, the carbon atoms are arranged in the zigzag configuration and it has been assumed that the bond angles are tetrahedral throughout. The carbon—hydrogen bond length is taken as 1.094 Å, and the carbon—carbon distance is 1.54 Å (13). On the basis of this knowledge of the structure of the sodium stearate unit cell, the second moment, S, of the proton magnetic resonance can be calculated (14).

For a polycrystalline sample the expression for the second moment S of the proton magnetic resonance in an assembly of protons and sodium nuclei is

[1]
$$S = \frac{716}{N} \sum_{j>k} r_{jk}^{-6} + \frac{55}{N} \sum_{j,f} r_{jf}^{-6},$$

where N is the number of protons whose interactions are considered, r_{jk} is the distance between any two protons j and k, and r_{jf} is the distance between any proton j and sodium nucleus f. The contribution of the second part of equation [1] is very small for sodium stearate. The intramolecular second moment for sodium stearate was found to be 18.9 gauss^2 and the intermolecular second moment was 9.4 gauss^2 for a total of 28.3 gauss^2.

This compares quite well with the experimental value of 28.0 ± 1.5 gauss^2 found at $-183°$ C and it is assumed that molecular motion at frequencies comparable to or greater than the resonance line width is absent (15).

According to the theory of Gutowsky and Pake (16), both the width and second moment of the resonance absorption line should decrease when molecular reorientation becomes sufficiently rapid. A more recent treatment of the theory has shown that molecular motion should cause a change in the line shape such that the second moment remains constant at its rigid lattice value (17); as the line width narrows due to the motion, the tails of the line become extended. However, experimentally observed second moments usually decrease as the line width decreases, in agreement with the earlier theory (16). This is because the amplitude of the extended tail part of the resonance absorption line is comparable to the amplitude of the spectrometer noise, hence it is not observed when the experimental line is obtained. This seems to be the case with sodium stearate; the second moment and line width behave in roughly the same way with changing temperature and no extended tails were detected on the resonance absorption line with the spectrometer signal-to-noise ratio of 30.

Since the molecules in solid sodium stearate are arranged side by side as in a bundle of rods, one of the most likely forms of motion would be a rotation or oscillation about the longitudinal axis of the paraffin chain. The reduction in the intramolecular second moment due to the complete reorientation of the sodium stearate molecules about their longitudinal axes can be calculated by means of the treatment of Gutowsky and Pake (16). Also for some kinds of motion likely in solid long-chain paraffins, Andrew (18) has found that the intra- and inter-molecular contributions are reduced by about the same factor. Hence the total second moment for reorientation about the longitudinal axes of sodium stearate molecules is about 8.1 gauss^2. This corresponds to the experimental second moment found around $110°$ C or just prior to the supercurd–subwaxy transition as shown in Fig. 2. The second moment expected for torsional oscillation of the paraffin chains about their long axes in solid sodium stearate is given by the graph in Fig. 3. This was calculated by means of equation [2] originally derived by Andrew (18).

[2] $$\rho = 1 - \tfrac{3}{4}[(1 - J_0^{\,2}(\alpha)) \sin^2 2\gamma + (1 - J_0^{\,2}(2\alpha)) \sin^4 \gamma].$$

Here ρ is the ratio of the second moments for the oscillating and rigid cases, α is the angular amplitude of oscillation, γ is the angle between the internuclear vector and the axis of reorientation, and J_0 is a Bessel function.

The model of a paraffin chain undergoing torsional oscillation or complete reorientation about its longitudinal axis seems sufficient to account for most of the experimental results below $113°$ C. So far, however, the possible effect of the ionic layer formed at the carboxyl ends in solid sodium stearate has been ignored. It would seem reasonable to suppose that the portion of the paraffin chain nearest the strongly bonded ionic layer would be able to undergo torsional oscillation to a somewhat lesser extent than the portions of the chain farthest away from the ionic layer. Moreover, it has been shown that such a twisting about the longitudinal axis of the paraffin chain may require less energy of activation than is required in the case where the whole chain must be lifted over the potential barrier at the same time (19). A rigid ionic layer may also prevent the complete reorientation of the chain predicted for a second moment of about 8 gauss^2. However, this value could also be accounted for by a twisting chain that is also free to oscillate slightly in a direction perpendicular to the chain axis.

The very narrow line width which occurs between $113°$ C and $114°$ C is usually taken
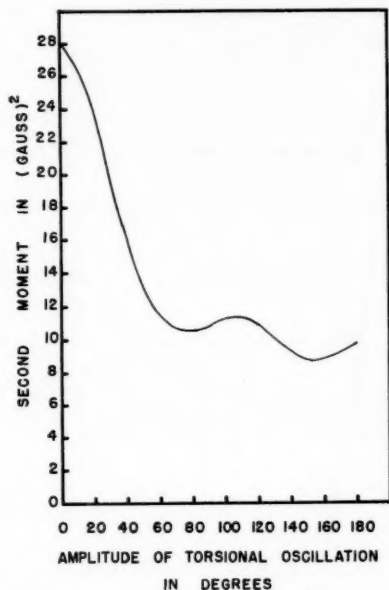
FIG. 3.   Calculated effect of torsional oscillation on the second moment of sodium stearate.

to indicate that the whole molecule is reorienting about more than one axis (15). If molecular reorientation is isotropic, the intramolecular contribution to the second moment should average to zero. However, so long as the centers of mass of the molecules remain fixed, the intermolecular contributions will not average to zero and a small but finite second moment should be observed (20). The supercurd to subwaxy transition between 113° C and 114° C in sodium stearate appears to involve a change from rotation or twisting about the longitudinal axis of the paraffin chain to a condition where reorientation may be possible about other axes. Yet the second moment of 1.2 gauss² at 114° C suggests that the sodium stearate molecules are still fixed in the crystal lattice. This seems to agree with the conclusions drawn from recent X-ray studies on sodium stearate (2). Above the supercurd–subwaxy transition the lattice structure consists of a set of parallel ribbons, indefinite in length and packed in a rectangular array. The sodium carboxylate ends of the molecules fit into the ribbon and the hydrocarbon chains, in a liquid-like state (3), fill up the rest of the lattice.

The correlation frequency ν_c of the motion responsible for narrowing proton magnetic resonance absorption lines may be calculated (16) by means of the following equation:

[3] $$\nu_c = 4260\Delta H/\tan\left[(\pi/2)(\Delta H^2 - B^2)/(A^2 - B^2)\right].$$

Here ΔH is the line width in the line-narrowing region, B is the line width at temperatures above this region, and A is the line width below it. For sodium stearate B is taken as 2.8 gauss, which is the line width at 113° C just prior to the supercurd–subwaxy transition and A is 16.1 gauss, which is considered to be the rigid lattice line width at −182° C. The second moments, previously discussed, indicated that only motion about the molecular longitudinal axis is likely between these limits. It is assumed that for a

given temperature this motion can be described by a single correlation frequency which varies with temperature T as

[4] $$\nu_c = \nu_0 \exp (V/RT),$$

where V is analogous to an activation energy for the motion and R is the gas constant. The correlation frequencies from sodium stearate line widths, shown in Fig. 4, gave two
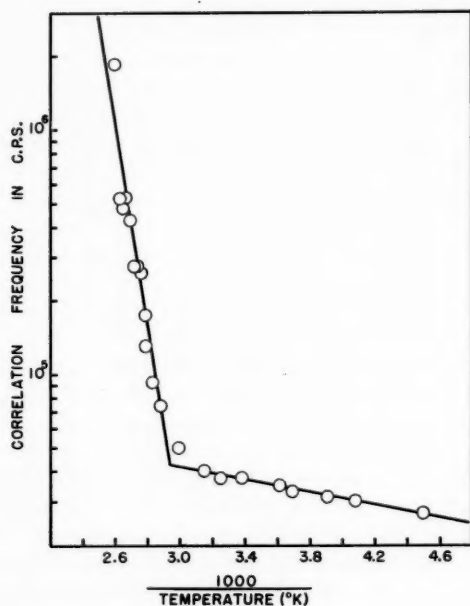
FIG. 4.   Correlation frequency for sodium stearate as a function of inverse temperature.

activation energies: below about 65° C, V was 0.8 kcal/mole, and above 65° C, V was 19.2 kcal/mole. Finding two activation energies by this method may not be unusual, for a similar situation has been reported for polyethylene (21). For the small activation energy at low temperatures in polyethylene a small-amplitude torsional oscillation has been postulated, while at high temperatures the large activation energy is ascribed to rotational and translational modes of large amplitude (21). The case for sodium stearate may be similar, although the known crystal structure would not be expected to allow large translational modes below the supercurd–subwaxy transition. The activation energy of 19.2 kcal/mole seems to be of the right magnitude for a violent twisting or rotation of the paraffin chains (19) which leads to a radical change in the crystal structure.

ACKNOWLEDGMENTS

REFERENCES

1. G. H. BROWN and W. G. SHAW.   Chem. Revs. **57**, 1049 (1957).
2. A. SKOULIOS and V. LUZZOTI.   Nature (London), **183**, 1310 (1959).
3. D. CHAPMAN.   J. Chem. Soc. 784 (1958).
4. R. F. GRANT, N. HEDGECOCK, and B. A. DUNELL.   Can. J. Chem. **34**, 1514 (1956).
5. J. B. BROWN and D. K. KOLB.   Progress in the chemistry of fats and other lipids. Vol. 3. Pergamon Press, Ltd., London. 1955. p. 58.
6. G. STAINSBY, R. FARNAND, and I. E. PUDDINGTON.   Can. J. Chem. **28**, 838 (1951).
7. R. F. GRANT and B. A. DUNELL.   Can. J. Chem. **38**, 359 (1960).
8. G. E. PAKE and E. M. PURCELL.   Phys. Rev. **74**, 1184 (1948).
9. E. R. ANDREW.   Phys. Rev. **91**, 425 (1953).
10. A. STOSICK.   J. Chem. Phys. **18**, 1035 (1950).
11. G. KOKOTAILO.   Thesis, Temple University. 1955.
12. V. VAND, A. AITKEN, and R. K. CAMPBELL.   Acta Cryst. **2**, 398 (1949).
13. L. PAULING.   The nature of the chemical bond. Cornell University Press, Ithaca. 1948. p. 189.
14. J. H. VAN VLECK.   Phys. Rev. **74**, 1168 (1948).
15. N. BLOEMBERGEN, E. M. PURCELL, and R. V. POUND.   Phys. Rev. **73**, 679 (1948).
16. H. S. GUTOWSKY and G. E. PAKE.   J. Chem. Phys. **18**, 162 (1950).
17. E. R. ANDREW and R. A. NEWING.   Proc. Phys. Soc. (London), A, **72**, 959 (1958).
18. E. R. ANDREW.   J. Chem. Phys. **18**, 607 (1950).
19. H. FRÖHLICH.   Theory of dielectrics. 2nd ed. Oxford University Press, 1958. p. 128.
20. E. R. ANDREW.   Nuclear magnetic resonance. Cambridge University Press. 1956. p. 173.
21. D. W. MCCALL and W. P. SLICHTER.   J. Polymer Sci. **27**, 171 (1957).

CONSTITUTION OF AN ACIDIC XYLAN FROM TAMARACK (LARIX LARICINA)[1]

G. A. ADAMS

ABSTRACT

An acidic xylan isolated from tamarack wood contained arabinose, xylose, and uronic acid (1:17:3) and was homogeneous on examination by electrophoresis and sedimentation. Molecular weight estimations by four different methods showed a degree of polymerization of 20. Methylation and periodate oxidation showed that the xylan consisted of ca. 16 β-D-xylopyranose units joined by $1 \rightarrow 4$ glycosidic bonds with the possible occurrence of one $1 \rightarrow 3$ linkage. To this unbranched structure were attached as side branches, three single units of 4-O-methyl-D-glucuronic acid through C_2 and one unit of L-arabofuranose through C_3.

INTRODUCTION

The many xylans that have been isolated from land plants have all shown the same basic structure (1, 2, 3, 4). Variations in the xylans from individual species are provided by differences in the nature and number of single-unit side chains which are attached to the xylan chain and these differences have been summarized for a number of species of wood (4).

Xylans from softwoods have not been studied as extensively as those from hardwoods mainly because of the difficulty of separating them from glucomannans and other hemicelluloses. However, improved methods of fractionation will now permit this separation and the present paper reports the isolation and structure of an acidic xylan from tamarack.

The starting material was holocellulose prepared by chlorite delignification of extractive-free tamarack wood. Extraction with dilute alkali yielded a mixture of hemicelluloses from which the acidic xylan was separated by copper complexing. Evidence for the homogeneity of the purified hemicellulose was provided by single symmetrical peaks shown in the electrophoretic and sedimentation patterns (Fig. 1).
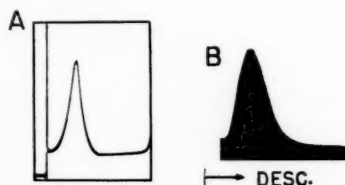
FIG. 1. (A) Sedimentation pattern of tamarack acidic xylan. (B) Electrophoresis pattern of tamarack acidic xylan.

The yield of purified hemicellulose, $[\alpha]_D$ $-35°$, was 1% (based on extractive-free wood) and arabinose, xylose, and uronic acid were present in a molar ratio of 1:17:3. There was a trace of rhamnose in the xylan hydrolyzate but no structural significance could be assigned to this sugar.

Hydrolysis of the hemicellulose yielded an aldobiouronic acid as the main acidic

product. Acetylation of the methyl ester methyl glycoside of the acid yielded a crystalline acetate (1) which established the identity of the original aldobiouronic acid as 2-O-(4-O-methyl-α-D-glucopyranosyl uronic acid)-D-xylopyranose. The hemicellulose was methylated and fractionated to give one main fraction. Methanolysis and hydrolysis yielded the following products: (1) methylated aldobiouronic acid (3.0 moles); (2) 2-O-methyl-D-xylose (1.0 mole); (3) 3-O-methyl-D-xylose (trace); (4) 2,3-di-O-methyl-D-xylose (10 moles); (5) 2,4-di-O-methyl-D-xylose (1.0 mole); (6) 2,3,4-tri-O-methyl-D-xylose (1.0 mole); (7) 2,3,5-tri-O-methyl-L-arabinose (0.90 mole).

Isolation of crystalline methyl-2-O-(2,3,4-tri-O-methyl-D-glucopyranosyl)-3-O-methyl-β-D-xyloside (2) from reduction of component 1 confirmed the earlier identification of the aldobiouronic acid and showed that the uronic acid was attached to C_2 of a xylose unit in the main chain.

The 2-O-methyl-D-xylose (component 2) represented branch points in the xylan chain and was found in the same molar amount as 2,3,5-tri-O-methyl-L-arabinose (component 7). It is probable, therefore, that the 2-O-methyl-D-xylose arose from those units in the xylan chain that carried single-unit L-arabofuranose side chains linked through C_3. The 3-O-methyl-D-xylose (component 3) probably arose from a slight amount of hydrolysis of the partially methylated aldobiouronic acid.

The 2,3-di-O-methyl-D-xylose (component 4) represented the main structural feature of the xylan, i.e. D-xylopyranose units joined in a straight chain by glycosidic bonds through C_1 and C_4. The presence of 1 mole of 2,4-di-O-methyl-D-xylose (component 5) could be accounted for by either a $1 \rightarrow 3$ linkage in the main chain or by incomplete methylation. It was unlikely that this component represented a non-reducing terminal xylose unit substituted at C_3 by an arabofuranose residue because all of the latter was accommodated by attachment to C_3 of xylose units in the chain. Xylans of red algae have been shown to contain $1 \rightarrow 3$ and $1 \rightarrow 4$ linkages (6) and there is evidence for $1 \rightarrow 2$ linkages in some of the xylans of aspen wood (7). On the other hand, Croon and Timell (8) have shown that C_3 is less reactive than C_2 in xylans and hence may not be completely methylated. Attempts to resolve this question by enzymic degradation of the tamarack xylan are now in progress.

The 2,3,4-tri-O-methyl-D-xylose (component 6) represented nonreducing terminal units and the amount found indicated a degree of polymerization (D.P.) of 20. The 2,3,5-tri-O-methyl-L-arabinose (component 7) was the only -O-methyl ether of arabinose present in the mixture and showed that all the residues of this sugar were attached as single-unit side chains. The ease with which the arabinose units were removed from the original hemicellulose by mild acid hydrolysis also confirmed that they were in the furanose form and attached as terminal groups. It has not been proved that these single arabofuranose units were attached directly to the main xylan chain with no xylose units interposed. However, this point has been established in other araboxylans by two different methods (9, 10) and it is very likely that the present araboxylan is similar.

From the foregoing evidence it was clear that the arabomethoxyglucuronoxylan consisted of 16 β-D-xylopyranose units linked $\beta1 \rightarrow 4$ with the possible occurrence of one $\beta1 \rightarrow 3$ linkage. To this unbranched structure were attached, as single-unit side chains, three 4-O-methyl-D-glucuronic acid units through C_2 and one L-arabofuranose unit through C_3.

Such a molecule would consume 0.85 mole of periodate and yield 0.15 mole of formic acid per monomer unit and the experimental values of 0.87 mole of periodate and 0.15 mole of formic were in agreement with these calculations. The D.P. of the polysaccharides

was 19–20 based on formic acid production by periodate oxidation and 20 on the basis of nonreducing terminal D-xylose units in the methylated products. The values are in reasonable agreement with those given by viscosity (D.P. 20–22) and by the method of vapor pressure lowering (11, 12) (D.P. 16). On the basis of this agreement between four methods of molecular weight estimation the molecule is considered to contain about 20 sugar units. This value is small in comparison with the D.P. values reported for xylans which range from 85–220 (13, 4). The xylan under examination was less than 10% of the original crude hemicellulose and represents a molecular species which is about equivalent in size to the repeating unit of other softwood xylans (14, 15). It seems probable that the xylans from one wood species exist in a wide range of molecular sizes. It has already been shown that xylans from one wood source have differences in chemical composition (16).

The structure of the arabomethoxyglucuronoxylan from tamarack is similar, in general, to that of other xylans isolated from coniferous woods. While the xylan of loblolly pine (16) and Norway spruce (17) do not contain L-arabinose units, those of European larch (18), Sitka spruce (15), and western hemlock (14) all contain small amounts of arabinose. The proportions of 4-O-methyl-D-glucuronic acid, L-arabinose, and D-xylose are almost the same in Sitka spruce (15), western hemlock (14), and tamarack.

EXPERIMENTAL

All specific rotations are equilibrium values unless otherwise stated, melting points are corrected, and all evaporations were done at 35° C or less.

Paper Chromatography

Chromatographic separations were carried out using the following solvent systems (v/v ratios): (a) pyridine:ethyl acetate:water (2:1:2); (b) methyl ethyl ketone:water (2:1); (c) ethanol:benzene:water (47:200:15); (d) n-butanol:ethanol:water (40:11:19); (e) ethyl acetate:acetic acid:formic acid:water (18:3:1:4). Separations were made by the descending technique on Whatman No. 1 filter paper. Sugars were located on the paper by p-anisidine hydrochloride spray reagent (19).

Preparation of the Hemicellulose

A tamarack (Larix laricina) log, 47 years old, was converted to shavings, and then ground in a Wiley mill. The wood particles were thoroughly extracted successively with benzene:ethanol (2:1), ethanol, and water. From the aqueous solution an arabogalactan was recovered in about 6% yield; its constitution has been determined and was the subject of an earlier publication (20).

The water-extracted residue was converted to chlorite holocellulose (21) and was extracted with sodium hydroxide solution (1%) at room temperature for three successive 24-hour periods. The alkaline solutions and washings were combined, neutralized with acetic acid, concentrated at 25° C under reduced pressure, and the salts removed by dialysis in running water. The crude hemicellulose was recovered by freeze-drying, and the yield was 12.9% (extractive-free wood basis). Hydrolysis of the hemicellulose in N sulphuric acid for 12 hours at 100° C and chromatographic examination of the hydrolyzate ($[\alpha]_D^{25} +22°$) showed the presence of xylose, arabinose, rhamnose, mannose, glucose, galactose, and a uronic acid. The number of sugars in the hydrolyzate indicated that more than one polysaccharide was present. Further evidence of heterogeneity was provided by electrophoretic examination in a Tiselius-type apparatus in borate buffer which showed two main peaks and indications of additional minor components.

Fractionation of the Hemicellulose

The crude polysaccharide (53 g) was dissolved, with stirring, in water (5 l.) and the insoluble material (fraction 1) was removed by centrifuging. A solution of 7% copper acetate solution (142 ml) was added to the supernatant and the precipitate which formed was removed by centrifuging (fraction 2). Addition of ethanol gave a series of fractions (No. 3 – No. 8) which were centrifuged off, freed of copper by acidification and dialysis, and recovered by freeze-drying. The results are shown in Table I.

TABLE I
Fractionation of hemicellulose
(53.14 g in 5 liters of water)

Fraction No.	Precipitating agent	Yield, g	Sugars present*				
			Xyl.	Arab.	Gal.	Glu.	Rham.
1	—	8.50	x	x	x	Tr.	Tr.
2	7% Copper acetate (143 ml)	3.41	x	x	x	Tr.	Tr.
3	Ethanol (570 ml)	22.91	x	x	x	Tr.	Tr.
4	Ethanol (142 ml)	1.22	x	x	x	Tr.	Tr.
5	Ethanol (199 ml)	2.01	x	x			Tr.
6	Ethanol (241 ml)	1.32	x	x			Tr.
7	Ethanol (285 ml)	1.24	x	x	Tr.		Tr.
8	Ethanol (570 ml)	1.72	x	x	x		Tr.
9	—	2.96	x	x	x		Tr.

*All fractions contain uronic acids.

On the basis of these results fractions No. 4 and No. 7 were combined and refractionated. The purified material was then combined with fractions No. 5 and No. 6. The last trace of copper was removed from the hemicellulose by passage of its aqueous solution over Amberlite IR-120.

The yield of purified xylan was 8.0% of the original crude hemicellulose. Analysis gave an arabinose:xylose:uronic acid ratio of 1:17:3; methoxyl, 2.9%; nitrogen, nil; and $[\alpha]_D^{25}$ −34.8° (c, 1.03% in water). The sugar mixture obtained on acid hydrolysis had $[\alpha]_D^{25}$ +24°.

Graded Hydrolysis

Hemicellulose (51 mg) was heated on a boiling-water bath with 5 ml of hydrochloric acid (0.01 N). At 30-minute intervals the hydrolyzate was examined chromatographically in solvent (a). In 3.5 hours the arabinose had been removed from the hemicellulose along with only a minor amount of xylose. The degraded hemicellulose was recovered with ethanol. Hydrolysis with N sulphuric acid and chromatographic examination of the hydrolyzate showed mainly xylose, some uronic acids, and only traces of arabinose.

Periodate Oxidation

Tamarack hemicellulose (100 mg duplicate samples) was dissolved in water (50 ml) and oxidized by 0.1 M sodium metaperiodate (50 ml) in the dark at 16° C. Analysis for periodate consumption and formic acid production (22) gave the following results.

Time, hours	24	48	72	120
Formic acid, moles per anhydropentose unit	0.14	0.145	0.15	0.16
Periodate consumption, per anhydropentose unit	0.54	0.61	0.86	0.87

In a separate experiment, the hemicellulose (50 mg) was oxidized for 120 hours as pre-viously described. The excess periodate was destroyed by ethylene glycol and the solution was dialyzed. The oxidized hemicellulose was recovered by freeze-drying and then hydrolyzed with N sulphuric acid. Chromatographic examination of the hydrolyzate showed only xylose to be present; the amount was approximately 25% of that originally present in the hemicellulose.

Preparation of Uronic Acids from the Xylan

Xylan (100 g) was stirred overnight in 0.5 N sulphuric acid at room temperature and then heated at 100° C for 8 hours. After neutralization of the acid, the neutral sugars and uronic acids were separated on a column of Dowex 1-X⁴ (HCO₃⁻) and the uronic acids recovered by elution with N formic acid by procedures already described (23). Chromatographic examination in solvent (e) showed the presence of four components with R_x values (movement relative to xylose) as follows: 0.29, 0.42, 0.70, and 1.30 (fractions 1, 2, 3, and 4). Fraction 4 was chromatographically identical with 4-O-methyl-D-glucuronic acid.

The uronic acid fractions (2.1 g) were separated on a cellulose column (27×2.5 cm) using solvent (e). Fraction No. 3 was mixed with some of fraction No. 4 and was purified by reseparating on sheets of Whatman No. 1 filter paper using solvent (e). The acids were eluted with water and concentrated in vacuo. Hydrolysis of fraction No. 3 with N sulphuric acid for 20 hours at 100° C yielded xylose and 4-O-methyl-D-glucuronic acid.

Identification of 2-O-(4-O-Methyl-α-D-glucopyranosyluronic acid)-D-xylopyranose

The aldobiouronic acid (fraction No. 3) was a slightly yellowish solid, $[\alpha]_D^{25}$ +98° (c, 1.0% in water). Anal. Calc. for $C_{12}H_{20}O_{11}$: OCH₃, 9.1%. Found: OCH₃, 9.0%. The acid (57 mg) was converted to methyl 2-O-[methyl-(4-O-methyl-α-D-glucopyranosyl)uronate]-D-xylopyranoside by heating with 2.5% methanolic hydrogen chloride (3 ml) for 8 hours. The methyl ester methyl glycoside was acetylated according to Timell (24). The acetyl-ated product was recovered and crystallized from ethyl ether, yield 30.7 mg. Recrystal-lization three times from ethyl ether yielded crystalline methyl-2-O-[methyl-(2,3-di-O-acetyl-4-O-methyl-α-D-glucopyranosyl)uronate]-3,4-di-O-acetyl-D-xylopyranoside, m.p. 201–203°, $[\alpha]_D^{25}$ +106° (c, 1.0% in chloroform). Anal. Calc. for $C_{22}H_{32}O_{15}$: OCH₃, 17.3%. Found: OCH₃, 17.2%. These values are in good agreement with the reported values (24).

Methylation of the Xylan

The xylan (6.1 g) was methylated five times with dimethyl sulphate (65 ml) and 45% sodium hydroxide (120 ml) and the product was isolated from the reaction mixture by continuous extraction with chloroform after acidification. Material that was not ex-tracted by chloroform was recovered from the aqueous solution by dialysis and freeze-drying. The combined products (6.2 g) showed a definite hydroxyl absorption at 3500–3600 cm⁻¹. Four methylations with Purdies reagents (methyl iodide, 60 ml, and silver oxide, 10 g) yielded the fully methylated xylan (5.28 g) showing no hydroxyl absorption at 3500–3600 cm⁻¹; $[\alpha]_D^{25}$ −30° (c, 1% in chloroform); methoxyl, 39.23% (calculated methoxyl, 40.83%). Fractionation of this material by mixtures of chloroform:petroleum ether gave one main fraction constituting 94% of the mixture and having the same analytical values as given above.

Hydrolysis of Methylated Xylan

The fully methylated xylan (4.9 g) was heated in 8% methanolic hydrogen chloride at 80° C for 16 hours. Acid was removed by silver carbonate and the filtrate was evapo-rated by a stream of air at room temperature. The residue was heated at 65° C for 2

hours with a saturated solution of barium hydroxide to convert the uronosides to their barium salts. Methylated glucosides (3.78 g) were recovered from this solution by extraction with chloroform and methylated uronic acids (1.53 g) were isolated by evaporation of the aqueous residue after removal of the barium ions by Amberlite IR-120.

Methyl glucosides of the neutral sugars were analyzed by gas–liquid partition chromatography (25, 26) giving the quantitative data cited in the discussion. The procedure also provided additional evidence for the identities of the components by comparison of their relative retention volumes with those of authentic samples. To obtain sufficient amounts of the methylated sugars for complete identification the mixture of glycosides was hydrolyzed by 88% formic acid at 97° C for 24 hours. The mixture of sugars (2.43 g) recovered from the hydrolyzate after neutralization with Amberlite IR-4B(OH) showed the following components on paper chromatography in solvents (b) and (c): 2,3,5-tri-O-methyl-L-arabinose, R_g 1.07, R_g 1.02; 2,3,4-tri-O-methyl-D-xylose, R_g 1.03, R_g 0.89; 2,3-di-O-methyl-D-xylose, R_g 0.69, R_g 0.25; 2,4-di-O-methyl-D-xylose, R_g 0.55, R_g 0.25; 2-O-methyl-D-xylose, R_g 0.26, R_g 0.04; 3-O-methyl-D-xylose, R_g 0.27, R_g 0.08. An attempt to resolve this mixture by chromatography on a cellulose column using solvent (b) was unsuccessful, all fractions obtained being mixtures of two or more components. Separations were therefore carried out on paper sheets (Whatman No. 3 MM with Whatman No. I wicks) using solvents (b), (c), and (d).

Identification of Methylated Sugars

2,3,5-Tri-O-methyl-L-arabinose

The sugar was dissolved in water, clarified with charcoal, and dried to constant weight (134 mg), $[\alpha]_D^{25}$ −33° (c, 1% in water), and OMe, 48.0% (calculated for $C_8H_{16}O_5$: OMe, 48.4%). Chromatographic examination in solvents (b) and (c) showed that the sugar had a rate of movement identical with that of authentic 2,3,5-tri-O-methyl-L-arabinose. A portion of the sugar (70 mg) was oxidized with bromine to yield 2,3,5-tri-O-methyl-L-arabonic acid. Distillation (bath temperature, 120–145° C at 0.020 mm) lactonized the acid, which on treatment with methanolic ammonia, yielded 2,3,5-tri-O-methyl arabonamide in crystalline form. Recrystallization from methanol – petroleum ether solution yielded pure crystals, m.p. 136° C, $[\alpha]_D^{25}$ −18° (c, 1% in water); these values agree closely with those reported for this compound (27).

2,3,4-Tri-O-methyl-D-xylose

Chromatographic examination in solvents (b) and (c) showed the syrup to be 2,3,4-tri-O-methyl-D-xylose units with a trace of the trimethyl arabinose. The syrup was dissolved in ether and a few drops of petroleum ether added; on seeding with 2,3,4-tri-O-methyl-D-xylose, crystallization occurred. Recrystallization from the same solvent yielded crystals having a melting point of 88–89° C, $[\alpha]_D^{25}$ +20° (c, 1.0 in water). Anal. calc. for $C_8H_{16}O_5$: OMe, 48.4%. Found: OMe, 48.2%.

2,3-Di-O-methyl-D-xylose

The syrup (1492 mg) had $[\alpha]_D^{25}$ +23° (c, 1.1% in water) and OMe, 34.5%. Calculated for $C_7H_{14}O_5$: OMe, 34.8%. Chromatographic examination in solvents (b) and (c) showed that it moved at the same rate as 2,3-di-O-methyl-D-xylose. On cooling an ethyl ether solution of the sugar, crystals were obtained which on recrystallization from the same solvent had a melting point of 91–92° (undepressed with an authentic sample). The anilide was formed by refluxing aniline (200 mg) with the sugar (300 mg) in methanol (5 ml) for 2.5 hours. The crystalline anilide was recrystallized twice from ethyl acetate and had a melting point of 123–124° (undepressed with an authentic sample of 2,3-di-O-methyl-N-phenyl-D-xylosylamine.

2-O-Methyl-D-xylose

The syrup (139 mg) had the same rate of movement on paper in solvents (b) and (c) as 2-O-methyl-D-xylose. After clarification with charcoal in 50% methanol, the syrup crystallized partially. Recrystallization from methanol – petroleum ether solution yielded 2-mono-O-methyl-D-xylose, m.p. 132–133°, $[\alpha]_D^{25}$ +34° (c, 1% in water).

3-O-Methyl-D-xylose

Electrophoresis of this sugar on paper strips in borate buffer (pH 9.2), with known references differentiated it from 2-O-methyl-D-xylose, which moves only slightly compared with the rapid migration of the 3-O-methyl sugar. The amounts recovered were too small to permit other identification.

Methylated Aldobiouronic Acid

The methylated aldobiouronic acid (1.53 g) which had been separated from the neutral glycosides was converted to the methyl ester methyl glycoside by refluxing for 6 hours with 4% methanolic hydrogen chloride. This product was then reduced with lithium aluminum hydride in ether solution to yield methyl 2-O-(2,3,4-tri-O-methyl-D-gluco-pyranosyl)-3-O-methyl-β-D-xyloside, which crystallized partially on standing. Recrystallization from ethyl acetate yielded a product with a melting point of 166–168° and $[\alpha]_D^{25}$ +80° (c, 1.05% in water) in good agreement with the reported values (14). Anal. Calc. for $C_{16}H_{20}O_{10}$: C, 50.25%; H, 7.91%; OMe, 40.6%. Found: C, 50.10%; H, 8.01%; OMe, 40.2%.

Electrophoresis

Hemicellulose (150 mg) was dissolved in 0.05 M borate buffer and dialyzed against the buffer at 4° C for 24 hours. The electrophoretic separation was made in a Spinco apparatus Model H for 270 minutes; the acidic xylan moved as a single symmetrical peak with mobility (μ) = 5.65×10^{-5} cm² v⁻¹ sec⁻¹. The diagram is shown in Fig. 1.

Sedimentation

Hemicellulose (2%) in 0.05 M borate buffer was centrifuged in a Model E Spinco ultracentrifuge. The rotor speed was 59,780 r.p.m. and the photograph was taken on attaining full speed (after 8 minutes). The pattern shows one sharp peak (Fig. 1).

Molecular Weight

Two physical methods of estimating molecular weight were used.

Viscosity.—Viscosity measurements were made on cupriethylenediamine solutions of the hemicellulose at concentrations of 0.08, 0.04, 0.02, 0.01, and 0.005%. Flow times were measured in an Ostwald-Cannon-Fenske type viscometer in a bath maintained at 20°± 0.02° C. The value for intrinsic viscosity [η] was substituted in the equation D.P. = K [η], where value of K = 212 (13), D.P. value = 20–22.

Vapor Pressure.—The method used was that developed by Sirianni and Puddington (11). The methylated hemicellulose was dissolved in benzene and the difference in vapor pressure between the pure solvent and the solution was measured at concentrations of 5.20, 3.72, 3.01, 2.56, 2.11, 1.90, 1.06% (g/100 g solution). The molecular weight at infinite concentrations was calculated according to Raoult's law. A straight line was fitted through the experimental points and extrapolated to infinite dilution. The observed molecular weight (number average) was 2900, therefore D.P. = 16.

ACKNOWLEDGMENTS

REFERENCES

1. R. L. Whistler.   Advances in Carbohydrate Chem. **5**, 269 (1950).
2. R. L. Whistler and C. L. Smart.   Polysaccharide chemistry. Academic Press Inc., New York. 1953. p. 134.
3. W. J. Polglase.   Advances in Carbohydrate Chem. **10**, 299 (1955).
4. G. O. Aspinall.   Advances in Carbohydrate Chem. **14**, 446 (1959).
5. T. E. Timell, C. P. T. Glaudemans, and J. K. Gillham.   Pulp Paper Mag. Can. **59**, 243 (1958).
6. E. G. V. Percival and S. K. Chanda.   Nature, **166**, 787 (1950).
7. J. K. N. Jones, E. Merler, and K. E. Wise.   Can. J. Chem. **35**, 634 (1957).
8. I. Croon and T. E. Timell.   Can. J. Chem. **38**, 720 (1960).
9. C. T. Bishop.   J. Am. Chem. Soc. **78**, 2840 (1956).
10. G. O. Aspinall and R. J. Ferrier.   J. Chem. Soc. 4188 (1957).
11. A. F. Sirianni and I. E. Puddington.   Can. J. Chem. **33**, 755 (1955).
12. R. Tremblay, A. F. Sirianni, and I. E. Puddington.   Can. J. Chem. **36**, 725 (1958).
13. C. P. T. Glaudemans and T. E. Timell.   Svensk Papperstidn. **61**, 1 (1958).
14. G. G. S. Dutton and F. Smith.   J. Am. Chem. Soc. **78**, 3744 (1956).
15. G. G. S. Dutton and K. Hunt.   J. Am. Chem. Soc. **82**, 1682 (1960).
16. J. K. N. Jones and T. J. Painter.   J. Chem. Soc. 573 (1959).
17. G. O. Aspinall and M. Carter.   J. Chem. Soc. 3744 (1956).
18. G. O. Aspinall and J. E. McKay.   J. Chem. Soc. 1059 (1958).
19. L. Hough, J. K. N. Jones, and W. H. Wadman.   J. Chem. Soc. 1702 (1950).
20. G. A. Adams.   Can. J. Chem. **38**, 280 (1960).
21. L. E. Wise, M. Murphy, and A. A. D'Addieco.   Paper Trade J. **122**, 35 (1946).
22. S. K. Chanda, E. L. Hirst, and E. G. V. Percival.   J. Chem. Soc. 1240 (1951).
23. H. C. Srivastava and G. A. Adams.   J. Am. Chem. Soc. **81**, 2409 (1959).
24. T. E. Timell.   Can. J. Chem. **37**, 827 (1959).
25. A. G. McInnes, D. H. Ball, F. P. Cooper, and C. T. Bishop.   J. Chromatog. **1**, 556 (1958).
26. C. T. Bishop and F. P. Cooper.   Can. J. Chem. **38**, 388 (1960).
27. R. W. Humphreys, J. Pryde, and E. T. Waters.   J. Chem. Soc. 1298 (1931).

PYRAZOLINES. PART II[1]

DONALD E. MCGREER, WING WAI, AND GEORGE CARMICHAEL

ABSTRACT

Product analysis has been carried out on the pyrolysis reaction in the liquid and vapor phase of 4- and 5-methyl-3-carbomethoxy-Δ^2-pyrazolines and 3-methyl-3-carbomethoxy-Δ^1-pyrazoline. The proportion of cyclopropane product was found to be greater than earlier reports had indicated and was higher for the vapor-phase pyrolysis than for the liquid-phase reaction. Vapor-phase pyrolysis of Δ^2-pyrazolines was found to require a catalyst, such as potassium hydrogen phosphate, which is believed to make possible the transformation of the Δ^2-pyrazoline into the pyrolyzable Δ^1-pyrazoline.

The pyrolysis of carbalkoxypyrazolines and related compounds has been shown to be a useful synthetic method for the preparation of derivatives of cyclopropane only in a limited number of cases. The method is particularly useful when there are carbalkoxy groups in the pyrazoline nucleus at positions 3 and 4 (1–5) and when there is an alkyl substituent and carbalkoxy substituent at the 3 position (1, 6, 7). For example, von Auwers (1) reported that 3-methyl-3-carbomethoxypyrazoline gave a product which contained 63% of methyl 1-methylcyclopropanecarboxylate and that 3,4-dicarbomethoxy-4-methylpyrazoline gave methyl 1-methylcyclopropane-1,2-dicarboxylate as the sole product. In general it has also been found that 3-carbomethoxypyrazolines with alkyl substitution at the 4 or 5 positions yield no cyclopropane product.

Recently we reported (8) that 3-carbomethoxy-Δ^2-pyrazoline yields a product which contains 32% of methyl cyclopropanecarboxylate. In a continuation of this work the 4- and 5-methyl-3-carbomethoxy-Δ^2-pyrazolines and 3-methyl-3-carbomethoxy-Δ^1-pyrazoline have been found to yield products containing cyclopropane derivatives. Upon further investigation of the pyrolysis reaction we have found that the proportion of cyclopropane derivative in the product is increased considerably when the pyrolysis is carried out in the vapor phase. For example, under these conditions 3-carbomethoxy-Δ^2-pyrazoline yields a product which contains 62% of methyl cyclopropanecarboxylate, an increase of 30% over the liquid-phase reaction.

The results of the pyrolysis of the three isomeric methyl-3-carbomethoxypyrazolines is shown in Table I and illustrated in Chart I. The liquid-phase pyrolyses were carried out by heating the pyrazoline in a distillation apparatus to a temperature at which nitrogen evolution was rapid and distillation of the product occurred as it was formed. The vapor-phase pyrolyses were carried out by dropping the liquid pyrazoline on beads or other packing material in a vertical tube heated to about 200° and connected to a vacuum system which maintained a pressure of 2 to 5 mm in the tube. The Δ^1-pyrazoline readily pyrolyzed when a glass bead packing was used but the Δ^2-pyrazolines were unchanged even with the beads at 500° unless the tube was charged with a catalyst (potassium hydrogen phosphate was used) to promote transformation of the Δ^2-pyrazoline to the Δ^1-form. This observation may be taken as further evidence that it is the Δ^1-form of the pyrazoline which pyrolyzes and not the Δ^2-form. Jones (9) and Beech et al. (10) have also obtained strong evidence in support of this postulate.

It is not possible to determine with certainty whether pyrolysis in the tube is occurring in the vapor phase or on the surface of the packing material. The catalyst, potassium

TABLE I

Product analysis from pyrazoline pyrolyses

Substituent in 3-carbomethoxy-pyrazoline	Phase	Proportion of components in the product in %				
		Cyclo-propane	α,β-Unsaturated ester		β,γ-Unsaturated ester	
			cis	trans	cis	trans
None	Liquid	32	30	31	7	
	Vapor	62	20	12	6	
3-Methyl	Liquid	65	15	15	5*	
	Vapor	85	7	4	4	
4-Methyl	Liquid	4	88		8	
	Vapor	26	62		12	
5-Methyl	Liquid	29	23*	43*	—	5
	Vapor	74†	12	10	—	4

*These compounds have not been previously reported and are tentatively identified from their N.M.R. and infrared spectra.
†Chromatography through a dinonyl phthalate or Ucon Polar column did not effect separation of the cis and trans esters. Infrared analysis of the acid obtained from the ester by hydrolysis indicated it to be 40% cis and 60% trans.

hydrogen phosphate, when added to the liquid-phase pyrolysis of 3-carbomethoxy-Δ^2-pyrazoline gives a lower yield of product which has approximately the same composition as the normal liquid-phase pyrolysis product. Because of this fact and since the boiling points of the pyrazolines at 2.5 mm are below the temperature at which pyrolysis occurs it is assumed that the pyrolysis takes place in the vapor phase. Further studies are now underway to determine the effect of catalyst, temperature, and pressure on the vapor-phase pyrolysis and to develop the method as a synthetic route to cyclopropane derivatives.

The pyrazolines used in the pyrolysis studies were prepared by the addition of diazomethane to the appropriate α,β-unsaturated ester. 3-Methyl-3-carbomethoxy-Δ^1-pyrazoline is a colorless liquid whereas the 4- and 5-methyl and the unsubstituted 3-carbomethoxypyrazolines are low-melting colorless solids which readily become straw-colored in the presence of air. The latter three are assigned the Δ^2-structure resulting from conjugation of the double bond with the ester carbonyl on the basis of their infrared spectra, which show N—H stretch and a conjugated carbonyl absorption.

The products from the pyrazoline pyrolyses were isolated by vapor chromatography and were identified from their physical properties. Three of these products (methyl 2-methyl-3-butenoate and methyl cis- and trans-2-pentenoate) have not previously been reported and the structures are tentatively assigned from the analysis, N.M.R., and infrared data and from the fact that each occur in equilibrium studies on known isomeric olefins. The evidence for these assignments is given in the experimental section.

The composition of the olefin portion of the pyrolysis product is in general not an equilibrium mixture as can be seen by a comparison of the equilibrium results in Table II with the pyrolysis results in Table I. The equilibrium values were determined by heating olefin samples at 250° for 2 weeks. The equilibrium was reached in each case by starting with two isomeric olefins and the equilibrium mixtures were analyzed by vapor chromatography. In general the olefin product from the pyrolysis reaction is richer in the cis-α,β-unsaturated olefin than is the equilibrium mixture and in many cases the cis-to-trans ratio approaches 1. A ratio of about 1 would be expected if both olefins were formed from the same high-energy intermediate for which the transition state to each olefin would be approximated by the intermediate rather than the product (11).

TABLE II

Equilibrium composition in % after equilibration at 250° C

Initial olefin	α,β-Unsaturated ester		β,γ-Unsaturated ester	
	cis	trans	cis	trans
Methyl *trans*-crotonate (8)	12	83	5	
Methyl *cis*-crotonate (8)	12	84	4	
Methyl tiglate	14	84	2	
Methyl 2-methyl-3-butenoate	14	82	4	
Methyl senecioate		84	16	
Methyl 3-methyl-3-butenoate		86	13	
Methyl *trans*-2-pentenoate	7	47	—*	46
Methyl *cis*-2-pentenoate	7	48	—*	45

*A new peak appeared in the chromatogram having one-half the area of the *cis*-2-pentenoate but was not identified.

The percentage of β,γ-unsaturated ester formed in the various reactions studied thus far seems remarkably constant and does not seem to be dependent on the relative stability of α,β- and β,γ-unsaturated products. This may mean that the β,γ-unsaturated product is also formed from the same intermediate from which the other products are formed and possibly by a proton migration (12).

The change in product composition between the liquid-phase reaction and the vapor-phase reaction is quite interesting and may make the vapor-phase reaction a feasible method for the preparation of a number of cyclopropane derivatives not readily available at the present time. The effect of the phase on the reaction may indicate that at least part of the olefin product in the liquid phase is formed by a bimolecular process which is reduced in favor of unimolecular processes in the high dilution of the vapor phase. It is therefore possible that high dilution in a solvent may also be useful for the preparation of cyclopropane derivatives where reaction in the vapor phase is not possible.

EXPERIMENTAL

Melting points and boiling points are uncorrected. Most boiling points were determined by the micro inverted capillary method. Infrared spectra were measured with a Perkin–Elmer Model 21 spectrometer using sodium chloride optics. N.M.R. spectra were recorded on a 40 Mc/s Varian spectrophotometer with field stabilizer VK 3506 and the methylene chloride used as an external standard was observed to have a value of 4.60 τ. The vapor chromatograph unit was an Aerograph model A-100-C.

Methyl-3-carbomethoxypyrazolines

The pyrazolines were prepared from diazomethane plus methyl methacrylate, diazomethane plus methyl crotonate, and diazoethane plus methyl acrylate. Ether solutions of the diazoalkane were prepared from the corresponding nitrosourea by treatment with 40% potassium hydroxide and were dried over potassium hydroxide but were not distilled. The α,β-unsaturated ester was added slowly to the ether solution until the color of the diazoalkane disappeared. The reaction to form the 4-methyl derivative took several hours but the 3- and 5-methylpyrazolines formed almost immediately at room temperature. These pyrazolines have been reported previously (1) but the following physical constants were not included in the report. The yields given are based on the reagent used in lowest molar quantity indicated in parentheses after the yield.

3-Methyl-3-carbomethoxy-Δ^1-pyrazoline: b.p. 89°/1.5 mm, yield 57% (nitrosourea).

MCGREER ET AL.: PYRAZOLINES. II

The infrared spectrum (10% in chloroform) showed no absorption due to N—H or C=N. The ester carbonyl appeared at 1734 cm⁻¹.

4-Methyl-3-carbomethoxypyrazoline: b.p. 98/1.2 mm, m.p. 26–27°, yield 35% (nitrosourea). The infrared spectrum (10% in chloroform) had bands at 3400, 1705, and 1566 cm⁻¹ assigned to the N—H, C=O, and C=N functions (13).

5-Methyl-3-carbomethoxypyrazoline: b.p. 96°/1 mm, m.p. 37–38°, yield 77% (methylacrylate). The infrared spectrum (10% in chloroform) had bands at 3420, 1706, and 1568 cm⁻¹ assigned to the N—H, C=O, and C=N functions (13).

Pyrolysis of 3-Methyl-3-carbomethoxy-Δ¹-pyrazoline

3-Methyl-3-carbomethoxy-Δ¹-pyrazoline (10 g, 0.07 mole) was heated in a distillation apparatus in an oil bath. At a bath temperature of 110° pyrolysis was indicated by the evolution of a gas and at 150° it became vigorous. Distillation yielded 7.0 g (88%) of a colorless product boiling up to 141°. Four components were isolated by vapor chromatography and were identified as indicated below where boiling point, refractive index, retention time in the vapor chromatogram using a 10-ft Ucon Polar column of 0.25-in. diameter with a helium flow rate of 67 cc/minute, and percentage of the total product determined by the weights of paper cuts of the peaks are given. In all chromatographic analyses it is assumed that the thermal conductivities of the components are close enough to each other compared to helium to be assumed equal.

Methyl tiglate: b.p. 137–139°, n_D^{24} 1.4353 (lit. (14) b.p. 139.4–139.6°, n_D^{20} 1.4370), 29.1 minutes, 15%.

Methyl angelate: b.p. 127–128°, n_D^{20} 1.4320 (lit. (14) b.p. 127.6–127.8°, n_D^{20} 1.4321), 19.5 minutes, 15%.

Methyl 1-methylcyclopropanecarboxylate: b.p. 122.5–123° (lit. (15) b.p. 121–123°), n_D^{24} 1.4198, 17.9 minutes, 65%.

Methyl 2-methyl-3-butenoate: b.p. 115–116°, n_D^{24} 1.4091, 13.3 minutes, 5%. Calc. for $C_6H_{10}O_2$: C, 63.11; H, 8.84. Found: C, 62.81; H, 8.79. The physical constants for the isomer methyl α-ethylacrylate are b.p. 122–123° and n_D^{20} 1.4243 (14). The structure was confirmed from the infrared spectrum (10% in carbon tetrachloride), which showed absorption at 1740 cm⁻¹ and 1640 cm⁻¹ indicative of a non-conjugated ester and a carbon–carbon double bond (16). The N.M.R. spectrum (0.20 ml per ml of carbon tetrachloride) had a complex multiplet in the olefin hydrogen region with peaks at 4.14, 4.36, 4.57, 4.82, 4.89, 5.22, and 5.27 τ. Other peaks were due to the ester methyl, 6.42 (singlet), the tertiary hydrogen, 6.88 (quartet with $J \simeq 7$ c.p.s.), and the alkyl methyl, 8.83 (doublet with $J \simeq 7.2$ c.p.s.) (17).

Vapor-Phase Pyrolysis of 3-Methyl-3-carbomethoxy-Δ¹-pyrazoline

The lower portion of a 50 cm ×25 mm tube was placed in a vertical position in a tube furnace 25 cm in length and heated to 200°. The tube was filled to 35 cm from its lower end with ⅝ in. diameter pyrex beads. The portion of the tube above the furnace was heated to 100° with a heating coil. The tube was fitted at the top with a pressure-equalized dropping funnel and at the bottom with two traps in series connected to a vacuum system. The traps were cooled with acetone – Dry Ice mixtures.

Two grams of 3-methyl-3-carbomethoxypyrazoline, b.p. 89°/1.5 mm, was added dropwise to the pyrolysis tube held at a pressure of 2 to 5 mm. The pyrolysis product was analyzed by vapor chromatography as in the analysis of the liquid-phase pyrolysis product and was found to contain 4% of methyl 2-methyl-3-butenoate, 85% of methyl 1-methylcyclopropanecarboxylate, 7% of methyl angelate, and 4% of methyl tiglate.

Isomerization Studies on Methyl Tiglate and Methyl 2-Methyl-3-butenoate

Ampoules containing 100 mg of methyl tiglate and methyl 2-methyl-3-butenoate isolated from the pyrolysis mixture were heated in a furnace at 250° for 2 weeks. The samples were analyzed by vapor chromatography in the same manner as the product from the pyrolysis of 3-methyl-3-carbomethoxypyrazoline and was found to contain from methyl tiglate and methyl 2-methyl-3-butenoate, respectively, methyl 2-methyl-3-butenoate 2%, 4%; methyl angelate 14%, 14%; and methyl tiglate 84%, 82%. The only new peak which might possibly be due to the isomer methyl α-ethylacrylate was a peak at 11.7 minutes, which showed a maximum area of 0.5 that of the methyl 2-methyl-3-butenoate. Analysis with a dinonyl phthalate column failed to show any new peaks.

Vapor-Phase Pyrolysis of 3-Carbomethoxy-Δ²-pyrazoline

The apparatus used was identical with that used for the pyrolysis of 3-methyl-3-carbomethoxy-Δ¹-pyrazoline except that the pyrolysis tube above the furnace was heated with heating tape to 90° and the 15-cm portion of the tube in the center of the tube furnace was packed with potassium hydrogen phosphate. Pyrolysis of a 2-g sample yielded a colorless product which was shown by vapor chromatographic analysis (8) to contain methyl vinylacetate 6%, methyl cis-crotonate 20%, methyl cyclopropanecarboxylate 62%, and methyl trans-crotonate 12%.

Pyrolysis of 3-Carbomethoxypyrazoline in the Presence of Potassium Hydrogen Phosphate

In a distillation apparatus was placed 5.2 g of 3-carbomethoxy-Δ²-pyrazoline and 1.5 g of potassium hydrogen phosphate and the mixture was heated in an oil bath to 190°. Analysis of the distillate (1.8 g, 44%) (8) showed methyl vinylacetate 6%, methyl cyclopropanecarboxylate 27%, methyl cis-crotonate 35%, and methyl trans-crotonate 32%.

Pyrolysis of 4-Methyl-3-carbomethoxy-Δ²-pyrazoline

4-Methyl-3-carbomethoxy-Δ²-pyrazoline (23 g, 0.15 mole) was pyrolyzed in a distillation apparatus at 190° in a similar manner to that described for 3-methyl-3-carbomethoxy-Δ¹-pyrazoline to give 15 g (80%) of a colorless product boiling up to 138°. Three components were isolated by vapor chromatography and identified as indicated below where boiling point, refractive index, retention time in the vapor chromatogram using a 10-ft Ucon Polar column of 0.25-in. diameter with a helium flow rate of 67 cc/minute, and percentage of the total product are given.

Methyl senecioate: b.p. 136°, n_D^{24} 1.4368, 31.2 minutes, 88%. This sample was identical in all respects with an authentic sample prepared by the procedure of Wagner (18).

Methyl 3-methyl-3-butenoate: b.p. 125°, n_D^{23} 1.4171 (lit. (18) b.p. 41°/27 mm, n_D^{20} 1.4168), 21.2 minutes, 8%.

Methyl 2-methylcyclopropanecarboxylate: —, n_D^{23} 1.4220, 26.8 minutes, 4%. The infrared and N.M.R. spectra of this compound were identical with those of the sample isolated from the pyrolysis of 5-methyl-3-carbomethoxypyrazoline.

Vapor-Phase Pyrolysis of 4-Methyl-3-carbomethoxy-Δ²-pyrazoline

The pyrolysis was carried out at 225° by the procedure described for the vapor-phase pyrolysis of 3-carbomethoxy-Δ²-pyrazoline. Under these conditions 10% of the pyrazoline was not pyrolyzed and was frozen out of the product. Analysis of the product by vapor chromatography showed that the product contained methyl senecioate 62%, methyl 2-methylcyclopropanecarboxylate 26%, and methyl 3-methyl-3-butenoate 12%.

Isomerization Studies on Methyl Senecioate and Methyl 3-Methyl-3-butenoate

Samples of methyl senecioate and methyl 3-methyl-3-butenoate were heated at 250°

for 2 weeks. Analysis of the product showed, respectively, methyl senecioate 84%, 87%; and methyl 3-methyl-3-butenoate 16%, 13%.

Pyrolysis of 5-Methyl-3-carbomethoxy-Δ²-pyrazoline

5-Methyl-3-carbomethoxy-Δ²-pyrazoline (5.0 g, 0.33 mole) was pyrolyzed in a distillation apparatus at 190° in a similar manner to that described for 3-methyl-3-carbomethoxy-Δ¹-pyrazoline to give 3.0 g (80%) of a colorless liquid boiling up to 142°. Four components were isolated and identified as indicated below where boiling point, refractive index, retention time in the vapor chromatogram using a 10-ft Ucon Polar column at 100° with a helium flow rate of 45 cc/minute, and percentage of the total product are given.

Methyl *trans*-2-pentenoate: b.p. 142°, n_D^{21} 1.4315, 37.2 minutes, 43%. Calc. for $C_6H_{10}O_2$: C, 63.11; H, 8.84. Found: C, 62.90; H, 8.91. The infrared spectrum (10% in carbon tetrachloride) showed bands at 1712, 1662, and 981 cm⁻¹ characteristic of a *trans-α,β-*unsaturated ester (16). The N.M.R. spectrum (0.5 g per cc of carbon tetrachloride) showed vinyl hydrogen signals at 3.16 τ (sextet with $J_{trans} \simeq 16$ c.p.s. and $J_{CH_2} \simeq 6.4$ c.p.s.) and 4.41 τ (doublet), ester methyl hydrogens at 6.50 τ (singlet), methylene hydrogens at 7.78 τ (multiplet), and alkyl methyl hydrogens at 9.05 τ (triplet $J \simeq 7.2$ c.p.s.). These data are consistent with the *trans-α,β-*unsaturated structure assigned to this compound (17).

Methyl *cis*-2-pentenoate: b.p. 128°, n_D^{20} 1.4281, 23.6 minutes, 23%. Calc. for $C_6H_{10}O_2$: C, 63.11; H, 8.84. Found: C, 62.91; H, 9.14. The infrared spectrum (10% in carbon tetrachloride) showed bands at 1723 and 1643 cm⁻¹ characteristic of an α,β-unsaturated ester (16). The N.M.R. spectrum (0.5 g per cc of carbon tetrachloride) was similar to that of the trans ester except for the value of the vinyl splitting constant, which was smaller in magnitude. Signals were found at 3.89 τ (sextet $J_{cis} \simeq 11.6$ c.p.s. and $J_{CH_2} \simeq 6.8$ c.p.s.), 4.46 τ (doublet), 6.55 τ (singlet), 7.56 τ (multiplet), and 9.23 τ (triplet $J \simeq 7.2$). These data are consistent with the *cis-α,β-*unsaturated structure assigned to this compound (17).

Methyl 2-methylcyclopropanecarboxylate: b.p. 130°, n_D^{20} 1.4228, 27.2 minutes, 29%. Calc. for $C_6H_{10}O_2$: C, 63.11; H, 8.84. Found: C, 63.28; H, 8.76. Hydrolysis with 10% sodium hydroxide of a 2-g sample obtained from a large-scale pyrolysis run, from which the olefin product was removed by oxidation with potassium permanganate, gave 1 g of 2-methylcyclopropanecarboxylic acid, b.p. 190–191° (lit. (19) b.p. 190–191°), n_D^{26} 1.4381. The infrared spectrum (10% in carbon disulphide) showed bands at 1174 cm⁻¹ and 1013 cm⁻¹ characteristic of the cis and trans acids, respectively, as well as the other prominent bands reported for these acids (20). The mixture was analyzed by the baseline method of Heigl (21) using the bands at 1174 and 1013 cm⁻¹ and the spectra of the pure cis and trans acids kindly provided by D. E. Applequist and A. H. Peterson and was found to be 40% cis and 60% trans.

Methyl *trans*-3-pentenoate: b.p. 137°, n_D^{21} 1.4220 (lit. (22) b.p. 128°/625 mm, n_D^{20} 1.4217), 30.4 minutes, 5%. No reason can be found for the discrepancy in the boiling point. A sample isolated from the isomerization mixture (see below) had a boiling point of 136°. The infrared spectrum (10% in carbon tetrachloride) showed bands at 1740 and 970 cm⁻¹ characteristic of a trans olefin and an ester but no bands were found in the 1600 to 1700 cm⁻¹ region possibly due to the symmetry of the double bond (16). The N.M.R. spectrum (0.3 g per cc of carbon tetrachloride) showed bands at 4.62 τ (multiplet), 6.46 τ (singlet), 7.12 τ (broad), and 8.50 τ (broad) as would be expected for the assigned

3-Methyl-3-carbomethoxy-Δ^1-pyrazoline
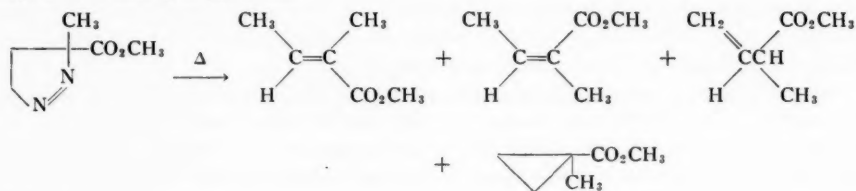
4-Methyl-3-carbomethoxy-Δ^2-pyrazoline
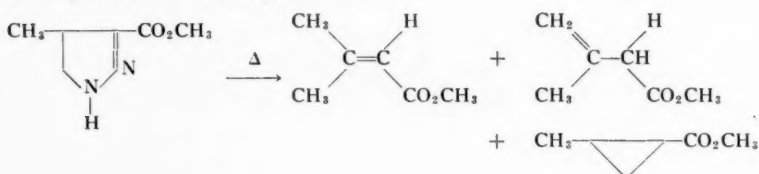
5-Methyl-3-carbomethoxy-Δ^2-pyrazoline
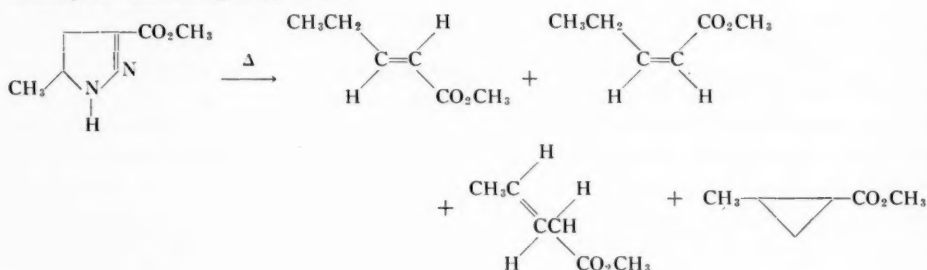
CHART I.

structure with broadening of the signals due to the large amount of long-range splitting possible (23).

Vapor-Phase Pyrolysis of 5-Methyl-3-carbomethoxy-Δ^2-pyrazoline

The pyrolysis was carried out at 225° by the procedure described for the vapor-phase pyrolysis of 3-carbomethoxy-Δ^2-pyrazoline. Analysis of the product showed the presence of methyl *trans*-2-pentenoate 10%, methyl *cis*-2-pentenoate 12%, methyl 2-methyl-cyclopropanecarboxylate 74%, and methyl *trans*-3-pentenoate 4%.

Isomerization Studies on Methyl trans-2-Pentenoate and Methyl cis-2-Pentenoate

Samples of methyl *trans*-2-pentenoate and methyl *cis*-2-pentenoate were heated at 250° for 2 weeks. Analysis of the product showed, respectively, methyl *cis*-2-pentenoate 7%, 7%; methyl *trans*-2-pentenoate 47%, 48%; and methyl *trans*-3-pentenoate 46%, 45%. In addition to these components a peak which had not previously been observed appeared in the chromatogram at 20.8 minutes. This peak was approximately one half of the area of that for methyl *cis*-2-pentenoate and might possibly be due to methyl *cis*-3-pentenoate. No new peaks were found when a dinonyl phthalate column was used.

REFERENCES

1. K. VON AUWERS and F. KONIG. Ann. **496**, 252 (1932).
2. H. STAUDINGER, E. ANTHES, and F. PFENNINGER. Ber. **49**, 1928 (1916).
3. L. J. SMITH and K. L. HOWARD. J. Am. Chem. Soc. **65**, 159 (1943).
4. P. C. GUHA and D. K. SANKARAN. Ber. **70**, 1688 (1937).
5. W. M. JONES. J. Am. Chem. Soc. **81**, 5155 (1959).
6. D. GOTKIS and J. B. CLOKE. J. Am. Chem. Soc. **56**, 2710 (1934).
7. P. C. GUHA and D. K. SANKARAN. Ber. **71**, 2673 (1938).
8. D. E. McGREER. J. Org. Chem. **25**, 852 (1960).
9. W. M. JONES. J. Am. Chem. Soc. **82**, 3136 (1960).
10. S. G. BEECH, J. H. TURNBULL, and W. WILSON. J. Chem. Soc. 4686 (1952).
11. G. S. HAMMOND. J. Am. Chem. Soc. **77**, 334 (1955).
12. W. G. YOUNG, L. J. ANDREWS, S. L. LINDENBAUM, and S. J. CRISTOL. J. Am. Chem. Soc. **66**, 810 (1944).
13. J. A. MOORE. J. Org. Chem. **20**, 1607 (1955).
14. M. NASTER and A. GAVRILOFF. Bull. soc. chim. Belges, **42**, 519 (1933).
15. M. KOHN and A. MENDELEWITSCH. Monatsh. **42**, 227 (1921).
16. L. J. BELLAMY. The infra-red spectra of complex molecules. Methuen & Co., Ltd., London. 1958. pp. 34, 175.
17. L. M. JACKMAN. Applications of nuclear magnetic resonance spectroscopy in organic chemistry. Pergamon Press, New York. 1959. pp. 50, 85.
18. R. B. WAGNER. J. Am. Chem. Soc. **71**, 3214 (1949).
19. R. MARBURG. Ann. **294**, 111 (1897).
20. D. E. APPLEQUIST and A. H. PETERSON. J. Am. Chem. Soc. **82**, 2372 (1960). The authors are deeply indebted to D. E. Applequist and A. H. Peterson for providing copies of these spectra.
21. J. J. HEIGL, M. F. BELL, and J. U. WHITE. Anal. Chem. **19**, 293 (1947).
22. H. L. GOERING, S. J. CRISTOL, and K. DITTMAR. J. Am. Chem. Soc. **70**, 3314 (1948).
23. R. R. FRASER. Can. J. Chem. **38**, 549 (1960).

THE KINETICS OF THE TERTIARY-AMINE-CATALYZED REACTION OF ORGANIC ISOCYANATES WITH THIOLS[1]

Yoshio Iwakura and Hisao Okada

ABSTRACT

The kinetics of the reactions of isocyanates with thiols in the presence of tertiary amines were examined. The rate of the reaction was of the first order with respect to the concentration of isocyanate, thiol, and tertiary amine. The catalytic action of tertiary amines decreased in the order of triethylenediamine, triethylamine, diethylcyclohexylamine, tributylamine, N-methylmorpholine, pyridine, and quinoline. The relative rate of the reaction of phenyl isocyanate with thiols decreased in the order of phenylmethanethiol, 1,4-butanedithiol, 1-butanethiol, 1-dodecanethiol, and thiophenol. The reaction took place more smoothly in strong ionizing solvents. These facts can be explained by the reaction mechanism indicated by the equations [6] to [8].

INTRODUCTION

The kinetics of the reactions of phenyl isocyanate in the presence of triethylamine with 1-butanethiol, 1-dodecanethiol, and 2-methylpropane-2-thiol in toluene solution at 25° have been investigated by Dyer and Glenn (1). Their work revealed the strong catalytic effect of triethylamine in the reaction, but did not elucidate the mechanism of the reaction. In the absence of a catalyst, the reaction of organic isocyanates with thiols proceeds at high temperatures (2, 3, 4). In the presence of triethylamine, however, the reaction proceeds very smoothly even at room temperature. In the presence of diethyl-cyclohexylamine, aromatic isocyanates react preferentially with the thiol group rather than the hydroxyl group in 2-mercaptoethanol (5).

In the present work, the catalytic effect of tertiary amines in the reaction between isocyanates and thiols has been kinetically studied and a reaction mechanism has been proposed. The results are compared with similar data from the reactions of isocyanates with alcohols (6, 7) and with carboxylic acids (8).

RESULTS AND DISCUSSION

It has been reported that, in the reaction of phenyl isocyanate with 1-butanethiol in the presence of triethylamine in toluene solution at 25°, the catalytic action was of the first order with respect to concentration of the amine; the reaction approximately followed the second-order kinetics during the early stages of the reaction (1).

The reaction of phenyl isocyanate in the presence of 0.0050 mole/liter of tributylamine catalyst with various initial concentrations of 1-dodecanethiol in benzene solution at 35° was examined kinetically and the results obtained are plotted in Fig. 1. The rate constants calculated for a second-order reaction are almost constant over the full course of the reaction and do not vary according to the initial concentration of 1-dodecanethiol. This indicates that the reaction followed second-order kinetics. Figure 1 and other data are summarized in Table I.

The reaction velocity of organic isocyanate with thiol in the presence of tertiary amine
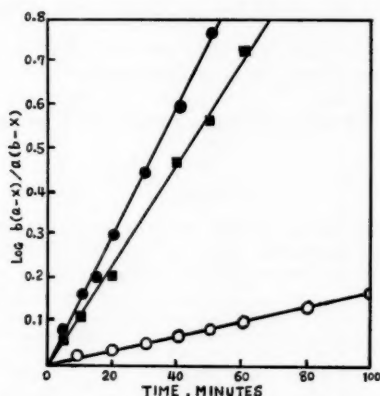
FIG. 1. Representative second-order rate plots for the reaction of phenyl isocyanate with 1-dodecane-thiol in the presence of 0.0050 mole/liter tributylamine in toluene at 35°.
Ordinate: variables in the equation [12].
Initial concentration: $b = C_6H_5NCO = 0.1250$ mole/liter.
$a = C_{12}H_{25}SH = 0.1498$ mole/liter ○.
$C_{12}H_{25}SH = 0.2995$ mole/liter ■.
$C_{12}H_{25}SH = 0.3603$ mole/liter ●.

TABLE I

The reaction of phenyl isocyanate with thiols at $35\pm0.02°$
(Initial concentration: $[C_6H_5NCO] = 0.1250$ mole/liter)

Thiol	Initial concn. of thiol (mole/liter)	Solvent	Tertiary amine	Concn. of tertiary amine (mole/liter)	Second-order rate constant (liter mole^{-1} min^{-1})
n-C$_{12}$H$_{25}$SH	0.1498	Benzene	Tributylamine	0.0050	0.154
"	0.2995	"	"	0.0050	0.153
"	0.3603	"	"	0.0050	0.144
n-C$_4$H$_9$SH	0.0750	p-Dioxane	N-Methylmorpholine	0.010	0.0456
"	0.1250	"	"	0.010	0.0518
"	0.2500	"	"	0.010	0.0466
"	0.3750	"	"	0.010	0.0441
n-C$_{12}$H$_{25}$SH	0.1250	Dibutyl ether	Tributylamine	0.0025	0.0309
"	0.3750	"	"	0.0025	0.0255

is of the first order with respect to the concentration of isocyanate, thiol, and tertiary amine, and is shown to follow equation [1]:

[1] $$-d[\text{R—NCO}]/dt = k[\text{R—NCO}][\text{R—SH}][\text{R}_3\text{N}].$$

If $[\text{R}_3\text{N}]$ is regarded as constant through a run, equation [2] is applicable, where k' is $k[\text{R}_3\text{N}]$:

[2] $$-d[\text{R—NCO}]/dt = k'[\text{R—NCO}][\text{R—SH}].$$

To compare the catalytic effects of tertiary amines in the reaction of phenyl isocyanate with 1-butanethiol, the rates of reaction catalyzed by seven tertiary amines were studied in toluene solution at 30°. In the absence of a catalyst, the reaction proceeded very

slowly and the rate constant was regarded as almost zero, that is, k_0 was negligible in the equation [3],

$$[3] \qquad\qquad\qquad k_{obs} = k_0 + k_c[R_3N],$$

where k_{obs} is the second-order rate constant observed. The results obtained are listed in Table II.

TABLE II

The reaction of phenyl isocyanate with 1-butanethiol in toluene solution at 30°
(Initial concentration: $[C_6H_5NCO] = [n\text{-}C_4H_9SH] = 0.1250$ mole/liter)

Tertiary amine	pK_a	Concn. of tertiary amine (mole/liter)	Second-order rate constant (liter mole^{-1} min^{-1})	Catalytic coefficient, k_c
Triethylenediamine	8.60	0.000468	0.0365	77.9
Triethylamine	10.78	0.0050	0.345	68.6
,,		0.0025	0.174	
Diethylcyclohexylamine		0.00994	0.375	39.6
,,		0.00497	0.178	
Tributylamine	9.93	0.0050	0.0754	15.6
,,		0.0025	0.0364	
N-Methylmorpholine	9.29	0.10	Too fast	1.08
,,		0.010	0.0108	
Pyridine	5.23	0.10	0.00314	
,,		0.010	Too slow	0.0314
N,N-Dimethylaniline	5.00	0.10	—	0.0

N,N-Dimethylaniline did not show any catalytic effect. This phenomenon confirms evidences obtained for the reaction of phenyl isocyanate with methyl alcohol (6a), the polymerization reaction of isocyanates (9), and the reaction of diisocyanates with polyols (10). The plot of [R₃N] against k_{obs} gave a straight line, showing that the catalytic effect was directly proportional to the concentration of tertiary amines. The catalytic coefficient k_e in the equation [3] was calculated from this slope for each of the tertiary amines used; the value obtained are listed in the fifth column in Table II. The catalytic coefficients fall almost in the same order as the basicity of the tertiary amines with the exception of triethylenediamine. With such strongly basic tertiary amines as triethylamine, diethyl-cyclohexylamine, and tributylamine the catalytic coefficients for the reaction of phenyl isocyanate with 1-butanethiol are larger than for the reaction of phenyl isocyanate with ethanol in dibutyl ether (6), but with weakly basic tertiary amines the opposite is true, that is, the coefficients for the reaction with alcohol are larger. This possibly explains the difference in reactivity of the hydroxyl and the thiol group of 2-mercaptoethanol in the presence of diethylcyclohexylamine (5). Triethylenediamine was much more effective catalytically than would be expected from its basicity, but this effect was less than that in the reaction between phenyl isocyanate and alcohol (11, 12).

The reactions of phenyl isocyanate with a large excess of 1-dodecanethiol in toluene at various temperatures were kinetically examined. The second-order rate constants and the apparent energies of activation calculated from the Arrhenius equation are listed in Table III with respect to the seven tertiary amines.

The reactions between phenyl isocyanate and 1-butanethiol in the presence of tertiary amines were studied in various solvents; the results obtained are listed in Table IV. The rate constants of the reaction increased in the order of benzene, toluene, dibutyl ether, dioxane, methyl ethyl ketone, and nitrobenzene. This solvent effect increased with increasing ionizing power of the solvents and was contrary to the result of the reaction

TABLE III

The reaction of phenyl isocyanate (0.1 mole/liter) with a large excess of
1-dodecanethiol (2 g) in toluene solution

Tertiary amine	Second-order rate constant (liter mole⁻¹ sec⁻¹)			Apparent energies of activation (cal/mole)
	20°	30°	40°	
Triethylenediamine	—	—	1.07	—
Triethylamine	0.765	0.877	1.03	2500
Diethylcyclohexylamine	0.617	0.704	0.811	2500
Tributylamine	0.363	0.406	0.470	2600
N-Methylmorpholine	0.0165	0.0201	0.0246	3600
Pyridine	0.000299	0.000427	—	5800
Quinoline	0.000232	0.000319	—	5800

TABLE IV

The reaction of phenyl isocyanate with 1-butanethiol in various solvents
(Initial concentration: $[C_6H_5NCO] = [n\text{-}C_4H_9SH] = 0.1250$ mole/liter)

Solvent	Tertiary amine	Concn. of tertiary amine (mole/liter)	Second-order rate constant (liter mole⁻¹ min⁻¹)	Reaction temperature (±0.02°)
Toluene	Triethylamine	0.0050	0.345	30
,,	,,	0.0025	0.174	,,
p-Dioxane	,,	0.0053	1.68	,,
,,	,,	0.0026	0.826	,,
Methyl ethyl ketone	,,	0.0025	1.17	,,
Nitrobenzene	,,	0.0025	2.27	,,
Methyl ethyl ketone	Pyridine	0.050	0.0158	35
Nitrobenzene	,,	0.050	0.0169	,,

of organic isocyanates with alcohols (7). This indicates that the rate-controlling step is represented by equation [8] and that the attack of the thiols on the complex-2 is accelerated by ionization of the thiols. In a powerful ionizing solvent, that is, a solvent having a greater dielectric constant, the thiols undergo ionization to a greater degree and gain more acidic character.

The reactions of phenyl isocyanate with different thiols in toluene at 30°, in the presence of triethylamine or diethylcyclohexylamine, was examined. The results obtained are listed in Table V. The reactivity of the thiols increased in the order of thiophenol,

TABLE V

The reaction of phenyl isocyanate with thiols in toluene solution at 30°
(Initial concentration: $[C_6H_5NCO] = [R\text{—}SH] = 0.1250$ mole/liter)

Thiol	pK_a*	Catalyzed with diethylcyclohexylamine (0.0050 mole/liter)	Catalyzed with triethylamine (0.0050 mole/liter)
1-Dodecanethiol	13.8	0.162	0.306
1-Butanethiol	12.4	0.178	0.345
Phenylmethanethiol	11.8	2.6	3.1
Thiophenol	8.3	Too slow	Too slow
1,4-Butanedithiol	—	—	0.92

NOTE: Unit of second-order rate constant, liter mole⁻¹ min⁻¹.
*Compt. rend. **232**, 2428 (1951).

1-dodecanethiol, 1-butanethiol, 1,4-butanedithiol, and phenylmethanethiol. No satisfactory explanation can be suggested at this time for the low activity of thiophenol.

In order to compare the reactivity of aromatic and aliphatic isocyanates and to examine the catalytic effect of tertiary amines on the two types, the kinetics of the reaction of ethyl isocyanate with 1-butanethiol in the presence of triethylamine in toluene at 30° were studied. The rate constants were 0.0422 liter mole^{-1} min^{-1} for 0.050 mole/liter and 0.0219 liter mole^{-1} min^{-1} for 0.025 mole/liter of triethylamine. The catalytic co-efficients of triethylamine were 68.6 for phenyl isocyanate and 0.86 for ethyl isocyanate in their reaction with 1-butanethiol.

The work of Baker and Gaunt (6) indicates that the probable mechanism of the catalyzed reaction of phenyl isocyanate and alcohol follows the path shown by formulae [4], [5]:

$$\begin{cases} R\text{—}NCO + R_3N \rightleftharpoons \begin{pmatrix} R\text{—}N{=}C{=}O \\ \ \ \ | \\ \ \ R_3N \end{pmatrix}_{\text{(complex)}} & [4] \\ \text{complex} + R\text{—}OH \rightarrow RNHCO_2R + R_3N. & [5] \end{cases}$$
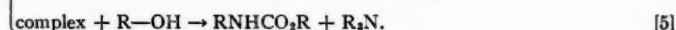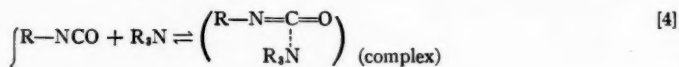
In equation [5], the active hydrogen-containing compound attacks the complex consisting of isocyanate and tertiary amine. In this case the rate of reaction is controlled by the acidity of the active hydrogen compound. Thiols are more acidic than alcohols; therefore, the catalytic coefficient of strongly basic tertiary amines in the reaction of isocyanate with thiol is larger than in the reaction with alcohol. With very weakly basic tertiary amines, however, the catalytic coefficient does not agree with the above presumption. From previously published (13) spectroscopic evidence of interaction between tertiary amines and thiols and from the experimental results given above, the probable mechanism of the catalyzed reaction of isocyanate and thiol seems to follow the kinetic scheme outlined below:

$$\begin{cases} R\text{—}SH + R_3N \underset{k_2}{\overset{k_1}{\rightleftharpoons}} (R\text{—}SH\text{---}NR_3) & [6] \\ \qquad\qquad\qquad \text{complex-1} \\ \\ \text{complex-1} + R\text{—}N{=}C{=}O \underset{k_4}{\overset{k_3}{\rightleftharpoons}} \begin{pmatrix} \text{complex-1} \\ \ \ \ \ | \\ R\text{—}N{=}C{=}O \end{pmatrix} & [7] \\ \qquad\qquad\qquad\qquad \text{complex-2} \\ \text{complex-2} + R\text{—}SH \overset{k_5}{\rightarrow} RNHCOSR + R_3N + R\text{—}SH. & [8] \end{cases}$$
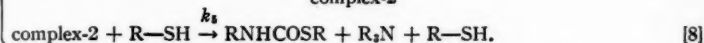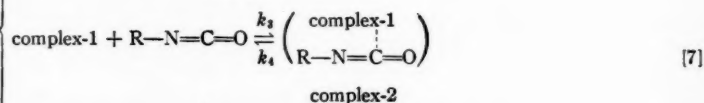
Assuming a steady-state concentration of the complex, the following kinetic equation is obtained:

$$[9] \qquad \frac{d[\text{RNHCOSR}]}{dt} = \frac{k_1 k_3 k_5 [R_3N][R\text{—}NCO][R\text{—}SH]^2}{(k_2 + k_3[R\text{—}NCO])(k_4 + k_5[R\text{—}SH])}.$$

In this equation, if

$$[10] \qquad\qquad k_2 \gg k_3[R\text{—}NCO], \qquad k_4 \ll k_5[R\text{—}SH]$$

are effective, the equation [9] stands for the equation [1].

EXPERIMENTAL

Procedures

The reaction vessel used was a long-necked, round-bottomed flask of approximately 50-ml capacity. A thiol – tertiary amine solution was prepared using a volumetric flask at a specified reaction temperature. Two milliliters of the thiol – tertiary amine solution

was pipetted into the reaction vessel. The isocyanate solution was prepared by the same method as the thiol – tertiary amine solution. A kinetic run was initiated by adding 2 ml of the isocyanate solution into the reaction vessel. To the reaction mixture in each of the reaction vessels (seven or eight) 10 ml of dibutylamine–acetone solution was periodically added and allowed to stand for about 15 minutes to react completely the remaining isocyanate in the vessel. Reaction rates were determined by following the disappearance of the isocyanate group by a modified Stagg method (14). Unreacted dibutylamine in a reaction vessel was then titrated with 0.05 N hydrochloric acid – ethanol solution, using a semimicroburette and bromophenol blue as the indicator. Blank titration of dibutylamine and tertiary amine was also carried out and normality of the isocyanate solution was determined. In the case of a reaction with a large excess of thiol, 1 ml of tertiary amine solution and about 2 g of 1-dodecanethiol were mixed and 2 ml of isocyanate solution was added. Reproducibility of the experiments was good and agreement of duplicate runs was ±2%.

Data were calculated and plotted according to the usual second-order reaction rate equation for reactants either at equal or at different initial concentration,

[11]
$$kt = \frac{x}{a(a-x)},$$

[12]
$$kt = \frac{2.303}{a-b} \log \frac{b(a-x)}{a(b-x)},$$

where a and b are initial concentration of isocyanate and thiol and x is concentration reacted at time t. In the case of a large excess of thiol, calculations were carried out using the first-order reaction rate equation. Representative rate plots are given in Fig. 1. Rate constants were determined from the slope of the best straight line drawn through the points of the plot (by the method of least squares).

In the literature (1) the autocatalytic effect of the product in this kind of reaction was described, but, in this present study, the autocatalytic phenomenon was not examined in detail. In the reaction catalyzed with a very weakly basic tertiary amine, however, very weak autocatalytic acceleration effect on the reaction was observed.

Materials

Diethylcyclohexylamine was prepared from hexylamine and ethyl iodide by a method described in the literature (15) and distilled, b.p. 185–192°. Triethylenediamine was recrystallized from ether, m.p. 156–157°. Other tertiary amines were dried over potassium hydroxide and fractionally distilled: b.p. triethylamine, 87–89°; tributylamine, 98–99°/19 mm; pyridine, 115.5°; N-methylmorpholine, 114°; N,N-dimethylaniline, 93°/29 mm; quinoline, 112°/14 mm. Commercial thiophenol was distilled, b.p. 68°/20 mm. Other thiols were synthesized starting from the corresponding alcohol or bromide and dried over calcium oxide and fractionally distilled under nitrogen atmosphere prior to use: b.p. 1-butanethiol, 95–99°; 1,4-butanedithiol, 96°/28 mm; 1-dodecanethiol, 116.5–117°/3 mm; phenylmethanethiol, 118°/29 mm. Commercial phenyl isocyanate and synthesized ethyl isocyanate were distilled before use: b.p. phenyl isocyanate, 164–165°; ethyl isocyanate, 60°. Toluene (16), dibutyl ether (6a), benzene (17), and dioxane (18) were purified by distillation from sodium. Nitrobenzene was dried over phosphorus pentoxide and distilled. Methyl ethyl ketone was dried over anhydrous potassium carbonate, refluxed for 2 days with a small amount of phenyl isocyanate, and fractionally distilled. Acetone, dibutylamine, and ethanol were used after distillation.

REFERENCES

1. E. Dyer and J. F. Glenn. J. Am. Chem. Soc. 79, 366 (1957).
2. H. L. Snape. Ber. 18, 2432 (1885).
3. H. Goldschmidt and A. Meissler. Ber. 23, 272 (1890).
4. S. Petersen. Ann. 562, 205 (1949).
5. J. F. Smith and E. C. Friedrich. J. Am. Chem. Soc. 81, 161 (1959).
6. (a) J. W. Baker and J. B. Holdsworth. J. Chem. Soc. 713 (1947).
   (b) J. W. Baker and J. Gaunt. J. Chem. Soc. 9, 19, 24, 27 (1949).
7. S. Ephrain, A. E. Woodward, and R. B. Mesrobian. J. Am. Chem. Soc. 80, 1326 (1958).
8. S. Ozaki and S. Shimada. Nippon Kagaku Zasshi, 80, 430 (1959).
9. R. G. Arnold, J. A. Nelson, and J. J. Verbanc. Chem. Revs. 57, 57 (1957).
10. J. H. Saunders et al. Ind. Eng. Chem. 46, 1498 (1954).
11. A. Farkas, G. A. Mills, W. E. Erner, and J. B. Maerker. Ind. Eng. Chem. 51, 1299 (1959).
12. A. Farkas and K. G. Flynn. J. Am. Chem. Soc. 82, 642 (1960).
13. W. Gordy and S. C. Stanford. J. Am. Chem. Soc. 62, 497 (1940).
14. H. E. Stagg. Analyst, 71, 557 (1946).
15. A. Skita and H. Rolfes. Ber. 53, 1252 (1920).
16. L. F. Fieser. Experiments in organic chemistry. D. C. Heath & Co. 1955. p. 292.
17. L. F. Fieser. Experiments in organic chemistry. D. C. Heath & Co. 1955. p. 282.
18. L. F. Fieser. Experiments in organic chemistry. D. C. Heath & Co. 1955. p. 284.

THE LOCATION OF XANTHATE GROUPS IN PARTIALLY SUBSTITUTED STARCH XANTHATES[1]

E. G. Adamek[2] and C. B. Purves

ABSTRACT

The rate of xanthation of starch with carbon disulphide in 17.8% potassium hydroxide at 23° was followed by converting the potassium salts to the S-methyl xanthate esters, and analyzing the latter for sulphur. These esters were tritylated without changing the xanthate D.S., and unity minus the trityl D.S. was assumed to represent xanthate D.S. in the primary alcohol positions of the starch. About 62% of the xanthate groups occupied secondary positions after 100 minutes of xanthation, but after 3350 minutes about 58% of the surviving xanthate groups were primary.

A sodium chlorite – pyridine – lactic acid mixture reduced the sulphur content of a fully acetylated starch S-methyl xanthate by about nine-tenths with little loss of acetyl groups, but the residual sulphur could not be eliminated and the resulting starch acetate could not be completely reacetylated or tosylated. The location of the hydroxyl groups in this acetate thus could not be studied by the tosylation–iodination method.

INTRODUCTION

A previous article (1) described attempts to discover the distribution of xanthate groups among the 2-, 3-, and 6-positions of cellulose sodium xanthates whose average degree of substitution (D.S.) ranged from 0.66 to 0.41. The xanthate salts were converted to the much more stable S-methyl esters, and the latter to completely substituted acetates, without significant loss in xanthate D.S. Attempts to dexanthate this acetate at 0° with chlorine dioxide buffered to pH 4.5, however, occasioned small losses in acetyl groups, and about one-tenth of the original sulphur content remained associated in an unknown chemical state with the dexanthated cellulose acetate. Fractional precipitation or dialysis of this acetate failed to remove the residual sulphur compounds. This failure diminished the reliability of the subsequent work, which consisted of determining distribution of unsubstituted hydroxyl groups in the dexanthated cellulose acetate (and hence of xanthate groups in the original cellulose xanthate) by the tosylation–iodination procedure. The present research was begun with a repetition of the above series of reactions with starch, since it was reasonable to hope that the great difference in the colloidal state of cellulose and starch might facilitate the study, particularly in the dexanthation step. A search of the literature (2) revealed a few articles and patents on the preparation and uses of starch sodium xanthates, but none on the distribution of the xanthate groups.

Since the primary object of the work was to explore possible methods of determining this distribution, it did not seem necessary to separate the original starch into the amylose and amylopectin components. The error caused by any incompleteness, or loss of acetyl groups, in dexanthation was reduced by starting with a starch potassium xanthate of relatively high D.S. (near unity). As expected (2), this product could be converted to the fully acetylated S-methyl ester with little or no change in the xanthate D.S. Subsequent attempts to remove the S-methyl xanthate groups selectively by aqueous chlorine dioxide, as used in the parallel work with cellulose S-methyl xanthates (1), resulted in poor yields of a starch acetate markedly deficient in acetyl groups and retaining 2.4, 4.6% of sulphur as residual sulphur compounds. About 20 attempts, briefly outlined

in the Experimental portion, were made to find a more selective method of dexantha-
tion. Hydrogen peroxide or peracetic acid in buffered aqueous solution, or sodium
persulphate – sodium chlorite in aqueous pyridine, degraded the starch acetate to water-
soluble products on those occasions when they reduced the sulphur content substantially.
The S-methyl xanthate group, unlike the primary tosyl group, was not eliminated by
heating with sodium iodide in a ketone solvent.

Sanyal and his co-workers (3), however, had dexanthated a cellulose S-methyl xanthate
acetate with sodium chlorite in 90% acetic acid, and it seemed worth while to explore
the use of nearly anhydrous systems in which chlorine dioxide was liberated from
sodium chlorite. Alkali chlorites were known to be reduced in aqueous solution by
aldehydes (4), carbohydrates (5), formic acid, oxalic acid, citric acid (6, 7), and acetic
anhydride (4), the action in at least the latter case appearing to be catalytic. Trial
showed that formic acid or acetic anhydride, but not formaldehyde, in a glacial acetic
acid – sodium acetate medium removed most of the S-methyl xanthate groups from
the acetylated starch derivative. Since these additives might have altered the acyl
substitution, they were replaced by lactic acid as the reducing or catalytic agent for
the chlorite, and in its final form the method removed about 90% of the sulphur content
of the starting material with the loss of only about 6% of the acetyl groups.

After dexanthation, the residual sulphur compounds in the resulting starch acetate
were not removed by mercuric chloride. One of these dexanthated acetates was extracted
with pyridine, in which 33% dissolved, but both the soluble portion and the undissolved
gel retained the original sulphur content. Since the starch contained 33% of amylose,
it was possible that the fractionation followed the amylose–amylopectin ratio rather
than any difference in substitution. Such experiments, together with similar negative
results in the cellulose field (1, 3) strengthened the view that the residual sulphur was
part of groupings that were chemically combined with, rather than tenaciously adsorbed
on, the residual starch acetate. The groups in question were probably thioesters, because
complete deacetylation with sodium methylate yielded a nearly sulphur-free starch; fur-
ther acetylation, provided the catalyst was sulphuric acid, also greatly reduced the
sulphur content. The simplest, but not necessarily the correct, explanation was that
the supposed thioesters were monothiocarbonates of the —O—CO—SCH₃ type formed
as a by-product in the dexanthation. If so, the monothiocarbonate group was fairly
stable toward chlorine dioxide or chlorite, and was hydrolyzed at a rate comparable
to that of acetyl groups.

Repeated attempts were then made to reacetylate the dexanthated starch acetates
to the maximum theoretical substitution of 3.0, but customary methods of acetylation,
even if successful with the original starch S-methyl xanthate or repeated two or three
times, yielded products of D.S. 2.0 to 2.4. Pacsu and Mullen (8) previously noted the
resistance of starch itself to complete acylation, but successfully overcame it by first
swelling the starch in aqueous pyridine. Their method increased the D.S. to only 2.6
in the present case and to 2.8 after a second identical acetylation. As might be expected
from these negative results, the sulphur content of the dexanthated starch acetate
increased by only 1.9% when tosylated under conditions that produced extensive sub-
stitution with the similar cellulose derivative. The tosylation–iodination method of
locating S-methyl xanthate groups in starch was thus inapplicable and other methods
had to be investigated.

An attempt was made to hydrolyze starch S-methyl xanthate to the corresponding
mixture of glucose S-methyl xanthates, and to identify the latter by paper chromatog-

raphy with butanol–water as eluent. Although this hydrolysis required much less drastic conditions than those required in the parallel hydrolysis of cellulose S-methyl xanthate (3) the result was the same; the two spots of R_F 0.56 and 0.70 derived from glucose 6-S-methyl xanthate were evident, but the 2- and 3-derivatives had failed to survive the hydrolysis. Neither a dextrinizing nor a saccharifying enzyme preparation produced glucose from starch S-methyl xanthate, although starch itself was readily degraded, even in presence of the xanthate.

Preliminary experiments then showed that starch and starch S-methyl xanthates, like cellulose (9) and cellulose S-methyl xanthates (1), could be successfully condensed with triphenylmethyl chloride (trityl chloride) in pyridine. The determination of the trityl group in the starch S-methyl xanthates was by weighing the triphenylmethyl carbinol produced by acid hydrolysis (9), but the earlier uncertainties originating in the formation of colloidal sulphur and traces of mercaptans (1) were overcome by correcting the weight of the crude carbinol for its sulphur content. In the final work, starch was xanthated by the "emulsion" technique while dispersed in aqueous potassium hydroxide, and samples of the starch potassium xanthate, isolated at various times by precipitation into methanol, were promptly converted to the pure S-methyl xanthates. These xanthate esters were then tritylated, over-all yields from the potassium salts being in all cases close to theoretical, and the D.S. of the products with respect to both trityl and S-methyl xanthate groups was determined by analysis. Comparison of the data (Table I, columns

TABLE I

Tritylation of starch S-methyl xanthates

Starch S-methyl xanthate[a]			Tritylated starch xanthate[b]				Trityl carbinol
Xanthation, minutes	% S	D.S. xanthate	% S	% Trityl	D.S. xanthate	D.S. trityl[c]	% S
10	6.3	0.17	2.5	56.0	0.16	0.92	0.20
20	9.4	0.28	4.1	54.0	0.25	0.89	0.41
40	16.4	0.54	8.9	45.9	0.54	0.73	2.1
60	21.1	0.76	11.7	43.6	0.74	0.73	1.6
75	24.0	0.92	14.5	40.0	0.92	0.67	5.3
105	26.8	1.09	17.2	35.2	1.07	0.58	10.2
170[d]	26.8	1.09	19.0	29.8	1.10	0.46	14.0
250	29.3	1.26	22.7	23.1	1.27	0.34	22.5
330	28.6	1.21	20.7	27.1	1.19	0.41	15.9
740	23.4	0.89	16.3	32.0	0.91	0.47	13.9
1940	19.0	0.66	12.0	38.5	0.68	0.57	8.0
3350	18.3	0.63	10.3	42.1	0.60	0.65	3.7

[a]Starch, 30 g, shaken at 23° with 350 ml of aqueous 17.8% potassium hydroxide and 150 ml of carbon disulphide. Aliquots, 50 ml, withdrawn at times stated and products promptly converted to the S-methyl xanthates.

[b]Tritylations with excess trityl chloride in pyridine at 70° for 3 days.

[c]Corrected for sulphur content noted in right-hand column.

[d]Residual xanthation slurry (a), 150 ml, diluted with 50 ml of carbon disulphide and 100 ml of 17.8% potassium hydroxide. Aliquots, 60 ml, taken at times stated.

3 and 6) showed that none of the S-methyl xanthate groups were lost during tritylation, and that the accuracy of the analytical work (D.S. ± 0.03) was satisfactory. By assuming that the trityl group selectively and completely substituted the primary alcohol positions left unoccupied by the S-methyl xanthate group, the substitution of the latter in the 6-position of the starch was calculated as unity minus the trityl D.S. given in column 7. The primary S-methyl xanthate D.S. thus being known, the average substitution in the

secondary 2- and 3-positions of the starch was found by difference from the total xanthate substitution (column 3 or 6).

When the rates of xanthation were plotted against time (Fig. 1), the plot for secondary
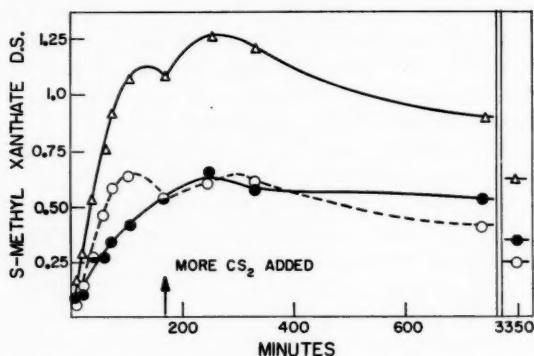
FIG. 1.   Rate of xanthation of starch (see Table I, footnotes *a* and *d*). Total substitution, $\triangle$; primary substitution, ●; secondary substitution, ○.

S-methyl xanthate D.S. (open circles) went through a maximum near 100 minutes which was reflected in the plot for total D.S. (triangles) but not in that for primary D.S. (filled circles), which continued to increase. About 38% of the substitution was in the primary, and 62% in the secondary, positions at this maximum. It was also evident from the shape of the plots that xanthation proceeded more rapidly in the secondary positions. When the maximum near 100 minutes was past, the addition of more carbon disulphide and alkali to the xanthating mixture produced higher maxima in all three plots after 250 to 300 minutes, and in this period the amounts of primary and secondary xanthation were almost the same. Thereafter, the substitution in the secondary positions declined more rapidly than that in the first; the plots crossed, and after 3350 minutes, when the experiment was terminated, almost 60% of the surviving xanthate groups occupied primary positions in the starch macromolecule. The course of the xanthation of starch was thus similar to that of cellulose, which was discussed in the previous publication (1) and which has now been studied in much greater detail by Philipp and Liu (10).

EXPERIMENTAL

Materials and Analytical Methods

The wheat starch used was a defatted, purified sample kindly supplied by Dr. K. M. Gaver of Ogilvie Flour Mills Limited, Montreal, Quebec. Preparation of the purified starch potassium xanthates, of D.S. near unity, and from them the corresponding S-methyl esters, were as previously described (2). All products were dried by solvent-exchange into ether and then *in vacuo* over phosphorus pentoxide at room temperature.

Analyses for sulphur by the Parr semimicro bomb method, for ash, and for acetyl groups by distillation with 30% chromic acid, were as previously described (1, 2). The method for acetyl was the most reliable found, but the results tended to be slightly high. In the analyses of tritylated starch S-methyl xanthate for trityl content by the method of Hearon and his collaborators (9), a 0.5-g sample was digested in 10 ml of concentrated sulphuric acid for 2 hours at room temperature. Dilution of the resulting clear, brown solution with 100 ml of water, which was added with cooling and shaking

as a fine stream, caused the precipitation of the crude triphenyl carbinol. After being allowed to settle overnight, the slurry could be conveniently filtered in a tared porous crucible. The residue was washed several times with water, was dried *in vacuo* over phosphorus pentoxide, and was weighed. The sulphur content of the triphenyl carbinol was determined and the weight of carbinol corrected accordingly. If the corrected weight was a, and the original sample weight was b, then % trityl = $24,300a/260b$.

If x and y represented the D.S. of trityl and S-methyl xanthate groups, respectively, in starch, their values were found by solving the simultaneous equations:

$$\% \text{ trityl} = 24300x/(162+242x+90y),$$
$$\% S = 6400y/(162+242x+90y).$$

The corresponding equations for S-methyl xanthates and their acetates were reported previously (1).

Acetylated Starch S-Methyl Xanthate

As noted previously (2), the acetylation of the S-methyl xanthate with sulphuric acid as catalyst gave a white, completely substituted product but occasioned a small loss in the xanthate D.S. Several acetylations with pyridine – acetic anhydride showed that no loss of S-methyl xanthate groups occurred, but that acetylations at 55° or 95° for 20 to 30 hours yielded a total D.S. of about 2.9. Prolonged acetylations of the above kind gave brown products, and one particularly dark sample contained 0.56% of nitrogen. This amount corresponded to the presence of 3.2% of pyridine, but extraction with cold N hydrochloric acid for 2 days at 5° failed to alter the sulphur and acetyl analyses significantly. The following method illustrated the final procedure.

Twenty grams of starch S-methyl xanthate (D.S. 1.20), 240 ml of pyridine, and 120 ml of acetic anhydride were heated together under gentle reflux (112°) for 45 minutes, with exclusion of moisture. After cooling, the turbid reaction mixture was poured slowly into 2 liters of vigorously stirred ice water. The resulting precipitate was recovered on a filter of coarse sintered glass; was washed several times with water, methanol, and ether in succession; was ground in a mortar; and was subjected once more to the washing sequence. When dried, the product was a white powder which was dispersible in chloroform and trichloroethylene but not to clear solutions. Yield, 23.6 g or 93% of theory. Found: S, 23.0; acetyl, 21.5%. Calculated for starch substituted to D.S. 1.25 with S-methyl xanthate and to D.S. 1.74 with acetyl groups: S, 23.0; acetyl, 21.5%. The total substitution was thus 2.99. When chloroform solutions of such products were examined in a Perkin–Elmer Model 21 double-beam spectrophotometer, the characteristic stretching frequencies of unsubstituted hydroxyl groups between wave numbers 3100 cm^{-1} and 3600 cm^{-1} were absent.

Attempted Dexanthations of Starch S-Methyl Xanthate Acetate

(a) Three grams of the above S-methyl xanthate acetate, 3 g of sodium iodide, 150 ml of acetonyl acetone, and 20 ml of allyl alcohol to remove any free iodine that formed were heated for 2 hours at 98° under reflux. The product, recovered by filtration, retained almost the original amount of sulphur. Yield, 2.9 g with S, 22.6%.

(b) The original S-methyl xanthate acetate, 1.5 g, dispersed in 40 ml of glacial acetic acid containing an excess of sodium acetate, was shaken with 12 ml of aqueous 30% hydrogen peroxide for 20 hours at room temperature. After dilution with 250 ml of water, the suspension was filtered and the product isolated. Yield, 1.1 g. Found: S, 7.3; acetyl, 24.4%. A repetition of this dexanthation caused the loss of more than half of the product

in the liquors. The remainder had S, 0.8%. Dexanthation with hydrogen peroxide at 5° proceeded very slowly, and hardly at all with peracetic acid in buffered acetic acid at room temperature during 16 hours at 23°.

(c) A highly viscous dispersion of 1.5 g of the S-methyl xanthate acetate in 28 ml of pyridine was mixed with 60 ml of water containing sodium persulphate, 14 g, and sodium chlorite, 14 g. The mixture was heated under reflux for 45 minutes, but no starch acetate separated when it was poured into water, presumably because the product was highly degraded.

(d) Two grams of another starch S-methyl xanthate acetate (S, 18.8; acetyl, 25.5%), dispersed in 25 ml of chloroform, was transferred into a black-painted flask containing 20 ml of glacial acetic acid, 20 ml of acetic anhydride, and 10 g of sodium acetate. The mixture was cooled to 0° before 10 g of powdered sodium chlorite and then 10 ml of water were added; the initial reaction was vigorous, and the stopper of the flask was kept loose to permit large volumes of chlorine dioxide gas to escape. After being kept near 0° for 30 minutes, the flask and contents were tightly stoppered and shaken mechanically for 22 hours at room temperature. After recovery by precipitation into water saturated with sodium acetate, the product was washed and dried. Yield, 1.6 g. Found: S, 2.6; acetyl, 31.1%. The analysis showed that 90% of the S-methyl xanthate and 8.5% of the acetyl groups had been removed.

The replacement of the acetic anhydride, acetic acid, and sodium acetate in the above experiment with 30 ml of pyridine and 21 ml of anhydrous formic acid caused the loss of 92% of the S-methyl xanthate and no loss of acetyl groups.

(e) Another starch S-methyl xanthate acetate (with S, 24.1; acetyl, 20.3%; D.S. 1.22 and 1.65) was used in the last seven dexanthations, each of which was restricted to an 8-g scale to reduce the risk of chlorine dioxide exploding in the apparatus used. The sample, 8 g, dispersed in 60 ml of chloroform, was contained in a wide-necked, black-painted 350-ml jar equipped with a glass stopper. A mixture of 40 ml of pyridine and 30 ml of 85 to 90% lactic acid was added, and the whole was cooled to 0°. The addition of 15 g of powdered sodium chlorite caused a vigorous evolution of chlorine dioxide gas and the stopper was kept loose. When the initial reaction had been completed at 0°, the jar was stoppered and shaken mechanically at room temperature for 1 hour. The mixture, still yellow-green in color, was then poured with stirring into 1.5 liters of diethyl ether. The soft precipitate was recovered and kneaded several times with ether, and then with small amounts of water, alternated with grinding in a mortar. After drying in the air, and further washings with ether, the white product was dried *in vacuo*. Found: S, 3.0; acetyl, 28.4% (D.S. 0.11, 1.58). In this case 91% of the S-methyl xanthate and 4% of the acetyl groups had been lost; in other cases the losses ranged as high as 93% and 10%, respectively. A repetition of the dexanthation gave a product with S, about 0.4% with the loss of 15% of the acetyl groups.

Examination of the Dexanthated Starch S-Methyl Xanthate Acetate

(a) A 0.4-g sample (S, 6.5; acetyl, 29.3%) was extracted at room temperature with 10-ml volumes of pyridine, which were separated from a swollen, gelatinous portion on the centrifuge. The extraction was repeated until, after the fifth, a drop of the supernatant liquor yielded no precipitate when diluted with ether. The combined extracts were then poured into much ether and the precipitate washed with water and ether and dried. Yield, 0.13 g or 33%. Found: S, 6.2; acetyl, 28.8%. The gel insoluble in pyridine was recovered in the same way. Yield, 0.21 g or 53%. Found: S, 6.4; acetyl, 28.8%.

(b) The above dexanthated starch S-methyl xanthate, 1.7 g, was deacetylated by being heated under reflux for 20 minutes with 100 ml of anhydrous methanol in which 1 g of sodium had been dissolved. After recovery on a filter, the product was ground in a mortar and deacetylated again in the same way. After washing in dilute acetic acid, methanol, and ether, the product weighed 1.3 g. Found: S, 0.29%. This sulphur content was not changed when an aqueous suspension was dialyzed through "Cellophane" against water for 55 hours.

(c) Another sample, 0.5 g, of dexanthated starch S-methyl xanthate acetate (with S, 2.0%; acetyl, 34.4%) was kept at 80° for 10 minutes while suspended in 20 ml of glacial acetic acid containing 1 g of mercuric acetate. The mixture was kept near 20° for 24 hours before being poured into water to isolate the product, which agreed with the original sample in yield and sulphur content.

(d) A sample, 0.8 g, of the composition noted in (c) was dispersed in 15 ml of dry pyridine to which 4.3 g of pure p-toluenesulphonyl chloride was added. The product was isolated after being kept near 20° for 24 hours, a period long enough to tosylate a similar cellulose derivative extensively (1). Found: S, 3.9%. The starch acetate thus resisted tosylation.

(e) Acetylation of similar dexanthated starch S-methyl xanthate acetates with pyridine and acetic anhydride, under conditions that led to the complete acetylation of the original starch S-methyl xanthate (see above) diminished the sulphur content somewhat but failed to raise the total substitution above 2.4, even when the acetylation was repeated. The use of sulphuric acid as the catalyst, of chloroacetic acid as impeller with magnesium perchlorate as catalyst (11), or of acetyl chloride in pyridine (12) gave no better results, although these methods gave complete, or almost complete, substitution with cellulose. Dexanthated starch S-methyl xanthates that had never been dried did not acetylate more completely than other samples. Although still unsatisfactory, the best method of acetylation found was that of Pacsu and Mullen (8). Two grams of a sample (with S, 2.3%; acetyl, 33.0%) was soaked in 30% aqueous pyridine, which was then replaced by 30 ml of anhydrous pyridine by distillation of the pyridine–water azeotrope. Acetic anhydride, 30 ml, was then added and the mixture kept at 115° for 1 hour. Found for the nearly white product: S, 1.9; acetyl, 39.4%, corresponding to D.S. 0.08, 2.52, respectively. The total D.S. was thus only 2.6.

Tritylation of Starch S-Methyl Xanthate

The procedure for tritylating cellulose (9) was slightly modified. In a typical experiment the pure, dry starch S-methyl xanthate, 2.5 g, was dispersed in 30 ml of pyridine contained in a flask fitted with a reflux condenser and protected from atmospheric moisture. The flask and contents were heated at 70° for 3 days, since it was found that some dexanthation occurred when a higher temperature (106°) was used for 20 hours. After being cooled, the light brown liquor was poured with stirring into 500 ml of ice and water, and the resulting precipitate was recovered on a filter of sintered glass. The product was washed with water, methanol, and ether, was ground in a mortar, washed again in the same sequence, and dried. Yields were close to those calculated from the content of S-methyl xanthate and trityl groups.

REFERENCES

1. E. P. SWAN and C. B. PURVES. Can. J. Chem. **35**, 1522 (1957).
2. E. G. ADAMEK and C. B. PURVES. Can. J. Chem. **35**, 960 (1957).
3. A. K. SANYAL, E. L. FALCONER, D. L. VINCENT, and C. B. PURVES. Can. J. Chem. **35**, 1164 (1957).
4. J. W. MELLOR. Comprehensive treatise on inorganic and theoretical chemistry. Suppl. II, Part I. Longmans, Green & Co., Inc., New York. 1956. p. 523.

5. W. Becher. Brit. Patent No. 345,190(1929); Chem. Abstr. **26**, 264 (1932).
6. E. Stossel and E. Zerner. U.S. Patent No. 2,338,268(1944); Chem. Abstr. **38**, 3786 (1944).
7. C. A. Hampel. Brit. Patent No. 561,229(1944); Chem. Abstr. **39**, 5057 (1945).
8. E. Pacsu and J. W. Mullen. J. Am. Chem. Soc. **63**, 1487 (1941).
9. W. M. Hearon, G. D. Hiatt, and C. R. Fordyce. J. Am. Chem. Soc. **65**, 2449 (1943).
10. B. Philipp and K. T. Liu. Faserforsch. u. Textiltech. **10**, 555 (1959).
11. H. T. Clark and C. J. Malm. U.S. Patent No. 1,880,808 (1932); Chem. Abstr. **27**, 600 (1933).
12. C. J. Malm, J. W. Mench, D. L. Kendall, and G. D. Hiatt. Ind. Eng. Chem. **43**, 684 (1951).

REACTIONS OF OXODELCOSINE AND INTERRELATION OF DELCOSINE AND DELSOLINE[1]

VINKO SKARIĆ[2] AND LÉO MARION

ABSTRACT

The oxidation of diacetyldelcosine produces a lactam which, after hydrolysis of the acetyl groups, can be oxidized further to a diketo-lactam in which one of the keto groups is in a five- and the other in a six-membered ring. This result leads to an alteration of the previously suggested structure of delcosine. The new structure suggests a close relationship between delcosine and delsoline which is confirmed by the methylation of the former. The reaction is selective and gives rise to a monomethyldelcosine identical in every way with delsoline. Reduction of the diketo-lactam (didehydro-oxodelcosine) with sodium borohydride gives oxodelcosine. Dehydro-oxodelcosine is also described, and its oxidation with lead tetraacetate as well as that of oxodelcosine lead to the formation of keto-products which lend supporting evidence for the structure assigned to delcosine.

Delcosine, an alkaloid isolated from *Delphinium consolida* L., has been investigated previously. The results then obtained (1) are best interpreted by assuming that the alkaloid possesses the same carbon–nitrogen skeleton as lycoctonine (2), and have led to the suggestion of tentative structure I (R = CH₃, R′ = R″ = H) for delcosine.

I
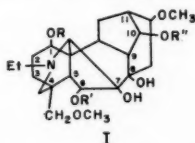
Although in this formula R″ = H has been established and the presence of a ditertiary vicinal glycol has been demonstrated chemically (3), the evidence for R′ = H is very meager and rests only on the interpretation of the formation of a carbinolamine ether (1) which requires the presence of a hydroxyl in the vicinity of the nitrogen. The work now described was designed to establish the nature of the substituents R and R′ in I.

It has already been shown that the oxidation of delcosine ($C_{24}H_{39}O_7N$) with chromic acid in acetic acid gives rise to dehydrodelcosine (II) in which the keto group forms part of a five-membered ring (1). When diacetyldelcosine (4) is oxidized with potassium permanganate, or with chromic acid – pyridine complex (Sarett's method), a lactam, diacetyl-oxodelcosine (III), m.p. 103–108° ($C_{28}H_{41}O_{10}N$), is obtained, which on hydrolysis, produces the neutral product, oxodelcosine (IV) ($C_{24}H_{37}O_8N$), m.p. 245–246°. Oxodelcosine (IV) in glacial acetic acid is oxidized by sodium dichromate to a diketone, dide-hydro-oxodelcosine (V) ($C_{24}H_{33}O_8N$), m.p. 211–212°, which in the infrared shows absorption bands at 1757 cm⁻¹ (five-membered cyclic ketone), 1720 cm⁻¹ (six-membered cyclic ketone), and 1653 cm⁻¹ (six-membered lactam). The product V, which is also obtainable by direct oxidation of delcosine with Sarett's reagent, is converted back to oxodelcosine (IV) by reduction with sodium borohydride.

This result confirms that the nitrogen forms part of a six-membered ring, but indicates that contrary to the original assumption only one of the two secondary hydroxyl groups

present in delcosine is on a five-membered ring, while the other is on a six-membered ring. The substituents, therefore, cannot be as represented in structure I (R = CH$_3$, R' = R'' = H) since, were R' = H, both keto groups in V should have been in five-membered rings. To account for this experimental result and the formation of the carbinolamine ether previously described (1), which requires that one hydroxyl group be in close proximity to the nitrogen, it is necessary to alter the suggested structure of delcosine to I (R = R'' = H, R' = CH$_3$). This new structure has already been reported in a preliminary communication (5).

The fact that one of the two secondary hydroxyl groups is attached to a six-membered ring is confirmed by the oxidation with Sarett's reagent of monoacetyldelcosine (4), which gives rise to a monoacetyldehydro-oxodelcosine (VI) (C$_{26}$H$_{37}$O$_9$N), m.p. 107–110°, hydrolyzed by potassium hydroxide to dehydro-oxodelcosine (VII) (C$_{24}$H$_{35}$O$_8$N), m.p. 228–229°, in which the keto group, according to the infrared spectrum (1719 cm^{-1}), is in a six-membered ring. The formation of VII from monoacetyldelcosine also establishes
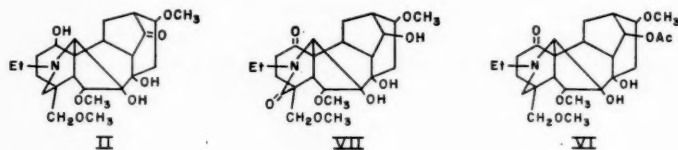
that it is the secondary hydroxyl group attached to the five-membered ring that is more readily and preferentially acetylated. Hence, compound II should be designated 10-dehydrodelcosine, whereas compound VII is 1-dehydro-oxodelcosine.

If structure I (R = R'' = H, R' = CH$_3$) be the correct one, then delcosine must be very closely related to delsoline, which has been assigned structure I (R = H, R' = R'' = CH$_3$) (6). In order to ascertain this point, delcosine was methylated by means of sodium hydride and methyliodide in dioxane according to the method used by Carmack *et al.* (7) in establishing the relationship of deltaline, delphaline, and lycoctonine. The product obtained after chromatography on alumina melted at 215–216°, undepressed on admixture with delsoline, and its optical rotation, infrared spectrum, and Debye–Scherrer diagram were all identical with the corresponding physical constants of delsoline. The methylation was therefore selective and affected only the secondary hydroxyl located on the five-membered ring which is also the hydroxyl that is the more readily acetylated.

The selective methylation of delcosine occurred only if the reaction was allowed to proceed at room temperature. When the reaction mixture was heated under reflux, the methylation was no longer selective and the product was di-*O,O*-methyldelcosine, C$_{26}$H$_{43}$O$_7$N, m.p. 203–206°.

The oxidation with periodic acid of the carbinolamine ether, anhydro-hydroxydelcosine, indicating the presence of a vicinal glycol in delcosine, has been reported previously (3). The action of lead tetraacetate on oxodelcosine has now been investigated. Preliminary studies showed that 1 mole of the oxidizing agent is consumed in 1 hour. In this oxidation oxodelcosine is converted to a compound VIII (C$_{24}$H$_{35}$O$_8$N), m.p. 191–193°, which in the infrared shows two absorption bands (3408 and 3360 cm^{-1}) in the hydroxyl region, a band at 1763 cm^{-1} attributable to a five-membered cyclic ketone, and one at 1654 cm^{-1} due to the lactam carbonyl. This oxidation indicating a vicinal glycol should give rise to a dicarbonyl derivative. The absence of an absorption band in the infrared region

1700-1720 cm^{-1} shows that the expected six-membered cyclic ketone carbonyl is not present, and consequently that it must have become masked by a secondary reaction. On the other hand, the further oxidation of VIII with Sarett's reagent gives rise to a compound IX ($C_{24}H_{33}O_8N$), m.p. 209–210°, which in the infrared contains only one hydroxyl band (3320 cm^{-1}) and two five-membered cyclic ketone carbonyls (1766, 1758 cm^{-1}) as well as the lactam carbonyl (1657 cm^{-1}). Hence, of the two hydroxyl groups present in VIII, only one (on a five-membered ring) is secondary. These results are explainable
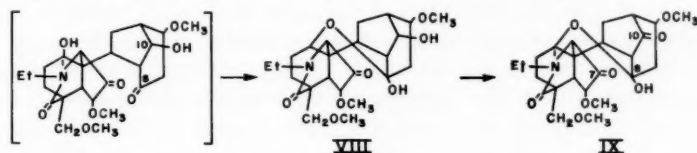
if in the secodiketone originally formed in the reaction, the carbonyl at 8 is assumed to have condensed with the secondary hydroxyl at 1 to form a hemiketal. There would result a tertiary hydroxyl at 8, and in the further oxidation of VIII to IX only the hydroxyl at 10 could be converted to a keto group.

In support of this interpretation, 1,10-didehydro-oxodelcosine (V), in which no secondary hydroxyl group is present, is oxidized by lead tetraacetate to 1,10-didehydroseco-oxodelcosine diketone (X) ($C_{24}H_{31}O_8N$), m.p. 175–177°, which according to its infrared absorption spectrum contains no hydroxyls. Further, 1-dehydro-oxodelcosine (VII), in which the hydroxyl at 1 is no longer present, is oxidized by lead tetraacetate to 1-dehydro-seco-oxodelcosine diketone (XI) ($C_{24}H_{33}O_8N$), m.p. 181–183°. In the infrared XI shows a hydroxyl band at 3344 cm^{-1}, one five-membered cyclic ketone (1776 cm^{-1}), two six-membered cyclic ketones (1712; 1688 cm^{-1}), and a lactam carbonyl (1655 cm^{-1}). Hence, in the absence of a secondary hydroxyl in ring A (position 1) no hemiketal is formed in the secodiketones.

Every one of the reactions of delcosine reported so far is accommodated by the new structure I (R = R″ = H, R′ = CH_3) assigned to the alkaloid, including the formation
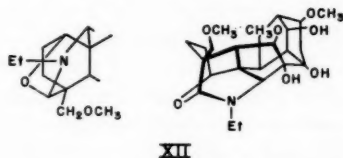
of the carbinolamine ether previously described (1). Notwithstanding a recently expressed view that the structure XII assigned to the carbinolamine ether (anhydrohydroxy-delcosine) is geometrically impossible (8), this structure when built with Courtauld models is remarkably strainless. It involves boat conformations for ring A and the nitrogen-bearing ring, and in this structure the ethyl group attached to the nitrogen is much less hindered than in delcosine itself. Consequently, the above statement of Büchi (8) does not appear to constitute a very serious argument.

It had been suggested previously (4) that the alkaloid delphamine (9) was very probably identical with delcosine. Due to the courtesy of Drs. L. S. Chetverikova and A. D. Kuzovkov, who sent us a sample of delphamine for comparison, this has been confirmed. The two bases have the same melting point, which is not depressed on admixture, and the infrared spectra and X-ray powder diagrams of both are identical.

As already reported by Ochiai, Okamoto, and Kaneko (10), their Takaobase-I has been found to be identical with delcosine. Through the kindness of Professor Ochiai, we have been able to compare their Shimoburobase-II with 10-dehydrodelcosine and find that the melting points of the bases and their mixture, their infrared spectra, and their X-ray powder diagrams are identical.

The alkaloids lucaconine and monoacetyllucaconine have been described in the literature (11) and some degradative work on the former has been recorded recently (12) as well as a corrected formula (13), which is the same as that of delcosine. The physical and chemical properties of lucaconine and its derivatives are so strikingly similar to those of delcosine and its corresponding derivatives that it is most probable that the two bases are identical and that monoacetyllucaconine is identical with monoacetyldelcosine.

EXPERIMENTAL

The physical constants were determined as follows: the melting points, uncorrected, were taken on a Kofler hot stage; optical rotations were measured in chloroform unless otherwise stated; the ultraviolet spectra were measured in 95% ethanol on a Beckman DU spectrophotometer, and the infrared absorption spectra were recorded on a Perkin–Elmer double-beam instrument Model 21B. The infrared absorption bands are reported in wave numbers followed by a number in parentheses which designates the percentage absorption. The neutral alumina used for adsorption chromatography was standardized according to Brockmann.

Diacetyloxodelcosine (III)

Diacetyldelcosine prepared as previously described (4) (200 mg) was dissolved in acetone (4 ml) containing water (0.15 ml) and acetic acid (0.1 ml) and the solution heated under reflux. To the refluxing solution powdered potassium permanganate (220 mg) was added portionwise with agitation over a period of 2 hours. The reaction mixture was then kept at room temperature overnight. Sulphur dioxide was bubbled in the solution, which was subsequently filtered and evaporated under reduced pressure to a syrup. The syrup was partitioned between 0.5 N sulphuric acid and chloroform and the chloroform solution washed with 4% aqueous sodium carbonate. The chloroform extract was dried, evaporated under reduced pressure, and the microcrystalline residue (169 mg) fractionally recrystallized from ether–hexane. The middle fractions (80.3 mg) were recrystallized from hexane from which diacetyloxodelcosine separated as colorless microcrystals, m.p. 103–105°. $[\alpha]_D^{25}$ +24.6±1.4° (c, 0.71). Found: C, 60.95; H, 7.42. Calc. for $C_{28}H_{41}O_{10}N$: C, 60.96; H, 7.49%. Infrared (nujol mull): 3454(50), 1738(92), 1644(84), 1245(95) cm^{-1}.

Diacetyloxodelcosine is also obtained in 65% yield from diacetyldelcosine by oxidation with chromic anhydride – pyridine complex.

Oxodelcosine (IV)

Diacetyloxodelcosine (54.0 mg) was refluxed for 2 hours with 5% potassium hydroxide in (1:1) aqueous methanol. After it was cooled, the solution was evaporated to a syrup under reduced pressure, water was added, and the product extracted with chloroform. The chloroform extract was washed with 0.5 N sulphuric acid, washed with water, dried, and evaporated under reduced pressure. The residue (47.9 mg) was crystallized from ether, m.p. 236–245°, dissolved in benzene, and chromatographed on alumina (activity II). Elution of the column with chloroform gave oxodelcosine, which crystallized from

a mixture of acetone, ether, and hexane as colorless prisms, m.p. 245–246.5, $[\alpha]_D^{23}$ +44.3 ±0.6° (c, 1.83). Found: C, 61.75; H, 7.93. Calc. for $C_{24}H_{37}O_8N$: C, 61.65; H, 7.98%. Ultraviolet spectrum: shoulder λ_{max} 210 mμ, log ε 3.8. Infrared spectrum (nujol mull): 3446(72), 3406(69), 1649(93), 1622(56) cm^{-1}; (chloroform solution): 3608(17), 3468(43), 1638(86) cm^{-1}.

1,10-Didehydro-oxodelcosine (V)

(a) *From oxodelcosine.*—To a solution of oxodelcosine (200 mg) in glacial acetic acid (15 ml), sodium dichromate (100 mg) dissolved in glacial acetic acid (15 ml) was added dropwise. The solution was set aside for 1 hour at room temperature. Sulphur dioxide was bubbled into the reaction mixture to destroy excess reagent and the solvent was removed under reduced pressure, leaving a residue which was partitioned between 0.5 N sulphuric acid and chloroform. The chloroform layer was washed with 4% sodium carbonate, dried, and evaporated under reduced pressure. The residue was crystallized from acetone–ether–hexane (wt. 136.3 mg, m.p. 202–208°), dissolved in benzene, and chromatographed on alumina (activity II–III) and eluted with benzene. Didehydro-oxodelcosine (88.3 mg) obtained from the eluate was recrystallized from benzene–hexane, m.p. 208–211°. Further elution with methanol gave another 46.5 mg of the product, m.p. 202–206°. On recrystallization from benzene–hexane the product was obtained as colorless prisms, m.p. 211–212°, $[\alpha]_D^{21}$ +135±0.9° (c, 1.11). Found: C, 62.35; H, 7.12. Calc. for $C_{24}H_{33}O_8N$: C, 62.19; H, 7.18%. Ultraviolet spectrum: λ_{max} 297 mμ, log ε 2.07, λ_{min} 267 mμ, log ε 1.63. Infrared spectrum (nujol mull): 3446(69), 1757(90), 1720(80), 1653(92) cm^{-1}; (chloroform solution): 3540(25), 3476(27), 1761(81), 1721(72), 1643(89) cm^{-1}.

(b) *From delcosine.*—Chromic anhydride (1.5 g) was added gradually with stirring to dry, freshly distilled pyridine (15 ml) previously cooled to 0°. The yellow complex began to precipitate and the mixture was allowed to warm to room temperature. A solution of delcosine (0.5 g) in pyridine (10 ml) was then added and the mixture allowed to stand at room temperature for 20 hours in a stoppered flask. The solvent was distilled off under reduced pressure, and, to the residue, cracked ice and 0.5 N sulphuric acid were added. Sulphur dioxide was bubbled into the solution which was then extracted with chloroform. The extract was washed with 0.5 N sulphuric acid, with 4% aqueous sodium carbonate, and with water. The didehydro-oxodelcosine recovered from the chloroform solution was purified as described above, m.p. 209–211°, wt. 233.9 mg.

Reduction of Didehydro-oxodelcosine

To a solution of didehydro-oxodelcosine (100 mg) in 80% methanol (25 ml), sodium borohydride (600 mg) was added and the mixture was kept at room temperature for 2 hours. The solvent was evaporated, 0.5 N sulphuric acid added to the residue and the mixture was extracted with chloroform. The extract was washed with 4% aqueous sodium carbonate and evaporated under reduced pressure. The residue was crystallized from ether (wt., 88 mg) and purified by chromatography in chloroform on neutral alumina and recrystallization from acetone–hexane, m.p. 241–243°, $[\alpha]_D^{23}$ +43.6±0.8°. The infrared spectrum (in chloroform solution) was superimposable on that of oxo-delcosine.

10-Monoacetyl-1-dehydro-oxodelcosine (VI)

Monoacetyldelcosine (4) (190 mg) in pyridine (3.6 ml) was oxidized with chromic oxide – pyridine complex. The complex was prepared in the usual way from chromic anhydride (360 mg) and pyridine (3.6 ml). The product was isolated exactly as described above. The monoacetyldehydro-oxodelcosine thus obtained and crystallized from

hexane consisted of microcrystals, m.p. 107–110°, $[\alpha]_D^{26}$ +94.6±1.3° (c, 0.74). Found: C, 62.01; H, 7.68. Calc. for $C_{26}H_{37}O_9N$: C, 61.52; H, 7.35%. Ultraviolet spectrum: λ_{max} 298 mμ, log ϵ 1.873 and shoulder at λ 214 mμ, log ϵ 3.382. Infrared spectrum (nujol mull): 3436(53), 1738(86), 1721(78), 1645(86), 1253(86) cm^{-1}; (in chloroform solution): 3520(18), 3440(25), 1732(75), 1723(79), 1645(81), 1248(84) cm^{-1}.

1-Dehydro-oxodelcosine (VII)

Monoacetyldehydro-oxodelcosine (186 mg) was saponified by refluxing for 2 hours with 5% potassium hydroxide in 1:1 methanol–water. The solution was evaporated to a syrup under reduced pressure, water was added, and the mixture was extracted with chloroform. The extract was washed with 0.5 N sulphuric acid, dried, and evaporated under reduced pressure. The residue (137 mg) was dissolved in benzene and chromatographed on a column of alumina of activity IV. The column was eluted with benzene and the eluate yielded a fraction of the product (86 mg), m.p. 221–225°, and a less pure fraction (43 mg), m.p. 208–216°. The first fraction was crystallized twice from acetone–hexane from which it separated in long, colorless needles, m.p. 228–229°, $[\alpha]_D^{23}$ +120±0.9° (c, 1.08). Found: C, 61.83; H, 7.45. Calc. for $C_{24}H_{35}O_8N$: C, 61.92; H, 7.58%. Ultraviolet spectrum: λ_{max} 297 mμ, log ϵ 1.937 and shoulder at λ 211 mμ, log ϵ 3.479, λ_{min} 267 mμ, log ϵ 1.565. Infrared spectrum (nujol mull): 3476(34), 3358(64), 1719(53), 1633(91) cm^{-1}.

Di-O,O-Methyldelcosine

To a solution of delcosine (76 mg) in dioxane (6 ml), sodium hydride (80 mg) and methyliodide (2 ml) were added, and the mixture kept overnight at room temperature. It was then refluxed for 8 hours. After it had cooled the reaction mixture was filtered and the filtrate evaporated to dryness under reduced pressure. The residual product (quantitative yield) was crystallized from acetone–ether (49 mg), m.p. 203–206°, $[\alpha]_D^{24}$ +48.6±1.3° (c, 0.74). Found: C, 65.00; H, 9.06; OCH$_3$, 31.60. Calc. for $C_{26}H_{43}O_7N$: C, 64.84; H, 9.00; 5OCH$_3$, 32.21%.

O-Methyldelcosine (Delsoline)

To a solution of delcosine (45.4 mg) in dioxane (2 ml), sodium hydride (30 mg) and methyliodide (0.5 ml) were added and the mixture was allowed to stand at room temperature for 21 hours in a flask protected by a calcium chloride tube. After this period the mixture was filtered through a hyflo-supercel column and the filtrate was evaporated to dryness under reduced pressure. The residue, which was crystalline, was recrystallized from benzene–hexane, m.p. 213–216°, wt. 42 mg. It was dissolved in benzene, chromatographed on a column of alumina grade IV (370 mg), and eluted with benzene. The benzene eluate yielded 26 mg of base and further elution with methanol yielded another 11 mg. Recrystallization of the product in benzene–hexane gave colorless prisms, m.p. 215–216°, undepressed on admixture with an authentic sample of delsoline. Its optical activity, $[\alpha]_D^{22}$ +53.4±0.5° (c, 2.04), was the same as that of delsoline, $[\alpha]_D^{27}$ +53.5±0.5° (c, 2.11). Found: C, 64.43; H, 8.79. Calc. for $C_{25}H_{41}O_7N$: C, 64.22; H, 8.84%. The infrared spectrum of the product was superimposable on that of delsoline, and its Debye-Scherrer powder diagram was identical with that of delsoline.

Internal Hemiketal of Seco-oxodelcosine Diketone (VIII)

Oxodelcosine (75 mg) was dissolved in a saturated solution of lead tetraacetate in glacial acetic acid (50 ml) and the solution was kept in the dark for 2 hours at room temperature. Excess lead tetraacetate was reduced with sulphur dioxide, water was

added, and the mixture was cooled for 1 hour. The precipitate was filtered off and the filtrate evaporated under reduced pressure to dryness. Sulphuric acid (0.5 N) was added to the residue and the mixture extracted with chloroform. The extract was washed with 4% aqueous sodium carbonate, dried, and evaporated. The neutral residue was crystallized in acetone–hexane, wt. 50 mg, m.p. 183–186°. Several recrystallizations from dichloromethane–ether yielded colorless prisms, m.p. 191–193°, $[\alpha]_D^{24}$ +1.5±0.8° (c, 0.65). Found: C, 62.06; H, 7.42. Calc. for $C_{24}H_{35}O_8N$: C, 61.92; H, 7.58%. Ultraviolet spectrum: λ_{max} 215 mμ, log ϵ 3.72, λ_{max} 322 mμ, log ϵ 2.40, λ_{min} 275 mμ, log ϵ 1.86. Infrared spectrum (nujol mull): 3408(55), 3360(52), 1763(84), 1654(93) cm⁻¹.

Internal Hemiketal of 10-Dehydroseco-oxodelcosine Diketone (IX)

To dried, freshly distilled pyridine (2.2 ml) cooled to 0°, chromic anhydride (116 mg) was added portionwise with shaking. The mixture from which a yellow complex had separated was allowed to warm to room temperature and to it was added a solution of the hemiketal of seco-oxodelcosine diketone (58 mg) in pyridine (1.2 ml). The reaction flask was stoppered and allowed to stand at room temperature for 20 hours. The solvent was then removed under reduced pressure and to the residue ice and 0.5 N sulphuric acid were added. Excess oxidizing agent was destroyed with sulphur dioxide and the solution was extracted with chloroform. The extract was washed with 0.5 N sulphuric acid, with 4% aqueous sodium carbonate, dried, and evaporated. The neutral residue crystallized on trituration with ether (wt. 31 mg) and was recrystallized from benzene–hexane from which it separated as colorless needles, m.p. 209–210°, $[\alpha]_D^{26}$ +13.7±1.0° (c, 1.1). Found: C, 62.33; H, 7.19. Calc. for $C_{24}H_{33}O_8N$: C, 62.19; H, 7.18%. Ultraviolet spectrum: λ_{max} 319 mμ, log ϵ 2.52, shoulder λ 213 mμ, log ϵ 3.80, λ_{min} 270 mμ, log ϵ 2.11. Infrared spectrum: 3320(56), 1766(86), 1758(78), 1657(90) cm⁻¹.

1,10-Didehydroseco-oxodelcosine Diketone (X)

Didehydro-oxodelcosine (75 mg) was dissolved in a saturated solution of lead tetra-acetate in glacial acetic acid (50 ml) containing water (2.5 ml) and kept at room temperature in the dark for 3 hours. Sulphur dioxide was bubbled through the solution and the precipitate filtered off after the mixture had been cooled. The filtrate was evaporated to dryness under reduced pressure, 0.5 N sulphuric acid was added to the residue, and the mixture was extracted with chloroform. After it was washed with acid and sodium carbonate as described above, the extract yielded a product which crystallized on trituration with ether, wt. 46 mg, m.p. 161–167°. Recrystallization from benzene–ether gave colorless plates, m.p. 175–177°, $[\alpha]_D^{27}$ +77.4±1.0 (c, 1.2). Found: C, 62.34; H, 6.75. Calc. for $C_{24}H_{31}O_8N$: C, 62.45; H, 6.77%. Ultraviolet spectrum: λ_{max} 312 mμ, log ϵ 2.29, λ_{min} 272 mμ, log ϵ 1.98. Infrared spectrum (nujol mull): 1780(84), 1764(77), 1717(89), 1652(87) cm⁻¹; (in chloroform solution): 1776(89), 1722(85), 1658(84) cm⁻¹.

1-Dehydroseco-oxodelcosine Diketone (XI)

1-Dehydro-oxodelcosine (49 mg) was oxidized with a saturated solution of lead tetra-acetate in glacial acetic acid (35 ml) and water (1.8 ml). The solution was kept for 1.5 hours in the dark at room temperature and the product isolated exactly as described above, wt. 30 mg. After recrystallization from benzene–ether the product consisted of colorless hexagonal prisms, m.p. 181–183°, $[\alpha]_D^{28}$ +57.1±2.1° (c, 0.28). Found: C, 62.36; H, 6.90. Calc. for $C_{24}H_{33}O_8N$: C, 62.19; H, 7.18%. Ultraviolet spectrum: λ_{max} 323 mμ, log ϵ 2.36, λ_{min} 274 mμ, log ϵ 1.87. Infrared spectrum (nujol mull): 3344(55), 1776(70), 1712(73), 1688(81), 1655(92) cm⁻¹.

REFERENCES

1. R. ANET, D. W. CLAYTON, and L. MARION. Can. J. Chem. **35**, 397 (1957).
2. M. PRZYBYLSKA and L. MARION. Can. J. Chem. **34**, 185 (1956).
3. R. ANET and L. MARION. Can. J. Chem. **36**, 766 (1958).
4. W. I. TAYLOR, W. E. WALLES, and L. MARION. Can. J. Chem. **32**, 780 (1954).
5. V. SKARIĆ and L. MARION. J. Am. Chem. Soc. **80**, 4434 (1958).
6. F. SPARATORE, R. GREENHALGH, and L. MARION. Tetrahedron, **4**, 157 (1958).
7. M. CARMACK, J. P. FERRIS, J. HARVEY, JR., P. L. MAGAT, E. W. MARTIN, and D. W. MAYO. J. Am. Chem. Soc. **80**, 497 (1958).
8. F. W. BACHELOR, R. F. C. BROWN, and G. BÜCHI. Tetrahedron Letters, **10**, 1 (1960).
9. M. S. RABINOVICH and R. KONOVALOVA. J. Gen. Chem. U.S.S.R. **12**, 321, 329 (1942).
10. E. OCHIAI, T. OKAMOTO, and M. KANEKO. Chem. and Pharm. Bull. **6**, 730 (1958).
11. T. AMIYA and T. SHIMA. Bull. Chem. Soc. Japan, **31**, 1083 (1958).
12. S. FURUSAWA. Bull. Chem. Soc. Japan, **32**, 399 (1959).
13. H. SUGINOME and S. FURUSAWA. Bull. Chem. Soc. Japan, **32**, 354 (1959).

THE ORTON REARRANGEMENT IN APROTIC SOLVENTS

SOME OBSERVATIONS ON THE REACTIONS OF p-SUBSTITUTED N-BROMOACYLANILIDES IN CHLOROBENZENE AND TRICHLOROACETIC ACID[1]

J. M. W. SCOTT[2]

ABSTRACT

The qualitative and kinetic behavior of a series of p-substituted N-bromoacylanilides when treated with trichloroacetic acid in chlorobenzene has been studied. The abnormal reaction which was previously demonstrated for the o-nitro derivative has been shown to occur with the p-isomer. The mechanisms of the normal and abnormal reactions are discussed. Some derivatives of 4-fluoro-3-bromoaniline are described.

Recently interest in the Orton rearrangement has been revived with a view to substantiating the 'π-complex' mechanism originally proposed by Dewar (1). In one of a series of publications (2) evidence for the production of an intermediate (acetyl hypobromite) was reported which appeared to support the alternative mechanism proposed by Soper (3). A closer examination of the experimental conditions under which this intermediate was produced has revealed that the intermediate was due to a slight trace of impurity in the reaction media (4). Although a further attack on the problem has been made using tracer techniques some aspects of the problem of the mechanism remained unsolved (5).*

One of the most interesting facts which the previous work revealed, and one with which this paper is particularly concerned, was the failure of N-bromo-2-nitroacetanilide to rearrange when treated with trichloroacetic acid in chlorobenzene (6). The bromine migrated to the solvent to give p-bromochlorobenzene. There are several mechanistic alternatives for this migration and it is of interest to assess their relative merits, and examine any implications they may have with respect to the normal rearrangement.

The rate-determining step for the rearrangement is considered to be a proton transfer and there is much evidence to support this (7–9). On the Dewar mechanism this yields an ion pair which rapidly and irreversibly forms a 'π-complex'. On the Soper mechanism it has been proposed (2) that the proton transfer is accompanied by a concerted attack of the carbonyl oxygen on the bromine atom to give a cyclic transition state which subsequently breaks down into the anilide and the acid hypohalite. These alternatives are represented schematically for both the 'normal (N)' and 'abnormal (A)' reactions:
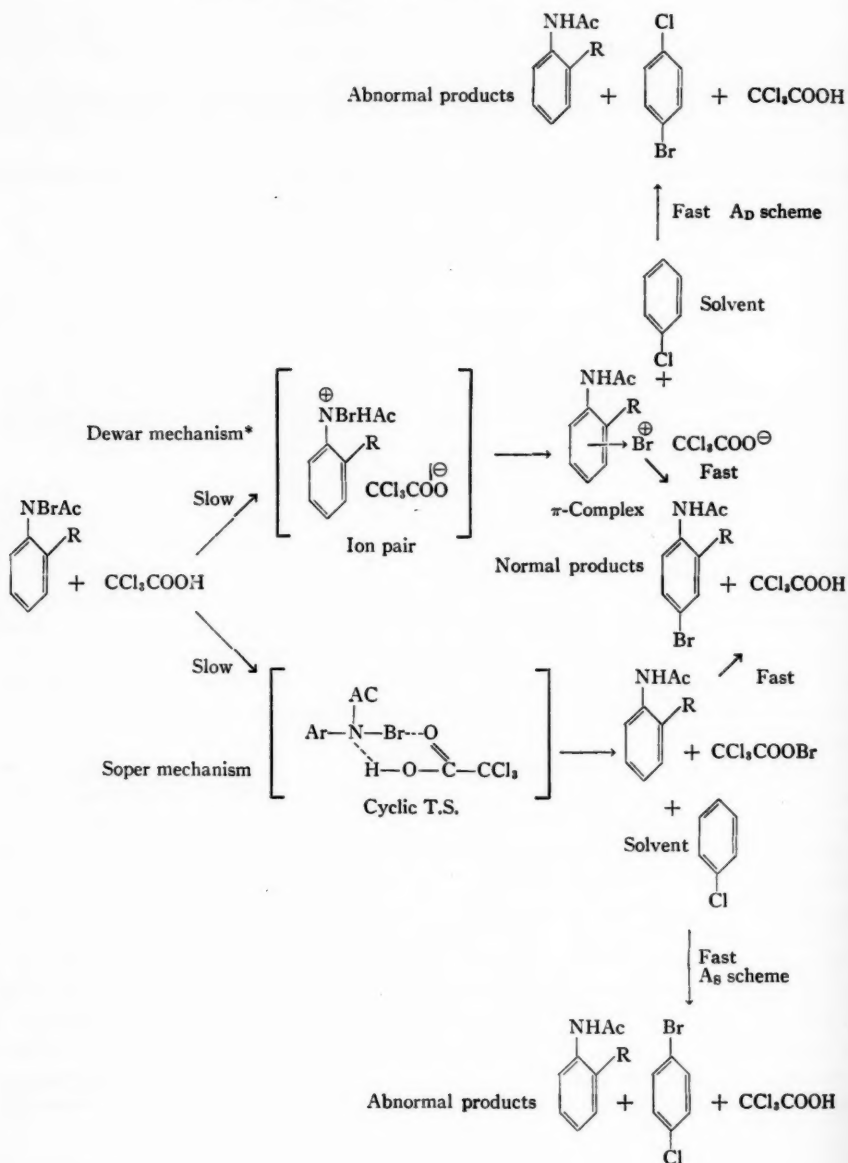
It is possible that the stages N-bromoanilide + acid → ion pair → π-complex may be concerted.

On the A_D scheme the 'π-complex' acts as a brominating agent, the reactivity of the bromine being enhanced in the particular instance $R = NO_2$ by the electron-withdrawing properties of the nitro substituent. A similar explanation has been advanced by Dewar to account for the intermolecular transfer observed by Soper *et al.* (3) when N-bromo-

acetanilide was treated with acetic acid in phenetole and anisole. On the Soper scheme the A_S reaction results from the competition for the bromine in the second bimolecular step between the anilide and the solvent. In the case $R = NO_2$ although the anilide may possibly have a more reactive p-position than the solvent, this is offset by the high concentration of the latter. The preceding discussion demonstrates that both mechanisms will superficially account for the observed experimental facts for both the A and N reactions. However, the possibility of other transition states for the A reaction must be considered. Two other schemes may be invoked in the case of $R = NO_2$. The first of these consists of a termolecular reaction:

(I)
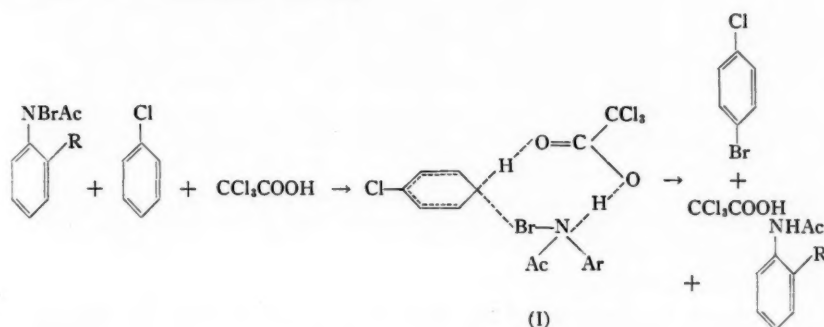
Some evidence for such transition states has been obtained when N-bromoacetanilide is 'rearranged' in the presence of anisole, i.e.

$$\text{rate} = k[\text{anisole}]^n[\text{N-bromoacetanilide}][\text{acid}].$$

However, the order (n) with respect to anisole shows a complex behavior with variation in the anisole concentration (4), which precludes any simple formulation of transition states such as I.

The transition state (I) bears obvious analogy to that proposed for the N_S reaction, the ring now being effectively six-membered instead of five. It would bear some resemblance to the transition state for the A_D fast reaction since the same molecules must be involved. Finally it may be envisaged that the bromine, the ion pair, or π-complex stage, forms some type of internal complex with the o-nitro group. This could then brominate the solvent. This hypothesis may be safely discarded since it has been demonstrated (see below) that the p-nitro compound behaves similarly and in this case the possibility of such an intermediate is very unlikely.

The problem, at this stage, appears to be reduced to deciding between the termolecular scheme on one hand and Dewar and Soper schemes on the other, since the latter appear almost indistinguishable experimentally. This was approached in the following manner. If the transition states leading to the A and N reactions are identical the rate of reaction for a series of p-substituted N-bromoacylanilides should presumably be related by the equation $\log k = x \log K_b +$ constant where K_b is the dissociation constant of the amine corresponding to the N-bromoacylanilide and x is a constant. If the abnormal reaction involves a termolecular transition state, this should not obey equation [1]. The use of equation [1] implies the use of a single catalyzing acid to compare the rates.

The above discussion shows that the investigation of the series of compounds $R = NO_2$, Cl, F, Br, Me, Ph, and H might be expected to aid in the elucidation of the problem and the result of such investigations is reported below.

EXPERIMENTAL

Materials

Acetanilides

p-Nitro-, *p*-bromo-, *p*-methyl- and *p*-chloro-acetanilides were purchased commercially and purified where necessary. *p*-Aminobiphenyl was purchased commercially and acylated with acetyl chloride in dry pyridine (10). *p*-Fluoroacetanilide was prepared by the route described for the *o*-isomer (6).

N-Bromo-4-fluoroacetanilide

p-Fluoroacetanilide (2.2 g) in chloroform (150 ml) was vigorously stirred (30 minutes) with a solution of sodium hypobromite prepared by dissolving bromine (5 ml) in 0.5 *N* NaOH (500 ml) also containing potassium bicarbonate (4 g). The chloroform layer was then washed with dilute potassium bicarbonate solution and dried over anhydrous sodium sulphate. Removal of the chloroform under reduced pressure and treatment with light petroleum (b.p. 40–60°) yielded a pale yellow solid which crystallized in plates from benzene and light petroleum (b.p. 40–60°), m.p. 95–97° (decomp.). (Active bromine 34.5, 34.6. C_8H_7NOBrF requires Br, 34.4%.)

N-Bromo-4-nitro-, chloro-, and bromo-acetanilides all previously characterized were prepared in the same way as the 2-fluoro derivative. The 4-nitro compound could not be obtained pure.

N-Bromo-p-acetaminobiphenyl

This compound was prepared by the same route as was used for the *o*-isomer (6). It crystallized from chloroform and light petroleum (b.p. 40–60°) yellow prisms, m.p. ca. 83° (decomp.). (Active bromine 27.3, 27.2. $C_{14}H_{13}NOBr$ requires Br, 27.5%.) N-Bromo-4-methylacetanilide was prepared by the dioxane method (6). It had previously been characterized and was found to be extremely labile.

3-Bromo-4-fluorotoluene

2-Bromo-*p*-toluidine hydrochloride (10 g) was suspended in hydrofluoroboric acid solution (10.3 g, 42% w/w) and cooled to 0°. Sodium nitrite (4 g) in the minimum of water was added dropwise with vigorous stirring, maintaining the temperature of the solution below 10°. After a further 30 minutes the diazonium salt was collected, washed with several small portions of ether, and dried over phosphorus pentoxide in a vacuum desiccator (11.8 g, 73.5%). The dry diazonium salt was decomposed in 30- to 50-g portions, the reaction being moderated by an equal weight of dry sand. The product was washed with dilute alkali and steam distilled. It was dried over calcium chloride and distilled under reduced pressure, b.p. 69–70°/11 mm (76.7 g, 43%). Found: C, 45.2; H, 3.5. C_7H_6BrF requires C, 44.5; H, 3.2%.

3-Bromo-4-fluorobenzoic Acid

3-Bromo-4-fluorotoluene (30 g) was oxidized with aqueous potassium permanganate (50 g). (For details see reference 2.) The product crystallized from aqueous alcohol in needles (10 g), m.p. 137°. Found: equivalent, 219; C, 38.7; H, 1.8. $C_7H_4O_2BrF$ requires equivalent, 219; C, 38.4; H, 1.8%. K_D (uncorr.) = 1.38×10^{-5} in 50/50 absolute ethanol water by volume, $T = 21-22°$.

3-Bromo-4-fluorobenzoyl Chloride

3-Bromo-4-fluorobenzoic acid (5 g) was boiled with thionyl chloride for 1 hour. The excess thionyl chloride was removed under reduced pressure and the residue distilled, b.p. 110–112°/11 mm. The distillate solidified giving colorless blades which were crystallized from light petroleum (b.p. 40–60°), m.p. 43–45°. Found: solvolysable Cl, 14.9. $C_7H_3O_2ClBrF$ requires Cl, 14.9%).

3-Bromo-4-fluorobenzamide crystallized in fine needles from anisole and light petroleum (b.p. 100–120°), m.p. 133° C. Found: C, 38.8; H, 2.3; N, 6.4. C_7H_5NOBrF requires C, 38.6; H, 2.3; N, 6.4%.

3-Bromo-4-fluorobenzanilide crystallized in needles from toluene, m.p. 148–149°. Found: C, 53.4; H, 3.3; N, 4.9. $C_{13}H_9NOBrF$ requires C, 53.1; H, 3.1; N, 4.8%.

3-Bromo-4-fluorobenz-p-toluidide crystallized in needles from toluene, m.p. 153–155°. Found: C, 54.3; H, 3.7; N, 4.7. $C_{14}H_{11}NOBrF$ requires C, 54.6; H, 3.6; N, 4.6%.

3-Bromo-4-fluoroaniline

3-Bromo-4-fluorobenzoic acid (6.6 g) in chloroform (200 ml) was treated with hydrazoic acid (2 moles) and concentrated sulphuric acid (40 ml) at 50–55° C on a steam bath. Working up in the usual fashion gave an amine (2 g, 36%) distilling at 124°/11 mm.

The *3-bromo-4-fluoroacetanilide* crystallized from toluene in prisms, m.p. 114°. Found: C, 41.4; H, 2.9; N, 6.1. C_8H_7NOBrF requires C, 41.4; H, 3.0; N, 6.0%.

The *3-bromo-4-fluoroformanilide* crystallized in needles from benzene – light petroleum (b.p. 40–60°), m.p. 91–92°. Found: C, 38.6; H, 2.1; N, 6.3%. C_7H_5NOBrF requires C, 38.6; H, 2.3; N, 6.4%.

The *N-benzoyl-3-bromo-4-fluoroaniline* crystallized from aqueous alcohol in plates, m.p. 125–127°. Found: C, 54.3; H, 2.8; N, 5.0. $C_{13}H_9NOBrF$ requires C, 53.1; H, 3.1; N, 4.8%.

Rearrangements

These were all carried out in a solution of 0.617 N A.R. trichloroacetic acid in chlorobenzene, the solution being prepared as described in the section dealing with the kinetic data. The rearranging solutions of the N-bromoamide and acid were left in the dark until they displayed negligible oxidizing properties towards acid potassium iodide solution. The N-bromoacylanilides were pure samples unless otherwise stated.

(*a*) *N-Bromo-p-methylacetanilide* (16 g) on treatment with the acid solution (ca. 30 ml) gave on removal of acid and the bulk of solvent a gummy product (11.8 g, 73.5%). Chromatography of a portion of the product on alumina from benzene/light petroleum (b.p. 60–80°) yielded a compound which crystallized from the same solvent in fine white needles, m.p. 117° C (lit. 2-bromo-4-methyl acetanilide 117° C). Because of the tarry nature of the product this reaction was not studied kinetically.

(*b*) *N-Bromo-p-acetaminobiphenyl* (5 g) on treatment with acid solution (ca. 10 ml) yielded a clean product (4.67 g, 81.4%), m.p. 139–142° C. C, 58.5; H, 4.1; N, 5.00; Br, 26.9. Calc. for $C_{14}H_{12}NOBr$: C, 58.0; H, 4.2; N, 4.8; Br, 27.5%. Hydrolysis of the product yielded an amine crystallizing in needles from light petroleum (b.p. 40–80°), m.p. 66–68° (lit. for 2-bromo-*p*-aminobiphenyl 66° C).

(*c*) *N-Bromo-4-bromoacetanilide* (10.35 g) on treatment with acid solution (ca. 20 ml) yielded a very clean product (9.6 g, 92.7%), m.p. 145–147° (lit. for 2,4-dibromoacetanilide 146° C).

(*d*) *N-Bromo-4-chloroacetanilide* (9.97 g) on treatment with acid solution yielded a very clean product (8.39 g, 84%), m.p. 134–136° (lit. for 2-bromo-4-chloroacetanilide 135°). Hydrolysis of product yielded an amine which crystallized in needles from light petroleum, b.p. 40–60°, m.p. 65–67° (lit. for 2-bromo-4-chloroaniline 69°).

(*e*) *N-Bromo-4-fluoroacetanilide* (1 g) on treatment with acid (2 ml) gave a clean product which appeared to be a mixture of the ring-brominated product and anilide formed possibly by loss of bromine to the solvent. Separation of the product was not achieved.

(*f*) *N-Bromo-4-nitroacetanilide* (10.84 g), 90.9% pure, when treated with acid yielded
p-bromochlorobenzene (3.5 g, 50%), m.p. 64–67° C (lit. 67° C), and unchanged anilide
(4.28 g, 72.2%), m.p. 215° C (lit. 215° C).

Kinetic Experiments

The kinetic experiments were mainly carried out as previously described (2) but with
certain modifications. All the glass apparatus used was carefully washed with distilled
water and dried in a vacuum oven.*

Chlorobenzene

Chlorobenzene was treated as previously (2) and then distilled twice from an all-glass
apparatus with liberal rejection of initial and tail fractions. Its physical properties were
essentially the same as those previously reported.

Solutions of Trichloroacetic Acid

A suitable weight of trichloroacetic acid (A.R. grade) was introduced into a 250-ml
flask which was then attached to a vacuum line. The flask was then warmed (ca. 50° C)
and pumped for about 2 hours. Air was then admitted through the silica-gel drying train,
followed by a suitable volume of purified chlorobenzene. The solutions so prepared were
standardized as before (2).

Solutions of the N-Bromoacylanilides

These were prepared and stored as previously described (2). The purity of each sample
was >97% except in the case of N-bromo-4-nitroacetanilide, which could be obtained only
ca. 90% pure. In consequence the purity of the sample was determined and the weight of
the impure sample required to give a solution of the desired strength calculated. The
solutions thus prepared eventually precipitated unchanged 4-nitroacetanilide (obviously
the main impurity) and this was removed by filtration. The precipitation of the anilide
was not due to any reaction of the N-bromo-4-nitroacetanilide with the solvent since the
oxidative power of the solutions towards acid potassium iodide solution remained constant
over a period of months.

Comparison of Rates

The meaningful comparison of rate constants between the various N-bromoacylanilides
is rather uncertain for the following reasons.

(*a*) The reaction is not strictly first-order with respect to the N-bromoacylanilide,
the first-order constants showing a variation with the initial concentration (C_1) of the
N-bromo compound (see references 2 and 8).

(*b*) The variation of the first-order rate constants with the concentration (C_a) of the
catalyzing acid is complex (see Bell (7)).

The following procedure was adopted. The first-order rate constants (k) for each
N-bromoacylanilide were determined for three values of C_1 and three values of C_a giving
nine rate constants at 45° C. A second-order rate constant k_m for each compound was
evaluated from these results in the following rather arbitrary manner.

Within the range C_a 0.2 *M*–0.1 *M*, k is approximately linear in C_a. The measured
rates were consequently reduced to unit acid concentration to give nine values of a
quantity k_u. Bell and Levinge (8) have shown that the variation of k with C_1 can be
represented by an equation of the form

$$1/k = A + BC_1$$

where A and B are empirically determined constants. Thus three k_u values for a given

*The spurious production of an intermediate previously reported was almost certainly due to traces of acetone
in the reacting system; in consequence the use of acetone for washing glassware was completely avoided.*

value of C_a were fitted to the above equation by the method of least squares and a value of k_u for $C_i = 0.01$ N was determined from the above equation. This procedure was repeated on the k_u values from the remaining two C_a values giving in all, three values of k_u at $C_i = 0.01$ N. The mean of these three values of k_u was defined as k_m and was expressed with a standard deviation.

This procedure for treating the reported rate data was found satisfactory for the 4-nitro-, 4-chloro-, 4-bromo-, and 4-fluoro-N-bromoacylanilides. One rate constant for the N-bromo-4-bromoacetanilide ($C_i = 0.0309$ N; $C_a = 0.199$ M, see Table I below) failed

TABLE I
Rate data for N-bromo-4-bromoacetanilide

C_i C_a	0.046 N $k \times 10^4$ sec^{-1}	0.0309 N $k \times 10^4$ sec^{-1}	0.00939 N $k \times 10^4$ sec^{-1}	0.01 N $k_u \times 10^4$ sec^{-1} mole^{-1}l.
0.199 M	1.75	1.66	2.00	10.8
0.150 M	1.36	1.41	1.56	10.6
0.102 M	0.89	0.975	1.17	11.3

$$k_m = 10.9 \pm 0.5 \times 10^{-4} \text{ sec}^{-1} \text{ mole}^{-1} \text{l}.$$

to conform to the general pattern observed and the rates of the N-bromo-4-phenylacetanilide showing a curious minimal reactivity at the intermediate N-bromoamide concentration. In consequence the rate constants for the latter compound are reported without the evaluation of k_m. The anomalous behavior of the odd N-bromo-4-bromoacetanilide rate constant and all the N-bromo-4-phenylacetanilide rate constants do not invalidate the general conclusions which we wish to make in this instance.

TABLE II
Rate data for N-bromo-4-chloroacetanilide

C_i C_a	0.046 N $k \times 10^4$ sec^{-1}	0.0279 N $k \times 10^4$ sec^{-1}	0.00961 N $k \times 10^4$ sec^{-1}	0.01 N $k_u \times 10^4$ sec^{-1} mole^{-1}l.
0.199 M	1.66	1.80	2.00	9.94
0.150 M	1.31	1.44	1.60	10.6
0.102 M	0.89	0.953	1.19	11.2

$$k_m = 10.6 \pm 0.6 \times 10^{-4} \text{ sec}^{-1} \text{ mole}^{-1} \text{l}.$$

TABLE III
Rate data for N-bromo-4-fluoroacetanilide

C_i C_a	0.0464 N $k \times 10^4$ sec^{-1}	0.0281 N $k \times 10^4$ sec^{-1}	0.0110 N $k \times 10^4$ sec^{-1}	0.01 N $k_u \times 10^4$ sec^{-1} mole^{-1}l.
0.199 M	1.75	1.88	1.95	9.65
0.150 M	1.34	1.39	1.56	9.96
0.102 M	0.891	0.986	1.08	10.3

$$k_m = 9.97 \pm 0.5 \times 10^{-4} \text{ sec}^{-1} \text{ mole}^{-1} \text{l}.$$

TABLE IV
Rate data for N-bromo-4-nitroacetanilide

C_i C_a	0.0500 N $k \times 10^4$ sec^{-1}	0.0289 N $k \times 10^4$ sec^{-1}	0.0104 N $k \times 10^4$ sec^{-1}	0.01 N $k_u \times 10^4$ sec^{-1} mole^{-1}l.
0.199 M	1.45	1.51	1.55	7.95
0.150 M	1.11	1.16	1.27	8.74
0.102 M	0.78	0.83	0.88	8.97

$$k_m = 8.55 \pm 0.5 \times 10^{-4} \text{ sec}^{-1} \text{ mole}^{-1} \text{l}.$$

TABLE V

Rate data for N-bromo-4-phenylacetanilide

C_i	0.0445 N	0.0273 N	0.00922 N
C_a	$k \times 10^4$ sec^{-1}	$k \times 10^4$ sec^{-1}	$k \times 10^4$ sec^{-2}
0.199 M	3.23	2.77	3.38
0.150 M	2.31	2.14	2.67
0.102 M	1.36	1.31	1.67

TABLE VI

Rate constants and pK_b values of the related amines

	pK_b (amine)	k_m, sec^{-1} mole^{-1}l. $\times 10^4$
N-Bromoacetanilide*	9.39	11.3±0.8
N-Bromo-4-nitroacetanilide	12.95	8.55±0.5
N-Bromo-4-fluoroacetanilide	9.48	9.97±0.5
N-Bromo-4-chloroacetanilide	10.19	10.6±0.6
N-Bromo-4-bromoacetanilide	10.09	10.9±0.5

*The calculation of the rate constant for N-bromoacetanilide at 45° C was made in the follow-ing way. The first-order rate constants ($C_i = 0.01\ N$) reported by Bell (7) at 15° C are linear in C_a over a range 0.07 M–0.2 M. Values of k at 15° C $C_a = 0.102\ M$, 0.150 M, and 0.199 M were thus interpolated from Bell's results, and from these, three values of k_u calculated. Using these values in conjunction with the Arrhenius equation ($E_a = 11.8$ kcal) three values of k_u at 45° C were calculated. These were then averaged and the mean value indentified with k_m as in the previous treatment. It should be noted that Bell's rate constants must be multiplied by a factor 2.3026/3600 to bring them to the units used in this paper.

DISCUSSION

The examination of the reaction products which preceded the kinetic studies revealed that the reactions of the 4-substituted N-bromoacylanilides were similar to those of the corresponding 2-substituted compounds. The 4-nitro compound was again exceptional, the bromine being transferred to the solvent to give 4-nitroacetanilide and 4-bromo-chlorobenzene. The products from the rearrangement of N-bromo-4-fluoroacetanilide also appeared complex and possibly contain 2- and 3-bromo-4-fluoroacetanilides, 4-fluoroacetanilide, and 4-bromo-chlorobenzene. An unambiguous synthesis of 3-bromo-4-fluoroacetanilide was devised with the hope that both 2- and 3-bromo-4-fluoroacetani-lides could be characterized. However, the complexity of the products from the re-arrangement of N-bromo-4-fluoroacetanilide (which it was hoped would yield 2-bromo-4-fluoroacetanilide as the sole product) prevented this project from being completely realized.

The recent work of Dewar and Couzens (4, 5) show that the premises on which the kinetic work was based are vastly oversimplified. It now appears that the Dewar and Soper formulations as originally postulated are insufficient to account for the observed complexities of the reacting system. However, two useful points appear to emerge from the present investigation.

(a) There is a rough correlation between log k_m and the logarithm of the dissociation constant of the parent amine (Table IV and Fig. 1). The slope of this line is very small, i.e. the reaction is very insensitive to substituent effects.

(b) Although the 2- or 4-substituted nitro group and possibly the 4-fluoro group induce the reaction to give different products, this does not appear to alter the nature of the rate-determining step, i.e. the differentiation in products occurs subsequent to the rate-determining step.
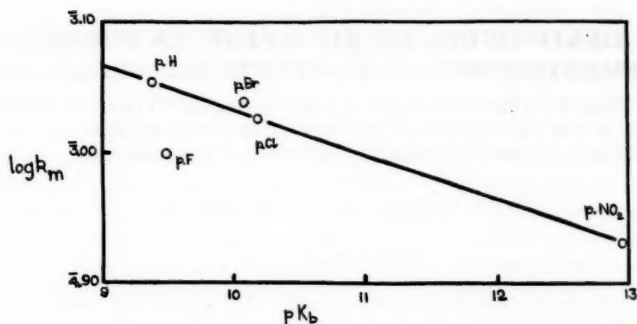
FIG. 1.   Correlation between log k_m and pK_b for a series of p-substituted N-bromoacylanilides.

The author wishes to acknowledge assistance from Mr. D. Allardyce during the investigation and some useful criticisms from Dr. R. F. Garwood.

REFERENCES

1. M. J. S. DEWAR.   Electronic theory of organic chemistry. Oxford University Press. 1949. p. 225.
2. M. J. S. DEWAR and J. M. W. SCOTT.   J. Chem. Soc. 2676 (1957).
3. C. G. ISRAEL, A. W. N. TUCK, and F. G. SOPER.   J. Chem. Soc. 547 (1945).
4. P. J. COUZENS.   Ph.D. Thesis, London. 1959.
5. M. J. S. DEWAR.   Kekule Symposium. International Union of Pure and Applied Chemistry, Organic Chemistry Section. Butterworth Scientific Publications, London. 1957. p. 179.
6. M. J. S. DEWAR and J. M. W. SCOTT.   J. Chem. Soc. 1445 (1957).
7. R. P. BELL.   Proc. Roy. Soc. (London), A, **143**, 377 (1934).
8. R. P. BELL.   Proc. Roy. Soc. (London), A, **151**, 211 (1935).
9. R. P. BELL.   J. Chem. Soc. 1154 (1936).
10. H. A. SCARBOROUGH and W. A. WATERS.   J. Chem. Soc. 89 (1927).

POTASSIUM DERIVATIVES OF FLUORENE AS INTERMEDIATES IN THE PREPARATION OF C₉-SUBSTITUTED FLUORENES

II. COMPARATIVE REACTIVITIES OF THE ALKALI METALS, LITHIUM, SODIUM, AND POTASSIUM, WITH FLUORENE IN GLYCOL DIMETHYL ETHER, GLYCOL DIETHYL ETHER, TETRAHYDROFURAN, AND DIOXANE[1]

G. W. H. Scherf and R. K. Brown

ABSTRACT

In the solvents 1,2-dimethoxyethane (DME), 1,2-diethoxyethane (DEE), tetrahydrofuran (THF), and dioxane, potassium reacts much more readily with fluorene than does sodium or lithium. Lithium is generally more reactive than is sodium. The order of effectiveness of the ethers is DME > DEE ≃ THF > dioxane. Although practically no reaction of these metals with fluorene occurs in toluene, the addition of small amounts of these ethers to toluene does accelerate such reaction. All three organometallic compounds are soluble in refluxing and cold (22°) DME, THF, and DEE except the 9-fluorenyllithium, which precipitates largely from cold DEE. The results are explained in terms of the relative electropositivities of the metals, their size, and the structure of the ethers. It is suggested that these ethers actually participate in the formation of the organometallic compound from the metal.

Sodamide and lithium amide react as readily as or more readily than the metals with fluorene in DME to produce the organometallic compounds.

Diphenylmethane and triphenylmethane react reasonably well with potassium in DME, but too slowly with lithium and sodium to be useful.

INTRODUCTION

It was recently reported (1) that 9-fluorenylpotassium could be prepared by the direct action of potassium with fluorene in dioxane solvent. The organometallic compound was a reddish-brown precipitate singularly free of tarry impurities and quite useful for the synthesis of 9-substituted fluorenes. The simplicity of preparation led us to study the scope of this reaction in greater detail.

In a preliminary examination of the effects of solvents on the preparation of 9-fluorenylpotassium (2), it was found, in agreement with general information already established in the literature (3), that dioxane, dialkyl, alkylaryl, or diaryl ethers as well as tertiary amines promoted the reaction of potassium with fluorene. Generally no reaction was observed in hydrocarbon solvents. The tertiary amines proved to be either less effective than the ethers or themselves reacted with the organometallic substance formed.

Since, of all the pure ethers examined, dioxane was the most effective, and because addition of ethers to the normally ineffective hydrocarbons to the extent of 20% gave reactions of the metal with fluorene in the case of dioxane but not for dialkyl or arylalkyl ethers, it was suggested that the presence of *two* ether oxygen atoms in a single molecule, suitably situated as in the unstable boat form of dioxane, and/or sterically less hindered oxygen atoms (4) might be responsible for the preferred reaction found for dioxane. This viewpoint, augmented by the reports that certain ethers such as those of ethylene glycol (5, 6) dissolve small amounts of potassium metal at low temperatures to form blue, electrically conducting solutions, while dialkyl ethers do not, led to the investigation of the comparative efficiencies of ethers of ethylene glycol, as well as tetrahydrofuran as solvents for the reaction of the alkali metals, lithium, sodium, and potassium, with fluorene. This paper presents the results of experiments in this direction.

Gilman and Gorsich (7) have reported that lithium does react directly with fluorene and with cyclopentadiene in tetrahydrofuran to form the corresponding 9-fluorenyllithium and cyclopentadienyl lithium. Recently a paper by Normant and Angelo (8) described the metalation of a number of hydrocarbons with reactive hydrogen atoms in tetrahydrofuran, primarily with sodium but in some examples with lithium or potassium, using as the intermediate metalating agent the product arising from the combination of the metal with naphthalene. The mixture of naphthalene, tetrahydrofuran, metal, and active hydrogen compound gave metalation of a number of hydrocarbons which previously had reacted very slowly or failed to react at all with metallic sodium. The use of amines and of special ethers such as dimethyl ether and 1,2-dimethoxyethane to facilitate the addition of alkali metals to hydrocarbons such as naphthalene, biphenyl, etc., and the utility of these addition compounds to prepare alkali metal salts of active hydrogen-containing hydrocarbons had been pointed out previously by Scott *et al.* (9). However, the presence of naphthalene and the dihydronaphthalene by-product complicated isolation and purification. The results of our work show that in the case of fluorene, the hydrocarbon under examination in this laboratory, the addition of naphthalene is an unnecessary factor in the reaction of alkali metals with fluorene to form the organometallic compound and hydrogen.

RESULTS AND DISCUSSION

For the comparative studies, equivalent amounts of metal and fluorene were used in the appropriate solvent. The particular quantities upon which time and extent of reaction are quoted were 0.05 mole of fluorene, 0.05 gram-atom of the metal, and 50 ml of the solvent. Reactions were protected by nitrogen atmosphere and anhydrous conditions were employed at all times. The results are compiled in the accompanying table for convenience. The metals lithium, sodium, and potassium were studied while the solvents examined were 1,2-dimethoxyethane (DME), 1,2-diethoxyethane (DEE), and tetrahydrofuran (THF). The results in these solvents are compared with those obtained for dioxane in the previous work (2). For those cases where the metal remained solid under the conditions employed, we did attempt to use pieces of roughly similar size, about 1 mm³. Solid pieces of sodium, especially at higher temperatures, had a strong tendency to stick together, hence presenting a smaller surface area to the reagent than was originally obtained. Molten sodium did not show this property. A similar behavior for potassium was not found, probably due to the greater rate of reaction with fluorene at the surface preventing adhesion of metal particles. Lithium particles did not stick together at all.

The extent of metalation was estimated by methylation of the salt by addition of methyl iodide, and, after isolation of the product, measurement of the amount of mono- and di-methylfluorene and of unchanged fluorene by infrared spectroscopy (1).

From the results shown in Table I, and from previous work (2), it is seen that, generally, hydrocarbon–ether mixtures are less effective solvents for the reaction of these alkali metals with fluorene than are the pure ethers, and also cause precipitation of the product even from the hot solutions. However, a mixture of 20% DME in *heptane* not only gave nearly complete metalation with potassium in 3 hours, but showed no precipitation of the organometal. Instead, during the reaction, there was observed the formation of a nearly colorless upper layer composed of heptane, unreacted fluorene, and some DME, and a dark-red lower layer containing 9-fluorenylpotassium and DME contaminated with some heptane. The formation of this lower layer apparently approximated the conditions for DME only as solvent and would account for the greater extent of reaction.

TABLE I

Solvent	Metal	Temperature	Observation	Extent of Metalation
Dioxane (98°/700 mm)	Li	Reflux	Little reaction in 4 hours	<5%
	Na	Reflux	Little reaction in 4 hours	<5%
	K	Reflux	Complete in 4 hours. Product largely insoluble hot	80–90%
	K	22°	Some reaction in 12 hours. Product largely insoluble hot	~30%
DME (85°/700 mm)	Li	22°	Small pieces. Complete reaction in ~5 hours. Product soluble R.T.	~80–90%
		Reflux	Small pieces. Complete reaction in ~5 hours. Product soluble R.T.	~80–90%
	Na	22°	Small pieces. Complete reaction in ~8 hours. Product soluble R.T.	~80–90%
		Reflux	Small pieces. Complete reaction in ~10 hours. Product soluble R.T.	~80–90%
	K	22°	Complete in 2 hours. Product soluble R.T.	~90–95%
		Réflux	Complete within 1 hour. Product soluble R.T.	~90–95%
DEE (118°/700 mm)	Li	22°	About 20% unreacted after 50 hours. Product largely insoluble R.T.	—
		Reflux	Complete in 5–6 hours. Product soluble in hot, insoluble R.T.	70–80%
	Na	22°	Incomplete in 50 hours	—
		Reflux	Nearly complete in 30 hours. Product largely soluble R.T.	70–80%
	K	22°	Complete in ~3 hours. Product soluble R.T.	~70–80%
		Reflux	Complete in ~2 hours. Product soluble R.T.	~70–80%
THF (65°/700 mm)	Li	22°	Little reaction in 4 hours. Complete in 50 hours. Product soluble R.T.	~80%
		Reflux	Complete in 7–8 hours. Product soluble R.T.	~80%
	Na	22°	Incomplete in 50 hours. Product soluble R.T.	—
		Reflux	Incomplete in 48 hours. Product soluble R.T.	—
	K	22°	Complete in ~2½ hours. Product soluble R.T.	—
		Reflux	Complete in 1 hour. Product soluble R.T.	~70%
Toluene +20% dioxane	K	Reflux	In 5 hours incomplete. Product largely insoluble hot	40–50%
Toluene +20% DME	K	Reflux	Complete in 2 hours. Product largely insoluble hot	60–70%
Toluene +20% DEE	K	Reflux	Nearly complete in 4 hours. Product largely insoluble hot	60–70%
Toluene +20% THF	K	Reflux	Incomplete in 4 hours. Product largely insoluble hot	~50–60%
Toluene +1% dioxane	K	Reflux	In 4 hours, very little reaction	—
Toluene +1% DME	K	Reflux	In 4 hours, red solution + some precipitate	~10–15%
Toluene	K	Reflux	In 4 hours very little reaction	~ 2–3%
Dioxane +10% DME	Li	Reflux	Complete in 10 hours. Product soluble at R.T.	~90%
	Na	Reflux	Incomplete in 24 hours. Product soluble at R.T.	~50%
	K	Reflux	Complete in 2 hours. Product largely soluble at R.T.	~90%
Heptane +20% DME	K	Reflux	Complete in 3 hours. Two layers. Product soluble R.T.	~90%

NOTE: R.T. = room temperature (22°).
In all solvents, solutions of the potassium salt were very dark red, those of the sodium or lithium salts were quite light red (those of the lithium salt somewhat lighter than those of the sodium salt).

The same separation into two layers, with the formation of no precipitate, was observed when a solution of 9-fluorenyl-potassium (-sodium or -lithium) in DME only was diluted with heptane. A similar dilution of a dioxane *solution* of 9-fluorenylpotassium caused the precipitation of most of the salt and when this salt was washed three times with hexane,

it was apparently free of dioxane since no ether–oxygen band was discernible in the infrared spectrum of a Nujol mull of the salt. However frequent, heptane washes of the dark-red layer obtained from the heptane diluted DME solutions failed to yield any solid precipitate or to remove the ether from the organometal. It is quite clear that with DME as solvent or cosolvent the diluting aliphatic hydrocarbon competed with the metalated fluorene for the ether far less effectively than did the hexane versus 9-fluorenyl-potassium for dioxane, no doubt due to the stronger association of the DME with the organometallic compound. Diethyl ether, a solvent more compatible with DME, and also capable of dissolving the 9-fluorenylpotassium only to a limited extent, did cause a precipitation of an oily solid which, however, could not be completely freed from ether. Toluene, however, added to a DME solution of 9-fluorenylpotassium slowly precipitated a portion of the red salt. In contrast, a DME solution of 9-fluorenyl*lithium* poured into excess diethyl ether caused much precipitation of solid 9-fluorenyllithium which was readily freed from ether by hexane washes, showing that the greater polar character of the potassium–carbon bond intensifies the association of the type shown below.
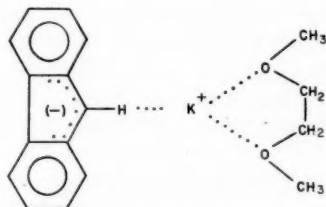
That the lithium salt remains quite soluble in DME is most likely due to the small size of the lithium atom which compensates largely for the lower polarity of the lithium–carbon bond. The lithium atom thus can approach the two oxygen atoms of the glycol ether more closely than can potassium or sodium and because of this close approach will develop more polar character and hence a stronger association of the type shown above. A similar structure has been suggested by Wittig (11) to explain the difficultly soluble molecular complex between phenyllithium and 1,2-dimethoxyethane.

The larger sodium and potassium ions must then depend primarily upon the original polar character of the metal–carbon bond (somewhat augmented upon approach to the ether) for their degree of association with the ether. On the basis of only the original polarity of the metal–carbon bond, the sodium salt should then associate with DME less firmly than does the potassium compound but more so than does the lithium compound. One might therefore expect that small steric factors should affect the degree of proximity of the lithium atom to the ether oxygens, therefore the degree of polarization of the lithium–carbon bond by the glycol ether and hence the strength of association, more than would be the case for the sodium or potassium analogues.

Some evidence for this is given in the results found for the solubilities of the organometallic compounds in DEE. The 9-fluorenyllithium is quite soluble in hot DEE but precipitates largely from the cold solution (at R.T.). On the other hand, both the potassium and sodium compounds remain almost completely soluble in DEE at room temperature. The larger steric interference of the ethyl group in DEE thus hinders close approach of the lithium to the two oxygen atoms. This small difference is of great significance in the association of 9-fluorenyllithium with the glycol ethers, but not as critical with the more ionic sodium and potassium compounds.

It is noteworthy that the red-orange solid 9-fluorenyllithium (obtained from DEE as above) dissolved readily in dioxane. Diethyl ether dissolved only a small amount of the lithium salt while toluene failed to dissolve any of it.

It is furthermore quite clear that for the preparation of the lithium, sodium, or potassium salts of fluorene, the solvents of choice are, in order of effectiveness, DME > DEE ≈ THF > dioxane > dialkyl ethers.* In all cases, potassium reacts much more vigorously with fluorene than does sodium or lithium, as expected on the basis of the difference in electropositivity between potassium and the other two metals. The presence of two favorably situated oxygen atoms such as found in the ethers of ethylene glycol promotes this reaction. The larger bulk of the ethyl group over that of the methyl group (in DEE vs. DME) is thus expected to, and does, offer steric hindrance to co-ordination. Ferguson (4), in his discussion of solubility of ethers in water, points out that the methyl groups of diethyl ether partially shield the oxygen atom from facile approach by water, thus accounting for the much greater water solubility of dimethyl ether, tetrahydrofuran, and dioxane over that of diethyl ether. That THF is a better solvent for the metalation reaction than is dioxane is also expected since the co-ordinating electrons of the oxygen atom in the former are exposed to a greater extent than they are in the latter molecule, a fact which is readily discerned by consideration of the models of these two molecules.

That the reactivity of lithium is similar to and sometimes greater than that of sodium,† although its electropositivity is less, is quite likely due to its smaller size, which permits closer approach to the favorably located and exposed oxygen atoms in DME, DEE, and THF.

The observation that the solid, dioxane-free 9-fluorenylpotassium, suspended in heptane, is quite definitely deeply colored, and that even the very reactive molten potassium shows no coloration of the bright surface of the metal, when it is refluxed with fluorene in heptane, but upon addition of dioxane a reaction does occur (2) indicates that the ether not only hastens metalation by removing the product from the surface of the metal but also actually participates in the formation of the organometallic compound. Further support for this point of view is given by the fact that ether-free 9-fluorenyllithium, made in DEE, dissolves readily in dioxane but that the reaction of lithium and fluorene in dioxane was found to be very slow, the refluxing solvent in 15 hours developing only a slight color. Removal of the product from the surface of the metal cannot therefore be the controlling factor in this case. A concerted reaction of the type suggested below is thus indicated.
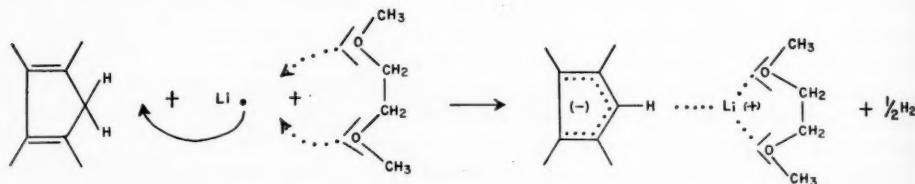
Generally, increased temperature facilitates metalation. Thus in tetrahydrofuran, DEE, and dioxane, both sodium and lithium react faster at reflux temperature than at room temperature while potassium does so in these three solvents *and* in DME. The

*Dimethyl ether, no doubt, is an exception since it has been shown to co-ordinate readily with water due to the lower steric effect of the methyl groups (4, 9).

†W. Schlenk and E. Bergmann (Ann. **463**, 1 (1928)) have found that lithium metal in ether suspension adds more readily to hydrocarbons, such as biphenyl and naphthalene, than does sodium.

similarity of the reaction of sodium at room temperature and at the boiling point in DME may be accounted for by the tendency of the warmed solid metal to agglomerate. However, though lithium reacts about equally well in DME at room temperature and at reflux temperature, the explanation offered for the behavior of sodium cannot apply. This similar time of reaction of lithium at high and low temperatures has been observed in several repetitions of the same experiment. It might be that the increasing rate of reaction due to elevation of temperature does occur but is offset by the increased thermal agitation of the molecule which hinders the attainment of the favorable conformation of the ether and hence the simultaneous close approach to the two oxygen atoms required for the reaction with lithium.

Reaction of Fluorene with Lithium Amide and Sodium Amide in DME

In DME, both lithium amide and sodium amide react quite readily with fluorene. 9-Fluorenylsodium of good quality can thus be prepared more rapidly using sodamide rather than metallic sodium. In 3 hours, 0.05 mole of a good grade of sodamide reacted completely with an equivalent amount of fluorene in refluxing DME as compared with 10 hours required for reaction of 0.05 mole of sodium under the same conditions. Extent of the reaction was again measured by methylation. The lithium amide used was a technical grade, but it reacted completely in 5 hours yielding about 60% metalation. The clear solutions of the organometallic compounds in DME obtained in this manner possessed a deeper red color than those obtained by the direct action of the metal with fluorene. This may be due to the presence of ammonia since the addition of dry gaseous ammonia to 9-fluorenylsodium prepared from sodium reacting with fluorene in DME actually caused intensification of color.

Reaction of Triphenylmethane and Diphenylmethane with Lithium, Sodium, or Potassium in DME as the Solvent

Triphenylmethane was found to react with potassium, showing the red color characteristic of the metal salt after 30 minutes of reflux, and being completely consumed in 10 hours. Reaction with benzyl chloride gave the expected 1,1,1,2-tetraphenylethane in good yield.

Both sodium and lithium under the same conditions reacted very slowly with triphenylmethane and in a period of 100 hours had reacted only to the extent of about 10% as judged by the weight of the unreacted metal.

Diphenylmethane after 3 days' reflux in DME had consumed nearly all the potassium. However, lithium under the same conditions in 30 hours showed only a slight accumulation of red solid on the surface of the metal but no solution of the product.

EXPERIMENTAL

Details for the comparative reactions of the metals in the various solvents and isolation and estimation of products followed published directions (1). In all cases, 0.05 mole of fluorene, 0.05 mole of metal, and 50 ml of purified, dry solvent were used. A constant stream of pure, dry nitrogen supplied a protective atmosphere for the reactions.

The solvents were generally commercially available reagent grade materials but were further purified by distillation from potassium. Only a technical grade of 1,2-diethoxyethane was available. This was treated carefully with metallic potassium, over which the liquid stood for 24 hours. Distillation from the metal gave a glycol ether of good quality.

Metalation of Triphenylmethane

Triphenylmethane (12.2 g, 0.05 mole) and potassium (1.95 g, 0.05 mole) were refluxed in 50 ml 1,2-dimethoxyethane. The solution showed a red color after 30 minutes and in 10 hours all the metal was consumed. To the deep-red solution, containing the completely dissolved triphenylmethylpotassium was added 6.3 g (0.05 mole) of benzyl chloride. The solution, which decolorized rapidly, was then diluted with 150 ml of water, extracted with ether, and the ether extracts dried ($CaCl_2$). Removal of the ether gave a yellow solid which was triturated with pentane to remove unreacted triphenylmethane. Colorless 1,1,1,2-tetraphenylethane requiring no further purification was obtained in good yield, m.p. 140° uncorr., lit. 140–142° (12).

When sodium replaced potassium in a similar experiment a light-red color developed only after 12 to 15 hours of reflux. The small pieces of sodium had formed a single spherical piece of metal. After 100 hours of reflux, 90% of the metal (by weight) remained unreacted. Lithium showed red coloration of the surface of the metal in 5 hours, but gave only 10% reaction of the metal after 100 hours reflux.

Metalation of Diphenylmethane

Details for the reaction between diphenylmethane and potassium followed those described for the triphenylmethane. Evidence of the reaction, via appearance of a red color in the solution, occurred within 3 hours. In 3 days, nearly all the potassium had disappeared giving a product quite soluble in DME. Treatment of the salt with benzyl chloride gave 1,1,2-triphenylethane, m.p. 53°, lit. 54° (13).

Lithium, under the same conditions, formed only a small amount of red precipitate on the metal surface but no change occurred after 30 hours of reflux.

ACKNOWLEDGMENTS

REFERENCES

1. G. W. H. SCHERF and R. K. BROWN. Can. J. Chem. **38**, 697 (1960).
2. Unpublished work.
3. M. S. KHARASCH and O. REINMUT. Grignard reactions of non-metallic substances. Prentice-Hall, Inc., New York. 1954.
4. L. M. FERGUSON. J. Am. Chem. Soc. **77**, 5288 (1955).
5. J. L. DOWN, J. LEWIS, B. MOORE, and G. WILKINSON. J. Chem. Soc. 3767 (1959).
6. F. CAFASSO and B. R. SUNDHEIM. J. Chem. Phys. **31**, 809 (1959).
7. H. GILMAN and R. D. GORSICH. J. Org. Chem. **23**, 550 (1958).
8. H. NORMANT and B. ANGELLO. Bull. soc. chim. France, 354 (1960).
9. N. D. SCOTT, J. F. WALKER, and V. L. HANSLEY. J. Am. Chem. Soc. **58**, 2442 (1936).
10. S. SEARLES and M. TAMRES. J. Am. Chem. Soc. **73**, 3704 (1951).
11. G. WITTIG. Naturwiss. **30**, 696 (1942).
12. J. SCHMIDLIN and H. H. HODGSON. Ber. **41**, 435 (1908).
13. A. KLAGES and S. HEILMANN. Ber. **37**, 1455 (1904).

THE MECHANISM OF THE CARBONYL ELIMINATION REACTION OF BENZYL NITRATE

KINETIC ISOTOPE EFFECTS AND DEUTERIUM EXCHANGE[1]

Erwin Buncel[2] and A. N. Bourns

ABSTRACT

The carbonyl elimination reaction ($E_{CO}2$) of benzyl nitrate has been investigated with the object of distinguishing between the concerted and carbanion mechanisms. A deuterium exchange experiment resulted in a very small amount of deuterium pickup. The nitrogen isotope effect, k_{14}/k_{15}, associated with formation of the nitrite ion was found to be 1.0196 ±0.0007 at 30° C. The two results taken together exclude the formation of a carbanion intermediate but are consistent with a concerted mechanism.

Benzyl-α-d_2 nitrate has been prepared and the rate of its carbonyl elimination reaction compared with that of the undeuterated compound. The deuterium isotope effect was 5.04±0.25 at 60° C. The significance of the magnitude of the nitrogen and deuterium isotope effects and of their interrelationship with the Hammett reaction constant *rho* is discussed in terms of the nature of the transition state and a comparison is made with other $E2$ elimination reactions.

Nitrate esters have been extensively studied during the last decade and are the subject of a recent review article (1). Several types of reaction have been observed with nucleophilic reagents (2, 3). The reaction followed in a given system depends on the structure of the nitrate, the nature of the nucleophilic reagent, and the solvent, and often two or more of the reactions take place simultaneously.

1. Substitution on carbon:

$$RCH_2—CH_2—O—NO_2 + Y^- \longrightarrow RCH_2CH_2—Y + NO_3^-.$$

2. Substitution on nitrogen:

$$RCH_2—CH_2—O—NO_2 + Y^- \longrightarrow RCH_2CH_2O^- + Y—NO_2.$$

3. β-Hydrogen elimination:

$$RCH_2—CH_2—O—NO_2 + Y^- \longrightarrow RCH=CH_2 + NO_3^- + YH.$$

4. α-Hydrogen elimination:

$$RCH_2—CH_2—O—NO_2 + Y^- \longrightarrow RCH_2CH=O + NO_2^{\doteq} + YH.$$

The substitution reaction on carbon has been shown (2) to follow either the S_N1 or the S_N2 mechanism, the factors determining the course of reaction being analogous to those for alkyl halides. For example, in 90% ethanol the rate of reaction of *tert*-butyl nitrate is first order, being independent of the hydroxide ion concentration, while for ethyl nitrate the rate is second order, being proportional to both the nitrate and the hydroxide ion concentrations. Evidence for substitution on nitrogen (reaction 2) is based on oxygen-18 studies of the position of bond fission in the hydrolysis of *n*-butyl and *n*-octyl nitrate (4) and on stereochemical studies in the hydrolysis of optically active 2-octyl nitrate (5). This reaction differs from the others in that it results in the nitration of the base, and this property has been utilized as a synthetic method for the nitration of amines and active methylene groups (6, 7). The β-hydrogen elimination of

alkyl nitrates (reaction 3) has also been shown to proceed by the unimolecular or bimolecular mechanisms (2) and often occurs concurrently with substitution on carbon.

Whereas the first three types of reaction cited have counterparts in the reactions of carboxylic esters or alkyl halides, the α-hydrogen elimination finds no direct analogy in the reactions of these compounds. It has been named a carbonyl elimination reaction (2) and has been designated $E_{co}2$ since it always shows the characteristics of a typical bimolecular reaction, viz., a strong base is necessary to remove the α-hydrogen atom and the reaction has never been observed under solvolytic conditions. From a thorough study Baker and Heggs concluded that the $E_{co}2$ reaction is strongly facilitated by increased acidity of the eliminated hydrogen and by substituent groups which can conjugate with the forming carbonyl bond (8). The importance of these factors in determining the rates of the $E_{co}2$ reaction and the yields of aldehyde product is demonstrated by the following data, obtained in 90% aqueous ethanol at 60° C (8): ethyl nitrate, 0.2×10^{-5} l. mole^{-1} sec^{-1}, 2%; p-methylbenzyl nitrate, 3×10^{-3} l. mole^{-1} sec^{-1}, 54%; benzyl nitrate, 8×10^{-3} l. mole^{-1} sec^{-1}, 87%; and p-nitrobenzyl nitrate, 3×10^{2} l. mole^{-1} sec^{-1}, 100%. The Hammett reaction constant ρ for m- and p-substituted benzyl nitrates has the high positive value of $+3.40$.

By analogy with other elimination reactions, two mechanisms must be considered for the carbonyl elimination reaction of organic nitrates.

Concerted mechanism

$$\hspace{8cm} [1]$$

transition state
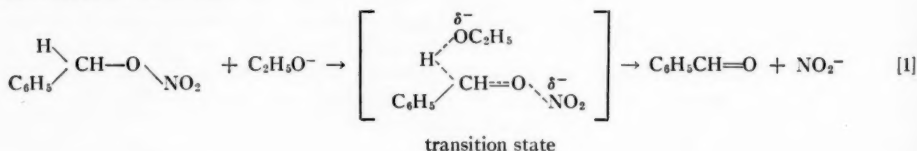
Two-step mechanism

$$\hspace{8cm} [2]$$

$$\hspace{8cm} [3]$$
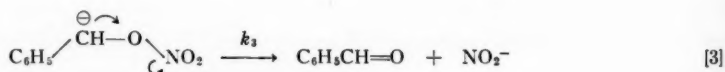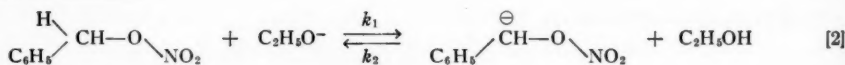
In the concerted mechanism the removal of hydrogen by base is synchronous with formation of the carbon–oxygen double bond and separation of nitrite ion. This is analogous to the $E2$ mechanism observed in olefin-forming eliminations of alkyl halides, ammonium and sulphonium salts (9). The alternative possibility is a two-step process in which the base first removes the hydrogen to form a carbanion intermediate which subsequently eliminates the nitrite ion with formation of aldehyde. This corresponds to the $E1cb$ mechanism suggested by Ingold as a possible path in olefin-forming eliminations, and may be designated $E_{co}1cb$ (8). Cristol has proposed that the $E1cb$ mechanism does indeed occur in cyclic systems where the eliminated groups have cis orientations (10, 11).

The carbonyl elimination reaction is one in which the carbanion mechanism is expected to be "inherently probable" (8), and a particularly favorable system should be that of

benzyl nitrate. The high positive value for the Hammett reaction constant ρ, $+3.40$, obtained for m- and p-substituted benzyl nitrates, and the fact that the σ^* value (12) for the para-nitro group must be used for a linear relationship to hold between log k and σ clearly show that the transition state of the reaction has a high degree of carbanion character. Further, the strongly electron-attracting nitrate group will have an appreciable effect on the acidity of the eliminated hydrogen, and this would be expected to promote reaction by a carbanion mechanism.[3]

The present investigation was undertaken with the object of establishing which of the two possible mechanisms, the concerted or the two-step, is being followed in the carbonyl elimination reaction of benzyl nitrate.

Deuterium Exchange Test

An established method for detecting a carbanion intermediate in an elimination reaction is the deuterium exchange test of Skell and Hauser (14). The reaction between substrate and base is carried out in hydroxyl-deuterated solvent (the solvent being the conjugate acid of the base) to partial completion and the unreacted substrate is isolated and examined for its deuterium content. If a true carbanion intermediate is present then the reverse of the first stage will result in deuterium pickup by the substrate.

An appreciable pickup of deuterium by the substrate would unquestionably prove that a carbanion intermediate is formed. The absence of deuterium pickup, however, would not necessarily exclude the intervention of a carbanion intermediate, since the rate at which the carbanion decomposes to product could be so much greater than its rate of return to reactant by combination with solvent (i.e., $k_3 \gg k_2$) as to preclude the observation of deuterium in the recovered substrate by the available experimental methods.

A deuterium exchange test was carried out with benzyl nitrate and ethoxide ion in anhydrous 99% ethanol-1-d. The reaction was interrupted at about 40% completion by the addition of p-toluenesulphonic acid. The unchanged benzyl nitrate was recovered and purified by fractional distillation. It was analyzed for deuterium by combustion to water and measurement of the O–D absorption at 2500 cm^{-1} (15). The purest sample of benzyl nitrate isolated, as judged by the identity of its infrared spectrum with authentic benzyl nitrate, analyzed for a deuterium content of 0.007 ± 0.003 atom% excess of deuterium. The significance of such a small deuterium content is open to more than one explanation. It could result from the actual presence of $C_6H_5CHDONO_2$ (0.05 mole% excess) formed by the reaction of a carbanion intermediate with deutero-ethanol. In this case the observed deuterium enrichment would require that for every one carbanion that reverts to reactant 1200 decompose to product (see Experimental), i.e., $k_3/k_2 = 1200$, where k_3 includes the concentration of solvent deutero-ethanol.[4] An alternative explanation, however, is that this very small deuterium enrichment is caused by the presence of some deuterium-containing contaminant.[5]

In past studies of elimination reactions the interpretation given to the observation of a very small deuterium enrichment in the recovered reactant has varied. Some workers

[3]*Cristol found that in a cis dehydrochlorination the replacement of a chlorine substituent by the strongly electron-attracting p-toluenesulphonyl group increased the rate of reaction by a factor of about 10^{10} (13).*

[4]*Because of a possible isotope effect associated with the reaction of deutero-ethanol with carbanion, the k_3/k_2 ratio in undeuterated ethanol may differ somewhat from this figure (16).*

[5]*Some enrichment will undoubtedly arise from a kinetic isotope effect involving the reactant, which originally has the natural isotopic abundance of deuterium. It can be shown, however, that this factor could account for no more than a quarter of the observed enrichment.*

have taken the result to mean the absence of exchange and have inferred that a concerted mechanism is being followed (14), while others have concluded that the enrichment is evidence in support of a carbanion intermediate (10).

Kinetic Nitrogen Isotope Effect

In previous applications of the deuterium exchange test the ambiguity presented by an apparent very small deuterium pickup could not be resolved. It has been possible to resolve this problem in the present reaction system by an evaluation of the kinetic nitrogen isotope effect. In the concerted process (equation [1]) the $O—NO_2$ bond is broken in the rate-determining step and this should result in a nitrogen isotope effect of considerable magnitude, i.e., of the order of 1–3% (vide infra). In the carbanion mechanism with $k_3 \gg k_2$, which is the only possibility for a carbanion mechanism permitted by the results of the deuterium study, the rate-determining step is the formation of the carbanion in which the bonds associated with nitrogen are still intact. In this case there should be no nitrogen isotope effect, or at the most an isotope effect of a few tenths of a per cent.

A kinetic nitrogen isotope effect study was undertaken with benzyl nitrate of normal isotopic composition. The procedure consisted of allowing reaction between benzyl nitrate and ethoxide ion to proceed to 10% completion and comparing the nitrogen isotopic composition of the formed nitrite ion with that of the starting benzyl nitrate. Since a simultaneous substitution reaction results in displacement of nitrate ion, a separation of the nitrate ion formed in the carbonyl elimination reaction was required.[6] This separation was achieved by selective reduction of the nitrite and nitrate ion to ammonia (17). The ammonia was subsequently oxidized to nitrogen (18), which was analyzed by mass spectrometry. The total nitrite and nitrate ion obtained from the 100% reaction was similarly converted to nitrogen and analyzed by mass spectrometry. The results of these experiments are shown in Table I.

TABLE I

N^{14}/N^{15} ratios in $E_{CO}2$ reaction of benzyl nitrate at 30° C

Expt. No.	Extent of reaction	N^{14}/N^{15}	
		$NO_2^- + NO_3^-$	NO_2^-
1	100	265.58	
2	100	265.78	
3	100	265.46	
4	100	265.66	
5	100	265.62	
6	10		270.52
7	10		270.54
8	10		270.66
9	10		270.42
10	10		270.74
Mean N^{14}/N^{15} ratios*		$265.62 \pm .12$	$270.58 \pm .12$

*The limits shown are the standard deviations.

The kinetic isotope effect, calculated from these isotopic ratios and the known extent of reaction (19), is

$$k^{14}/k^{15} = 1.0196 \pm 0.0007.$$

[6]Experiments using nitrogen-15 enriched nitrate ion established the absence of isotopic exchange between nitrite and nitrate ions under the reaction conditions and in the subsequent separation procedure. Details of this work will be published elsewhere.

This isotope effect, which is one of the largest observed for nitrogen in a rate process unequivocally establishes that the O—N bond is undergoing rupture in the rate-determining step. Since the observation of no significant deuterium exchange has ruled out a carbanion mechanism in which the step involving O—N bond rupture is rate determining, it follows that only a concerted process is consistent with the results of both the nitrogen isotope effect and the deuterium exchange studies.

Although the results of this investigation clearly exclude the carbanion mechanism for the reaction of benzyl nitrate the possibility still exists for reaction by this mechanism with reactants in which structural features would provide greater stability to a carbanion. Systems of this type are under investigation.

It was convenient to determine the nitrogen isotope effect in the competing substitution reaction forming nitrate ion since this had been converted to ammonia in the process of separating it from the elimination product. The isotopic ratio for the nitrogen of nitrate ion (combined products of experiments 6–10) was 265.52, which is identical, within the limit of measurement, with the mean value obtained for the product of 100% reaction. This observation of a zero isotope effect is consistent with a nucleophilic substitution of ethoxide ion on carbon with displacement of nitrate ion.

Hydrogen–Deuterium Isotope Effect

To gain greater insight into the nature of the transition state of the carbonyl elimination reaction the hydrogen–deuterium isotope effect for the reaction has also been determined. This was measured by separately evaluating the specific reaction constants for $C_6H_5CH_2ONO_2$ and $C_6H_5CD_2ONO_2$. Benzyl-α-d_2 nitrate was prepared by the lithium aluminum deuteride reduction of ethyl benzoate to benzyl-α-d_2 alcohol which was converted to benzyl-α-d_2 chloride and to benzyl-α-d_2 nitrate by usual procedures. The kinetics were conducted in anhydrous ethanol. The total rate was followed by acid–base titration and the rate constants for the carbonyl elimination reaction, $k_{E_{CO}2}$, and for the substitution reaction, $k_{S_{N}2}$, were evaluated from the relative yields of nitrite and nitrate ions. These yields remained constant throughout the reaction, demonstrating that the two ions were formed by reactions of the same kinetic order. The rate data are shown in Table II. It is seen that the carbonyl elimination reaction shows an isotope effect of 5.0 at 60° C. From the data given in Table II one may also calculate a k_H/k_D

TABLE II
Hydrogen–deuterium isotope effect at 60.2° C

	$C_6H_5CH_2ONO_2$	$C_6H_5CD_2ONO_2$
% $E_{CO}2$	88.7	64.4
% S_N2	11.3	35.6
$10^3 k_{total}$*	13.9	3.79
$10^3 k_{E_{CO}2}$	12.3	2.44
$10^3 k_{S_{N}2}$	1.57	1.35
	$(k_H/k_D)_{E_{CO}2} = (12.3/2.44) = 5.04 \pm 0.25$†	

*k in l. mole⁻¹ sec⁻¹.
†Estimated uncertainty based upon variation in yields of nitrite ion and rate constant values.

ratio of 1.16 for the substitution reaction. No significance, however, is attached to the difference between this value and unity because of the rather large percentage error in the determination of the small amount of nitrate ion.

Nature of the Transition State in the $E_{CO}2$ Reaction

Information concerning charge distribution and extent of bond rupture in the **transition** state of a bimolecular elimination reaction of the type

$$Z-C_6H_4-\underset{\underset{H}{|}}{C}H-Y-X \xrightarrow{B^-} \left[\overset{\delta^-}{\underbrace{Z=C_6H_4}} \overset{\delta^-}{=\underset{\underset{\underset{B}{\overset{\delta^-}{\diagup}}}{\overset{}{\vert}}}{C}H=Y}\overset{\delta^-}{\diagdown} X \right] \rightarrow Z-C_6H_4CH=Y + BH + X^- \quad [4]$$

<center>transition state</center>
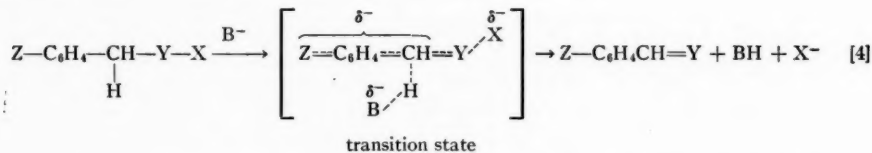
is provided by three quantities: (*a*) the deuterium isotope effect, (*b*) the isotope effect associated with the leaving group X, and (*c*) the Hammett ρ value. A large k_H/k_D value implies a large degree of carbon–hydrogen bond stretching with the release to the rest of the molecule of the electron pair associated with this bond. The resulting negative charge may reside largely on the carbon atom and its attached aryl group, in which case the transition state may be described as having a high degree of carbanion character and the reaction will be characterized by a large positive Hammett ρ, or the charge may reside in part or in whole on the leaving group X. Other factors being equal, the greater the extent to which this charge is accommodated in the transition state by the leaving group the more highly concerted the reaction, the larger the isotope effect associated with X, and the smaller the ρ value.

The k_H/k_D value of 5.0 at 60° C for the $E_{CO}2$ reaction of benzyl nitrate (X = NO$_2$, Y = O, and Z = H in equation [4]) is large, being only slightly smaller than that calculated (ca. 5.6) for the complete loss of the carbon–hydrogen bond stretching frequency in the transition state (16). The ρ value, +3.4, for the $E_{CO}2$ reaction of substituted benzyl nitrates is large also; indeed, it is larger than the ρ values observed in other bimolecular elimination reactions involving ethoxide ion (20), and is one of the largest found for a rate process (12). To a considerable extent, then, the negative charge which is developed as a result of the large carbon–hydrogen bond stretching resides on the benzyl carbon, and the transition state, therefore, may be described as having a high degree of carbanion character.

That the oxygen–nitrogen bond is also considerably weakened in the transition state of the $E_{CO}2$ reaction of benzyl nitrate is evident from the magnitude of the nitrogen isotope effect, 2.0% at 30° C. Although this value is considerably smaller than the 3.8%[7] calculated on the assumption of complete oxygen–nitrogen bond rupture in the transition state, it is significantly greater than the nitrogen isotope effect of 1.3% found in this laboratory (24) for the E2 Hofmann elimination reaction of β-phenylethyltri-methylammonium bromide (X = $\overset{+}{N}(CH_3)_3$, Y = CH$_2$, and Z = H in equation [4]) with ethoxide ion at the same temperature. Since the deuterium effect is also larger, 5.0 at 60° C compared with 3.0 at 50° C observed by Saunders for the Hofmann reaction (25), it would appear that rupture of both C—H and Y—X bonds is more fully developed in the transition state of the carbonyl elimination reaction. On the other hand, the transition state for the $E_{CO}2$ reaction must have considerably more carbanion character than that of the bimolecular elimination with ethoxide ion of the structurally related β-phenylethyl bromide (X = Br, Y = CH$_2$, and Z = H in equation [4]). The deuterium

---

[7]*This value is obtained from the Bigeleisen expression (21) using 860.6 cm^{-1} for the stretching vibration of the O—NO$_2$ bond (22) in evaluating the free-energy term and the Slater theorem for the effective mass term. Using the mass fragment method of evaluating the mass term (23), the calculated effect is 2.8%.*

isotope effect for this dehydrobromination reaction has the abnormally large value of 7.1 at 30° C (25), while the ρ value for the reaction of substituted β-phenylethyl bromides is only +2.18 (20), compared with the +3.4 found for the $E_{\mathrm{CO}}2$ reaction of the benzyl nitrates. More of the negative charge developed in the transition state must, therefore, reside on the bromine atom in the halide reaction than on the nitro group in the carbonyl elimination, and carbon–bromine bond rupture must have progressed further than oxygen–nitrogen bond rupture.

From these considerations it would appear that with respect to the extent to which bonds have been weakened, the transition state for the carbonyl elimination of benzyl nitrate is intermediate between the transition states for the $E2$ reaction of β-phenylethyltrimethylammonium ion and of β-phenylethylbromide.

EXPERIMENTAL

Materials

Benzyl nitrate.—This was prepared from benzyl chloride and silver nitrate in aceto-nitrile (26). The product, purified by fractional distillation from silver nitrate and calcium carbonate, was obtained in 75% yield (b.p. 45°/0.5 mm, n_{D}^{20} 1.5209).

Benzyl-α-d_2 nitrate.—The steps involved in the synthesis of benzyl-α-d_2 nitrate were: (1) reduction of ethyl benzoate to benzyl-α-d_2 alcohol with lithium aluminum deuteride; (2) conversion of benzyl-α-d_2 alcohol to benzyl-α-d_2 chloride with zinc chloride and hydrochloric acid; and (3) reaction of benzyl-α-d_2 chloride with silver nitrate in aceto-nitrile. The over-all yield of benzyl-α-d_2 nitrate (b.p. 45°/0.5 mm, n_{D}^{20} 1.5203) was 62%. A N.M.R. analysis[8] showed that the product was 99% $C_6H_5CD_2ONO_2$.

Benzyl-α-d_2 alcohol.—Ethyl benzoate (28.5 g, 0.190 mole) was reacted for 4 hours with lithium aluminum deuteride (3.94 g, 0.099 mole) in 400 ml ether which had been dis-tilled from lithium aluminum hydride, and the complex was then decomposed with 10% sulphuric acid. The product, recovered by ether extraction, was treated with aqueous alcoholic sodium hydroxide to hydrolyze any unreacted ethyl benzoate. After removal of ethanol and extraction with ether, distillation yielded benzyl-α-d_2 alcohol (b.p. 76°/5 mm, n_{D}^{20} 1.5398) in 84% yield.

Benzyl-α-d_2 chloride.—Benzyl-α-d_2 alcohol (17.4 g, 0.158 mole) was added during 1 hour to 77 g of a stirred solution of hydrochloric acid and zinc chloride (Lucas' reagent (27)) at 0° C. Stirring was continued for 1 hour at 0° C and 2 hours at room temperature. The reaction mixture separated into two layers and was extracted with a 1:1 mixture of ether and petroleum ether. Distillation yielded benzyl-α-d_2 chloride (b.p. 64°/12 mm) in 86% yield.

Deuterium Exchange Experiment

Ethanol-1-d was prepared by the action of 99.4% deuterium oxide on sodium ethoxide, prepared from molecular sodium (28) under strictly anhydrous conditions in a nitrogen atmosphere. The product was shown by N.M.R.[8] to be at least 99% deuterated on the hydroxyl group. A solution of sodium ethoxide in the deutero-ethanol (ca. 0.5 M) was prepared by dissolution of sodium metal and was standardized by titration with acid. Fifty milliliters of the ethoxide solution was added to an equimolar quantity of benzyl nitrate and reaction was allowed to proceed at 30° C to an appropriate extent of com-pletion when it was quenched by addition of p-toluenesulphonic acid. Solvent was removed under reduced pressure and the residue was taken up in ether and washed

---

[8]*N.M.R. analyses were performed by Dr. R. J. Gillespie.*

with ice-cold water. The extent of reaction was determined by an acid–base titration of the aqueous washings. The ethereal solution was evaporated and treated with three 25-ml quantities of methanol, each of which was removed by distillation through a Vigreux column. The purpose of this methanol treatment was to remove last traces of deutero-ethanol and to exchange any hydroxyl-deuterated benzyl alcohol which may have been formed by hydrolysis following the quenching. The product of this treatment was fractionally distilled through a 15-cm tantalum spiral column. Deuterium analysis was carried out by combustion of the recovered benzyl nitrate and measurement of the O—D absorption at 2500 cm^{-1} in the water formed (15).

In the first exchange experiment, carried to 44% completion, two fractions of benzyl nitrate were collected, both of which showed some contamination with benzaldehyde, as shown by a carbonyl absorption in the infrared spectra, although the higher boiling fraction was the purer. The analysis results for the two fractions were 0.029±0.006 and 0.015±0.003 atom% excess deuterium, respectively. In a second exchange experiment, carried to 37% completion, the recovered material was more carefully purified and a fraction which was almost completely carbonyl-free was obtained. This fraction was found to contain 0.007±0.003 atom% excess deuterium.

On the basis of the carbanion intermediate mechanism one can calculate the k_3/k_2 ratio corresponding to a deuterium pickup of 0.007 atom%. Assuming that only one hydrogen in the benzyl nitrate exchanges, the following can be derived from equations [2] and [3]. (The rate constant for the reverse step in equation [2] will here also be denoted by k_2 even though it now applies to the reaction of carbanion with deutero-ethanol.)

$$\frac{d}{dt}[C_6H_5CHDONO_2] = k_2[C_6H_5\overset{\ominus}{C}HONO_2][C_2H_5OD] \qquad [5]$$

$$\frac{d}{dt}[\text{product}] = k_3[C_6H_5\overset{\ominus}{C}HONO_2] \qquad [6]$$

Dividing equations [5] and [6] and integrating one obtains

$$\frac{[C_6H_5CHDONO_2]}{[C_6H_5CHDONO_2]+[C_6H_5CH_2ONO_2]} = \frac{k_2[C_2H_5OD]}{k_3} \qquad [7]$$

$$\times \frac{[\text{product}]}{[C_6H_5CHDONO_2]+[C_6H_5CH_2ONO_2]}.$$

Substituting $[(0.007 \times 7)/100] = 0.00049$ for the mole fraction excess of $C_6H_5CHDONO_2$ in the benzyl nitrate recovered after 37% reaction, it follows that

$$\frac{k_3}{k_2[C_2H_5OD]} = \frac{37}{63 \times 0.00049} = 1200.$$

Kinetic Measurements with $C_6H_5CH_2ONO_2$ *and* $C_6H_5CD_2ONO_2$

A solution of benzyl nitrate (0.04–0.05 M) and sodium ethoxide (0.05–0.08 M) in anhydrous ethanol was prepared by the addition of standard sodium ethoxide solution to a weighed amount of the nitrate and was maintained in a constant temperature bath to ±0.03° C. At suitable intervals of time aliquots of 2 ml each were removed and added to 15 ml of ice-cold water for quenching the reaction. Following titration with standard acid the unreacted nitrate ester was extracted with petroleum ether. The aqueous extract was analyzed for nitrite and nitrate ions by a modification of the method described by Varner *et al.* (17). This method is based on the differential rates of reduction

of nitrite and nitrate to ammonia. While nitrite ion is rapidly reduced by ferrous hydroxide alone, the presence of a silver ion catalyst is required for the reduction of nitrate ion.

The solution containing nitrite and nitrate was placed in a Kjeldahl-type distillation apparatus constructed with a double splash-head. A 40% aqueous sodium hydroxide solution (15 ml) was added and steam was passed through until all the ethanol had distilled over. This initial removal of ethanol was found to be necessary for quantitative reduction. A 20% aqueous solution of ferrous sulphate (5 ml) was added and steam distillation continued for 3 minutes during which time the nitrite ion was reduced to ammonia which was collected in 5% boric acid solution. The nitrate ion was then reduced on the addition of a saturated silver sulphate solution (5 ml) and the ammonia formed was distilled during 5 minutes into a fresh receiver containing boric acid solution. The ammonia from the reductions was titrated with $0.01\ N$ sulphuric acid using methyl red – methylene blue indicator. A complete analysis involving the reduction of both nitrite and nitrate was performed without interruption of steam distillation.

The over-all rate constant for the reaction was calculated from the usual second-order plot using the data from the acid–base titrations. At least two kinetic runs were performed with each compound at a given temperature, and rate constants agreed within $\pm 2\%$. The nitrite and nitrate analyses were performed for at least five points in each kinetic run. The yields of nitrite and nitrate ion were reproducible within $\pm 1\%$ absolute and the mean values were used to calculate the rate constants of the component $E_{Co}2$ and S_N2 reactions.

Nitrogen Isotope Effect

The kinetic nitrogen isotope effect in the $E_{Co}2$ reaction was obtained by comparing the nitrogen isotopic abundance in the nitrite ion formed in reactions carried out to some small known extent of completion with the isotopic abundance in the starting compound. The latter was obtained by measuring the isotopic abundance in the combined nitrite and nitrate ion product formed in reactions allowed to proceed to completion.

Benzyl nitrate ($0.05\ M$) and sodium ethoxide ($0.05\ M$) in 50 ml of anhydrous ethanol were allowed to react at $30°$ C for a length of time corresponding to 10% reaction. The solution was then added to a mixture of ice-cold petroleum ether and $0.1\ N$ aqueous sodium bicarbonate (5% excess over the remaining ethoxide) and the two layers were separated. The bicarbonate served to neutralize excess ethoxide which otherwise would react with the small amount of benzyl nitrate not removed in the petroleum ether. (Neutralization with $0.1\ N$ sulphuric acid resulted in some loss of nitrite and nitrate ion, possibly by reaction of nitrous acid with ethanol.) The aqueous ethanol solution was concentrated to a small volume on a rotary evaporator and the last trace of benzyl nitrate was extracted with petroleum ether. Nitrite and nitrate ion were separately reduced, following the procedure described in the previous section, and the ammonia absorbed in $0.01\ N$ sulphuric acid. The extent of reaction was calculated from the total yield of ammonia obtained in the reductions. The solution of ammonium sulphate obtained from the reduction of nitrite ion was concentrated to about 3 ml and transferred to a high-vacuum system where it was oxidized by means of sodium hypobromite solution (18) to nitrogen gas for mass spectrometric analysis. The nitrogen was purified by continuous circulation over copper and copper oxide, both at $750°$ C, and through a trap cooled in liquid nitrogen.[9] Sufficient ammonium sulphate was present to give on oxidation 2 ml of nitrogen at atmospheric pressure.

[9]*Details of the purification procedure will appear in a subsequent publication.*

Since the amount of nitrogen which would be formed from the nitrate ion produced in a single experiment would be much too small for mass spectrometric analysis, the ammonium sulphate solutions from all the nitrate ion reductions were combined and oxidized to give a single nitrogen sample for analysis.

The nitrogen isotopic abundance in the starting benzyl nitrate was determined as follows. Benzyl nitrate (0.04–0.05 M) was completely hydrolyzed by sodium ethoxide (0.05–0.10 M) in anhydrous ethanol at 60° C. An aliquot of 5 ml was then removed and the nitrite and nitrate reduced to ammonia by the method described in the section on Kinetic Measurements, except that no titration of ethoxide was performed and the ammonia from nitrite and nitrate was collected in the same acid solution. The ammonium sulphate solution was oxidized to nitrogen and the latter was measured mass spectrometrically as described previously. From two separate reactions carried out to completion a total of five nitrogen samples was prepared.

The mass spectrometric analysis was carried out using a 90° sector type instrument, similar to the one described by Wanless and Thode (29). It was capable of measuring *relative* isotopic abundance ratios, $N^{14} - N^{14}/N^{14} - N^{15}$, to ±0.02%.

The kinetic isotope effect was calculated from the expression (19)

$$k_{14}/k_{15} = \frac{\ln(1-f)}{\ln(1-rf)}$$

where

$$r = \frac{(N^{14}/N^{15})_{\text{reactant}}}{(N^{14}/N^{15})_{NO_2^-}}$$

and $f = 0.09$, the mole fraction of reactant which has undergone decomposition to nitrite ion.[10]

REFERENCES

1. R. Boschan, R. T. Merrow, and R. W. Van Dolah. Chem. Revs. **55**, 485 (1955).
2. J. W. Baker and D. M. Easty. J. Chem. Soc. 1193, 1208 (1952).
3. G. W. H. Cheeseman. J. Chem. Soc. 115 (1957).
4. M. Anbar, I. Dostrovsky, D. Samuel, and A. D. Yoffe. J. Chem. Soc. 3603 (1954).
5. S. J. Cristol, B. Franzus, and A. Shadan. J. Am. Chem. Soc. **77**, 2512 (1955).
6. W. D. Emmons and J. P. Freeman. J. Am. Chem. Soc. **77**, 4387, 4391 (1955).
7. H. Feuer and C. Savides. J. Am. Chem. Soc. **81**, 5826 (1959).
8. J. W. Baker and T. G. Heggs. J. Chem. Soc. 616 (1955).
9. C. K. Ingold. Structure and mechanism in organic chemistry. Cornell University Press, Ithaca, N.Y. 1953. Chap. VIII.
10. S. J. Cristol and D. D. Fix. J. Am. Chem. Soc. **75**, 2647 (1953).
11. S. J. Cristol and E. F. Hoegger. J. Am. Chem. Soc. **79**, 3438 (1957).
12. H. H. Jaffé. Chem. Revs. **53**, 191 (1953).
13. S. J. Cristol and R. P. Arganbright. J. Am. Chem. Soc. **79**, 3441 (1957).
14. P. S. Skell and C. R. Hauser. J. Am. Chem. Soc. **67**, 1661 (1945).
15. N. R. Jones and M. A. MacKenzie. Talanta, **3**, 356 (1960).
16. K. B. Wiberg. Chem. Revs. **55**, 713 (1955).
17. J. E. Varner, W. A. Bulen, S. Vanecko, and R. C. Burrell. Anal. Chem. **25**, 1528 (1953).
18. D. Rittenberg. *In* Preparation and measurement of isotopic tracers. J. W. Edwards. Ann Arbor, Michigan. 1946. p. 31.
19. W. H. Stevens and R. W. Attree. Can. J. Research, B, **27**, 807 (1949).
20. C. H. DePuy and C. A. Bishop. J. Am. Chem. Soc. **82**, 2532 (1960).
21. J. Bigeleisen. J. Chem. Phys. **17**, 675 (1949).
22. J. F. Brown. J. Am. Chem. Soc. **77**, 6341 (1955).
23. J. Bigeleisen and M. Wolfsberg. Advances in Chem. Phys. **1**, 15 (1958).
24. G. Ayrey. Private communication.
25. W. H. Saunders and D. H. Edison. J. Am. Chem. Soc. **82**, 138 (1960).
26. A. F. Ferris, K. W. McLean, I. G. Marks, and W. D. Emmons. J. Am. Chem. Soc. **75**, 4078 (1953).
27. A. I. Vogel. Practical organic chemistry. 3rd ed. Longmans, Toronto. 1956. p. 261.
28. A. I. Vogel. Practical organic chemistry. 3rd ed. Longmans, Toronto. 1956. p. 193.
29. R. K. Wanless and H. G. Thode. J. Sci. Instr. **30**, 395 (1953).

[10]*The error introduced by neglecting in the calculation of the isotope effect the 0.01 mole fraction of reactant which has produced nitrate ion without isotopic fractionation is insignificantly small.*

LES SPECTRES INFRAROUGES DE L'ACIDE SULFURIQUE ET DES OLÉUMS[1]

PAUL A. GIGUÈRE ET RODRIGUE SAVOIE

RÉSUMÉ

On a mesuré les spectres infrarouges, entre 2 et 30 μ, de l'acide sulfurique et de ses solutions aqueuses à diverses concentrations de même que celui de l'acide deutéré, D_2SO_4. On a aussi mesuré à l'état solide les spectres de l'acide pur et de ses hydrates à une, deux et quatre molécules d'eau. Les fréquences observées ont pu être attribuées aux différents modes de vibration de la molécule H_2SO_4. Les résultats confirment et complètent ceux déjà obtenus par d'autres méthodes quant à la nature et l'abondance relative des diverses espèces ioniques (y compris H_3O^+) et moléculaires présentes dans ces solutions. En particulier, on a vérifié l'auto-dissociation de H_2SO_4 pur et l'ionisation incomplète de l'eau, même dans l'acide très concentré. Enfin on a étudié de la même façon les spectres des oléums contenant jusqu'à 70% de l'anhydride SO_3. En augmentant la concentration de ce dernier, on voit apparaître graduellement les bandes de $H_2S_2O_7$, $H_2S_2O_{10}$ et enfin SO_3.

INTRODUCTION

Les spectres moléculaires de l'acide sulfurique et de ses solutions offrent un intérêt particulier en ce qu'ils permettent d'identifier les diverses espèces, ioniques et autres, présentes dans ces systèmes relativement complexes. D'autres méthodes physico-chimiques, surtout colligatives et partant moins sélectives, en particulier la conductivité électrique, la cryoscopie (voir les importants travaux de Gillespie, dans la revue récente (1)), la calorimétrie (2) et la résonance nucléo-magnétique (3), ont déjà servi à élucider la question. Quant aux spectres, seul l'effet Raman avait été étudié jusqu'ici surtout par Chédin (4) et plus récemment par Millen (5) et Young (6). Dans l'infrarouge, le caractère extrêmement corrosif et la grande absorptivité des solutions d'acide sulfurique présentaient des difficultés qui n'ont pu être surmontées que dernièrement grâce à l'invention du chlorure d'argent de qualité optique. C'est par ce moyen que Marcus et Fresco (7) ont obtenu un premier spectre infrarouge de l'acide pur au cours d'un travail sur les mélanges nitrifiants, et que dans ce laboratoire nous avons précédemment étudié les solutions diluées d'acide sulfurique (8) afin de mettre en évidence le spectre de l'ion H_3O^+. Il nous a semblé utile de compléter ce travail par une analyse systématique des spectres infrarouges de l'acide liquide et de ses solutions aqueuses, de même que ceux des hydrates à une, deux et quatre molécules d'eau à l'état solide. Comme prolongement naturel de ce travail nous avons été conduits à mesurer pour la première fois l'absorption infrarouge des oléums à des concentrations allant jusqu'à 70%. Rappelons que par convention le titre $X\%$ d'un oléum signifie une composition pondérale de X parties d'anhydride sulfurique SO_3 et $(100-X)$ parties d'acide sulfurique pur.

MÉTHODE EXPÉRIMENTALE

Pour l'étude des spectres entre 3500 et 500 cm^{-1} on préparait les échantillons simplement en pressant une goutte de solution de concentration appropriée entre deux disques de chlorure d'argent fraîchement polis au moyen d'une grande lime douce trempée dans l'eau. L'épaisseur des films ainsi obtenus est évaluée à quelque 10 μ d'après la quantité d'acide employée et la surface recouverte. Comme le chlorure d'argent commence à absorber vers 500 cm^{-1}, il a fallu utiliser du côté des basses fréquences des plaques d'iodure de césium protégées par un mince film de polyéthylène. En effet, ce matériau est à la

fois résistant à l'acide sulfurique et assez transparent dans l'infrarouge moyen, sauf pour une forte bande d'absorption vers 730 cm^{-1}; par contre il s'est révélé inutilisable avec les oléums. Il en fut de même du Teflon qui, bien que non attaqué par le liquide, semblait perméable aux vapeurs corrosives. En fait, aucun des matériaux couramment utilisés pour l'infrarouge n'a permis d'observer les spectres d'absorption des oléums dans la région des basses fréquences au delà de 450 cm^{-1}.

Pour l'étude des solides, on s'est servi d'une cellule de type conventionnel (9) dans laquelle les films de liquide pressé entre deux plaques de chlorure d'argent étaient refroidis, sous vide, à l'aide de mélanges d'acétone et de neige carbonique. Après une première solidification du film, on laissait remonter la température (mesurée avec un thermocouple) jusqu'à 4° ou 5° au-dessous du point de fusion de l'hydrate en question; puis on refroidissait de nouveau, et très lentement. Cette opération était répétée plusieurs fois afin d'obtenir un solide cristallin et non pas vitreux. Toutefois, si l'on en juge par l'allure des bandes, il n'est pas certain que ce but ait été atteint entièrement.

L'acide sulfurique commercial (96%) fut employé tel quel, soit pur, soit additionné d'eau distillée ou d'oléum à 23% suivant le cas. Ce dernier (General Chemical Co.) était d'abord distillé dans un appareil en Pyrex assemblé par rodages et comprenant une colonne Vigreux mais sans réfrigérant. Pour obtenir des concentrations supérieures à 23%, on faisait barboter à froid dans cet oléum des vapeurs provenant de la distillation d'un autre échantillon du même oléum. De cette façon, on a pu atteindre progressivement un titre de quelque 70%. Tous les échantillons étudiés au cours de ce travail étaient liquides à température ordinaire, sauf celui à 28.5% qui cristallisa partiellement au bout de quelques semaines. Une étude préliminaire de l'absorption infrarouge des vapeurs blanches dégagées par les oléums a montré les bandes de l'acide sulfurique et celles, beaucoup plus faibles, de l'anhydride SO_3. Le titre des oléums fut déterminé par alcalimétrie selon la méthode usuelle. L'échantillon de D_2SO_4 fut obtenu en faisant absorber très lentement dans un peu d'eau lourde (à 99% de D_2O), refroidie dans la glace, des vapeurs d'anhydride sulfurique provenant de la distillation d'oléum commercial. Par titrations et dilutions successives, on a réussi à atteindre exactement la concentration $100 \pm 0.2\%$ de D_2SO_4.

Pour enregistrer les spectres, on s'est servi alternativement d'un spectrophotomètre Beckman (modèle IR-4) à double faisceau, et d'un appareil Perkin–Elmer (modèle 112-C) avec prismes de chlorure de sodium et de bromure de césium. Afin de diminuer l'absorption par le gaz carbonique et l'humidité, on faisait circuler un courant d'azote sec à travers l'appareil avant et pendant les mesures.

DISCUSSION DES RÉSULTATS

Les fréquences au maximum des diverses bandes d'absorption sont énumérées dans les Tableaux I, II, III et IV; quelques spectres infrarouges sont reproduits dans les Figures 1 et 2. Pour faciliter la discussion, on considérera successivement les solutions aqueuses, l'acide sulfurique pur, les hydrates solides et enfin les oléums.

(A) Les solutions liquides

Dans les solutions diluées l'espèce moléculaire la plus abondante H_2O cause une forte absorption dans les régions de 3400 cm^{-1} (ν_3), 1650 cm^{-1} (ν_2) et 730 cm^{-1} (ν_R). Les deux premières sont encore nettement visibles dans les solutions à environ 80% (Fig. 1, A); c'est là une confirmation directe de la déduction de Gillespie (10), basée sur des données cryoscopiques, à l'effet que l'ionisation de l'eau est incomplète dans l'acide sulfurique même aux fortes concentrations. Fait remarquable, l'addition de H_2SO_4 affecte à peine

la fréquence de libration ν_R de l'eau, contrairement aux électrolytes du type KCl qui l'abaissent considérablement (8). La différence vient de ce que ces électrolytes affaiblissent la structure de l'eau liquide en diminuant le nombre de liaisons hydrogène. Dans
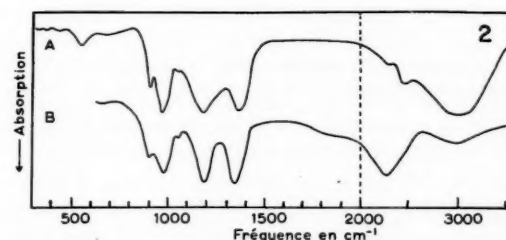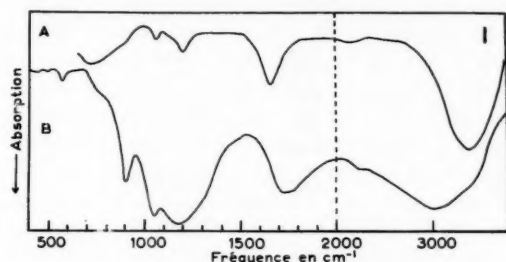
Fig. 1.   Spectres infrarouges des solutions aqueuses d'acide sulfurique. (A) 8.5% H_2SO_4; (B) 78.5% H_2SO_4.
Fig. 2.   Spectre d'absorption infrarouge de l'acide sulfurique (A) et deutérosulfurique (B).

TABLEAU I

Fréquences (en cm^{-1}) des bandes d'absorption dans les spectres infrarouges de l'acide sulfurique et de ses solutions aqueuses

8.5%	25.5%	46%	78.5%	90.5%	95.5%	100% H_2SO_4
—	—	—	—	332	332	332 f
—	—	—	—	372	372	372 f
—	—	—	—	420	420	420 f
445	445	442	444 f	—	—	—
500	500	500	500 f	—	—	—
—	—	—	549	549	549	549 F
584	584	584	584 F	584	584	—
—	—	—	—	(675)	(675)	675 ff
720 m	720 mf	—	—	—	—	—
—	—	—	740 f	735 f	740 f	?
890 ff	890 m	895 m	907 F	907 F	907 F	907 F
—	—	—	967 ff	966 F	967 F	967 FF
1052 f	1052 F	1050 FF	1050 FF	1052 m	1052 m	1050 f
1100 ff	—	—	—	—	—	—
—	—	—	1155 f	1160 m	1165 m	1170 FF
1205 m	1195 F	1192 FF	1190 FF	(1190)	(1190)	—
—	—	?	?	?	(1240)	(1240)
—	(1350)	(1350)	(1350)	1355 F	1365 F	1368 FF
1655 F	1650 F	1655 m	1650 ff	—	—	—
(1750)	1750 f	1750 m	1740 F	(1710)	(1700)	—
2150 ff	—	—	2250 f	2225 m	2250 m	2250 f
—	—	2450 ff	2450 ff	2450 f	2450 m	2450 m
—	—	(2910)	(2950)	2950 F	2970 FF	2970 FF
3400 FF	3400 FF	3400 F	(3400)	—	—	—

SYMBOLES: ff = très faible; f = faible; m = moyenne; F = forte; FF = très forte. Les fréquences entre parenthèses indiquent des bandes incertaines (épaules, etc.).

TABLEAU II

Fréquences (en cm⁻¹) des bandes Raman
et infrarouges de H_2SO_4 et HSO_4^-

	Raman	Infrarouge
H_2SO_4	—	332 ± 10
	395	372 ± 10
	430	420 ± 10
	560	549 ± 5
	917	907 ± 5
	972	967 ± 5
	1140	1170 ± 10
	—	1240 ± 25
	1370	1365 ± 5
	—	2450 ± 50
	—	2970 ± 50
HSO_4^-	595	584 ± 5
	895	890 ± 8
	1036	1052 ± 5

TABLEAU III

Fréquences (en cm⁻¹) des principales bandes dans le spectre
infrarouge de l'acide sulfurique et de ses hydrates à l'état solide

H_2SO_4	$H_2SO_4.H_2O$	$H_2SO_4.2H_2O$	$H_2SO_4.4H_2O$
?	732 F	(735)	735 ff
—	890 F	900 F	890 F
910 FF	—	—	—
980 F	—	—	—
1030 f	1046 FF	1045 FF	1045 FF
—	—	—	1100
—	1142	1153 FF	1160 FF
1165 F	1180	—	—
1225 m	—	—	—
—	1240 F	—	—
1375	—	(1320) f	(1340) f
—	—	—	1650 F
—	1730 F	1710 F	1750 F
2150 f	2125 F	2050 ?	—
2400 F	?	2400 m	(2500)
—	2775 FF	2700 f	—
2980 FF	—	2950 F	3000 m
—	—	—	3350 F

TABLEAU IV

Spectres infrarouges des oléums (Les fréquences sont données en cm⁻¹)

6.5%	12.5%	23%	28.5%	46.5%	51%	69% SO_3
(472)	(475)	472 f	472 f	472 f	476 f	476 f
—	—	—	510 f	513 f	510 f	516 f
—	?	538 mf	538 F	538 F	538 F	540 FF
550 F	555 F	555 F	550 F	552 f	552 f	—
618 ff	618 f	619 mf	618 m	619 mF	620 F	618 F
?	655 f	640 mf	640 mf	640 mF	635 mf	640 mf
—	—	—	688 ff	688 ff	688 f	688 f
732 f	732 mf	732 m	732 m	732 mF	730 mF	728 mF
806 f	807 mf	809 FF	808 FF	806 FF	806 FF	806 FF
907 F	908 mF	906 m	905 mf	(905)	(905)	—
970 FF	970 FF	969 FF	969 FF	969 FF	965 FF	965 FF
—	—	—	—	1075 ff	1075 ff	1075 f
1180 FF	1185 FF	1190 FF	1190 FF	1190 FF	1200 FF	1200 FF
1365 FF	1365 FF	1370 FF	1370 FF	1370 FF	1370 FF	1370 FF
—	—	1430 f	1430 mf	1430 m	1430 m	1430 m
2250 f	2250 f	2200 f	2200 f	2200 mf	2200 mf	2200 mf
2450 F	2450 F	2425 F	2425 F	2425 F	2424 F	2425 F
2970 FF	2970 FF	3000 FF	3000 FF	3000 FF	3000 FF	3000 FF

l'acide sulfurique, au contraire, on a en moyenne le même nombre de liaisons hydrogène (soit quatre) par molecule (ou ion).

Viennent ensuite les espèces ioniques: d'abord H_3O^+ dont les bandes caractéristiques à 1750 et 1200 cm^{-1} (8) augmentent d'intensité avec la concentration jusqu'à un maximum vers 80% d'acide (Tableau I). Il en est de même de l'ion bisulfate HSO_4^- pour lequel Young et ses collaborateurs (5) ont établi avec précision les fluctuations de concentration en se basant sur l'intensité des bandes Raman. Plusieurs des bandes de l'anion HSO_4^- se confondent avec celles de la molécule H_2SO_4 comme on pouvait le prévoir; les trois plus caractéristiques, à 584, 890 et 1052 cm^{-1}, ont leur équivalent en Raman (Tableau II). Les deux ions H_3O^+ et HSO_4^- sont donc les plus abondants dans les solutions aqueuses d'acide sulfurique. À noter que la bande à 1050 cm^{-1} est encore perceptible dans le spectre de H_2SO_4 pur, une autre confirmation expérimentale de l'auto-dissociation déjà démontrée par la cryoscopie et la conductivité électrique (1). Les spectres Raman ne permettent pas de vérifier ce point, pas plus d'ailleurs que mettre en évidence l'ion H_3O^+ (11).

Quant à l'anion sulfate SO_4^{--} sa concentration maximum (moins de la moitié de celle de l'ion bisulfate) se trouve entre 40 et 60% d'acide, toujours d'après les spectres Raman (5). C'est de cette façon que varie l'intensité des deux bandes à 445 et 500 cm^{-1} que nous attribuons pour cette raison aux modes de déformation asymétrique de l'ion sulfate. Dans les spectres infrarouges des sulfates ioniques cristallins (12) ces fréquences sont notablement plus élevées, soit environ 600–650 cm^{-1}. Le décalage observé dans les solutions d'acide provient peut-être de l'hydratation des ions. Par ailleurs la bande très faible à 1100 cm^{-1} dans la solution la plus diluée, et qui va se perdre dans la forte absorption vers 1050 cm^{-1} aux grandes concentrations d'acide, provient également de l'anion sulfate (12). Elle est due à la vibration de valence S—O asymétrique; la fréquence symétrique correspondante est 982 cm^{-1} en Raman (13).

Au delà de 80% d'acide, une douzaine de bandes appartenant à la molécule H_2SO_4 (Tableau II) émergent graduellement alors que celles de l'ion bisulfate s'affaiblissent. Au moins trois de ces bandes (i.e. à 907, 1365 et 2950 cm^{-1}) sont communes à l'acide et à l'anion comme le prouvent les variations d'intensité avec la composition. Le problème de la constitution des solutions très concentrées (au-dessus de 80%) d'acide sulfurique n'est pas entièrement élucidé. Dans l'acide pur, outre l'auto-dissociation déjà mentionnée,

$$2H_2SO_4 \rightleftarrows HSO_4^- + H_3SO_4^+; \hspace{3cm} [1]$$

une seconde, moins importante, est censée exister (1), soit

$$2H_2SO_4 \rightleftarrows H_3O^+ + HS_2O_7^-. \hspace{3cm} [2]$$
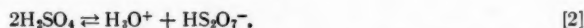
Cependant les ions ainsi produits sont si peu abondants qu'on ne saurait les déceler par spectroscopie, sauf dans les cas les plus favorables (telle la bande de HSO_4^- à 1050 cm^{-1} citée plus haut). Ainsi il est à prévoir que le spectre du cation $H_3SO_4^+$ diffère assez peu de celui de la molécule H_2SO_4. Les seuls indices qu'on pourrait lui attribuer dans les présents spectres, en se basant sur le critère intensité, sont deux bandes très diffuses, l'une vers 740 cm^{-1} et l'autre à 2250 cm^{-1}. La première, en particulier, a une fréquence appropriée pour un mode de balancement (wagging) des hydrogènes. Par contre, la seconde fréquence à 2250 cm^{-1} semble un peu trop basse pour une vibration de valence O—H; elle doit plutôt appartenir à quelque combinaison ou harmonique des bandes plus fortes de H_2SO_4.

Par ailleurs, diverses propriétés physiques (14) conduisent à postuler l'existence d'un ion solvaté $H_3O^+(H_2SO_4)$ dans les solutions très concentrées (au-delà de 90%). La présence

des bandes caractéristiques de l'ion hydroxonium dans les solutions à plus de 95% d'acide renforce cette hypothèse au détriment d'une autre mise récemment de l'avant par Young et Walrafen (15) et qui fait appel à une espèce nouvelle $H_5SO_5^+$. En effet, tout laisse prévoir que ce cation hypothétique aurait une structure, et partant un spectre de vibration nettement différents de ceux des espèces H_2SO_4, $H_3SO_4^+$ et HSO_4^-.

(B) Les vibrations normales de H_2SO_4

Dans les travaux antérieurs sur le spectre moléculaire de l'acide sulfurique on ne s'est pas préoccupé d'attribuer les fréquences des bandes observées aux divers modes de vibration de la molécule. La diffraction aux rayons-X (16) a confirmé la structure la plus probable, soit un arrangement quasi-tétraédral des oxygènes autour du soufre, les deux hydrogènes étant normalement situés dans le plan Z (Fig. 3). La molécule appartient
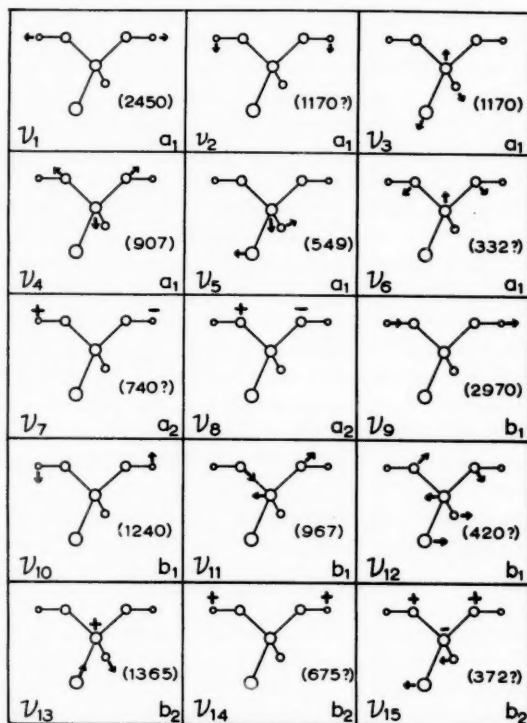
FIG. 3. Modes de vibration de la molécule H_2SO_4. Les nombres entre parenthèses indiquent les fréquences en cm^{-1}.

donc au groupe de symétrie C_{2v} et la théorie (17) prévoit que ses 15 vibrations normales sont réparties en deux classes: soit 8 symétriques par rapport à l'axe (dont 6 du type a_1 et 2 du type a_2) et 7 asymétriques (dont 4 du type b_1 et 3 du type b_2). Les vibrations de type a_2 étant inactives en infrarouge, on observera donc au maximum 13 vibrations fondamentales, du moins pour la molécule à l'état libre. Pour fins d'identification on peut séparer les vibrations en deux groupes de 6 et 9 respectivement, suivant qu'elles font intervenir directement ou non les atomes d'hydrogène. On a représenté sur la Fig. 3

ces divers modes de vibration de la molécule H_2SO_4 avec la fréquence probable de chacune. Les vibrations de valence O—H, ν_1 et ν_9, se retrouvent ici presque exactement aux mêmes fréquences que dans le cas de l'acide sélénieux (18); elles sont décalées à 1860 et 2280 cm^{-1} dans D_2SO_4. Ces fréquences relativement basses confirment l'existence de fortes liaisons hydrogène dans l'acide sulfurique et ses solutions. D'autre part, les vibrations de déformation $\angle SOH$ sont difficiles à identifier parce qu'elles tombent dans une région de forte absorption due aux bandes de valence S—O. Pour la même raison, les décalages isotopiques dans D_2SO_4 sont de peu d'utilité ici. Cependant, en comparant minutieusement les spectres des deux molécules on peut déceler dans le cas de H_2SO_4 un léger excédent d'absorption vers 1240 cm^{-1} qui doit provenir d'une bande de déformation $\angle SOH$. Etant donné sa faible intensité, il s'agit peut-être de la vibration asymétrique ν_{10} qui affecte assez peu le moment polaire de la molécule. Si cette explication est valide, il est alors possible que la vibration symétrique correspondante soit comprise dans la forte bande à 1170 cm^{-1} (ν_3) qui effectivement semble encore plus large pour H_2SO_4 que pour D_2SO_4. Dans les solutions aqueuses d'acide sélénieux, on ne trouve qu'une seule bande intense de déformation $\angle SeOH$ à 1236 cm^{-1}. Enfin, le seul des deux modes de balancement (wagging) des hydrogènes qui soit actif en infrarouge, ν_{14} n'a pas lui non plus été identifié avec certitude dans les présents spectres. Par analogie avec diverses molécules, en particulier des alcools et des acides organiques, on peut prévoir pour ce mode une fréquence de l'ordre de 650 à 700 cm^{-1}. La bande assez floue à 675 cm^{-1} conviendrait bien à cet égard, quoique son intensité semble un peu faible. Dans l'anion HSO_4^- ce mouvement de l'unique hydrogène se traduit par une bande à 584 cm^{-1}.

Pour sa part le groupe SO_4 dans l'acide sulfurique possède neuf vibrations caractéristiques non dégénérées. Du côté des hautes fréquences on rencontre d'abord les vibrations de valence double S=O, ν_3 à 1170 et ν_{13} à 1365 cm^{-1}, soit presque exactement les mêmes valeurs que dans SO_2. Les distances interatomiques sont aussi identiques, 1.42 Å (19). Les deux vibrations de valence simple S—O ont des fréquences sensiblement plus basses, ν_4 à 907 et ν_{11} à 967 cm^{-1}, en accord avec les longueurs plus grandes, 1.52–1.55 Å, de ces liaisons. Dans l'anion HSO_4^- les fréquences correspondantes se trouvent à 895 et 1052 cm^{-1} respectivement. Quant aux diverses fréquences de déformation, nous avons essayé de les identifier par comparaison avec la molécule SO_2F_2 déjà étudiée par spectroscopie infrarouge (20) et centimétrique (21). Outre que la symétrie est la même dans les deux cas, les masses et les distances diffèrent assez peu. Ainsi, on retrouve dans les deux spectres une bande à environ 550 cm^{-1} attribuable au mode de déformation commun $\angle OSO$. Des trois autres bandes qui restent dans le spectre de H_2SO_4 à 420, 372 et 332 cm^{-1}, on serait porté a priori à assigner la première au mode de déformation $\angle OSO$ impliquant les groupements hydroxyles (ν_6) étant donné les liaisons hydrogène qui doivent en augmenter la fréquence. Cependant, seules les deux faibles bandes à 420 et 372 cm^{-1} ont leur équivalent dans le spectre Raman (Tableau II). Vu la similitude des deux modes de balancement ν_{12} et ν_{15}, il semble plus logique de leur attribuer les deux premières bandes, ce qui laisse la dernière à 332 cm^{-1} pour ν_6. Toutefois, cette interprétation n'est que provisoire.

(C) Les hydrates solides

Lors de la solidification, les bandes infrarouges de l'acide sulfurique et de ses solutions aqueuses deviennent plus nettes et plus minces comme c'est généralement le cas. Par comparaison avec celui du liquide (Fig. 2, A) on note les particularités suivantes dans le spectre de l'acide pur à l'état solide (Fig. 4, A). Les deux bandes à 910 et 1050 cm^{-1}

caractéristiques de l'ion bisulfate sont nettement plus intenses, confirmant par là que l'auto-dissociation est plus forte à l'état solide. Par ailleurs, la bande de déformation $\angle$ SOH à 1225 cm^{-1} est maintenant très distincte de la bande de valence S=O à 1165 cm^{-1}. L'harmonique de cette dernière fréquence se retrouve sans doute dans la bande très diffuse à 2150 cm^{-1}, de même que la combinaison des deux fondamentales à 1365 et 910 cm^{-1}.

Le monohydrate $H_2SO_4 \cdot H_2O$ montre un spectre (Fig. 4, B) entièrement différent de ceux non seulement de l'acide pur mais encore des solutions liquides de composition voisine (comp. Fig. 1, B). Notons en passant que le monohydrate contient 84.5% de H_2SO_4, le dihydrate, 73.15% et le tétrahydrate, 57.7%. L'effet Raman (11) et la résonance nucléo-magnétique (22) ont donné pour ce solide des résultats compatibles avec
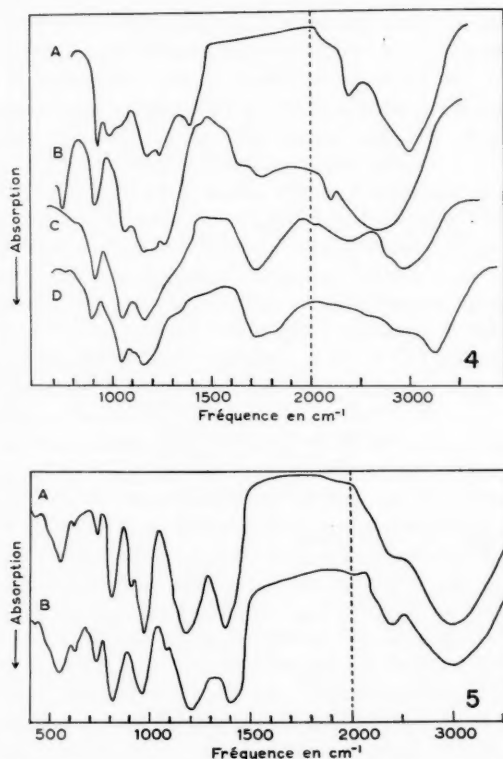
FIG. 4.   Spectres de l'acide sulfurique et de ses hydrates à l'état solide. (A) H_2SO_4; (B) monohydrate (C) dihydrate; (D) tétrahydrate.
FIG. 5.   Spectres infrarouges entre 2 et 25 μ des oléums. (A) 23% SO_3; (B) 69% SO_3.

la structure ionique $(H_3O^+)(HSO_4^-)$. Effectivement, la majorité des bandes rapportées ici (Tableau III) peuvent s'interpréter sans ambiguïté d'après ces deux ions, à savoir celles de H_3O^+ à 732, 1142, 1730 et 2125 cm^{-1} (23) et celles de HSO_4^- à 890, 1046 et 1240 cm^{-1} (12). Cependant, la bande à 732 cm^{-1} constitue ici une énigme en ce qu'elle est beaucoup trop intense pour provenir uniquement de l'ion hydroxonium. En effet,

elle est à peine visible dans les deux autres hydrates (Fig. 4, C et D). Nous nous proposons d'étudier cette question plus en détail. Dans les spectres du dihydrate toute trace d'acide non-ionisé a disparu et les bandes de H_2O sont bien évidentes. Enfin dans le cas du tétrahydrate la bande de l'ion sulfate à 1100 cm^{-1} se détache nettement de celle de l'ion bisulfate à 1045 cm^{-1} contrairement au cas des solutions liquides.

(D) Les oléums

Les spectres Raman des oléums à diverses concentrations sont déjà bien connus à la suite des travaux originaux de Chédin (4) et de ceux plus récents de Millen (5). Ce dernier a attribué les bandes observées à des acides supérieurs tels $H_2S_2O_7$, $H_2S_3O_{10}$, etc. dont l'existence avait été révélée par les mesures cryoscopiques de Gillespie (24). Les présents résultats (Tableau IV) confirment en général cette interprétation. Ainsi la bande d'absorption à 907 cm^{-1}, caractéristique de H_2SO_4, s'affaiblit graduellement lors de l'addition de SO_3 et finit par disparaître dans les oléums à environ 45%, composition correspondant à l'acide disulfurique $H_2S_2O_7$. Quant aux autres bandes de H_2SO_4 à 550, 970, 1170 et 1368 cm^{-1}, ainsi que les bandes de valence OH vers 3–4 μ, si elles semblent garder la même intensité à toutes concentrations, c'est qu'elles sont communes aux acides supérieurs et leurs ions, comme on pouvait le prévoir. Dans la plupart des cas on observe un léger déplacement du maximum de ces bandes suivant la concentration. En fait, seules quelques-unes des bandes rapportées ici peuvent servir à identifier sans ambiguïté l'une quelconque des espèces moléculaires ou ioniques présentes dans les oléums.

En se basant sur des considérations de structure on doit s'attendre à des vibrations caractéristiques du "pont" S—O—S présent dans tous les acides supérieurs de formule générale $H_2SO_4 \cdot (SO_3)_n$. Aussi attribuons-nous aux vibrations de valence de ce groupe les deux bandes à 732 et 806 cm^{-1} qui sont de fréquence et d'intensité relative appropriées. Comme la première seule apparaît en Raman, elle doit correspondre à la vibration symétrique S—O. En ceci, notre interprétation diffère de celle de Millen (5) qui considère cette bande comme un diagnostic sûr de la molécule $H_2S_2O_7$ à l'exclusion des acides supérieurs. En fait, nos spectres infrarouges ne montrent aucune diminution appréciable d'intensité des deux bandes à 732 et 806 cm^{-1} pour des concentrations supérieures à 45% (i.e. $H_2S_2O_7$) ce qui concorde bien avec l'explication que nous proposons ici. Les autres bandes, qui d'après la distribution d'intensité pourraient être assignées à la molécule $H_2S_2O_7$, se trouvent à 618 et 640–655 cm^{-1}; cette dernière appartient peut-être à l'anion $HS_2O_7^-$ sur la concentration duquel on ne possède pas de données précises.

Quant à l'acide trisulfurique $H_2S_3O_{10}$ qui, selon les mesures cryoscopiques de Gillespie (24) existe aux concentrations supérieures à 30%, on peut lui attribuer avec assez de certitude les deux bandes à 688 et 1430 cm^{-1}. Dans les spectres Raman on observe à 480 cm^{-1} une bande qui semble bien provenir de cet acide, du moins si l'on s'en rapporte à son intensité. Son équivalent (à 472 cm^{-1}) dans les présents spectres ne montre pas le même profil d'intensité, mais ceci provient sans doute de difficultés expérimentales (lumière diffractée, etc.) dans cette région située à la limite utile de notre instrument.

Par ailleurs, nous n'avons pu déceler dans les spectres des oléums, même les plus concentrés, d'indices certains de l'acide tétrasulfurique $H_2S_4O_{13}$. Des deux fréquences Raman attribuées par Millen à cet acide, la première à 245 cm^{-1} tombe loin en dehors de la région étudiée ici et la seconde à 688 cm^{-1} apparaît déjà à 28% dans nos spectres, d'où l'attribution à $H_2S_3O_{10}$ ci-haut. Enfin, la faible bande à 1075 cm^{-1} dans les oléums

à plus de 45% de SO_3 révèle la présence de cette dernière molécule comme l'a démontré Chédin (4) à partir des spectres Raman. Selon toute apparence, l'anhydride SO_3 se trouve ici à l'état de monomère puisque les bandes caractéristiques du polymère S_3O_9 (25), en particulier celle à 860 cm⁻¹, n'apparaissent pas dans les spectres infrarouges des oléums même à 70%. Notons en terminant que, pas plus que pour les solutions aqueuses d'acide sulfurique, nous n'avons pu trouver dans les spectres des oléums d'évidence positive pour l'espèce $H_3SO_4^+$ bien que, d'après la stoéchiométrie, ce cation doive exister dans ce milieu.

REMERCIEMENTS

SUMMARY

The infrared absorption spectra from 2 to 30 μ have been measured for sulphuric acid, its aqueous solutions at various concentrations, the solid acid and its three hydrates, and finally the deuterated acid D_2SO_4. The results confirm and extend our knowledge as to the nature and relative abundance of the ionic and molecular species present in these systems. In particular, direct evidence was found for the self-dissociation of the pure acid as well as for the incomplete ionization of water even in very concentrated sulphuric acid. It was possible to assign most of the observed frequencies to the various vibrational modes of the H_2SO_4 molecule. Likewise the infrared spectra of oleums in concentrations up to 70% have been studied, and the higher acids, $H_2S_2O_7$ and $H_2S_3O_{10}$, have been identified.

BIBLIOGRAPHIE

1. R. J. GILLESPIE. Revs. Pure and Appl. Chem. (Australia), 9, 1 (1959).
2. B. J. KIRKBRIDE et P. A. H. WYATT. Trans. Faraday Soc. 54, 483 (1958).
3. G. C. HOOD et C. A. REILLY. J. Chem. Phys. 27, 1126 (1957).
4. J. CHÉDIN. Compt. rend. 201, 724 (1935); Ann. chim. (Paris), 8(11), 432 (1937).
5. D. J. MILLEN. J. Chem. Soc. 2589 (1950).
6. T. F. YOUNG, L. F. MARANVILLE et H. M. SMITH. The structure of electrolytic solutions. Edité par W. J. Hamer. John Wiley & Sons, New York. 1959. Chap. 4.
7. R. A. MARCUS et J. M. FRESCO. J. Chem. Phys. 27, 564 (1957).
8. M. FALK et P. A. GIGUÈRE. Can. J. Chem. 35, 1195 (1957).
9. E. L. WAGNER et D. F. HORNIG. J. Chem. Phys. 18, 296 (1950).
10. R. J. GILLESPIE. J. Chem. Soc. 2493 (1950).
11. D. J. MILLEN et E. G. VAAL. J. Chem. Soc. 2913 (1956).
12. F. A. MILLER et C. H. WILKINS. Anal. Chem. 24, 1253 (1952).
13. L. A. WOODWARD et R. G. HORNER. Proc. Roy. Soc. (London), A, 144, 129 (1934).
14. P. A. H. WYATT. Trans. Faraday Soc. 56, 490 (1960).
15. T. F. YOUNG et G. E. WALRAFEN. Communication à la 136ième réunion de l'American Chemical Society, Atlantic City, N.J., Septembre, 1959.
16. R. PASCARD. Compt. rend. 240, 2162 (1955).
17. G. HERZBERG. Infrared and Raman spectra of polyatomic molecules. D. Van Nostrand Co., Inc., New York. 1945.
18. M. FALK and P. A. GIGUÈRE. Can. J. Chem. 36, 1680 (1958).
19. L. E. SUTTON (Editeur). Tables of interatomic distances. Special Publication No. 11, The Chemical Society, London. 1958.
20. W. D. PERKINS et M. K. WILSON. J. Chem. Phys. 20, 1791 (1952).
21. R. M. FRISTROM. J. Chem. Phys. 20, 1 (1952).
22. R. E. RICHARDS et J. A. S. SMITH. Trans. Faraday Soc. 47, 1261 (1951).
23. C. C. FERRISO et D. F. HORNIG. J. Chem. Phys. 23, 1464 (1955).
24. R. J. GILLESPIE. J. Chem. Soc. 2516 (1950).
25. H. GERDING et J. LECOMTE. Physica, 6, 737 (1939).

THE COPPER/ARSENIC SYSTEM AND THE
COPPER ARSENIDE MINERALS[1]

R. D. Heyding and G. J. G. Despault

ABSTRACT

In addition to the α solid solution of arsenic in copper, three intermediate phases exist in the copper/arsenic system. The ϵ phase, stable only below ca. 340° C, has the hexagonal A3 (D_{6h}^4, $P6_3/mmc$) structure with $a = 2.588$, $c = 4.226$ Å, and the approximate formula Cu_8As. The compound $Cu_{3-x}As$, with $0 \leqslant x \leqslant 0.3$, is trigonal ($D_{3d}^4$, $P\bar{3}c1$) with $a = 7.132$, $c = 7.304$ Å at $x = 0$. This compound has no polymorphic forms between 200° C and the melting point. The arsenic-rich compound $Cu_{5-u}As_2$, with $0 \leqslant u \leqslant 0.1$, melts incongruently at about 700° C, and decomposes at 300° C to arsenic and Cu_3As. The structure has not been determined, but the powder diffraction pattern is recorded. The solubility of copper in arsenic appears to be negligible.

It is suggested that the mineral α domeykite is a high-pressure phase, and that the mineral algodonite is a high-pressure modification of the ϵ phase. The mineral β domeykite is isostructural with Cu_3As.

According to the phase diagram (1), two compounds are formed in the binary copper/arsenic system. The first of these, Cu_3As, has been synthesized by Katoh (2) and the structure determined by Steenberg (3). It is trigonal (D_{3d}^4, $P\bar{3}c1$), and exists over a short composition range. A transition on the copper-rich side of Cu_3As at 380° C has been interpreted by Hansen (1) as the transformation of Cu_3As into a polymorphic low-temperature form, although Steenberg was unable to prepare Cu_3As with other than the trigonal structure mentioned above. Bolfa *et al.* (4) have reported the formation of a phase at relatively high pressure which is isostructural with the mineral *domeykite*, but the diffraction pattern and unit cell dimensions were not recorded.

Although the exact composition of the second compound in the binary phase diagram is not known, Hansen has assumed the formula to be Cu_5As_2, and has attributed the transitions at 700° and 300° C on the arsenic-rich side of Cu_3As to incongruent melting and peritectoid decomposition of this compound.

Recently, Schubert *et al.* (5) have reported the synthesis of a compound Cu_9As which does not appear on Hansen's phase diagram. It has the hexagonal close-packed A3 structure, and is stable only below 400° C.

The present study was undertaken to confirm the composition of the phase reported by Schubert, to search for transitions in Cu_3As, and to investigate the composition and structure of the arsenic-rich compound.

EXPERIMENTAL

Twenty-four alloys containing 2.5 to 36 at.% As in copper were prepared by heating the elements in sealed evacuated pyrex, vycor, or quartz tubes in the usual manner. The copper was prepared by reduction of powdered copper oxide with purified hydrogen. Spectroscopic analysis indicated impurity limits (in p.p.m.) of: Ag, 5–10; Fe, 5; Ni, 5; Si, 3; and Mg, 2. ASARCO metallic arsenic of 99.999% spectroscopic purity was sublimed prior to use to remove traces of oxide and to facilitate crushing.

Alloys containing less than 20 at.% As were melted and quenched, annealed at 680° C, and cooled slowly to room temperature. Filings of the specimens were placed in quartz

X-ray capillaries which were in turn sealed under vacuum in larger vycor or pyrex capillaries for heat treatment. Alloys containing more than 20 at.% As were readily crushed by mortar and pestle, and subsequent heat treatment was conducted on bulk powders.

Some of the copper-rich alloys were annealed at moderate pressures and temperatures by heating open capillaries or tubes in a steel bomb under argon at 1500 to 2500 p.s.i.

X-Ray diffraction patterns were obtained in Norelco 11.46-cm Debye–Scherrer cameras using CuK_α radiation.

RESULTS AND DISCUSSION

The Copper-rich Region: The ϵ Phase

Diffraction patterns of alloys containing less than 25% As quenched from temperatures between 350° and 660° C showed only patterns of the α solid solution, or the α solid solution and Cu_3As. The unit cell dimension of the saturated α phase in equilibrium with Cu_3As was found to be 3.647 ± 0.001 Å, in good agreement with Mertz and Mathewson's value of 3.6483 Å (6).

A third phase appeared in alloys quenched or cooled slowly from 300° C with a corresponding decrease in intensities of the patterns of the α phase and Cu_3As. This phase was never obtained pure, even after cold-working and prolonged annealing. It has the approximate composition Cu_8As, and is isostructural with the compound Cu_9As recorded by Schubert, with hexagonal unit cell dimensions $a = 2.588\pm0.001$, $c = 4.226\pm0.001$ Å, $c/a = 1.633$. This $A3$, Mg-type structure (D^4_{6h}, $P6_3/mmc$) is also found in the ϵ phases of the Cu/Sb, Ag/As, and Ag/Sb systems (1, 7), and by analogy, should be referred to as the ϵ phase. Like the other ϵ phases, decomposition occurs at relatively moderate temperatures. Our inability to prepare a uniphase specimen may have been due either to a sluggish transformation or to the existence of a lower stability limit such as that observed in the Ag/As system, or both. In either event, the unit cell dimensions are not sensitive to total alloy compositions, and consequently the homogeneity range appears to be quite narrow under normal conditions.

The mineral *algodonite* is obviously isostructural with the ϵ phase, although compositions reported for the mineral range from Cu_7As (8) to Cu_4As (3). The diffraction pattern given by Peacock (9) for algodonite with the composition Cu_6As is identical with that of the ϵ phase, with minor variations in intensities of some of the reflections. One might expect the homogeneity limit of this close-packed phase to alter under pressure at the expense of the Cu_3As phase, and indeed, we have found that even at 2500 p.s.i. appreciable quantities of the ϵ phase (with slightly altered lattice parameters) appear in alloys of the composition Cu_4As. The variation in composition of the mineral, and the apparent discrepancy between composition of mineral and synthetic specimens can be attributed to differences in ambient pressures during formation of the phase.

The transition at 380° C in the phase diagram is, as far as we are able to estimate, 30 to 80° C higher than the temperature at which the peritectoid decomposition of the phase occurred in our alloys. There is some uncertainty in the figure given in the diagram, since it is based on an inflection in the solubility limit of arsenic in copper. It is not likely that the transition would be observed by differential thermal analysis unless the alloys were cold-worked before analysis.

The Compound Cu_3As

In alloys containing 22 to 27 at.% As, hexagonal Cu_2As or Cu_3As and the second phase appropriate to the two-phase region (α solid solution or the ϵ phase) were the only phases observed regardless of formation temperature or heat treatment between

200° and 660° C. The unit cell dimensions and the analyses of homogeneous alloys at the copper- and arsenic-rich limits, quenched from 560° C, are:

As, (at.%)	Composition	a (Å)	c (Å)	c/a
24.92	$Cu_{3.01}As$	7.132	7.304	1.024
26.87	$Cu_{2.72}As$	7.113	7.272	1.022

These dimensions are in excellent agreement with Katoh's values for the terminal alloys (2), but the limits are somewhat richer in arsenic than those proposed by Katoh.

The mineral β *domeykite*, also with the formula Cu_3As, is isostructural with this phase, with unit cell dimensions of $a = 7.10$ kX and $c = 7.25$ kX (8).

There was no indication of a polymorphic transformation in Cu_3As within 2- to 3-week annealing periods at temperatures below 400° C. Moreover, an alloy prepared by heating the elements at 200° C for 2 months exhibited only the pattern of Cu_3As, although traces of unreacted copper and arsenic were visible under the microscope. We conclude that this phase exists only in the trigonal form described by Steenberg.

The Arsenic-rich Phase

Alloys containing 27 to 36 at.% As exhibited the diffraction patterns of Cu_3As and arsenic when quenched from 700° C or annealed and cooled slowly to room temperature from 280° C. A new phase was observed in alloys quenched from intermediate temperatures, with arsenic the second phase in alloys containing greater than 30 at.% As. Hansen's interpretation of the transformations at 700° and 300° C, incongruent melting and peritectoid decomposition of the arsenic-rich phase, is confirmed.

The decomposition at 300° C is rapid, and quenching was invariably attended by deposition of an arsenic mirror on the wall of the ampoule. Analysis of an alloy quenched from 550° C when in equilibrium with metallic arsenic at 450° C indicated a maximum copper content corresponding to $Cu_{2.5}As$ and a minimum content corresponding to $Cu_{2.45}As$.

The first 33 lines of the rather complicated diffraction pattern are recorded in Table I. The compound does not appear to be isostructural with any of the transition metal

TABLE I

Powder diffraction pattern of $Cu_{5-u}As_2$*

I†	d (Å)	hkl‡	I†	d (Å)	hkl‡
1	5.30	110	3	1.694	114
13	3.30	201	3	1.673	420
2	3.23	102	1	1.576	332
1	2.87	112	9	1.493	{500 430}
7	2.65	220			
1	2.56	202	7	1.445	413
6	2.47	221	2	1.431	314
21	2.43	212	4	1.395	105
3	2.35	310	11	1.373	115
13	2.16	113	7	1.343	324
100	2.075	320	13	1.324	440
90	2.022	302	2	1.313	215
100	1.991	321	4	1.295	522
17	1.960	312	13	1.197	523
11	1.925	213	13	1.177	{602 325}
13	1.780	004			
13	1.737	{322 104}	4	1.158	116
			33	1.146	504

*Uncertainty in composition: $0 \leqslant u \leqslant 0.1$.
†Intensities by visual comparison with density wedge.
‡Tentative tetragonal cell, $a = 7.48$ Å, $c = 7.12$ Å. Observed density 7.88 g/cc, $Z = 4$.

or copper family chalcogenides or phosphogenides of approximately the same composition, although there is some superficial similarity to $Ni_{2.5}As$ (10) and $Ni_{2-2.5}Sb$ (11). The pattern can be indexed on a tetragonal cell with $a = 7.48$ Å, $c = 7.12$ Å, but this analysis must be regarded as provisional.

The Copper/Arsenic Minerals Algodonite and Domeykite

Three copper/arsenic minerals are recognized: hexagonal algodonite mentioned previously, the trigonal Cu_3As mineral called β domeykite by Padĕra (8) and 'artificial domeykite' by Katoh (2) and Steenberg (3), and the cubic Cu_3As mineral called α domeykite by Padĕra and domeykite or mineral domeykite by Katoh and Steenberg. The uncertainty in composition of the phases these minerals represent and the misinterpretation of the transformations they undergo has led to some confusion in the literature not only with respect to the minerals but with respect to the phase diagram as well.

The cubic mineral α domeykite decomposes at 225° C with the formation of algodonite and trigonal Cu_3As.* The composition of cubic α domeykite corresponds to Cu_3As, and Steenberg has argued that if cubic α domeykite and trigonal β domeykite are both Cu_3As, the transition at 225° cannot be explained unless algodonite is also, ideally, Cu_3As. This interpretation has been the basis for the assumption in subsequent literature that Cu_3As has two or three modifications. We have found no such modifications. Moreover, Pearson (7) has observed that cubic α domeykite is isostructural with $Cu_{15}Si_4$, and has suggested that the correct formula is $Cu_{15}As_4$ rather than Cu_2As. Finally, algodonite itself decomposes to trigonal β domeykite and the α solid solution at 250° C (3, 12), an impossible transformation unless algodonite lies between the solid solution and Cu_3As in the phase diagram.

We attempted to repeat the synthesis of the high-pressure Cu_3As phase described by Bolfa (4) without success, probably because the pressures we could attain were too low. It is unfortunate that Bolfa and his co-workers did not give the diffraction pattern of their product, but we must assume that it was identical with the mineral they used for comparison, and that the mineral was indeed cubic α domeykite.

With this assumption, the relationship of the minerals to the binary phase diagram can be explained quite simply. Cubic α domeykite is a high-pressure phase, probably with the formula $Cu_{15}As_4$, which decomposes on heating to trigonal Cu_3As (which is identical with trigonal β domeykite) and the ϵ phase. Algodonite is a high-pressure modification of the ϵ phase with variable composition, which decomposes at 250° C, somewhat below the normal transition temperature, with the formation of the α solid solution and trigonal Cu_3As. Neither of the high-pressure phases, algodonite and α domeykite, will appear on the normal phase diagram, and there is no reason to expect that the compound Cu_3As exists other than with the trigonal lattice.

As a result of this investigation we submit that three modifications are required in the phase diagram shown and described in Hansen:

1. The transition at 380° C, on the copper-rich side of Cu_3As represents the peritectoid decomposition of the ϵ phase rather than a polymorphic transition in Cu_3As. The ϵ phase has very narrow homogeneity limits at about Cu_8As.

2. The homogeneity limits of Cu_3As at 560° C are $Cu_{3.0}As$ and $Cu_{2.7}As$, somewhat richer in arsenic than indicated in the diagram.

*The description in Hansen of cubic α domeykite as a high-temperature phase is obviously a misprint.

3. The composition of the arsenic-rich phase can be represented by the expression $Cu_{5-u}As_2$ in which u, the uncertainty, is within the limits $0 \rightarrow 0.1$. We have found no evidence to indicate that a compound richer in arsenic is formed at normal pressure.

ACKNOWLEDGMENTS

REFERENCES

1. M. HANSEN. Constitution of binary alloys. 2nd ed. McGraw-Hill. 1958. p. 160 et seq.
2. N. KATOH. Z. Krist, **76**, 228 (1930).
3. B. STEENBERG. Arkiv. Kemi, Mineral Geol. A, **12**, No. 26, 1 (1936–38).
4. J. BOLFA, R. PASTANT, and M. ROUBAULT. Compt. rend. **230**, 103 (1950).
5. K. SCHUBERT, H. BREIMER, W. BURKHARDT, E. GUNZEL, R. HAUFLER, H. L. LUKAS, H. VELTER, J. WEGST, and M. WILKENS. Naturwiss. **44**, 229 (1957).
6. J. C. MERTZ and C. H. MATHEWSON. Trans. Am. Inst. Mining Met. Engrs. **124**, 59 (1937).
7. W. B. PEARSON. Handbook of lattice spacing and structures of metals and alloys. Pergamon. 1958.
8. K. PADĚRA. Rozpravy České Akad. **61** (4), 22 (1951); Structure Reports, **16**, 23 (1952).
9. M. A. PEACOCK. X-Ray Powder Data File, Card 9-429.
10. R. D. HEYDING and L. D. CALVERT. Can. J. Chem. **35**, 1205 (1957).
11. U. FURST and F. HALLA. Z. physik. Chem. (Leipzig), B, **40**, 285 (1938).
12. C. PALACHE, H. BERMAN, and C. FRONDEL. Dana's system of mineralogy. Vol. 1. 7th ed. John Wiley & Sons. 1952. p. 170 et seq.

A METHOD FOR ADIABATIC COMPRESSION OF GASES UNDER CONTROLLED CONDITIONS[1]

G. D. GRAHAM[2] AND O. MAASS[3]

ABSTRACT

A preliminary account is given of an experimental technique by means of which the specific heats of gases may be measured at high temperatures and pressures. With the transducer employed consistent results were obtained up to 7000 p.s.i. and it is proposed to incorporate a transducer having a much higher pressure range where it is estimated that temperatures up to 10,000° K can be recorded.

INTRODUCTION

In a number of research directions it is of considerable interest to determine the properties of gases at high temperatures. In this paper an experimental procedure is described where the ratio of specific heats can be determined at temperatures above 1000° K.

This paper must be considered as a preliminary one in which the method of approach is described in some detail, and where measurements have been carried out as yet only to the relatively low temperature of 3000° K. By using the term low temperature it is implied that with the incorporation of a transducer which is adaptable to higher pressure measurements than the one used so far it is hoped that it will be possible to get useful information up to temperatures at least as high as 10,000° K. The procedure to be described involves the application of a high pressure impinging on one end of a double-headed piston which causes the other piston head to compress the gas under examination suddenly and under controlled conditions.

To make this possible the use of a double diaphragm is incorporated. This can be ruptured in such a way by an impinging pressure which exerts its full force on the upper piston head. This makes it possible to have an immediate and controlled impinging pressure to a high degree of accuracy whereby insuring reproducible results.

To recapitulate, the device to be described enables one to compress a gas to a predetermined volume with a high degree of accuracy and in a small fraction of a second.

The incorporation of a transducer which is adaptable to higher pressure measurements involving higher temperatures should make it possible to approach the main objective, namely to go to the high temperature mentioned above. This is under immediate consideration but it is thought that publication of the experimental procedure is warranted.

Before going on to a description of what has been accomplished so far, it may be pointed out that a transducer has been procured which will enable pressure measurements to be made up to 150,000 p.s.i. It is claimed by the manufacturer that this transducer can make reproducible measurements at this pressure but has been found to give non-reproducible results in the range below 10,000 p.s.i.

EXPERIMENTAL

The experimental procedure which is to be described may seem somewhat complicated and it is to be hoped that the diagrammatic sketch of the apparatus (Fig. 1) may help to elucidate this.
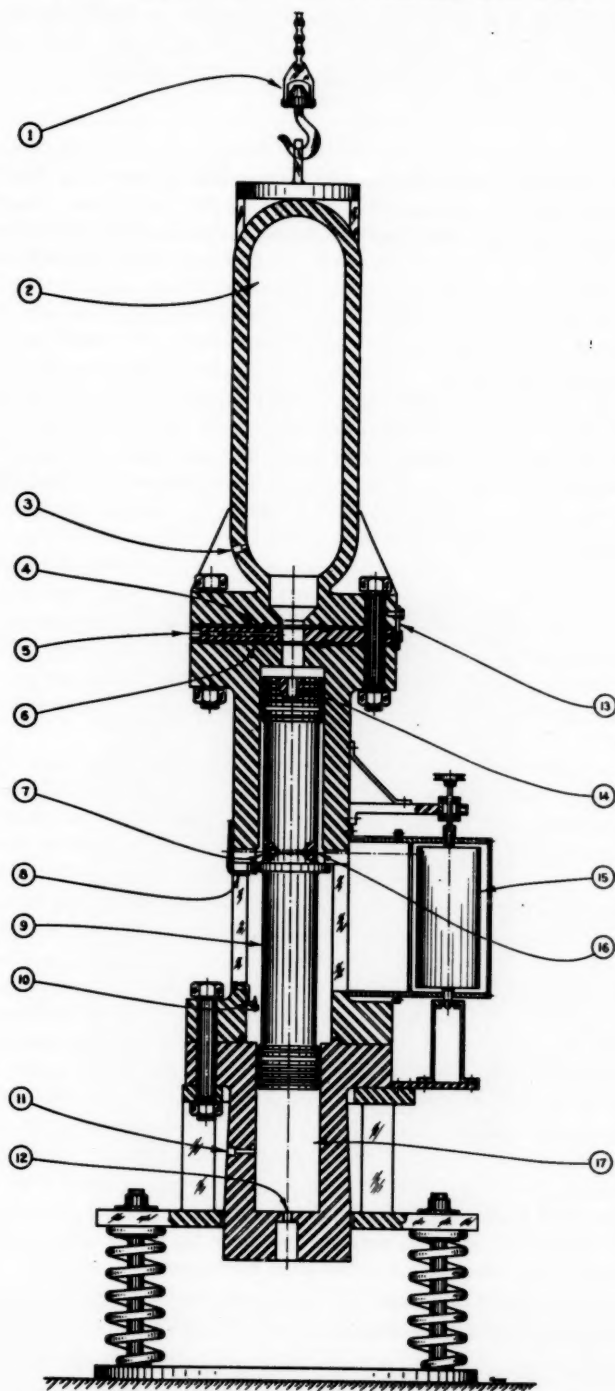
Fig. 1.

A gas of known volume is to be compressed suddenly and this to be done under controlled conditions in such a small fraction of time that adiabatic conditions prevail. This will be described under Apparatus, Measurements, and Procedure.

APPARATUS

The entire apparatus is mounted on eight automobile springs (Fig. 1). The gas under examination is contained in compression chamber (17)* which may be evacuated and filled through inlet (11). The chamber was forged from stainless steel No. 410 and was designed to withstand pressures of at least 150,000 p.s.i. The internal dimensions are 6 in. diameter and 16 in. high with a surface finish of 32 microns. In the bottom of the chamber is a threaded cavity (12) into which a suitable transducer can be flush mounted.

The double-headed piston (9) is of forged aluminum alloy weighing approximately 100 pounds and is fitted at both ends with five aircraft piston rings. Although the rings were fitted so as to have zero gap, as an added precaution against leakage, a rubber "O" ring was fitted to the bottom end in place of one of the piston rings. At its middle as shown in Fig. 1 the piston is flanged; this acts as a stop when the piston is raised into firing position and as a reference point in volume measurements. To facilitate dismantling and assembling there is a threaded hole (14) in the upper end of the piston into which a hoisting device may be inserted.

The upper end of the piston travels in a cylinder which was forged from stainless steel No. 410. To enable volume measurements to be carried out two openings were cut on opposite sides in the lower half of this cylinder. Both the compression chamber and cylinder are held securely together by means of sixteen 1 in. diameter bolts.

The air reservoir (2), which has a volume of 2 cubic feet, contains the propelling gas and is filled through inlet (3) from compressed air cylinders. This reservoir pressure is later on referred to as the impinging pressure.

Between the cylinder and air reservoir the firing assembly is located. This consists of two identical brass disks separated by a 1-in. thick, washer-shaped, steel plate. The volume so formed between the disks is known as the compensating chamber and has a volume of approximately 50 cc which is insignificant to the volume pressure changes which take place. Compressed air may be fed into this chamber through inlet (5). To insure a rigid and leakproof seal, "O" rings (6) are situated on both faces of each disk. The air reservoir, firing assembly, and cylinder are fastened together with sixteen 1 in. diameter bolts. Either disk will burst instantaneously if subjected to a force somewhat above its breaking pressure. Knowing the approximate breaking pressure of the disks, it is possible to contain a pressure in the air reservoir greater than the breaking pressure of the upper disk by admitting a balancing pressure to the compensating chamber. For example, if the desired impinging pressure is 200 p.s.i. one would select disks having a breaking pressure of approximately 150 p.s.i. plus or minus 15 p.s.i. In this case the compensating chamber may be pressurized to 100 p.s.i. and concurrently the air reservoir to 200 p.s.i. without fear of rupture of either disk. Release of the compensating pressure by bleeding through a valve will result in the bursting of the upper disk whereupon the 200 p.s.i. pressure will burst the lower disk, thus exerting the full force of the impinging pressure on the piston. It may be pointed out here that it is important to know the impinging pressure accurately so as to be able to reproduce and vary these impinging pressures. If only one disk is used it would be almost impossible to reproduce the impinging pressure because such a disk might have a variation in its breaking pressure of

*Throughout the paper, numbers in parentheses refer to circled numbers in Fig. 1.

possibly 20%. Furthermore in the investigation underway it was of considerable interest to be in a position to vary the impinging pressure by relatively small amounts. By having perfect metal disks that would break at say 95.0 p.s.i., 100.0 p.s.i., or 105.0 p.s.i. in a reproducible way enabling only one disk to be used would entail considerable cost in procuring such disks. With the double-disk procedure reproducible impinging pressures can be obtained at say 95 p.s.i., 100 p.s.i., or 105 p.s.i. or any other arbitrary pressure within small variations using the same sheet of foil from which the disks are cut. It also makes it possible to initiate the experiment with relative ease. The impinging pressure in the range used to date can be determined to within 0.5% by use of a pressure gauge with 1 p.s.i. per division markings.

MEASUREMENTS PROCEDURE

The maximum pressure attained in the initial compression is measured by means of a transducer. The choice of transducer is governed by the pressure range being investigated. For the work to date an Endevco No. 5000 piezoelectric gauge having a pressure range of 0 to 2500 p.s.i. has been used. The signal from the transducer is fed through a high-impedance (500-megohm) amplifier and then into a Hughes Memoscope Model No. 104. The peak height of the trace observed in the memoscope is measured by means of a cathetometer and from a previous calibration of the transducer this is converted to a pressure. A permanent record of the trace is obtained by photographing with a polaroid Land camera (see Fig. 2).
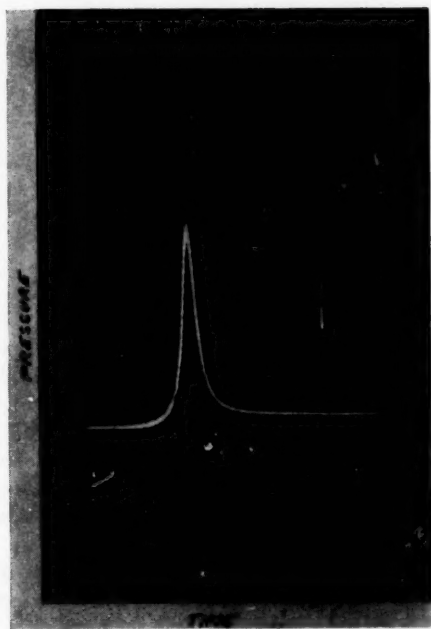
FIG. 2.

The volume at maximum pressure is measured by means of a small lead pyramid (10) which is attached by means of a screw to a small platform. When the piston is propelled downward the flange on the piston body strikes the lead. The depression of the lead is

then measured and the volume calculated. The accuracy of these volume measurements were confirmed by placing a lead pyramid directly under the piston during a run. This pyramid was then measured and it was found that the calculated volume based on the measurement of the outside pyramid was in agreement within 0.1%.

The drum camera (15), which records the oscillations of the piston, is mounted on the side of the apparatus at one of the openings. A variable speed motor drives the drum at any desired speed and by means of a zirconium arc lamp (7) inserted in the piston a light beam is pinpointed on the camera through lens (16). A manually operated shutter is opened just before the piston is propelled and closed after the oscillations have ceased. In Fig. 3 a photographic copy of a typical drum camera trace is shown. It is believed that considerable data can be obtained from such a trace.
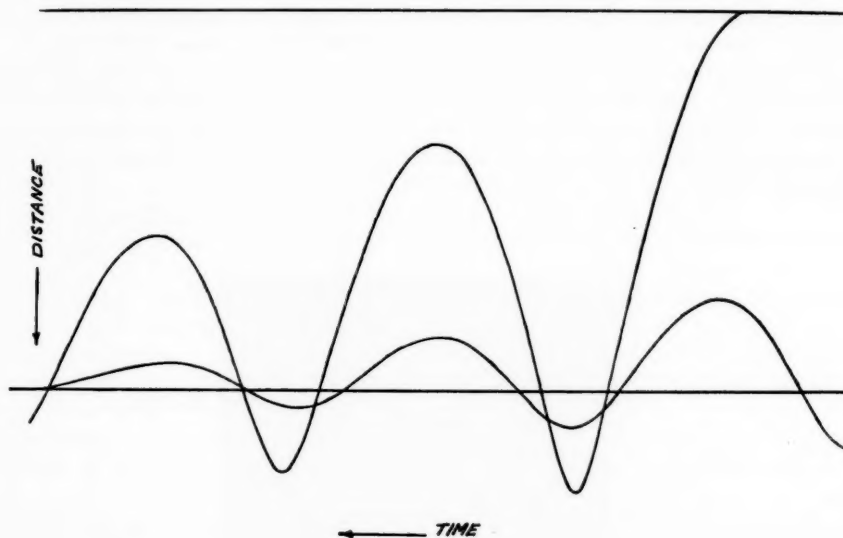
Fig. 3.

PROCEDURE

In Fig. 1 the apparatus is shown ready for an experiment. The propelling gas is fed into the cylinder and at the same time into the compensating chamber between the shims through inlet (5). When the desired pressures have been reached the valves are closed. The shutter on the drum camera (15) is opened and the compensating pressure is bled off through inlet (5). The disks break, as explained above, propelling the piston downward compressing the gas under observation in compression chamber (17). As the piston starts to move down it triggers the memoscope sweep by means of trigger (8).

To reload for the next experiment the piston is raised by opening inlet (11) and evacuating the reservoir above the piston. The bolts holding the upper sections are loosened and hooks (13) (there are three hooks spaced 120° apart) are set in place. By means of hoist (1) the air reservoir and steel plate are raised enabling the lower brass shim (6) to be replaced. The hoist is then lowered and the three hooks removed. The air reservoir is now hoisted alone and the upper shim (4) replaced. The air reservoir is again lowered and

the bolts tightened. The drum camera is reloaded and the lead volume indicator replaced. The piston is then held securely in position (by means of a wooden block placed between the piston flange and the lower edge of the opening) and the compression chamber (17) is evacuated. The gas under test is then fed into the chamber at atmospheric pressure and inlet (11) is closed. The wooden block holding the piston is removed and the apparatus is now ready for another experiment.

RESULTS

It is recognized that using ideal gas laws to make any calculations is not justified; nevertheless to make certain approximations is a reasonable approach. Having done this the following data is tabulated in Table I. The results of many experiments are summarized

TABLE I

Gas	Impinging pressure, p.s.i.	Temperature, °K	Pressure, p.s.i.	Ratio specific heats
Argon	140	1690	1280	1.630
	150	1790	1470	1.632
	170	1930	1984	1.634
	200	2000	2572	1.610
	450	3100	7203	1.603
Nitrogen	100	600	397	1.270
	110	675	544	1.290
	150	850	911	1.320
	190	1380	985	1.344
	200	1450	1029	1.354
Carbon dioxide	100	650	1411	1.203
	130	700	1500	1.224
	150	875	2675	1.258
	180	1000	4778	1.305
	200	1325	5880	1.327

as far as argon is concerned and the wide pressure and temperature range show how constant the specific heats remain. The results for nitrogen and carbon dioxide are consistent.

None of the results tabulated should be taken as establishing data which approach the accuracy of those previously established by others. It may be stated again that the purpose of this paper is to describe an experimental technique which is useful for exploring a higher-temperature region which has not yet been adequately explored.

REMARKS

There are a number of side issues for which this equipment can be usefully employed because a relatively large (5 liters) initial volume of gas can be used.

For example, it can be used to compress adiabatically a gas which undergoes chemical decomposition at high temperatures and under controlled conditions. The resulting products can be withdrawn for analysis and, as can be readily seen, a wide range of temperatures can be covered.

THE DETERMINATION OF ZIRCONIUM WITH
BENZOYLPHENYLHYDROXYLAMINE[1]

D. E. Ryan

ABSTRACT

Zirconium is completely precipitated by benzoylphenylhydroxylamine from 0.5 N acid solutions. The complex formed in sulphuric acid solutions has a constant composition, $Zr(C_{13}H_{10}O_2N)_4$, and is used for the direct weighing of zirconium; the factor is 0.0970. The product precipitated from hydrochloric acid solutions must be ignited to the oxide. The reaction is sensitive, 1 p.p.m. of zirconium being detectable, and quantitative determination of 0.2 mg is possible. Thorium and the rare earths do not interfere.

INTRODUCTION

Benzoylphenylhydroxylamine (BPHA),* where the benzoyl group has replaced the nitroso group in cupferron, has become an important reagent in the past 10 years. It has been used for the determination of iron, copper, aluminum, and titanium (1); for tin (2); for vanadium (3, 4); and for tantalum and niobium (5, 6, 7). It is recommended as superior to cupferron, when applicable, because it is more sensitive to hydrogen ion concentration, is much more stable to heat and light, and forms complexes that can, in some instances, be dried at 110° C (1, 2). BPHA has been stated to form a complex of definite composition with zirconium (8) that does not decompose at 110° C. Since only a few reagents, from the many precipitants available for zirconium, are suitable for direct weighing and as BPHA yields no precipitates with thorium or trivalent rare earths in acid solution, a detailed investigation into its possibilities for the determination of zirconium was considered worth while.

EXPERIMENTAL

From hydrochloric acid solutions of zirconium a flocculent white precipitate is obtained on adding a solution of BPHA; the precipitate becomes granular on digestion upon the steam bath and filters easily. No zirconium was detected by alizarin in filtrates from solutions containing 5% of concentrated hydrochloric acid. Under these conditions the following ions are not precipitated by the reagent: $Cu^{..}$, $Al^{...}$, $Bi^{...}$, $Cd^{..}$, $Cr^{...}$, $Pb^{..}$, $Mg^{..}$, $Mn^{..}$, $Ni^{..}$, $Zn^{..}$, $UO_2^{..}$, $Th^{....}$, $Y^{...}$, $Ce^{...}$, $Sm^{...}$, $La^{...}$, $Pr^{...}$, $Gd^{...}$, $Nd^{...}$, and $Dy^{...}$. The soluble 1:1 purple complex (9) is formed in ferric iron solutions whereas tin, vanadium V, cerium IV, and titanium react to give the usual precipitates.

Zirconium is readily precipitated by BPHA in sulphate solutions and precipitation is quantitative in 0.5 N sulphuric acid. BPHA fails to precipitate zirconium from solutions containing fluoride.

The compound precipitated from sulphate solutions contains, found after drying at 110° C and ignition to the oxide, 9.71% zirconium. $(C_{13}H_{11}O_2N)_4Zr$, in which four molecules of BPHA are combined with one atom of zirconium, has a zirconium content of 9.70%. This complex is stable to several hours' drying at 130° C but at 160° C some decomposition occurs, the compound becoming buff rather than white in color.

Reagents

N-*Benzoylphenylhydroxylamine.*—The reagent was prepared as previously described (2) and recrystallized from hot water; the compound can be purchased from leading chemical supply houses. A solution was prepared by dissolving 4 g in 100 ml of 95% ethyl alcohol.

Standard zirconium solutions.—The zirconium solutions were prepared from Matthey specpure zirconium oxychloride and zirconium sulphate. The chloride solutions, even in 5% hydrochloric acid, were found to be unstable over a convenient period of time and fresh solutions were prepared for each series of determinations. The sulphate solutions, in 2% sulphuric acid, caused no such difficulty. The zirconium content was determined gravimetrically by means of cupferron and mandelic acid.

Procedure

1. Ignition to the Oxide

Varying amounts of acid were added to samples of the zirconium standards and the solutions diluted to 150–200 ml. Reagent, in excess of the theoretical quantity required for the zirconium present, was added and the solutions digested for half an hour on the steam bath. After the samples were cooled to room temperature, they were filtered through Whatman No. 42 filter paper, washed with a saturated aqueous reagent solution, and ignited to the oxide. The results are shown in Table I.

TABLE I

Precipitation of zirconium by benzoylphenylhydroxylamine and subsequent weighing as the oxide

No.	Zr taken, mg	Zr found, mg	Conditions
1	2.70*	2.72	Solution 1% in concentrated HCl
2	2.70*	2.75	Solution 3% in concentrated HCl
3	2.70*	2.71	Solution 5% in concentrated HCl
4	2.70*	2.36	Solution 7% in concentrated HCl
5	8.42	8.42	Solution 5% in concentrated HCl
6	11.55	11.55	"
7	11.55	11.53	"
8	17.90	17.90	"
9	21.80	21.75	"
10	8.42	8.42	Solution 1.5% in concentrated H_2SO_4
11	8.42	8.31	Solution 2% in concentrated H_2SO_4
12	8.42	5.45	Solution 5% in concentrated H_2SO_4
13	8.42	5.50	Solution 10% in concentrated HCl
14	8.42	8.41	As sample No. 5 but 10 mg Th present
15	8.42	8.45	As sample No. 5 but 50 mg Th present
16	8.42	8.44	As sample No. 5 but 70 mg rare earths present
17	8.42	8.51	As sample No. 5 but 10 mg Ce···· present reduced with H_2O_2
18	8.42	8.54	As sample No. 5 but 10 mg Ti···· present complexed with H_2O_2

*These results were obtained independently by a member of this laboratory.

These results show that precipitation of zirconium by BPHA is quantitative in solutions containing up to 5% of concentrated hydrochloric acid and 1.5% of concentrated sulphuric acid (approximately 0.5 to 0.6 N in hydrogen ions); precipitation is incomplete at higher acidities. Thorium and the trivalent rare earths do not interfere. The interference of titanic and ceric ions is largely removed in one precipitation by complexing the titanium or reducing the cerium with hydrogen peroxide.

Attempts to remove interference of quinquevalent vanadium by complexing with hydrogen peroxide were unsuccessful; the result obtained for 8.42 mg of zirconium taken

was 9.91 mg in the presence of 10 mg of vanadium. In the presence of 20 mg of iron, the result was 0.5 mg higher than for the 8.42 mg of zirconium taken on a single precipitation.

THE DIRECT WEIGHING OF ZIRCONIUM COMPLEXES

Complexes that are capable of direct weighing eliminate the necessity of ignition to an oxide and permit, by virtue of their favorable factor, smaller quantities of metal ions to be determined more accurately. For zirconium, where one must invariably consider hafnium and its similar chemical behavior, there is the additional advantage that formation of such complexes permits the ready determination of the hafnium-to-zirconium ratio.

Of the many precipitants available for zirconium only 8-hydroxyquinoline, mandelic acid and its derivatives, and, more recently, tartrazine have been recommended as forming precipitates suitable for direct weighing. Balanescu (10) found that zirconium precipitates with 8-hydroxyquinoline could be dried at 140° C if precipitated from nitrate solutions buffered with acetate; precipitates varying in composition were obtained in chloride solutions.

There has been some disagreement regarding the mandelic acid derivatives. Oesper and Klingenberg (11) claimed good results on drying at 110° C for the p-bromo derivative whereas Belcher et al. (12) stated that consistent but low results were found with this same compound. Astanina and Ostroumov (13) found that mandelic acid gave zirconium precipitates that could be dried at 110° provided the final solutions were 20% by volume in concentrated hydrochloric acid; Hahn and Baginsky (14) reported also that complexes of constant composition were precipitated by mandelic acid from strong hydrochloric acid solutions and stated that low results in less acid solutions were due to basic salts; similar results have been found in this laboratory.

Tartrazine (15) has been recently recommended for the direct weighing of zirconium. The zirconium is precipitated at 80° C from chloride or nitrate solutions at pH 1; the factor used was for a compound with the formula Zr_3 (tartrazine)(OOH)$_3$. In view of the ease of hydrolysis of zirconium solutions and the failure to obtain precipitates of constant composition by well-known reagents under these conditions, further confirmation on the usefulness of this reagent is necessary.

The zirconium precipitates obtained with benzoylphenylhydroxylamine from 5% hydrochloric acid solutions are stable but are not of a constant composition; as expected, compounds precipitated from chloride solutions of zirconium at this acidity are not suitable for direct weighing. From sulphuric acid solutions, however, complexes having the composition $(C_{13}H_{11}O_2N)_4Zr$ are obtained and precipitation is complete at acidities up to 0.5 N; apparently the sulphate complexes of zirconium prevent the formation of unwelcome basic salts and permit compounds of unvarying composition to be precipitated. Mandelic acid, used subsequently in these solutions, gives also zirconium complexes suitable for direct weighing.

Procedure

2. Direct Weighing of Zirconium Complex with Benzoylphenylhydroxylamine

Samples of zirconium sulphate standard solution were diluted to 100–150 ml and the solutions made not more than 0.5 N in sulphuric acid. Reagent, in slight excess (not more than 40 mg for every 100 ml of solution) of the theoretical quantity required for the zirconium present, was added dropwise with stirring and the solutions digested on the steam bath for an hour. The samples, after cooling, were filtered through porous-

based porcelain crucibles and washed with cold water. The precipitates were then washed with two or three 5-ml aliquots of hot water (80° C) and dried at 110° C. The weight of the complex was multiplied by the theoretical factor 0.0970 to obtain the weight of zirconium. Results are shown in Table II.

TABLE II

Direct weighing of zirconium complex with benzoylphenylhydroxylamine

No.	Zr taken, mg	Zr found, mg	Remarks
1	8.38	8.36	—
2	8.41	8.42	—
3	8.41	8.41	—
4	8.41	8.45	—
5	8.41	8.38	Solution 0.7 N in H_2SO_4; 7.84 mg found after usual digestion period but an additional 0.54 mg precipitated from filtrate after standing overnight
6	16.76	16.75	—
7	16.82	16.85	—
8	25.23	25.23	—
9	0.85	0.70	Solution volume 50 ml; usual digestion period before filtering
10	0.51	0.51	As sample No. 9 but digested overnight
11	0.17	0.15	As sample No. 9 but digested overnight

The results show that benzoylphenylhydroxylamine is a suitable reagent for the direct weighing of zirconium when applied to dilute sulphuric acid solutions. Complete precipitation of the zirconium is possible from 0.7 N H_2SO_4 solutions, but at acidities greater than 0.5 N an overlong digestion period is necessary. Results 9, 10, and 11 show that a prolonged digestion period is required for solutions containing very small amounts of zirconium.

From 5% hydrochloric acid, although precipitation is complete, the weights of complex obtained are low and the compositions vary with the amount of zirconium present in solution; for 8.42 mg of zirconium, in one instance, the weight of complex found was 0.0845 g (theoretical 0.0868) and for 21.05 mg of zirconium was 0.2063 g (theoretical 0.2170). Since degree of hydrolysis in zirconium solutions is dependent on time, temperature, and acid present, these results are undoubtedly due to simultaneous precipitation of varying amounts of basic salts; a distinct cloudiness, for example, develops on heating 5% hydrochloric acid solutions of zirconium oxychloride for less than an hour on the hot plate.

From sulphuric acid solutions, zirconium complexes suitable for direct weighing are also precipitated by mandelic acid. A typical result obtained for 8.41 mg taken was 8.42 mg, the weight of mandelic acid complex (precipitated from 0.5 N sulphuric acid solution) being 0.0643 g.

Mandelic acid and its derivatives, although undoubtedly the most useful of the organic reagents used for zirconium, have been criticized (16) because of their non-sensitivity and the large amounts of reagent thus required for each precipitation. It is worth while noting, therefore, that benzoylphenylhydroxylamine detects as little as 0.1 mg of zirconium in 100 ml of solution and quantitative precipitation of 0.2 mg is possible.

REFERENCES

1. S. C. Shome. Analyst, 75, 27 (1950).
2. D. E. Ryan and G. D. Lutwick. Can. J. Chem. 31, 9 (1953).
3. S. C. Shome. Anal. Chem. 23, 1186 (1951).
4. D. E. Ryan. Analyst, 85, 569 (1960).
5. R. W. Moshier and J. E. Schwarberg. Anal. Chem. 29, 947 (1957).
6. A. K. Majumdar and A. K. Mukherjee. Anal. Chim. Acta, 19, 23 (1958).
7. F. J. Langmhyr and T. Hongslo. Anal. Chim. Acta, 22, 301 (1960).
8. G. D. Lutwick and D. E. Ryan. Can. J. Chem. 32, 949 (1954).
9. C. A. Armour and D. E. Ryan. Can. J. Chem. 35, 1454 (1957).
10. G. Balanescu. Z. anal. Chem. 101, 101 (1935).
11. R. E. Oesper and J. J. Klingenberg. Anal. Chem. 21, 1509 (1949).
12. R. Belcher, A. Sykes, and J. C. Tatlow. Anal. Chim. Acta, 10, 34 (1954).
13. A. A. Astanina, and E. A. Ostroumov. J. Anal. Chem. U.S.S.R. 6, 27 (1951).
14. R. B. Hahn and E. S. Baginsky. Anal. Chim. Acta, 14, 45 (1956).
15. Gh. Baiulescu and L. Turcu. Anal. Chim. Acta, 21, 33 (1959).
16. P. S. Marty and Bh. S. V. R. Rao. Z. anal. Chem. 141, 93 (1954).

THE APPLICATION OF THE HAMMETT EQUATION TO
ORTHO-SUBSTITUTED BENZENE REACTION SERIES[1]

Marvin Charton

ABSTRACT

The Hammett equation is directly applicable to ortho-substituted benzene reaction series in which reaction site and benzene ring are separated by some group Z, apparently due to the absence of steric effects in these series. The σ_p values are used in the correlations. Fourteen ortho-substituted benzene reaction series have been correlated. The electrical effect of a substituent in the ortho position is found to be about 0.75 times its effect in the para position. The effect of the side-chain Z in the transmission of substituent effects is $OCH_2 > SCH_2 > CH=CH > SeCH_2 > CH_2CH_2$.

INTRODUCTION

Linear free-energy relationships have been shown to be of great value for the correlation of reaction rates, equilibria, and physical properties with variations in structure. The Hammett equation,

$$[1] \qquad \log(K_X/K_H) = \rho\sigma_X,$$

has been widely applied to meta- and para-substituted benzene reaction series (2, 3) and to olefins (4, 5) and acetylenes (6). In modified form, it has been applied to aliphatic and to ortho-substituted benzene reaction series (7). Direct application of the Hammett equation to ortho-substituted benzene derivatives is unsuccessful, due to steric effects. Taft (7) has been able to correlate a few ortho-substituted benzene reaction series by an approach which is dependent upon the elimination of the steric effect in the evaluation of the substituent constants. Mammalis and Rydon (8) have suggested that substituent constants for ortho substituents be defined from reaction series in which the reaction site is not adjacent to the substituent. It has been suggested by a number of authors that the inductive and resonance effects of an ortho substituent are similar to those of the same substituent in the para position. It is of interest to compare the $\sigma_o{}^*$ substituent constants obtained by Taft (7), by elimination of steric effects, with the σ_p substituent constants. Considering the degree of uncertainty in the values of substituent constants, they are almost identical. These results suggested the possibility of direct application of the Hammett equation, using the σ_p substituent constants, to ortho-substituted benzene reaction series in which the reaction site is not directly attached to the ring (I). As the reaction site and substituent are not adjacent in such reaction series, hydrogen bonding and other secondary bonding interactions between them cannot occur, and no hindrance to the attack of reagent should exist. The literature was searched for reaction series of this type. Fourteen such reaction series have been examined, seven involving equilibrium data and seven involving rate data. The correlations were made by the method described by Jaffé.
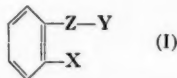
$$\text{(I)}$$

RESULTS AND DISCUSSION

Data and Correlations

The data used in the correlations are given in Table I. The substituent constants used are those given by Jaffé (3) and by McDaniel and Brown (9) except for the carbomethoxy group, which was taken from Charton and Meislich (4). A statistical factor of 1/2 was used in reaction series 12 for methyl phthalate to account for the presence of two potential reaction sites. The results of the correlation are shown in Table II; Figs. 1 and 2 are typical curves.
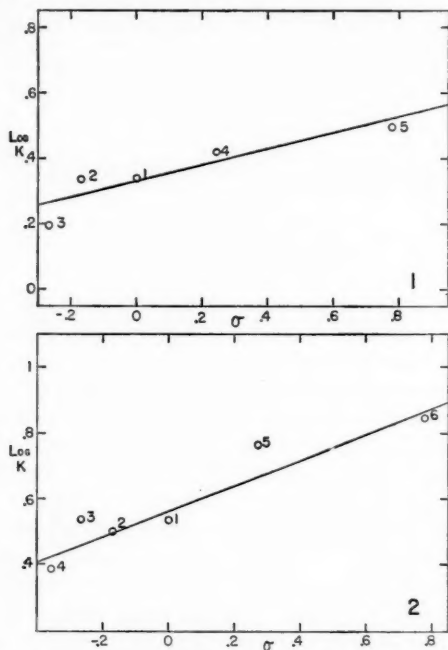
FIG. 1. Hammett equation plot of log $10^5 K$ vs. σ for 3-(2'-substituted)phenyl propanoic acids. The substituents are: 1, H; 2, Me; 3, MeO; 4, Cl; 5, NO$_2$.

FIG. 2. Hammett equation plot of log $10^5 K$ vs. σ for *trans*-2-substituted cinnamic acids. The substituents are: 1, H; 2, Me; 3, OMe; 4, OH; 5, Cl; 6, NO$_2$.

The results of the correlations are as good as those generally obtained for meta- and para-substituted benzene reaction series. Of the 14 reaction series examined, six show fair correlation ($0.90 \leqq r \leqq 0.95$), five show good correlation ($0.95 \leqq r \leqq 0.99$), and three show excellent correlation ($0.99 \leqq r$), according to the empirical scale proposed by Jaffé (3, 18). Jaffé (3) has pointed out that the correlation coefficients decrease with decreasing absolute values of ρ. Of the six reaction series which had fair correlation, the value of ρ_0 (19) was less than 0.400 in five (20).

Structural Requirements for Correlation

Apparently, the side-chain Z must consist of at least two atoms, for satisfactory correlation to result. No satisfactory correlation is obtained in the case of the ionization constants of 2-substituted phenylacetic acids, however, although the available data (for

$X = H$, Cl, Br, I, NO₂) is insufficient to support a conclusive statement. Examination of the Stuart–Briegleb models for this reaction series, and for others in which the side chain is a methylene group indicates the possibility of considerable interaction between the substituent and the reaction site.

TABLE I
Rate and equilibrium data

1. Ionization constants of 3-(2-substituted)phenyl propanoic acids in water at 25° C

Subst.	H	Me	MeO	Cl	NO₂	Ref.
$10^5 K$	2.19	2.17	1.57	2.65	3.13	10a, 10b

2. Ionization constants of *trans*-2-substituted cinnamic acids in water at 25° C

Subst.	H	Me	MeO	OH	Cl	NO₂	Ref.
$10^5 K$	3.65	3.165	3.45	2.44	5.83	7.07	10c

3. Ionization constants of 2-substituted propiolic acids in 35% dioxane–water at 25° C

Subst.	H	Cl	NO₂	OMe	Ref.
$10^4 K$	5.8	8.3	15.0	4.3	11

4. Ionization constants of 2-substituted phenoxyacetic acids in water

Subst.	MeO	Me	Cl	NO₂	Ref.
$10^4 K$	5.8	6.8	10.2	15.8	12

5. Ionization constants of 2-substituted phenylthioacetic acids in water

Subst.	MeO	Me	Cl	NO₂	Ref.
$10^4 K$	1.8	2.8	3.0	5.5	12

6. Ionization constants of 2-substituted phenylselenoacetic acids in water

Subst.	MeO	Me	Cl	NO₂	Ref.
$10^4 K$	1.4	1.5	2.3	3.2	12

7. Ionization constants of 2-substituted benzohydroxamic acids in 0.1 M KNO₃ at 30° C

Subst.	H	MeO	NH₂	Me₂N	NO₂	Ref.
$10^9 K$	15.9	12.6	10.0	8.91	63.1	13a

8. Rates of acid-catalyzed esterification of 2-substituted propiolic acids in methanol at 35° C

Subst.	H	Cl	NO₂	OMe	Ref.
$10^4 k$	5.3	4.8	4.1	7.3	11

9. Rates of acid-catalyzed esterification of 2-substituted propiolic acids in methanol at 35° C

Subst.	H	Cl	NO₂	OMe	Ref.
$10^4 k$	11.7	11.2	9.3	16.3	11

10. Rates of alkaline hydrolysis of 2-substituted cinnamic acid ethyl esters in 87.83% aqueous ethanol at 30° C

Subst.	H	OMe	F	Cl	Br	I	NO₂	Ref.
$10^2 k$	10.6	3.99	2.48	21.1	32.5	2.67	84.1	14a, 14b

11. Rates of reaction of 2-substituted benzohydroxamic acids with sarin in water at 30.5° C

Subst.	H	OMe	NH₂	Me₂N	NO₂	Ref.
k	2.61	21.1	35.3	37.5	7.4	13a

12. Rates of reaction of 2-substituted methyl benzoates with trimethylamine

Subst.	H	Me	Cl	CO₂Me	NO₂	Ref.
$10^2 k$	1.609	1.66	7.27	12.43	33	16

13. Rates of alkaline fission of 2-substituted benzoyloxymethyl dimethyl sulphinium iodides

Subst.	H	Me	OMe	Cl	NO₂	Ref.
k	356.5	314.1	291.1	673	1242	8

14. Rates of rearrangement of N-2-substituted benzyl-N-phenacyl-N,N-dimethyl quaternary ammonium halides at 16.4° C

Subst.	Me	OMe	Cl	Br	I	NO₂	Ref.
k	1.58	1.63	36.7	49.1	83.0	1070	15, 17

NOTE: Units of k are (a) l. mole⁻¹ sec⁻¹; (b) l. mole⁻¹ min⁻¹; (c) l. mole⁻¹ hr⁻¹.

The Effect of Side Chain on Transmission of Substituent Effect

A comparison of the ρ_o values obtained from the correlation of ortho-substituted benzene reaction series with the ρ values for the corresponding meta- and/or para-substituted benzene reaction series may be used to determine variation in transmission

of substituent effects through different side chains. The ratio of the $\rho_{o,Z}$ value for some side-chain Z to that for the CH_2CH_2 side chain, ρ_{o,Z^0}, for a given reaction under identical reaction conditions, provides a method of making such comparisons (3). Those values of ρ, r, s, n, and $-\log K$ for the corresponding meta- and/or para-substituted reaction series which are available are given in Table II.

Thus,

[2]
$$\rho_{oZ}/\rho_{oZ^0} = q_o, \qquad \rho_Z/\rho_{Z^0} = q.$$

Values of q_o obtained from reaction series 1, 2, 4, 5, and 6 are shown in Table II. The values for the OCH_2, SCH_2, and $SeCH_2$ groups are of about the same order of magnitude as that for the $CH=CH$ group, and increase in order of increasing electronegativity of the group VI element. This might be explained in the case of the SCH_2 and $SeCH_2$ groups by hyperconjugation and an expansion of the S or Se valence shell from an octet to a decet, but such an explanation is, of course, not possible for the OCH_2 group, which exhibits the greatest transmission of the substituent effect.

The values of q for the corresponding meta- and/or para-substituted reaction series are also given in Table II. It is notable that although the distance between the reaction site and the substituent is greater for meta- and para-substituted compounds than it is for ortho-substituted compounds, it appears that the effect of the substituent is not transmitted to the reaction site to as great an extent in the ortho-substituted reaction series as it is in the meta- and para-substituted reaction series. Transmission through the side chain from the limited data available appears to be about 1.5 times as effective for meta- and para-substituted compounds as for ortho-substituted compounds. This might be due to some distortion of the bond angle in the ortho-substituted reaction series which decreases the overlap of the p orbitals in O, S, and Se, or the π orbital of the $CH=CH$ group, with the π orbital of the ring.

The Magnitude of the Electrical Effect of an Ortho Substituent

In the absence of steric effects and secondary bonding,

[3]
$$\sigma_{oX} = C\sigma_{pX}.$$

The correlations made in this paper have used the Hammett equation in the following form,

[4]
$$\log(K_{oX}/K_H) = \rho_o\sigma_{pX}.$$

If the substituent constants for ortho substituents were available, then assuming steric effects are nonexistent, ortho-, meta-, and para-substituted benzene reaction series would be included in a single correlation with the same value for ρ. Thus

[5]
$$\log(K_{o,m,p\ X}/K_H) = \rho\sigma_{o,m,p\ X}$$

or considering only ortho substitution,

[5a]
$$\log(K_{oX}/K_H) = \rho\sigma_{oX}.$$

To a good first approximation, steric effects will not exist in ortho-substituted benzene reaction series of type I, and therefore use of equation 5a is justified for these reaction series. It is, of course, not applicable to ortho-substituted benzene reaction series in which the substituent and reaction site are directly attached to the ring.

TABLE II

Reaction series[a]	ρ_o[b]	r_o[c]	s_o[d]	$-\log K_{Ho}$	n_o[e]	ρ	r	s	n	$-\log K_H$ calc.	Ref.[f]	Z	g_o	q	g_o/q
1	0.243	0.905	0.055	4.669	5	0.212	0.979	0.016	8	4.551	3	CH_2CH_2	1	1	—
2	0.389	0.940	0.0661	4.413	6	0.466	0.977	0.040	9	4.447	3	$CH{=}CH$	1.60	2.20	1.38
3	0.524	0.997	0.019	3.223	4	—	—	—	—	—	11	—	—	—	—
4	0.408	0.994	0.0245	3.107	4	0.561	0.922	0.139	7	1.644	g	OCH_2	1.68	2.65	1.63
5	0.395	0.943	0.0824	3.576	4	0.419	0.930	0.209	5	1.873	g	SCH_2	1.63	1.98	1.38
6	0.351	0.990	0.0282	3.752	4	0.977	0.999	0.016	5	8.773	13b	$SeCH_2$	1.44	—	—
7	0.576	0.977	0.0839	7.704	5	−0.44	—	—	6	—	11	—	—	—	—
8	−0.221	0.928	0.0485	3.239	4	−0.44	—	—	7	—	11	—	—	—	—
9	−0.211	0.924	0.0474	2.887	4	1.329	0.996	0.046	7	—	3	—	—	—	—
10	1.211	0.941	0.153	0.911	7	−0.762	0.996	0.035	15	2.752	13b	—	—	—	—
11	−0.467	0.954	0.0986	−1.416	5	—	—	—	—	−1.328	—	—	—	—	—
12	1.394	0.955	0.185	1.634	5	0.768	0.987	0.050	6	—	8	—	—	—	—
13	0.636	0.984	0.0557	−1.968	5	—	—	—	—	—	—	—	—	—	—
14	2.376	0.962	0.266	2.823	6	—	—	—	—	—	—	—	—	—	—

[a]These numbers refer to Table I.
[b]The subscript "o" designates values for ortho-substituted reaction series, other values are for meta- and/or para-substituted reaction series.
[c]Correlation coefficient.
[d]Standard deviation.
[e]Number of compounds in series.
[f]References are for ρ, r, s, n, and $\log K_H$ calc. taken from the literature.
[g]Calculated from data of ref. 12.

From equations 2, 4, and 5a, equation 6 is obtained

[6] $$C = \rho_0/\rho$$

where C represents approximately the electrical effects of a substituent in the ortho position as compared with its electrical effects in the para position. Actually, C is subject to variations in ρ_0 due to phenomena such as a bulk effect between the ortho substituent and the side-chain Z which may cause decreased orbital overlap in unsaturated side chains, and to variations in solvation as compared with meta- and para-substituted benzene reaction series. Values of C obtained from those reactions series for which both ρ_0 and ρ are available are shown in Table II. Although the values of C vary considerably, they are all of the same order of magnitude, and in view of the uncertainties inherent in ρ values, the variation found is reasonable. The magnitude of $\bar{C}$ shows that the electrical effects of a substituent in the ortho and in the para positions are of the same order of magnitude.

TABLE III

Reaction series C		Reaction series C	
1	1.147	7	0.590
2	0.835	8	0.500
3	0.646	9	0.480
5	0.704	10	0.913
6	0.838	11	0.613
$\bar{C} = 0.736$		13	0.830

SUMMARY

On the basis of the above results, ortho-substituted benzene reaction series in which substituent and reaction site are not adjacent, can be correlated directly by the Hammett equation using the σ_p substituent constants. Ortho substituents in such reaction series have the same type of electrical effects as para substituents. These effects are about the same order of magnitude for ortho as for para substituents. Steric effects are largely absent for these reaction series.

REFERENCES

1. M. CHARTON. Abstracts, 134th Meeting of the American Chemical Society, Chicago, Ill. September, 1958. p. 9P.
2. L. P. HAMMETT. Physical organic chemistry. McGraw-Hill Book Co., Inc., New York. 1940. pp. 118–123, 173.
3. H. H. JAFFÉ. Chem. Revs. **53**, 191 (1953).
4. M. CHARTON and H. MEISLICH. J. Am. Chem. Soc. **80**, 5940 (1958).
5. M. CHARTON. Abstracts, 132nd Meeting of the American Chemical Society, New York. September, 1957. p. 78P.
6. M. CHARTON. Unpublished results.
7. R. W. TAFT. *In* Steric effects in organic chemistry. *Edited by* M. S. NEWMAN. John Wiley & Sons Inc., New York. 1957. p. 556.
8. P. MAMMALIS and H. N. RYDON. J. Chem. Soc. 1049 (1955).
9. D. H. MCDANIEL and H. C. BROWN. J. Org. Chem. **23**, 420 (1958).
10a. J. F. J. DIPPY and R. H. LEWIS. J. Chem. Soc. 1008 (1937).
10b. J. F. J. DIPPY and J. E. PAGE. J. Chem. Soc. 357 (1938).
10c. J. F. J. DIPPY and R. H. LEWIS. J. Chem. Soc. 1426 (1937).
11. M. S. NEWMAN and S. H. MERRILL. J. Am. Chem. Soc. 77, 5552 (1955).
12. O. BEHAGEL and M. ROLLMANN. Chem. Ber. **62**, 2693 (1929).
13a. M. A. STOLBERG and W. A. MOSHER. J. Am. Chem. Soc. **79**, 2618 (1957).
13b. R. SWIDLER, R. E. PLAPINGER, and G. M. STEINBERG. J. Am. Chem. Soc. **81**, 3271 (1959).
14a. K. KINDLER. Ann. **452**, 90 (1927).
14b. K. KINDLER. Ann, **464**, 278 (1928).
15. T. THOMSON and T. S. STEVENS. J. Chem Soc. 55 (1932)

16. L. P. HAMMETT and H. PFLUGER. J. Am. Chem. Soc. **55**, 4079 (1933).
17. T. THOMSON and T. S. STEVENS. J. Chem. Soc. 55 (1932), reported that 12–15% of a by-product which could not be further characterized was found in this reaction. They claimed to have developed an analytical method which allowed determination of both rearrangement products and unreacted starting material without interference from the by-product. For a further discussion of the results of these authors see J. H. BREWSTER and M. W. KLINE. J. Am. Chem. Soc. **74**, 5179 (1952).
18. It has also been suggested that for $r > 0.90$ correlation is very poor, for $r > 0.95$ correlation is fair.
19. ρ_o will be used to denote rho for the ortho-substituted benzene reaction series obtained by correlation with σ_p values. ρ will be used to denote rho for the meta- and/or para-substituted benzene reaction series obtained by correlation with the appropriate σ_m or σ_p constants.
20. One of the referees has pointed out that Wepster has shown one group ortho to a bulky substituent to be sufficient to appreciably decrease resonance interaction between the substituent and the benzene ring (B. M. WEPSTER. Progress in stereochemistry. Vol. II. Butterworth Scientific Publications, London. 1958. p. 99). This is a likely cause of the poorer results obtained in some of the correlations.

CONJUGATED FATTY ACIDS OF TRAGOPOGON AND CALENDULA SEED OILS[1]

MARY J. CHISHOLM AND C. Y. HOPKINS

ABSTRACT

The seed oil of *Tragopogon porrifolius* L. was found to contain about 4% of conjugated diene hydroxy fatty acids, identified as 9-hydroxy-10,12- and 13-hydroxy-9,11-octadecadienoic acids. On dehydration, the products were 8,10,12- and 9,11,13-octadecatrienoic acids. The diene acids were *cis,trans* or *trans,cis* and the triene acids were judged to be all-*trans*.

The conjugated triene acid of *Calendula officinalis* L. seed oil was isolated and identified as *trans*,8:*trans*,10:*cis*,12-octadecatrienoic acid by spectral analysis, by the structure of the maleic anhydride adduct, and by identification of degradation products. All-*trans*-8,10,12-octadecatrienoic acid was found to react with maleic anhydride at both the 8,11 and 10,13 positions.

INTRODUCTION

During the isolation of an epoxy fatty acid from the seed oil of *Tragopogon porrifolius* L. (family Compositae) (1) it was observed that a small proportion of an unsaturated acid of unusual characteristics was also present. It amounted to about 4% of the total fatty acids and had a conjugated diene linkage. On heating with glacial acetic acid it was converted to a conjugated triene acid. Both the diene and triene acids were unstable. Their structures were determined as described below, each proving to be a mixture of two position isomers.

The diene acids were found to have a hydroxy group and were identified as 9-hydroxy-10,12-octadecadienoic acid and 13-hydroxy-9,11-octadecadienoic acid. The triene acids were identified as 8,10,12- and 9,11,13-octadecatrienoic acids.

A naturally occurring triene acid was isolated from the seed oil of *Calendula officinalis* L. (family Compositae) and shown to be *trans*,8:*trans*,10:*cis*,12-octadecatrienoic acid. The isomerized form (all-*trans*) of this acid had been prepared previously by McLean and Clark from the same species (2). The configuration of the natural acid (*trans,trans,cis*) is opposite to that of α-eleostearic acid (*cis,trans,trans*).

Shortly after this work was completed, Morris, Holman, and Fontell reported the occurrence of two hydroxy diene acids in the seed oils of certain other species, apparently identical with the hydroxy acids described herein (3). Their evidence, based on spectral data and thin-layer chromatography, is in agreement with ours, which is based on spectral data and chemical degradative results. All of the results lead to the conclusion that the substances are 9-hydroxy-10,12- and 13-hydroxy-9,11-octadecadienoic acids.

RESULTS AND DISCUSSION

Conjugated Acids of Tragopogon Oil

The oil had ultraviolet absorption characteristic of diene conjugation, indicating the presence of about 4% of a diene acid, based on the total fatty acids. There was no appreciable triene absorption. After saponification in the cold and removal of unsaponifiable matter, the fatty acids were partitioned between petroleum ether and aqueous ethanol (1 volume, H_2O: 4 volumes EtOH). The alcoholic portion contained both diene acid and epoxy acid in about equal amounts. Further partitioning and crystallization from acetone

at low temperature yielded a concentrate consisting mainly of conjugated diene acid (ultraviolet max. 233 mμ). It had infrared absorption at 3580 cm^{-1}, indicating an hydroxyl group, and two peaks of nearly equal intensity at 945 and 980 cm^{-1}, characteristic of a conjugated *cis,trans* or *trans,cis* diene (4).

The substance was subjected to oxidative splitting by periodate–permanganate (5) and the acidic products were converted to methyl esters, avoiding loss of volatile components (6). The mixture of methyl esters was examined by gas chromatography. Peaks corresponding to hexanoate and azelate were observed, indicating unsaturated centers at the 12,13 and 9,10 positions, respectively. Since these could not both be present in one conjugated diene acid, it is concluded that the substance was a mixture of two acids, one being $\Delta^{9,11}$ and the other $\Delta^{10,12}$. Neither heptanoic nor sebacic esters appeared, hence the hydroxyl group must have been attached to the terminal fragment in the 9,11 acid and to the carboxyl fragment in the 10,12 acid (III, I).

Boiling the hydroxy diene acid mixture with glacial acetic acid gave a solid acid (or acids), shown by spectral analysis to have a conjugated triene structure and no hydroxyl group. This substance absorbed 3 moles of hydrogen to give stearic acid, hence it had a straight chain of 18 carbon atoms. The triene acid was split by periodate–permanganate and the fragments were shown by gas chromatography to consist of valeric, hexanoic, suberic, and azelaic acids. The substance was therefore a mixture of two octadecatrienoic acids (II and IV) having double bonds in the 8,10,12 and 9,11,13 positions, respectively.

$$CH_3(CH_2)_4CH{=}CHCH{=}CHCH(CH_2)_7COOH \tag{I}$$
$$\big| \qquad OH$$

$$CH_3(CH_2)_4CH{=}CHCH{=}CHCH{=}CH(CH_2)_6COOH \tag{II}$$

$$CH_3(CH_2)_4CHCH{=}CHCH{=}CH(CH_2)_7COOH \tag{III}$$
$$\big|\ OH$$

$$CH_3(CH_2)_3CH{=}CHCH{=}CHCH{=}CH(CH_2)_7COOH \tag{IV}$$
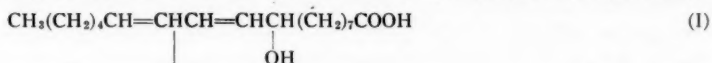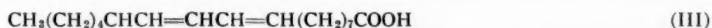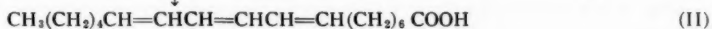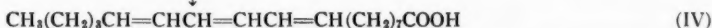
This result confirms the positions of the two double bonds in the diene acids as reported above (10,12 and 9,11). It also provides evidence for the location of the hydroxyl group. Thus, in the 10,12-diene acid, the hydroxyl group must be attached to carbon 8 or 9 to produce an 8,10,12-triene. Because of the ease with which dehydration takes place, it is almost certain that the hydroxyl is at position 9, where it is activated by the adjacent double bond (I). By similar reasoning, the 9,11-diene acid is considered to have the hydroxyl at position 13 (III), giving the 9,11,13-triene on dehydration. 9-Hydroxy-10,12-octadecadienoic is evidently a geometric isomer of dimorphecolic acid, discovered by Smith and co-workers (7), in which the double bonds are *trans,trans*, and which underwent dehydration with the same readiness.

Confirmation of the position of the hydroxyl group was obtained by hydrogenating the mixture of hydroxy diene acids. The product melted at 65–66° and appeared to be a mixture of monohydroxystearic acids. Oxidative splitting by solid permanganate in acetic acid was performed first on a model substance, 12-hydroxystearic acid. The fragments therefrom, identified by gas chromatography, were hexanoic, heptanoic, undecanedioic, and dodecanedioic acids. Thus splitting took place at two positions, 11,12 and 12,13. Minor proportions of azelaic and sebacic acids were also produced. Applying this procedure to the hydrogenated acids gave four monobasic acids, pentanoic, hexanoic, nonanoic, and decanoic (Table I), hence the original hydroxyl group must have been on the 13th

TABLE I

Oxidative splitting of hydrogenated acids

$CH_3(CH_2)_4\underset{\underset{OH}{\mid}}{CH}(CH_2)_{11}COOH \rightarrow$	$\begin{array}{l} CH_3(CH_2)_3COOH \\ CH_3(CH_2)_4COOH \end{array}$	$+$	$\begin{array}{l} HOOC(CH_2)_{11}COOH \\ HOOC(CH_2)_{10}COOH \end{array}$
$CH_3(CH_2)_8\underset{\underset{OH}{\mid}}{CH}(CH_2)_7COOH \rightarrow$	$\begin{array}{l} CH_3(CH_2)_7COOH \\ CH_3(CH_2)_8COOH \end{array}$	$+$	$\begin{array}{l} HOOC(CH_2)_7COOH \\ HOOC(CH_2)_6COOH \end{array}$

carbon atom in one acid (III) and on the 9th carbon atom in the other (I). There were minor amounts of heptanoic and octanoic acids. One pair of the corresponding dibasic acids was identified, viz. suberic and azelaic, both in substantial amount. The C_{12} and C_{13} dibasic acids were in smaller amount, apparently having been partially degraded by the oxidizing agent, as occurred in the oxidation of 12-hydroxystearic acid.

The two hydroxy diene acids appeared to be present in about equal amounts in the original oil. This was determined from the relative amounts of the respective fragments of the oxidized hydroxy diene acids and of the oxidized triene acids, estimated from the gas chromatograms.

The possible presence of 11-hydroxy-9,13-octadecadienoic acid was considered but was judged unlikely. Oxidation of the hydrogenated hydroxy acids gave no sebacic acid, one of the expected products from 11-hydroxystearic acid.

The concentrate of the hydroxy diene acids had infrared maxima of nearly equal intensity at 945 and 980 cm^{-1} (Fig. 1). By analogy with the spectra of the simple conjugated diene acids (4), this is strong evidence that both hydroxy acids are mainly, if not entirely, *cis,trans* or *trans,cis* in configuration. The mixture of the two triene acids obtained on dehydration, however, had a single strong infrared band at 990 cm^{-1} and no other maxima in the 900–1000 cm^{-1} region. It is concluded that these acids are all *trans*. Since the diene acids had one *trans* bond and dehydration may be expected to produce a second *trans* bond, the original *cis* bond must have isomerized spontaneously to *trans* during the dehydration to give the all-*trans* triene product. The all-*trans* structure was confirmed when an attempt to isomerize it by iodine in pentane produced no change in melting point or other properties.

Conjugated Acid of Calendula Oil

Saponification of calendula oil and crystallization of the acids from acetone at low temperature yielded a conjugated triene acid, $C_{18}H_{30}O_2$, as determined by elementary analysis and ultraviolet absorption. It gave stearic acid on hydrogenation. Oxidative splitting of the triene acid gave hexanoic and suberic acids, identified by gas chromatography. The double bonds must have been, therefore, at positions 8, 10, and 12 (V).

The infrared spectrum prepared from a solid film of the acid had a very strong peak at 990 cm^{-1} and a medium strong band at 940–975 cm^{-1}. The solution spectrum, in CS$_2$, had maxima at 987 (vs), 955 (m), and 920 cm^{-1} (m). This type of spectrum suggests a grouping of two *trans* and one *cis* bond, although it is not exactly the same as that of α-eleostearic acid (8). The ultraviolet spectrum showed maxima at 262, 272, and 283 mμ, also indicative of two *trans* and one *cis* bond in conjugation, by analogy with α-eleostearic acid (8, 9).
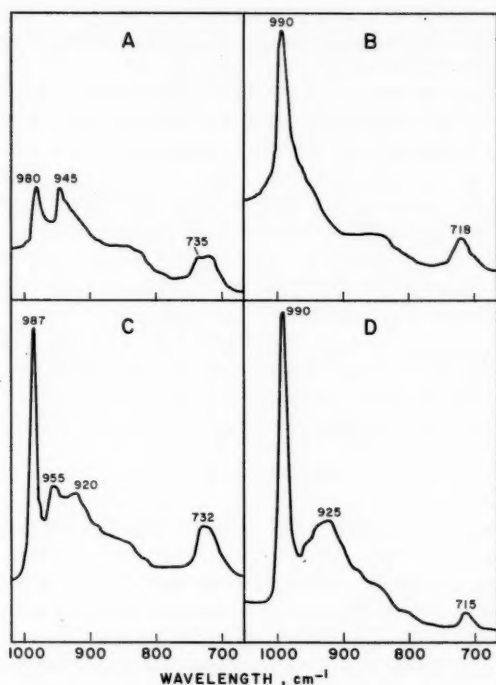
FIG. 1. Infrared spectra, between 700 and 1000 cm^{-1}, determined in CS$_2$ solution. A, concentrate of hydroxy diene acids from tragopogon; B, methyl esters of triene acids obtained by dehydration of the hydroxy diene acids; C, triene acid from calendula; D, all-*trans* isomer of triene acid from calendula.

The acid reacted readily with maleic anhydride and the adduct was easily purified, showing the presence of two adjacent *trans* double bonds. On splitting the adduct by permanganate–periodate, only one straight chain acid was obtained as a major product. It was identified by gas chromatography as hexanoic acid. There was only a trace of suberic acid. Thus the adduct must have been formed by reaction at the 8 and 11 positions, leaving the 12,13 double bond free (VI).

$$CH_3(CH_2)_4 \ \overset{c}{CH}{=}CHCH\overset{t}{=}CHCH\overset{t}{=}CH(CH_2)_6 \ COOH \qquad (V)$$
maleic
anhydride

$$CH_3(CH_2)_4 \ CH{=}CHCHCH{=}CHCH \ (CH_2)_6 \ COOH \qquad (VI)$$
$$CH\text{------}CH$$
$$OC\text{----}O\text{----}CO$$
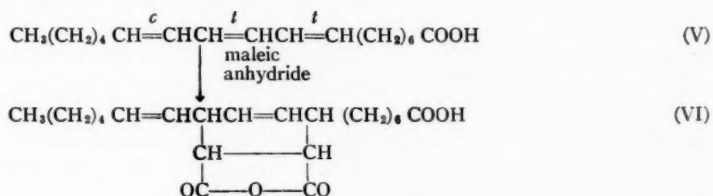
The infrared spectrum of the adduct (VI) had no peak in the region 950–975 cm^{-1} and hence no *trans* exocyclic double bond. The 12,13 double bond was therefore *cis* and the original acid was *trans*,8:*trans*,10:*cis*,12-octadecatrienoic acid. The reasoning is similar to that employed by Paschke and co-workers in determining the configuration

of the eleostearic acids (10). The maleic anhydride adduct of all-*trans*-8,10,12-octadeca-trienoic acid was prepared for comparison. Its infrared spectrum had a peak at 963 cm^{-1} (*trans* exocyclic double bond).

The *trans*,8:*trans*,10:*cis*,12 acid, m.p. 40–40.5°, was readily converted to the all-*trans* form, m.p. 77–78°, by treatment with iodine in pentane. The infrared spectrum (CS_2 solution) had a strong single peak at 990 cm^{-1}, indicative of the all-*trans* structure, and very little absorption in the vicinity of 950 cm^{-1}. An all-*trans* conjugated triene acid may be expected to react with maleic anhydride in two ways. Thus, Bickford and co-workers found evidence that addition occurs to β-eleostearic acid at both the 9,12 and 11,14 positions (11). In the present work, proof was obtained that two different adducts are formed in the reaction of all-*trans*-8,10,12-octadecatrienoic acid with maleic anhydride. The reaction product was oxidized by permanganate–periodate and the fragments were examined by gas chromatography. Both hexanoic acid and suberic acid were found in substantial amounts, showing that addition of maleic anhydride had occurred at the 10,13 as well as the 8,11 positions, forming two separate adducts.

The name calendic acid is proposed for *trans*,8: *trans*,10: *cis*,12-octadecatrienoic acid.

EXPERIMENTAL

Methods

Infrared spectral data were obtained with a Perkin–Elmer Model 21 infrared spectro-photometer with sodium chloride prism. Samples were in carbon disulphide solution unless stated otherwise. Ultraviolet measurements were made in cyclohexane or isooctane solution. Gas–liquid chromatography of methyl esters was conducted at various column temperatures from 70° to 170°, according to the chain length of the sample. The detector was a thermistor type of thermal conductivity cell. Column length was 1 meter, helium flow rate 95 ml/min, and inlet pressure 7 to 12 p.s.i., depending on the column tempera-ture. Identification of the various esters was made by comparing the emergence time with that of a standard sample of the same ester under the same conditions on the same day.

TRAGOPOGON OIL

Seed of *Tragopogon porrifolius* L. was purchased from a commercial seed house. It was of the current year's stock. The seed (450 g) was ground and extracted with petroleum ether by stirring with successive lots of the solvent at room temperature. The solvent was removed at 25–30° under nitrogen. The oil had ultraviolet absorption maximum at 233 mμ, $E_{1 cm}^{1\%}$ 47.5, equivalent to 4.0% conjugated octadecadienoic acid based on the total fatty acids. There was no measurable absorption at 268 mμ (conjugated triene).

The oil (83 g) was saponified at room temperature (25°) by letting it stand for 18 hours with a solution of 25 g of potassium hydroxide in 500 ml of ethanol. The unsaponi-fiable matter was removed by extraction and the fatty acids were partitioned between petroleum ether and ethanol:water (4 volumes EtOH:1 volume H_2O). The partitioning was carried out in three stages and the products recovered from the alcohol portions were analyzed for conjugated diene by ultraviolet absorption and for oxirane oxygen by Swern's method (12) with the following results:

Portion	Wt. of acids, g	Conjugated diene acid, %	Oxirane oxygen, %
1	7.0	32.0	2.1
2	7.2	8.7	1.2
3	4.4		0.7

The acids from the first portion were estimated to contain 32% conjugated diene acid and 37% epoxy acid, assuming that both are of chain length C_{18}. This mixture was treated further by solvent partition and the alcohol-soluble portion, on crystallization from acetone at $-70°$, yielded an oil (0.34 g) which was a concentrate of the conjugated diene acid. It had ultraviolet maximum 233 mμ and $E_{1cm}^{1\%}$ 561.

Identification of Diene Acids

The concentrate had an infrared peak at 3580 cm^{-1} (OH) and two peaks of equal intensity at 945 and 980 (conjugated *cis,trans* double bonds). Oxidative splitting by permanganate–periodate (5) and examination of the esterified fragments by gas chromatography (6) showed that they were hexanoate and azelate. There was no heptanoate or sebacate. There was some evidence of other compounds at longer emergence times, possibly fragments carrying the hydroxy group.

On hydrogenation of the diene acid concentrate (1.0 g) with Adams catalyst in ethyl acetate and successive crystallizations from ethyl acetate and from hexane, the product (0.33 g) melted at 65–66° and was evidently a mixture of monohydroxystearic acids. Calculated for $C_{18}H_{36}O_3$: C, 71.95; H, 12.08. Found: C, 71.83; H, 11.70. Infrared maximum, 3600 cm^{-1} (OH). Oxidative splitting of the hydrogenated product by solid permanganate in glacial acetic acid at 50° (13) gave a mixture of monobasic and dibasic acids which was esterified and submitted to gas chromatography. A similar oxidation of 12-hydroxystearic acid gave two monobasic acids, hexanoic and heptanoic, and two dibasic acids, undecanedioic and dodecanedioic, along with minor proportions of azelaic and sebacic acids. The monobasic acids obtained from the oxidation of the hydrogenated diene acids were chromatographed (as methyl esters) at 55°, 70°, and 93°. They were mainly pentanoic (15%), hexanoic (22%), nonanoic (25%), and decanoic (28%), with smaller amounts of heptanoic (5%), and octanoic acids (5%). Suberic and azelaic acids were observed in substantial amount (as esters) when chromatographed at 175°. There were also dodecanedioic and tridecanedioic acids, in smaller proportions, along with pimelic and undecanedioic. There was little or no sebacic acid.

Dehydration to Triene Acids

The mixed hydroxy diene acids were dehydrated as follows. The concentrate (3.4 g) was refluxed with glacial acetic acid (17 ml) for 4 hours, the acetic acid was removed under reduced pressure and the residue was heated for 1 hour with 35 ml of N alcoholic KOH. The crude acids were crystallized from 15 ml of acetone at $-35°$, giving 0.9 g of glistening plates, m.p. 58–60°. Further crystallization from ethyl acetate raised the melting point to 60–61° but no higher. (Found: C, 77.69; H, 10.65. Octadecatrienoic acid, $C_{18}H_{30}O_2$, requires C, 77.65; H, 10.85.) The substance had ultraviolet absorption maxima at 260, 269, 280 mμ (all-*trans* conjugated triene). The infrared spectrum (solid film) had a single strong peak at 985–995 cm^{-1}, also characteristic of the all-*trans* form. There was no OH peak. The spectrum of the methyl ester (in CS_2) showed a similar all-*trans* band at 990 cm^{-1}. When hydrogenated in methanol with Adams catalyst, the acid (0.37 g) absorbed 3.06 moles of hydrogen, and the product was stearic acid (0.34 g), m.p. and mixed m.p. 69–70°, equivalent weight 284.9 (calc. 284.4).

A portion of the triene acid was oxidized by periodate–permanganate (5) and the products were converted to methyl esters (6) for identification by gas chromatography. Valerate and hexanoate were identified at 80°, in approximately equal amounts (53:47). Suberate and azelate were observed at 170°. A larger portion was oxidized by the procedure of McLean and Clark (2). Azelaic acid, m.p. and mixed m.p. 104–105°, was

isolated with some difficulty by crystallizing the mixture of products. It was judged that more than one dibasic acid was present.

An attempt to isomerize the triene acids by iodine in hexane solution produced no change in melting point.

CALENDULA OIL

trans,8:trans,10:cis,12-Octadecatrienoic Acid (Calendic Acid)

Seed of *Calendula officinalis* L. was purchased from a commercial seed house. It was ground and the oil was extracted with petroleum ether in a Soxhlet. Ten grams of the oil was saponified by heating for 1 hour with 6% alcoholic potassium hydroxide under nitrogen. The unsaponifiable matter was removed and the fatty acids were crystallized fractionally from acetone at temperatures from $0°$ to $-40°$, giving 2.5 g of an acid, m.p. 40–40.5°. The acid was highly unstable in air, becoming sticky in a few minutes if exposed at room temperature. It was kept under nitrogen at the temperature of solid carbon dioxide. Calculated for $C_{18}H_{30}O_2$: C, 77.65; H, 10.85. Found: C, 77.97; H, 10.92. Ultraviolet maxima at 262, 272, and 283 mμ. Infrared maxima (solid film) at 990 (vs), 940–975 (m), and 740 (m); (in CS_2) at 987 (vs), 955 (m), 920 (m), and 732 cm^{-1} (m).

Hydrogenation with Adams catalyst in methanol gave stearic acid, m.p. and mixed m.p. 69.5–70°. The triene acid was oxidized by permanganate–periodate (5) and the products were examined as methyl esters by gas chromatography (6). Peaks corresponding to hexanoate and suberate were observed. There were no other peaks.

The triene acid was heated with maleic anhydride in benzene for 1 hour, forming an adduct, m.p. 73–74° after several crystallizations from ether:petroleum ether (1:5). Calculated for $C_{22}H_{32}O_5$: C, 70.18; H. 8.57. Found: C, 70.18; H, 8.55. The infrared spectrum showed no peak or shoulder in the region of 950–975 cm^{-1}. The adduct was oxidized by permanganate–periodate and the fission products were converted to methyl esters and chromatographed. There was a large peak identified by its emergence time as hexanoate and a very small peak identified as suberate.

The content of conjugated triene acid in the oil was estimated to be 47%.

All-trans-8,10,12-Octadecatrienoic Acid

On treatment with iodine in pentane, the triene acid (2.5 g), m.p. 40–40.5°, was quickly converted to the all-*trans* isomer which melted at 77–78° after crystallization from ethanol at 0° (1.9 g). Infrared maximum 990 cm^{-1} (vs); ultraviolet maxima 259, 269, and 280 mμ. McLean and Clark reported ultraviolet maxima 258, 268, and 280 mμ (2). The maleic anhydride adduct was prepared. It was more difficult to purify than that from the unisomerized acid and melted no higher than 70–71° (McLean and Clark, 71°). The yield was 1.5 g from 1.9 g of the *trans* acid. In admixture with the adduct from the unisomerized acid it melted at 56–58°. Its infrared spectrum showed a small but distinct peak at 963 cm^{-1}. The adduct was oxidized by permanganate–periodate and the fragments were identified by gas chromatography as hexanoate and suberate, both in considerable amount.

REFERENCES

1. M. J. Chisholm and C. Y. Hopkins.   Chem. & Ind. (London), 1154 (1959).
2. John McLean and A. H. Clark.   J. Chem. Soc. 777 (1956).
3. L. J. Morris, R. T. Holman, and K. Fontell.   J. Am. Oil Chemists' Soc. 37, 323 (1960).
4. J. R. Chipault and J. M. Hawkins.   J. Am. Oil Chemists' Soc. 36, 535 (1959).
5. R. U. Lemieux and E. von Rudloff.   Can. J. Chem. 33, 1701 (1955).
6. M. J. Chisholm and C. Y. Hopkins.   Can. J. Chem. 38, 805 (1960).
7. C. R. Smith, Jr., T. L. Wilson, E. H. Melvin, and I. A. Wolff.   J. Am. Chem. Soc. 82, 1417 (1960).
8. L. Crombie and A. G. Jacklin.   J. Chem. Soc. 1632 (1957).
9. F. D. Gunstone.   Chemistry of fats and fatty acids. Chapman and Hall Ltd., London. 1958. p. 25.
10. R. F. Paschke, W. Tolberg, and D. H. Wheeler.   J. Am. Oil Chemists' Soc. 30, 97 (1953).
11. W. G. Bickford, E. F. DuPre, C. H. Mack, and R. T. O'Connor.   J. Am. Oil Chemists' Soc. 30, 376 (1953).
12. D. Swern, T. W. Findley, G. N. Billen, and J. T. Scanlan.   Anal. Chem. 19, 414 (1947).
13. K. E. Bharucha and F. D. Gunstone.   J. Chem. Soc. 613 (1957).

STRUCTURAL AND SOLVENT EFFECTS ON THE $n \to \pi^*('U \leftarrow 'A)$ TRANSITIONS IN ALIPHATIC CARBONYL DERIVATIVES: EVIDENCE FOR HYPERCONJUGATION IN THE ELECTRONICALLY EXCITED STATES OF MOLECULES[1]

C. N. R. Rao,[2] G. K. Goldman,[3] and A. Balasubramanian

ABSTRACT

The $n \to \pi^*$ transition of the carbonyl group has been studied in solvents of varying degree of polarity and hydrogen-bonding ability, in a number of aliphatic carbonyl derivatives. Evidence for hyperconjugation of the alkyl groups in the electronically excited states of molecules has been presented.

INTRODUCTION

The long-wavelength low-intensity absorption between 2600 and 3000 Å in carbonyl compounds has been shown (1, 2) to be due to a singlet–singlet symmetry forbidden transition* arising from the excitation of an electron from a nonbonding orbital(n orbital) to an antibonding orbital (π^* orbital). Empirical criteria which permit distinctions between the pure π-electron transitions and the $n \to \pi^*$ transitions have been formulated (3, 4, 5). The solvent effects on $n \to \pi^*$ transitions have been characterized (4) and, in general, the transition energies are found to increase with the increase in the polarity of the solvent. We have now studied the substituent and solvent effects on the $n \to \pi^*$ transitions in aliphatic carbonyl derivatives with the purpose of understanding the nature of alkyl group interaction in the electronically excited states of molecules† since it has not been possible to evaluate the contributions from the inductive and the hyperconjugation effects from the earlier studies (6).

EXPERIMENTAL

All the solutes and solvents were subjected to suitable purification and fractionation before use. Particular care was taken in distilling trifluoromethylacetone from phosphorus pentoxide just before running the spectrum, since it readily forms the hydrate.

The ultraviolet absorption spectra were recorded using a Cary Model 11 recording spectrophotometer and a Hilger spectrophotometer, H700. The absorption maxima have been recorded in cm^{-1} (ν') and the intensities in terms of the molar extinction coefficients (ϵ).

RESULTS AND DISCUSSION

The $n \to \pi^*$ transition frequencies and intensities of some aliphatic carbonyl derivatives are summarized in Table I. The results are in general agreement with the earlier work (6). The results satisfy all the necessary criteria (3, 4, 5) proposed for $n \to \pi^*$ transitions. In Fig. 1 the $n \to \pi^*$ bands of acetaldehyde and methyl i-propyl ketone are reproduced.

TABLE I

The $n \rightarrow \pi^*$ transition of the carbonyl group in aliphatic carbonyl derivatives (RCOR′)

No.	R	R′	Solvent					
			Heptane		Methanol		Water	
			ν', cm^{-1}	ϵ_{max}	ν', cm^{-1}	ϵ_{max}	ν', cm^{-1}	ϵ_{max}
1	CH$_3$	H	34,360*	10.2	35,088	—	36,036	—
2	CH$_3$	CH$_3$	36,133	11.8	37,037	15.4	37,809	16.8
3	CH$_3$	C$_2$H$_5$	36,036	15.3	36,765	17.8	37,523	18.6
4	CH$_3$	i-C$_3$H$_7$	35,242	17.3	35,971	20.1	36,663	24.7
5	CH$_3$	t-C$_4$H$_9$	34,965	18.3	35,461	23.7	36,101	—
6	CH$_3$	CF$_3$	36,036	40.0	—	—	—	—
7	CH$_3$	CH$_2$CH$_2$COCH$_3$†	36,430	15.1	—	—	37,736	20.6
8	C$_2$H$_5$	C$_2$H$_5$	35,842	16.4	36,630	19.2	37,037	—
9	i-C$_3$H$_7$	i-C$_3$H$_7$	34,722	21.7	35,273	25.5	35,714	—
10	CH$_3$	n-C$_3$H$_7$	35,842	—	36,563	—	36,900	—
11	n-C$_3$H$_7$	n-C$_3$H$_7$	35,399	—	—	—	36,496	—
12	CH$_3$	i-C$_4$H$_9$	35,398	—	35,907	—	36,900	—
13	i-C$_4$H$_9$	i-C$_4$H$_9$	35,211	—	—	—	—	—
14	t-C$_4$H$_9$	t-C$_4$H$_9$	33,445	19.8	34,014	24.1	—	—
15	CH$_3$	n-C$_5$H$_{11}$	35,650	—	36,298	—	37,174	—
16	CH$_3$	n-C$_6$H$_{13}$	35,778	—	36,363	—	—	—

*Center of the nearly symmetric band system.

†Acetylacetone does not exhibit the $n \rightarrow \pi^*$ transition in this region. It gives a band around 37,175 cm^{-1} in heptane, which shows solvent red shift (4). This is because of the aromatic nature resulting from enolization.
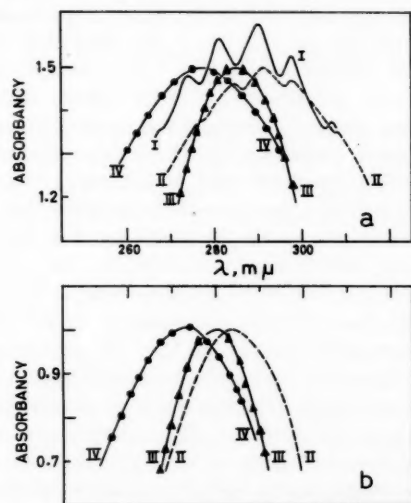
FIG. 1. The $n \rightarrow \pi^*$ transition of the carbonyl group of (a) acetaldehyde, (b) methyl i-propyl ketone: I, in gas phase; II, in heptane solution; III, in methanol solution; and IV, in water solution.

Acetaldehyde shows vibrational fine structure in heptane just as it does in gas phase except that there is a slight bathochromic shift in the former case. The fine structure is not seen in the spectrum taken in methanol or water. Ketones do not show any recognizable fine structure even in heptane solutions. However, all the carbonyl derivatives do show increasing $n \rightarrow \pi^*$ transition energies with the increasing polarity or hydrogen-bonding ability of the solvents.

The intensities of the $n \rightarrow \pi^*$ bands in all the derivatives studied are seen to be weak. The ϵ value for acetone is not much different from that of acetaldehyde, even though the two molecules differ in symmetry (C_{2v} and C_s). Similarly, methyl ethyl ketone and acetone exhibit nearly comparable intensities. The intensity of the forbidden $n \rightarrow \pi^*$ transition in all these molecules is undoubtedly derived in the same manner. Thus, all the aldehydes and saturated ketones seem to retain the C_{2v} symmetry characteristics of the formaldehyde molecule. The intensity-borrowing mechanism of the $n \rightarrow \pi^*$ transition in formaldehyde has been shown (5) to be due to the vibrationally induced mixing of the electronic states. The out-of-plane vibration, ν_6, is considered responsible for the intensity of the $n \rightarrow \pi^*$ transition in formaldehyde. The mode of motion responsible for the intensity of the transition in acetone should then be ν_6, in which the two carbon atoms and the oxygen atom bonded to the central carbon atom are displaced out of the plane of symmetry in one direction and the central carbon in the opposite direction. Among the saturated aliphatic ketones, the $n \rightarrow \pi^*$ transition intensity is least in acetone and it is slightly greater in other cases. It can be seen from the data in Table I that the $n \rightarrow \pi^*$ transition intensity increases with the increasing polarity or hydrogen-bonding ability of the solvent.

It has been generalized (5, 7, 8) that electron-donating substituents shift the $n \rightarrow \pi^*$ transition to shorter wavelengths due to the increase in the energy of the excited state caused by the accumulation of electronic charge in a localized region. In the $n \rightarrow \pi^*$ transition of the carbonyl group, the electronic charge is transferred from oxygen to carbon. Electron-donating groups like —Cl, —OCH$_3$, etc., when attached to the carbon atom, produce large intramolecular blue shifts of the transition. Interestingly enough, aliphatic carbonyl compounds (RCOR' where R = CH$_3$), with R' as CH$_3$, C$_2$H$_5$, i-C$_3$H$_7$, and t-C$_4$H$_9$, exhibit the $n \rightarrow \pi^*$ transitions at 36133, 36036, 35242, and 34965 cm^{-1}, respectively, in a hydrocarbon solvent. Such a trend cannot be explained in terms of inductive effect alone because acetaldehyde (R' = H) and trifluoromethylacetone (R' = CF$_3$) show the transition at 34360 and 36036 cm^{-1}, respectively, in heptane. There is no proportionality between the $n \rightarrow \pi^*$ frequencies and the polar effects of groups in these carbonyl derivatives, as can be seen from Fig. 2(a), where ν' is plotted against Taft's aliphatic polar substituent constants (9), $\Sigma\sigma^*$. However, the infrared carbonyl stretching frequencies in aliphatic ketones bear a linear relation to $\Sigma\sigma^*$ of groups (10, 11) showing that there may be no hyperconjugative effect of alkyl groups in the ground electronic states of molecules. In fact, it has been fairly well accepted nowadays that hyperconjugation may not play a prominent role in the electronic ground states of molecules (12). If one assumes that there is some contribution by the resonance interaction of the alkyl groups in the electronically excited states of molecules, one may be able to explain the observed $n \rightarrow \pi^*$ frequencies in the aliphatic carbonyl derivatives. The frequency is highest in acetone (where both R and R' are methyl groups), just what one would expect if there were electron donation by C—H hyperconjugation.

Kreevoy and Taft (13) applied the linear inductive energy relationship to study the nature of the electronic interaction of alkyl groups in the acid-catalyzed rates of hydrolysis of diethyl acetals and ketals. Assuming that only C—H hyperconjugation was operative in addition to the inductive effect, they proposed the relation

(i) $$\log (k/k_0) = (\Sigma\sigma^*)\rho^* + \Delta nh$$

where Δn is the difference in the number of α-hydrogens actually available for C—H
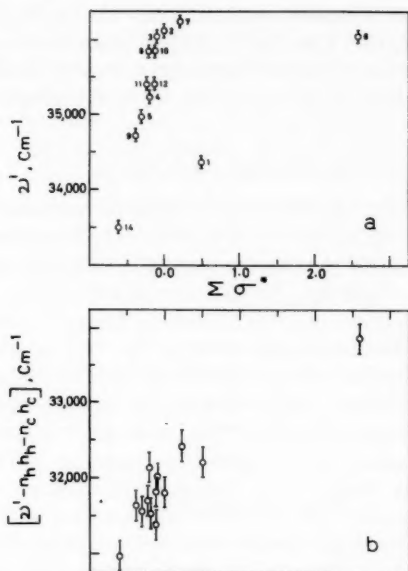
FIG. 2. (a) Plot of the $n \to \pi^*$ transition frequencies (ν') in aliphatic carbonyl derivatives against the polar substituent constants of Taft, $\Sigma\sigma^*$.

(b) Plot of ($\nu' - n_h h_h - n_c h_c$) against $\Sigma\sigma^*$. The maximum limits of uncertainty on the frequencies have been shown.

hyperconjugation compared with the maximum number of six and h is the hyperconjugation constant. A similar treatment of the $n \to \pi^*$ frequencies of aliphatic carbonyl derivatives, taking into consideration only the inductive and C—H hyperconjugative effects of alkyl groups, was carried out by employing the equation

(ii)
$$\nu' = \nu_0' + (\Sigma\sigma^*)\rho^* + n_h h_h$$

where ν' is the observed $n \to \pi^*$ frequency in cm^{-1}, n_h is the number of α-hydrogens available for C—H hyperconjugation, and h_h is the hyperconjugation constant. The value of h_h was estimated to be 385 cm^{-1} (in heptane solution) by solving simultaneous equations. The plot of ($\nu' - 385\ n_h$) versus $\Sigma\sigma^*$ showed considerable scatter of the points. The standard deviation of the points was found to be 348 cm^{-1} and the correlation coefficient was 0.557. In view of the rather poor correlation obtained, it was decided to consider possible contribution by the C—C hyperconjugation of the alkyl groups.

Taft and Lewis (14) have recently proposed a modified treatment which takes into account both C—H and C—C hyperconjugation. The quantitative relation between the measured reactivity effects and the sum of the inductive and the hyperconjugation effects has been expressed as

(iii)
$$\log (k/k_0) = (\Sigma\sigma^*)\rho^* + R$$

and $R = n_h h_h + n_c h_c$, where n_h and n_c are the number of α-C—H and α-C—C bonds of the alkyl group and h_h and h_c are the C—H and C—C hyperconjugation constants. The quantity $[\log(k/k_0) - R]$ should then depend only on the polar effects of groups.

Such a relation has been found to explain quantitatively the reaction rate data in several alkyl-substituted systems (14, 15). The effects of alkyl groups on the transition energies of the 0–0 bands of gaseous benzene spectra were also found to follow equation (iii). The $n \rightarrow \pi^*$ transition frequencies in Table I may be treated similarly, by employing the equation

(iv) $$\nu' = \nu_0' + (\Sigma\sigma^*)\rho^* + n_h h_n + n_c h_c.$$

By assuming a linear relation between the points for acetaldehyde and trifluoro-methylacetone in Fig. 2(a), the constants h_h and h_c were found to be approximately 720 and 410 cm^{-1}, respectively, for the data in heptane. An approximate proportionality is found between $(\nu' - 720\, n_h - 410\, n_c)$ and $\Sigma\sigma^*$ as shown in Fig. 2(b). The standard deviation of the points and the correlation coefficient are 276 cm^{-1} and 0.920, respectively.

It is seen that the correlation coefficient for equation (iv) is much greater than for equation (ii).* Thus, it appears that the contributions from the inductive and the C—H and C—C hyperconjugative effects are necessary to explain the $n \rightarrow \pi^*$ transition frequencies of aliphatic carbonyl derivatives. The ratio h_h/h_c is seen to be about 1.75, which is greater than the value of 1.3 generally found in aromatic systems (14). Apparently, the contribution from C—H hyperconjugation, compared with C—C hyperconjugation, is much greater in the aliphatic systems than in the aromatic systems.

The $n \rightarrow \pi^*$ frequencies of acetone, methyl ethyl ketone, methyl i-propyl ketone, and methyl t-butyl ketone in heptane solution are in the Baker-Nathan order, i.e., CH$_3$ > C$_2$H$_5$ > i-C$_3$H$_7$ > t-C$_4$H$_9$. The same trend is maintained in solvents of varying degree of polarity or/and hydrogen-bonding ability, as can be seen from Fig. 3. There is no indication of an inversion of this order with the change in solvents as observed by Schubert *et al.* (16) in *p*-alkylacetophenones and *p*-alkylnitrobenzenes. The results of Schubert
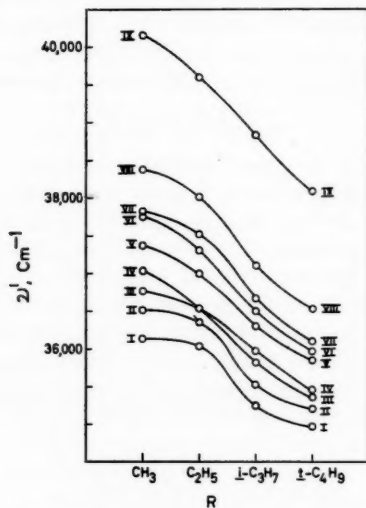
FIG. 3.   Solvent effects on the $n \rightarrow \pi^*$ transition frequencies of CH$_3$COR: I, heptane; II, acetonitrile; III, i-propanol; IV, methanol; V, acetic acid; VI, 2,2,2-trifluoroethanol; VII, water; VIII, 30% perchloric acid; and IX, 60% perchloric acid.

The authors are thankful to the referee for suggesting the statistical analyses of the relations.

et al. (16) may be explained (14) as due to possible errors in fixing the positions of the 0–0 bands and also due to the uncertainty in the mechanism of the substituent effects on the transition. In general, it may be said that the effect of alkyl groups on the near ultraviolet absorption spectra of aromatic systems is not consistent. The evidence for hyperconjugation in the excited states of molecules presented in this study seems to be quite reasonable because (*a*) the molecules studied are aliphatic and so no other type of resonance interaction can occur, (*b*) the infrared carbonyl stretching frequencies in these molecules are proportional to Taft's aliphatic polar parameters of groups, thus indicating that hyperconjugation may be unimportant in the ground electronic states, (*c*) the $n \rightarrow \pi^*$ transition is very sensitive to change in structure and solvent, and (*d*) similar trends of the $n \rightarrow \pi^*$ frequencies are found in solvents of varying degree of polarity or/and hydrogen bonding.

All the carbonyl derivatives show increasing solvent blue shifts* with the increasing polarity or/and hydrogen-bonding ability of the solvent.† In the series of ketones, RCOR′ (with R = CH$_3$), the solvent blue shift is maximum in acetone (where R′ is also a methyl group) in all the solvents studied. The significance of this observed effect is not completely clear.†

ACKNOWLEDGMENTS

REFERENCES

1. R. S. MULLIKEN. J. Chem. Phys. **3**, 564 (1935).
2. H. L. McMURRY. J. Chem. Phys. **9**, 231 (1941).
3. M. KASHA. Discussions Faraday Soc. No. 9, 14 (1950).
4. H. McCONNELL. J. Chem. Phys. **20**, 700 (1952).
5. J. W. SIDMAN. Chem. Revs. **58**, 689 (1958).
6. P. MARONI. Ann. chim. (Paris), **2** (13), 757 (1957).
7. A. BURAWOY. J. Chem. Soc. 1177 (1939).
8. S. NAGAKURA. Bull. Chem. Soc. Japan, **25**, 164 (1952).
9. R. W. TAFT, JR. *In* Steric effects in organic chemistry. *Edited by* M. S. Newman. John Wiley & Sons, Inc., New York. 1956. Chap. 13.
10. C. N. R. RAO, G. K. GOLDMAN, and C. LURIE. J. Phys. Chem. **63**, 1311 (1959).
11. H. W. THOMPSON and D. A. JAMESON. Spectrochim. Acta, **13**, 236 (1958).
12. C. N. R. RAO. Current Sci. (India), **28**, 231 (1959); Nature, **187**, 913 (1960).
13. M. M. KREEVOY and R. W. TAFT, JR. J. Am. Chem. Soc. **77**, 5590 (1955).
14. R. W. TAFT, JR. and I. C. LEWIS. Tetrahedron, **5**, 210 (1959).
15. J. W. BAKER. Tetrahedron, **5**, 135 (1959).
16. W. M. SCHUBERT, J. ROBINS, and J. L. HAUN. J. Am. Chem. Soc. **79**, 910 (1957).

Blue shift $\Delta \nu' = \nu'_{solvent} - \nu'_{heptane}$.

†*A detailed analysis of the solvent effects on the $n \rightarrow \pi^*$ transition of the carbonyl group is now in progress in this laboratory and will be published in the near future.*

CATALYZED RECOMBINATION OF NITROGEN ATOMS, AND THE POSSIBLE PRESENCE OF A SECOND ACTIVE SPECIES IN ACTIVE NITROGEN[1]

Roger Kelly[2] and C. A. Winkler

ABSTRACT

The reactions of ethylene, ethane, and ammonia with active nitrogen have been studied over the pressure range 0.3 to 4 mm *using an unheated reaction vessel*. The object was to determine why each reactant shows, as is well-known, a smaller extent of reaction at lower temperatures than would be predicted from the atom concentration. It was concluded that ethylene probably brought about *homogeneous catalyzed recombination*, i.e. the process $N + C_2H_4 \rightleftharpoons N \cdot C_2H_4$, followed by $N + N \cdot C_2H_4 \rightarrow N_2 + C_2H_4$. The over-all third-order rate constant appeared to be very large, about 1.8×10^{-28} cc^2 molecule^{-2} sec^{-1}. The behavior of ammonia was quite different from that of ethylene and it was, in fact, possible to show that the extent of reaction was not governed by the instantaneous atom concentration at all. The results can be explained qualitatively, however, if it is assumed that excited molecules formed in the course of homogeneous atom decay constitute a second active species in active nitrogen. This view serves also to explain the failure in such work as that of Kistiakowsky *et al.* to observe ammonia destruction or excited molecules when especially low atom concentrations are used. The few experiments involving ethane were sufficient to show that the reactivity was low for a different reason than with ethylene.

In a previous study (1), active nitrogen was produced in a condensed discharge at pressures between 0.3 and 4 mm and under conditions of approximately complete initial dissociation. It was then allowed to flow rapidly through a "decay tube" to a reaction vessel, where the limiting (i.e. maximum) rate of HCN production from ethylene or ethane at 350° C was assumed to measure the flowrate of residual N atoms. Information on the rate constants for N atom decay was thus obtained. The present experiments have been conducted along similar lines, the same apparatus being used; however, the "activity" of the active nitrogen has been derived *with the reaction vessel unheated*. Measurements were made of HCN production from ethylene and ethane, and also of the decomposition of ammonia.

Ethylene and ethane are of particular interest at lower temperatures since they are typical of several substances with which the extents of reaction at all temperatures approach well-defined limiting values as the flowrate of reactant is increased, yet these values are significantly temperature dependent and, except at the highest temperatures, are substantially less than might be expected from the available N atom concentration (2, 3, 1). An explanation for such behavior has been given by Forst *et al.* (4), who suggested that N atom reactions might be accompanied by extensive recombination of the atoms catalyzed by the *reactant*. (Such a process is not eliminated by increasing the flowrate of reactant provided it is of the same order in reactant as the main reaction. On the other hand, ordinary homogeneous and surface decay, as well as recombination catalyzed by a *product*, would necessarily be swamped in the presence of a large excess of reactant, and would therefore have no effect whatsoever on a limiting reactivity.) By contrast, the destruction of ammonia by active nitrogen, while occurring to only a small extent, appears to be unaffected by moderate changes in temperature, is quite rapid (5),

Can. J. Chem. Vol. 38 (1960)

is accompanied by only partial quenching of the afterglow (6, 7), and apparently does not involve N atoms in the rate-controlling step (6, 8).[3] The behavior of ammonia is therefore, at least superficially, not consistent with a combination of N atom attack plus catalyzed recombination and has, in fact, seemed to require an alternative explanation in which it is assumed that an active species other than the N atom is present in active nitrogen (see, for example, 5, 9, 10).

It will be the object of the present work to determine whether the depressed reactivity of each substance studied can be better explained in terms of catalyzed recombination or a second active species.

EXPERIMENTAL

The apparatus was identical with that described earlier (Fig. 1 of reference 1), except that a decay tube (volume = 281 cc) was used only in series 1 to 3. In series 4 and 5 the decay tube was removed altogether. The reaction vessel was then connected directly to the discharge tube at a point *near the end of one electrode* and with the usual constriction present at the entrance to the reaction vessel (Fig. 1). Nitrogen was admitted
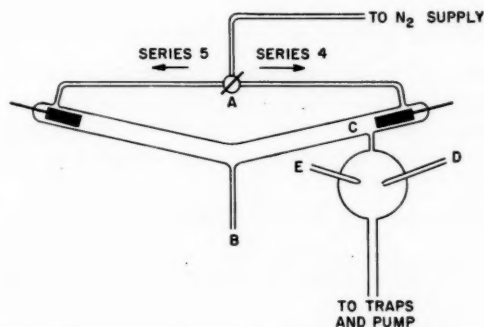
Fig. 1. Arrangement of the discharge tube and reaction vessel in series 4 and 5. (A) is a stopcock, according to the position of which the nitrogen enters the discharge tube either at the right electrode (series 4) or at the left (series 5). (B) is a constricted outlet from the discharge tube which served *in series 4* to set up a slight flow of gas *away* from the outlet to the reaction vessel, and thereby to minimize the diffusion of active nitrogen from region (C) into the reaction vessel. (D) is the reactant jet and (E) the thermocouple well. Further details of the apparatus are the same as in Fig. 1 of reference 1.

to the discharge tube either at the end to which the reaction vessel was sealed (series 4), or at the opposite end (series 5). The polarity of the electrodes was shown not to affect the results (cf. p. 2334 of reference 11).

In all experiments the system was poisoned with Na_2HPO_4 since this poison, in contrast to HPO_3, is unreactive towards ammonia. The electrical circuit and analytical procedures were as described previously (1) and, as before, the reactant flowrates were sufficiently high that the extents of reaction were at their limiting values for the temperatures used.

Whether or not complete initial dissociation was achieved is of no consequence to the arguments to follow.

[3]*The conclusion that N atoms do not participate in the rate-controlling step follows from the observations that, when ammonia is added to active nitrogen of microwave origin in amounts as great as 10 times the atom concentration, neither the atom concentration itself (6) nor the ability of the active nitrogen to destroy NO (8) is affected.*

THEORY

If the reactivity towards active nitrogen shown by a substance were depressed due to the fact that the substance catalyzed the recombination of the N atoms, then it should be possible to account for the details of the reaction by means of some combination of elementary N atom reactions. The possible elementary reactions include, firstly, those which lead to product formation:

$$[1] \qquad\qquad\qquad N + M \underset{k_{-1}}{\overset{k_1}{\rightleftharpoons}} NM,$$

followed by one of

$$[2] \qquad NM \xrightarrow{k_2} n(HCN, CNCl, NH, etc.) + p_2(\text{reactive fragments}), \quad (cf.\ 10,\ 12,\ 13)$$

$$[3] \qquad N + NM \xrightarrow{k_3} N_2 + M^*, \quad M^* \to p_3(\text{reactive fragments}),$$

$$\left.\begin{array}{c}\\ \\ \\ \\ \\ \end{array}\right\} (cf.\ 2,\ 10,\ 12,\ 14)$$

$$[4] \quad NM + NM \xrightarrow{k_4} N_2 + M + M^*, \quad M^* \to p_4(\text{reactive fragments}).$$
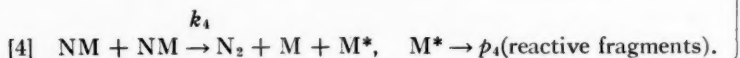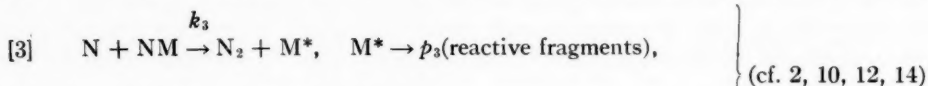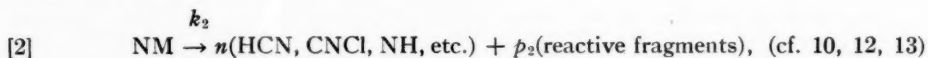
Here M is the reactant, M^* is an unspecified excited state of M, n is the number of molecules of HCN, etc., formed in the primary step of [2] (*one*, except in special cases, as when M is a cyanide), and p_2, p_3, and p_4 are the numbers of N atoms lost in rapid secondary reactions involving fragments of M. The values of p_2, etc. are not necessarily integral (cf. footnote 4).

Next there are reactions leading solely to recombination:

$$[5] \qquad\qquad\qquad N + NM \xrightarrow{k_5} N_2{}^* + M, \qquad\qquad (cf.\ 4)$$

$$[6] \qquad\qquad\qquad NM + NM \xrightarrow{k_6} N_2{}^* + 2M,$$

$$[7] \qquad\qquad\qquad NM + \text{surface} \xrightarrow{k_7} N \cdot \text{surface} + M,$$
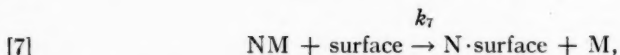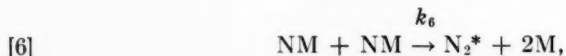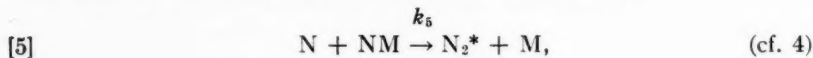
where $N_2{}^*$ represents an excited state of N_2. In principle, the M on the right side of [5], [6], and [7] might be excited; however, if so, it is assumed to revert to the ground state.

As mentioned previously, ordinary homogeneous and surface decay, as well as recombination catalyzed by a product, need not be considered provided the experiments are confined to conditions when the reactant is in excess.

If a low extent of reaction were due, not to catalyzed recombination, but to the fact that the reaction was initiated by a species other than the N atom, it is obviously true that experimental results would be consistent with no combination of elementary N atom reactions. However, a far simpler way of demonstrating the involvement of a second active species would be to show that the reactivity of a substance could be varied significantly by some act affecting the active nitrogen prior to its entry into the reaction vessel, yet which leaves the atom concentration within the reaction vessel essentially unchanged.

RESULTS AND DISCUSSION

The following abbreviation will be used henceforth: $[N]_a \equiv$ "apparent atom concentration" = reactivity.

Ethylene

In Figure 2 are shown the HCN production from ethylene as a function of pressure
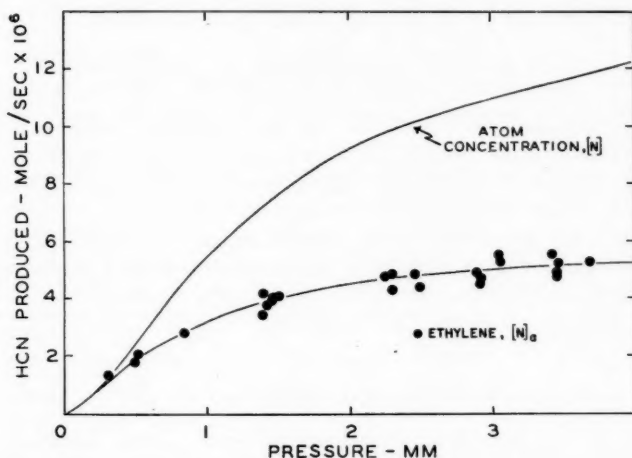
Fig. 2. Series 1. HCN production from ethylene as a function of pressure with both the decay tube and reaction vessel unheated. The reaction temperature varied between 55 and 85° C, depending on the pressure.

with both the decay tube and reaction vessel unheated (*series 1*), together with the corresponding atom concentrations, obtained by reacting ethylene or ethane at 350° C (identical with series 5 of reference 1). The reaction temperature varied from 55 to 85° C, depending on the pressure. The afterglow was completely extinguished in all the experiments of the series.

If the reactivity of ethylene at a given temperature is defined in terms of the HCN production, i.e. $[N]_a = [HCN]$, it follows from Fig. 2 that at the temperature used in the present work $[N]_a < [N]$. This is true in spite of the fact that the suggested mechanism for the ethylene reaction requires that $[N]_a = [N]$ (15, cf. 16). To determine whether the depression of the reactivity is due to catalyzed recombination or to a second active species, it will be noted that $[N]_a \rightarrow [N]$ as $[N] \rightarrow 0$. In other words, taking into consideration that, when the reactant is present in excess, the applicable elementary reactions will have the same order in M, the ethylene reaction appears to involve a combination of reactions [1] and [2] with *one or both* of [3] and [5]. The adequacy of these reactions may be tested by comparing the observed and predicted relations between $[N]_a$ and $[N]$. The predicted relations will be derived assuming (i) that the reactant M is in excess, (ii) that the NM complexes exist in steady-state (cf. footnote 5), and (iii) that reactions between N atoms and fragments of M give rise to HCN. Then, for the combination

[1] + [2] + ([3] and/or [5]), where $p_3 = 0$, one has

$$d[N]/dt = -(1+p_2)k_2[NM] - 2(k_3+k_5)[N][NM],$$

$$d[N]_a/dt = d[HCN]/dt = (n+p_2)k_2[NM].$$

Hence, proceeding as in reference 4,

[8]
$$[N]_a = \frac{(n+p_2)k_2}{2(k_3+k_5)} \ln\left\{1 + \frac{2(k_3+k_5)[N]}{(1+p_2)k_2}\right\}.$$

Similarly, for a combination [1] + [2] + [3], where $p_3 > 0$, one has

[9]
$$[N]_a = \frac{p_3[N]}{2+p_3} + \frac{k_2[2(n+p_2)+(n-1)p_3]}{(2+p_3)^2 k_3} \ln\left\{1 + \frac{(2+p_3)k_3[N]}{(1+p_2)k_2}\right\}.$$

For the ethylene reaction $n = 1$, while p_3 will lie somewhere between 0 and 2. The experimental data should therefore be consistent either (i) with equation [8] ($n = 1$), (ii) with equation [9] ($n = 1$, $p_3 = 2$), or (iii) with some intermediate type of behavior. It is seen in Table I that equation [8] is by itself sufficient to correlate the data. One thus concludes that the ethylene reaction can be adequately explained in terms of a combination of reactions [1] and [2] with [3] and/or [5], where $p_3 \to 0$, the last two processes being varieties of what may be called *homogeneous catalyzed recombination*. It is not necessary to introduce a second active species.

TABLE I

HCN production from ethylene in the region 55 to 85° C

Pressure (mm)	$[N]_a = [HCN]$* (mm)	$[N]$* (mm)	Predicted values of $[N]_a$ when $(k_3+k_5)/(1+p_2)k_2 = 8$ mm^{-1} or 2.8×10^{-16} cc molecule^{-1} (using equation [8] with $n = 1$)†	Predicted values of $[N]_a$ when $k_3/(1+p_2)k_2 = 32$ mm^{-1} (using equation [9] with $n = 1$ and $p_3 = 2$)†
0.5	.042	.054	.039	.035
1.0	.061	.103	.061	.062
1.5	.072	.139	.073	.081
2.0	.079	.164	.080	.094
3.0	.088	.190	.087	.108
4.0	.093	.210	.092	.118

*The experimental values of $[N]_a$ and $[N]$, as given in Fig. 2, have been converted from *micromole sec^{-1}* to *millimeter* using the factors given in Table I of reference 1. A slight error is associated with this change of units, since the conversion factors do not take into account the presence of the reactant and products. When referring to Table I of reference 1, the following change should be made in the heading of column 2: delete "$\times 10^6$".

†The values assigned to the constants $(k_3+k_5)/(1+p_2)k_2$ and $k_3/(1+p_2)k_2$ have been chosen by trial and error so as to give the best fit to the data at 1 mm pressure.

The conclusion that $p_3 \to 0$, i.e. that the reactive fragments formed in reaction [3] do not consume an appreciable quantity of N atoms, may seem surprising. However, it is in accord with the work of Dunford *et al.* (17), where th e was indication that ethylene which is excited by a process like [3] tends to revert to he ground state rather than to C_2H_2 or CH_2.

Several interesting rate constants can be obtained from the ratio $(k_3+k_5)/(1+p_2)k_2$ as given in Table I. Assuming that $p_2 = 1$,[4] and combining the above ratio with the over-all second-order rate constant for HCN production from ethylene as estimated by Milton and Dunford (18), i.e. $k_2 k_1/k_{-1} \approx 1.6 \times 10^{-13}$ cc molecule^{-1} sec^{-1} at 40° C, one obtains the over-all third-order rate constant for N atom recombination catalyzed by

[4]One CH_2 is believed to form in the ethylene reaction along with each primary HCN (15). The value $p_2 = 1$ therefore corresponds to complete conversion of the CH_2 to secondary HCN, so that a value slightly less than 1 might be more consistent with the recovery of small amounts of methane and ethane.

ethylene, namely $2(k_3+k_5)k_1/k_{-1} \approx 1.8\times10^{-28}$ cc^2 molecule^{-2} sec^{-1}.[5] Combining the ratio with *upper* limits for (k_3+k_5) and k_1, as derived from the collision frequencies, one obtains the values $1/k_2 \geqslant 1\times10^{-6}$ sec for the lifetime of the N·C$_2$H$_4$ complex with respect to decomposition into HCN + CH$_3$, and $1/k_{-1} \geqslant 5\times10^{-10}$ sec for the lifetime with respect to dissociation into N + C$_2$H$_4$. (In calculating (k_3+k_5) and k_1, the values $\sigma_N = 3\times10^{-8}$ cm and $\sigma_{C_2H_4} = \sigma_{N\cdot C_2H_4} = 5\times10^{-8}$ cm were used, and a temperature of 70° C was assumed.)

The value obtained for the rate constant of N atom recombination catalyzed by ethylene is compared with certain related constants in Table II. It is seen that the catalyzed

TABLE II

Comparison of third-order processes involving N atoms

Process*	Temperature (°C)	Third-order rate constant (cc^2 molecule^{-2} sec^{-1}×10^{33})	Lifetime of the relevant bimolecular complex with respect to dissociation (sec)	Reference
Homogeneous catalyzed recombination in the presence of C$_2$H$_4$	55 to 85	180,000	$\geqslant 5\times10^{-10}$ (i.e. $1/k_{-1}$)	Present
Homogeneous catalyzed recombination in the presence of CH$_3$CN	70	700	$\geqslant 2\times10^{-12}$ (i.e. $1/k_{-1}$)	4†
Collision rate ×2 (using $\sigma = 3\times10^{-8}$ cm)	70	40	$\sim 4\times10^{-13}$	—
Homogeneous decay	{ Ambient ~55	15 to 33 3 to 5‡	? ?	8, 19, 20 1, 21

*Though surface decay is not a third-order process, it is interesting to note that, as shown on p. 73 of reference 1, this process is perhaps an order of magnitude *more* efficient than homogeneous decay, and therefore much *less* efficient than the particular examples of catalyzed recombination.

†The rate constants in Table I of reference 4 have been extrapolated to 70° C in a plot of log k vs $1/T$. The value of $1/k_{-1}$ was then found as in the present work. The lifetime of the N·CH$_3$CN complex with respect to *reaction* (i.e. $1/k_2$) is not included in Table II; its value is $\geqslant 4\times10^{-6}$ sec, which is comparable to the value for N·C$_2$H$_4$ as given in the text.

‡The range of values 1.3 to 2.4 was given in reference 1; however, a recalculation of the results of reference 1 using improved values for the time of decay gives 3 to 5 (21).

recombination is particularly rapid, and, as would be expected, that the rapidity is associated with a relatively long-lived NM complex.

It is obvious that the preceding treatment of the ethylene reaction is valid only in so far as the elementary processes considered (equations [1] to [7]) represent all that are relevant.

Ethane and Ammonia

The production of HCN from ethane and the destruction of ammonia were next investigated, the reaction vessel being unheated and the decay tube either unheated (*series 2*), at 400° C (*series 3*), or removed altogether as shown in Fig. 1 (*series 4 and 5*). The results, together with the corresponding atom concentrations estimated from the reactions of ethylene or ethane at 350° C (for series 2 and 3 identical with series 5 and 6 of reference 1), are shown in Figs. 3A, 3B, and 3C. The afterglow was weakened, but not extinguished, in the presence of ammonia.

In marked contrast to ethylene, the extents of reaction of ethane and ammonia at lower temperatures, i.e. [N]$_a$, remain substantially less than the atom concentration in

[5]*The over-all rate constants for* HCN *production and catalyzed recombination take on the simple forms given only (i) if the* NM *complexes are in steady-state, i.e.* $k_{-1} \gg k_1[M]$ *(cf. equation [44] of reference 4), and (ii) if* $k_{-1} \gg (k_2+(k_3+k_5)[N])$. *That these inequalities are reasonable is borne out by the values actually obtained for the various constants.*

the limit $[N] \rightarrow 0$. The very low ammonia reactivity in the experiments of series 4 is perhaps especially to be noted. The low reactivities of ethane and ammonia are therefore clearly due to some effect other than the combination $[1] + [2] + ([3]$ and/or $[5])$ as with ethylene. Considering ammonia alone, all other combinations of elementary reactions can be eliminated on the basis of the fact that the reactivity of ammonia can be varied over wide limits by acts affecting the active nitrogen prior to its entry into the reaction vessel, yet which in certain cases leave the atom concentration within the reaction vessel essentially unchanged. For example, in series 2 at 1 mm pressure, $[N] = 5.4$ micromole sec^{-1} and $[N]_a = 0.50$; in series 5, on the other hand, though the value of $[N]$ at 1 mm was nearly the same (4.6), the value of $[N]_a$ was very low (0.00).
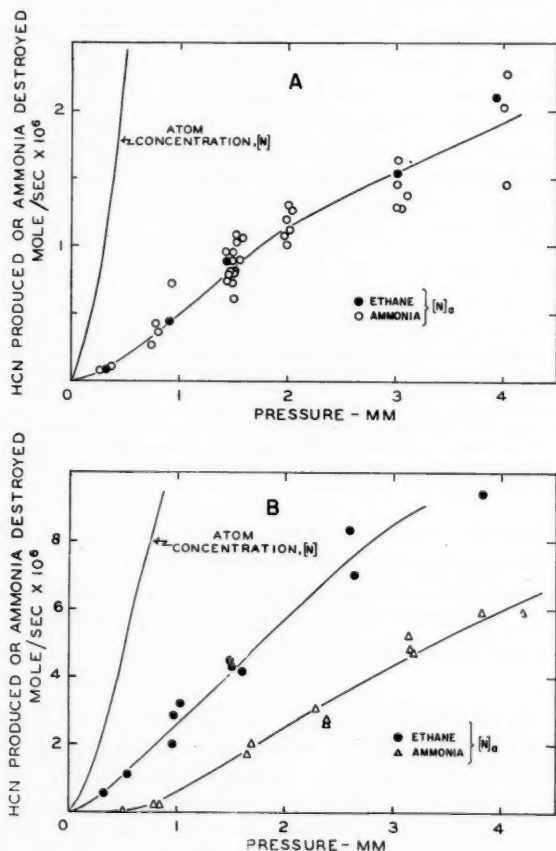
FIG. 3.   (A) Series 2. HCN production from ethane and ammonia destruction as functions of pressure with both the decay tube and reaction vessel unheated. Temperature of reaction vessel = 40 to 70° C.
    (B) Series 3. HCN production from ethane and ammonia destruction as functions of pressure with the reaction vessel unheated, as before, but the decay tube at 400° C. The reactivity of ethane is probably spuriously high due to the proximity of the hot decay tube. Temperature of reaction vessel = 50 to 130° C.
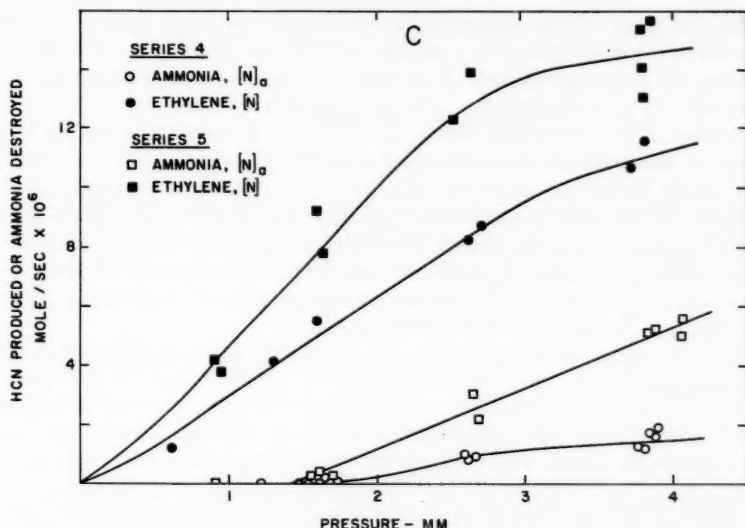
FIG. 3.   (C) Series 4 and 5. Ammonia destruction as a function of pressure with the reaction vessel attached directly to the discharge tube near an electrode. In series 4 the nitrogen entered the discharge tube at the end to which the reaction vessel was attached, while in series 5 it entered at the opposite end. The reaction vessel was unheated, the temperature being 55 to 100° C in series 4, and 60 to 150° C in series 5.

The failure of the ammonia reactivity to be governed by the instantaneous atom concentration is strong evidence that an active species other than the N atom initiates the ammonia reaction, a conclusion in essential agreement with previous work (see introductory section). Whether the ethane reaction involves a second active species, or merely a combination of elementary reactions different from those involved with ethylene, cannot be determined from the present data. In particular a better control of temperature is needed since, while the ammonia reaction is virtually independent of temperature in the region of interest (5), the ethane reaction is not. H atom attack might also serve to complicate the ethane reaction (3).

An indication of the mode of formation of the species which reacts with ammonia can be obtained from series 4. In this series, the reaction vessel was attached directly to the discharge tube *near the point of entry of the nitrogen*, so that the active nitrogen formed in the proximity of a metal electrode. The atom concentration therefore fell rapidly from the high value necessarily existing at the instant of each flash. Accordingly, the observation in series 4 that the ratio $[N]_a/[N]$ was lower at a given pressure than in any other series, and also lower than in the work of references 5, 22, and 23, implies that the second active species is formed by homogeneous atom decay.

A species formed by homogeneous atom decay is necessarily an excited molecule.

It is not possible, with the information available, to determine whether the reactivity of ammonia can be predicted quantitatively in terms of a second active species; however, the fact that the species is formed by a *multiorder* mode of atom decay is certainly consistent with the trend that is revealed by examining the data in Figs. 3A, 3B, and 3C for the ratio $[N]_a/[N]$ to increase as $[N]$ is increased. A similar trend was observed in references 22 and 23, in both of which a condensed discharge was used as in the present

work. A multiorder origin for the second active species also serves to explain the observations that, when a microwave discharge is used so that the atom concentration is very low even in the discharge tube, little or no ammonia destruction is found (6, 8), and excited molecules are not observed by mass spectrometry (11, 24).

The observation of Kaufman and Kelso (25) that, under conditions similar to those where essentially *no* ammonia destruction is observed (6, 8), certain thermal effects appear to be caused by excited molecules would seem at first sight contradictory to the present work. Note, however, that Dressler (26) has observed ground-state nitrogen in the first vibrational level as a component of active nitrogen. Provided this species were formed in the discharge process, it would be expected to persist even at the very low atom concentrations of reference 25; moreover, though the species would be comparatively inert chemically, it could lead to simple thermal effects.

The subject of the identity of the species reacting with ammonia will be considered in a subsequent paper.

REFERENCES

1. R. KELLY and C. A. WINKLER. Can. J. Chem. 37, 62 (1959).
2. D. M. WILES and C. A. WINKLER. Can. J. Chem. 35, 1298 (1957).
3. P. A. GARTAGANIS and C. A. WINKLER. Can. J. Chem. 34, 1457 (1956).
4. W. FORST, H. G. V. EVANS, and C. A. WINKLER. J. Phys. Chem. 61, 320 (1957).
5. G. R. FREEMAN and C. A. WINKLER. J. Phys. Chem. 59, 371 (1955).
6. G. B. KISTIAKOWSKY and G. G. VOLPI. J. Chem. Phys. 28, 665 (1958).
7. K. D. BAYES and G. B. KISTIAKOWSKY. J. Chem. Phys. 32, 992 (1960).
8. J. T. HERRON, J. L. FRANKLIN, P. BRADT, and V. H. DIBELER. J. Chem. Phys. 30, 879 (1959).
9. H. G. V. EVANS and C. A. WINKLER. Can. J. Chem. 34, 1217 (1956).
10. H. G. V. EVANS, G. R. FREEMAN, and C. A. WINKLER. Can. J. Chem. 34, 1271 (1956).
11. D. S. JACKSON and H. I. SCHIFF. J. Chem. Phys. 23, 2333 (1955).
12. S. E. SOBERING and C. A. WINKLER. Can. J. Chem. 36, 1223 (1958).
13. H. B. DUNFORD and B. E. MELANSON. Can. J. Chem. 37, 641 (1959).
14. R. A. WESTBURY and C. A. WINKLER. Can. J. Chem. 38, 334 (1960).
15. J. VERSTEEG and C. A. WINKLER. J. Chem. Phys. 31, 1 (1953).
16. J. T. HERRON, J. L. FRANKLIN, and P. BRADT. Can. J. Chem. 37, 579 (1959).
17. H. B. DUNFORD, H. G. V. EVANS, and C. A. WINKLER. Can. J. Chem. 34, 1074 (1956).
18. E. R. V. MILTON and H. B. DUNFORD. J. Chem. Phys. To be published.
19. P. HARTECK, R. R. REEVES, and G. MANNELLA. J. Chem. Phys. 29, 608 (1958).
20. T. WENTINK, J. O. SULLIVAN, and K. L. WRAY. J. Chem. Phys. 29, 231 (1958).
21. R. A. BACK, W. DUTTON, and C. A. WINKLER. Can. J. Chem. 37, 2059 (1959).
22. D. A. ARMSTRONG and C. A. WINKLER. J. Phys. Chem. 60, 1100 (1956).
23. G. J. VERBEKE and C. A. WINKLER. J. Phys. Chem. 64, 319 (1960).
24. J. BERKOWITZ, W. A. CHUPKA, and G. B. KISTIAKOWSKY. J. Chem. Phys. 25, 457 (1956).
25. F. KAUFMAN and J. R. KELSO. J. Chem. Phys. 28, 510 (1958).
26. K. DRESSLER. J. Chem. Phys. 30, 1621 (1959).

NOTES

INDOLYL-3-ACETALDOXIME

A. Ahmad, I. Eelnurme, and Ian D. Spenser

In connection with our work on the biosynthesis of indolyl-3-acetonitrile (1) we have prepared and characterized indolyl-3-acetaldoxime, which had been postulated (2) as the biological precursor of indolyl-3-acetonitrile, but does not appear to have been described.

EXPERIMENTAL

Indolyl-3-acetaldoxime

The sodium bisulphite adduct of indolyl-3-acetaldehyde (3) (1.310 g, 0.005 mole) was suspended in water and the pH of the mixture was adjusted to pH 8 by addition of 5% Na_2CO_3 solution. A solution of hydroxylamine hydrochloride (0.380 g, 0.0055 mole) in water, similarly adjusted to pH 8, was added, the mixture was stirred for a few minutes, filtered, and kept at 5°. After 12 hours the product (0.450 g, 52%), melting at 127–128° was filtered off. Recrystallization from chloroform gave indolyl-3-acetaldoxime as silvery plates, melting at 140–141°. (Found: C, 68.8; H, 5.9; N, 15.9. $C_{10}H_{10}N_2O$ requires: C, 69.0; H, 5.8; N, 16.1%.) Infrared absorption in Nujol (cm^{-1}): 3385 (s), 3220 (s), 1642 (m). Ultraviolet absorption (λ_{max}, mμ (log ϵ)) in ethanol: 220(4.58), 275 (shoulder) (3.83), 281(3.85), 290(3.77).

Conversion of Indolyl-3-acetaldoxime to Indolyl-3-acetonitrile

The oxime (0.210 g, 0.0012 mole) was dissolved in 5 ml acetic anhydride and allowed to stand 18 hours at room temperature. The dark mixture was treated with excess 10% NaOH solution and extracted with ether. The ether extract was dried (Na_2CO_3) and concentrated, and the residual oil was distilled at 100–110° and 2.10^{-3} mm yielding indolyl-3-acetonitrile as an oil (0.055 g, 30%) whose infrared absorption was identical with that of an authentic specimen (1). The oil crystallized on seeding with authentic indolyl-3-acetonitrile, melting point 34–36°.

The same product was obtained when $POCl_3$ was used in place of acetic anhydride.

Reduction of Indolyl-3-acetaldoxime to Tryptamine

A solution of the oxime (0.250 g, 0.00144 mole) in dry ether was added dropwise to a boiling suspension of $LiAlH_4$ in ether. After complete addition the mixture was refluxed for 1 hour, allowed to cool, decomposed by pouring into water, and acidified with 2 M H_2SO_4 until a clear solution was obtained, which was extracted with ether. The aqueous layer was made alkaline with 10% NaOH and some LiOH was filtered off. The filtrate was repeatedly extracted and the precipitate washed with ether. The combined ether extracts and washings were dried (NaOH), the solvent evaporated, and the oily residue distilled at 105–110° and 5.10^{-3} mm yielding tryptamine (0.132 g, 57%), melting at 116–118°, identical with an authentic specimen in melting point, mixed melting point, and infrared absorption.

1. A. Ahmad and I. D. Spenser. Can. J. Chem. **38**, 1625 (1960).
2. W. N. Dannenburg and J. L. Liverman. Plant Physiol. **32**, 263 (1957).
3. R. A. Gray. Arch. Biochem. Biophys. **81**, 480 (1959).

STRETCHING VIBRATIONS OF THE FREE $\overset{+}{N}H_3$ GROUP

P. Chevalier and C. Sandorfy

The usual method of measuring vibrational frequencies of free X–H groups i.e. taking the spectra of dilute solutions in a non-polar solvent cannot be applied to the case of the protonated amino group because of the insolubility of amine salts in such solvents.

Even if they were soluble the hydrogen bonds which are of the $\overset{+}{N}$—H— — — halogen$^-$ type would probably still prevail.

The only possibility seems to be, therefore, to prepare salts with bulky anions where steric hindrance would prevent the formation of hydrogen bonds. This method was applied by Nakamoto, Margoshes, and Rundle (1) and by Nakanishi, Goto, and Ohashi (2), who used the tetraphenylborate anion. They obtained $\overset{+}{N}H_3$ stretching bands which lie around 3100 cm^{-1} for methyl and ethyl amine salts.

There is some doubt, however, whether these bands can be considered as "free" $\overset{+}{N}H_3$ stretching bands. First, the half-width of these bands as found by us is between 30 and 40 cm^{-1} while, for example, the half-width of the free OH band in phenol is about 15 cm^{-1}. Secondly, we have observed (3) that perchloric acid salts of amines have $\overset{+}{N}H_3$ stretching bands in the same frequency range but they are broad. It seems to be likely therefore that the bonds described by the above-mentioned authors correspond actually to weakly hydrogen-bonded $\overset{+}{N}H_3$ groups and the really free $\overset{+}{N}H_3$ groups give bands at higher frequencies.

Whether the $\overset{+}{N}H_3$ groups are "free" or hydrogen-bonded seems to depend, even in the case of tetraphenylborates, on the particular spacial requirements in the given crystal.

Here are some of the frequencies and half-widths related to cases where the $\overset{+}{N}H_3$ group appears to be "free" in a very good approximation:

Anilinium tetraphenylborate	3286 cm^{-1}	3225 cm^{-1}
	11 cm^{-1}	12 cm^{-1}
α-Naphthylammonium tetraphenylborate	3313 cm^{-1}	3260 cm^{-1}
	12 cm^{-1}	13 cm^{-1}
β-Naphthylammonium tetraphenylborate	3313 cm^{-1}	3260 cm^{-1}
	14 cm^{-1}	16 cm^{-1}
Cyclohexylammonium tetraphenylborate	3286 cm^{-1}	3246 cm^{-1}
	9 cm^{-1}	11 cm^{-1}

Figure 1 gives the spectrum of the anilinium salt, and Fig. 2 the one of the cyclo-hexylammonium salt (dried in vacuum at 105° C). They were measured in fluorocarbon oil mulls.

Since this work was started Kynaston, Larcombe, and Turner (4) reported the spectra of a number of tetrachloroborates and a few tetrafluoroborates. They found the bands pertaining to the free $\overset{+}{N}H_3$ group in the case of methylammonium tetrafluoroborate to
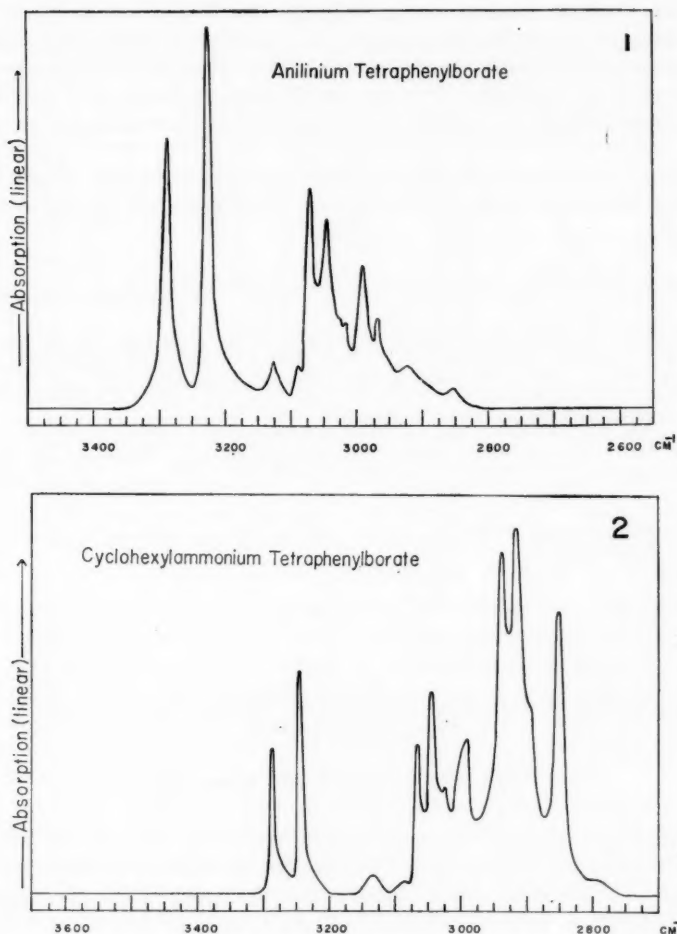
FIGS. 1 AND 2.

lie at 3282 and 3223 cm⁻¹. As may be inferred from their data, weak hydrogen bonds occur in all the other compounds.

From our data it is possible to measure the shift from the "free" bands to the bands in hydrochlorides.

Taking the arithmetic means of the two free $\overset{+}{N}H_3$ frequencies and the "center of gravity" of the broad composite hydrochloride bands (see 5 and 6) we obtain the following values:

Cyclohexylammonium	3266–2980	= 286 cm⁻¹
Anilinium	3256–2810	= 446 cm⁻¹
α-Naphthylammonium	3286–2810	= 476 cm⁻¹
β-Naphthylammonium	3286–2850	= 436 cm⁻¹

These values indicate medium strong hydrogen bonding in the hydrochlorides.

It is of interest to mention in this respect that Côté and Thompson (7) found 3332 cm^{-1} for the frequency of the triply degenerate stretching vibration of the ammonium ion in NH_4BF_4 where it very probably does not form hydrogen bonds and that Wagner and Hornig (8) found the corresponding band of the hydrogen-bonded ion at 3086 cm^{-1} in NH_4Cl.

Work is going on in this laboratory in order to prepare tetraphenylborates of many more primary, secondary, and tertiary amines. The results and further discussion will be given later.

We acknowledge a stimulating conversation with Professor D. F. Hornig.

1. K. NAKAMOTO, M. MARGOSHES, and R. E. RUNDLE. J. Am. Chem. Soc. **77**, 6480 (1955).
2. K. NAKANISHI, T. GOTO, and M. OHASHI. Bull. Chem. Soc. Japan, **30**, 403 (1957).
3. C. BRISSETTE. M.Sc. Thesis, Université de Montréal, Montréal, Qué. 1959.
4. W. KYNASTON, B. E. LARCOMBE, and H. S. TURNER. J. Chem. Soc. 1774 (1960).
5. B. CHENON and C. SANDORFY. Can. J. Chem. **36**, 1181 (1958).
6. C. BRISSETTE and C. SANDORFY. Can. J. Chem. **38**, 34 (1960).
7. G. L. CÔTÉ and H. W. THOMPSON. Proc. Roy. Soc. A, **210**, 217 (1951).
8. E. L. WAGNER and D. F. HORNIG. J. Chem. Phys. **18**, 296 (1950).

LITHIUM ALUMINUM HYDRIDE REDUCTION OF STERICALLY HINDERED AROMATIC NITRO COMPOUNDS

F. A. L. ANET AND J. M. MUCHOWSKI

In connection with another research problem it became necessary to prepare 2,6-di-(2-hydroxyethyl)-aniline (II). When 2,6-di(methoxycarbonylmethyl)-nitrobenzene (I) was subjected to lithium aluminum hydride reduction none of the azo compound was obtained; instead the desired amino di-alcohol was isolated in 54% yield. This reduction

was unexpected as it has been reported (1–5) that aromatic nitro compounds on lithium aluminum hydride reduction give rise to the corresponding azo compounds exclusively. Indeed, the immediate appearance of a red "azo" color on treatment of an ether solution of lithium aluminum hydride with an aromatic nitro compound has been suggested as a sensitive test for such compounds (1, 6, 7).

To test the generality of the reaction several mono- and di-ortho substituted nitro benzenes were reduced (see Table I). Obviously, the increase in amine formation parallels

TABLE I

Reduction products of aromatic nitro compounds with lithium aluminum hydride

Nitro compound	Azo derivative		Amine		
	% Yield	M.p., °C	% Yield	M.p., °C	Picrate, m.p., °C
Nitrobenzene	73.5	67–68[a]	—	—	
o-Nitrotoluene	30.9	53–54[a]	25.5	—	213[a]
o-Nitro-β-phenylethanol	41.2	138–139[b]	30.9	—	181.5–183.5[c]
1,3-Dimethyl-2-nitrobenzene	20.9	44.5–45[d]	53.1	—	184.5–186[a]
Nitromesitylene	10.7	73–75[e]	61.2	—	189–190[a]
2,6-Di(methoxycarbonyl)-nitro-benzene	—	—	44.4	120–121[f]	—
2,6-Di(methoxycarbonylmethyl)-nitrobenzene[g]	—	—	54.4	101–102[h]	—

[a] These melting points are in agreement with those stated in "A textbook of practical organic chemistry", *edited by* A. I. Vogel. Longmans, Green and Co. Ltd., London, 1948.

[b] Recrystallized from ethanol – petroleum ether (b.p. 80–100°). Calc. for $C_{14}H_{16}O_2N_2$: C, 71.09; H, 6.71%. Found: C, 71.33; H, 6.70%.

[c] Recrystallized from ethanol. Calc. for $C_8H_{11}ON$, $C_6H_3O_7N_3$: C, 45.90; H, 3.85%. Found: C, 46.19; H, 3.97%.

[d] J. T. Edward (J. Chem. Soc. 222 (1956)) reported m.p. 46–47°.

[e] P. Grammaticakis (Bull. Soc. chim. France, 951 (1951)) reported m.p. 75°.

[f] Recrystallized from ethanol – petroleum ether (b.p. 80–100°). Calc. for $C_8H_{11}O_2N$: C, 62.72; H, 7.24%. Found: C, 63.13; H, 7.22%.

[g] F. A. L. Anet and E. Nishizawa (unpublished work) give m.p. 144–145°.

[h] Recrystallized from ethanol – petroleum ether (b.p. 80–100°). Calc. for $C_{10}H_{15}O_2N$: C, 66.27; H, 8.34%. Found: C, 65.96; H, 8.33%.

increasing steric hindrance around the nitro group. The formation of azo compounds is known to take place by the condensation of the nitroso compound and the hydroxylamine or the amine (10) and these reactions would be expected to be sensitive to steric hindrance. The 2,6-disubstituted nitrobenzenes investigated gave mainly the amine. On the other hand, Nystrom and Brown (1) report a 71% yield of azomesitylene, while in our hands 61% mesidine and 11% azomesitylene were obtained on reduction of nitromesitylene, even under conditions identical with those given by these workers.

It appears that such anomalous reductions are not completely unknown. Ried and Müller (8) obtained 4,4'-diaminoazobenzene by lithium aluminum hydride reduction of 4,4'-dinitroazobenzene. Adams *et al.* (9) were unable to reduce 3-chloro-2-nitroanisole to the azo derivative. They do not, however, mention what, if any, product was isolated. Wiberg and Jahn (11) have reported the formation of p-toluidine from p-nitrotoluene by reduction with lithium aluminum hydride, but only in presence of aluminum chloride. In the absence of aluminum chloride p-azotoluene was the main product.

EXPERIMENTAL

Melting points and boiling points are uncorrected.

The lithium aluminum hydride reductions were carried out in one of two ways depending on the solubility of the starting material in ether.

(i) When the nitro compound was ether soluble, its ether solution was added in a dropwise manner to a suspension of a half-molar excess of the hydride in anhydrous ether. When the addition was complete, the mixture was boiled under reflux for 6 hours. Amines formed were extracted with 10% hydrochloric acid and identified as their picrates (melting points and mixed melting points). The azo compounds were crystallized from the appropriate solvent and identified by comparing their properties with those given in the literature.

(ii) If the nitro compounds* were only slightly soluble in ether, they were introduced to the hydride suspension (over a period of 24 hours) by the Soxhlet extractor technique. No azo compounds were formed in these cases and the amines were isolated by filtration of the organic layer, evaporation to dryness, and crystallization of the solid residue from the appropriate solvent system.

ACKNOWLEDGMENT

1. R. NYSTROM and W. G. BROWN. J. Am. Chem. Soc. **70**, 3738 (1948).
2. G. M. BADGER, J. H. SAIDLER, and B. THOMSON. J. Chem. Soc. 3207 (1951).
3. N. G. GAYLORD and J. A. SNYDER. Rec. trav. chim. **72**, 1007 (1953).
4. T. W. CAMPBELL, W. A. MCALLISTER, and M. T. ROGERS. J. Am. Chem. Soc. **75**, 864 (1953).
5. W. THEILACKER and F. BAXMANN. Ann. **581**, 117 (1953).
6. H. GILMAN and TH. N. GOREAU. J. Am. Chem. Soc. **73**, 2939 (1951).
7. L. S. NELSON and D. E. LASKOWSKI. Anal. Chem. **23**, 1495 (1951).
8. W. RIED and F. MÜLLER. Ber. **85**, 470 (1952).
9. R. ADAMS, R. HOLMES, and J. W. WAY. J. Am. Chem. Soc. **75**, 5901 (1953).
10. N. V. SIDGEWICK. The organic chemistry of nitrogen. Oxford University Press, Oxford. 1937. p. 436.
11. E. WIBERG and A. JAHN. Z. Naturforsch. **76**, 581 (1952).

*2,6-Di(methoxycarbonyl)-nitrobenzene and 2,6-di(methoxycarbonylmethyl)-nitrobenzene.

NOTE ON THE THERMAL NEUTRON CAPTURE CROSS SECTION OF Cs[133]*

A. P. BAERG† AND R. M. BARTHOLOMEW

During the course of recent investigations relating to the detection efficiency of 4π beta proportional counters for Cs^{134m} (1) it was noted that in the neutron irradiation of Cs^{133} the amount of Cs^{134m} produced is several orders of magnitude greater than would be estimated from the 17-millibarn cross section quoted for this reaction (2). The $Cs^{133}(n,\gamma)$ Cs^{134m} cross section was therefore re-examined. At the same time it was possible to check the cross section for the reactions leading to the ground state.

Irradiations

Samples of about 500 μg each of CsCl, together with cobalt wire neutron flux monitors (0.0127 cm diameter) (3), were irradiated in an empty fuel rod position of the NRX reactor. The CsCl was prepared by weighing a solution of known concentration into quartz tubes. These samples were evaporated to dryness in the tubes, which were then sealed for irradiation. Two samples in iron capsules were irradiated for 3 hours each and two others, in 0.076-cm cadmium-lined iron capsules, for a period of 16.5 hours each. The reactor power remained constant during any one irradiation and to within a few per cent throughout these irradiations.

Purification and Counting

The irradiated quartz capsules were crushed under a solution 9 N in hydrochloric acid

and the resulting solution of cesium was then passed through a Dowex A-1 anion exchange column to remove particulate silica. The effluent was evaporated to dryness and the cesium further purified by elution from a Dowex-50 cation resin column (1). Quantitative recovery of the cesium, to within $1/10\%$, throughout the purification was ensured by suitable monitoring. Weighed aliquots of the cesium solution from the cation resin column were mounted and dried on thin plastic, gold-coated films (4) for counting.

Special precautions were taken to ensure that the cesium was pure and, in particular, free of 2.6-hour Si^{31} from the quartz irradiation capsules. In each experiment, portions of the purified cesium solution were taken for precipitation of the cesium as silicotungstate (5). This cesium was then extracted several times with an amyl acetate solution of sodium tetraphenyl boron (see reference 1). This extraction, though very inefficient for macro amounts of cesium, provided ample activity for study. The decay characteristics of this specially purified material were carefully compared with those of the samples used for the cross-section measurements. The beta decay of all samples showed a half-life of 2.91 ± 0.01 hours (1) after subtraction of the 2.19-year Cs^{134} contribution (less than 1%).

The cobalt wire flux monitors were dissolved, and weighed aliquots dried on plastic films for counting.

All samples were counted with a 4π beta–gamma coincidence counter similar to that described by Campion (6). The method used for determining the detection efficiency of the 4π beta counter for Cs^{134m} is described in reference 1. In the counting of Cs^{134}, the gamma rays in the energy range 0.47 to 1.17 Mev were counted in coincidence with the beta radiations to arrive at the absolute disintegration rates.

Calculations and Results

The distintegration rates observed, referred to the end of the irradiations, are given in Table I together with irradiation times and the cadmium ratios (i.e. the ratio of observed

TABLE I

Experimental data

Irradiation	Irradiation time, hours	Counting rate at end of irradiation d.p.s./μg of target element		
		Co^{60}	Cs^{134m}	Cs^{134}
1. Uncovered	3	1.091×10^3	5.50×10^5	1.308×10^3
2. Uncovered	3	1.075×10^3	5.40×10^5	1.318×10^3
3. Cadmium-covered	16.5	1.882×10^2	2.55×10^5	2.052×10^3
4. Cadmium-covered	16.5	1.892×10^2	2.44×10^5	1.971×10^3
Cadmium ratio (average)		20.26 ± 0.5	4.19 ± 0.12	3.59 ± 0.09

rates of reaction without and with cadmium filter). The half-life values used to calculate the reaction rates are given in Table II. Self-shielding correction factors of 1.04 and 1.62, respectively, for uncovered and cadmium-covered irradiations were also applied to the cobalt data (7).

The cross-sections were calculated using the convention described by Westcott (8) (see also reference 9). A very brief outline only is given here to indicate the method which was used.

The measured reaction rate, R, is equated to the product of the effective cross section, $\hat{\sigma}$, and the conventional flux, nv_0, where n is the neutron density and v_0 is 2200 m/sec.

[1] $$R = \hat{\sigma}nv_0.$$

<div align="center">

TABLE II

Values of parameters used in calculations of cross sections

</div>

Co^{59} self-shielding correction factor, cadmium-covered	1.62 (7)
Co^{59} self-shielding correction factor, uncovered	1.04 (7)
Half-life of Co^{60}	5.28 years (2)
Half-life of Cs^{134m}	2.91 hours (1)
Half-life of Cs^{134}	2.19 years (10)
Co^{59} 2200 m/sec cross section	36.68 barns (2)
Co^{59} resonance integral, RI	75 barns (13)
$r\sqrt{T/T_0}$ (measured for irradiation position used)	0.0223 ± 0.0004

The effective cross section is defined by

$$[2] \qquad \hat{\sigma} = \sigma_0(g + rs)$$

where σ_0 is the 2200 m/sec cross section, r is a measure of the relative density of epithermal neutrons, and g and s are factors which depend on the departure of the cross sections from the $1/v$ law. In the present experiment it is assumed that $g = 1$ and the factor s is written as $\sqrt{(T/T_0)}s_0$; thus

$$[3] \qquad \hat{\sigma} = \sigma_0\left(1 + r\sqrt{\frac{T}{T_0}}s_0\right)$$

where T is the neutron temperature and T_0 is 293.6° K corresponding to 2200 m/sec neutrons. The term $r\sqrt{T/T_0}$, which is a constant of the reactor for the irradiation position used, is then related to the cadmium ratio, R_{Cd}, and s_0 as follows:

$$[4] \qquad r\sqrt{\frac{T}{T_0}} = \frac{1}{R_{Cd}\{s_0 + (1/K)\} - s_0}.$$

Here K is a function of the cadmium cross section and the thickness of filter used, having the value 2.2 in the present experiment (8). The factor s_0, in turn, is given by

$$[5] \qquad s_0 = \sqrt{\frac{4}{\pi}\left(\frac{RI}{\sigma_0}\right) - \frac{1}{K}}$$

where RI is the resonance integral, evaluated above the cadmium cutoff and includes the $1/v$ part above this energy.

The conventional flux, nv_0, is first obtained in the following way from the cobalt data. The factor s_0 is calculated from the known values of RI and σ_0 for cobalt (Table II). The factor $r\sqrt{T/T_0}$ is obtained from equation 4 using the measured cadmium ratio for cobalt and the calculated value of s_0. Then the effective cross section for cobalt (equation 3) is used in equation 1 to get the conventional flux, nv_0.

The effective cross section for cesium was obtained from equation 1 using the observed reaction rate and the conventional flux, nv_0 from the cobalt data. The factor s_0 for cesium is calculated (equation 4) from the observed cadmium ratio and the already known value of $r\sqrt{T/T_0}$. The 2200 m/sec cross section, σ_0, then follows from equation 3 and the resonance integral, RI, from equation 5.

The average cross-section values obtained in this way are given in Table III. The errors quoted are based on an estimated combined uncertainty of 1% in the determination of distintegration rates and a 2% uncertainty in the relative neutron fluxes for the cadmium-covered and uncovered irradiations. Possible errors associated with the parameters listed in Table II (except for $r\sqrt{T/T_0}$) have not been included.

TABLE III

Cross sections calculated from experimental data and the parameters of Table II

Reaction	$Co^{59}(n, \gamma)Co^{60}$	$Cs^{133}(n, \gamma)Cs^{134m}$	All reactions leading to the ground state
Effective cross section, $\hat{\sigma}$ (barns)	38.19 ± 0.04	3.67 ± 0.07	41.6 ± 0.9
2200 m/sec cross section, σ_0 (barns)	—	2.82 ± 0.07	30.4 ± 0.8
Resonance integral, RI (barns)	—	34.4 ± 1.9	461 ± 25

The value obtained in this work for σ_0 (2.82 ± 0.07 barns) for the production of Cs^{134m} is very much greater than that (17 millibarns) quoted in reference 2.

The effective cross section for the reactions leading to the ground state Cs^{134} (41.6 ± 0.9 barns) is found to be in good agreement with those obtained by Bidinosti et al. (40 barns) (11) and Brown et al. (40.9 ± 4.1 barns, which was also measured in a vacant fuel rod position in the NRX reactor) (12). The value obtained for σ_0 is in good agreement with 30 ± 1 barns reported in BNL-325 (2) but differs by somewhat more than the combined errors from the value obtained by Brown. The difference would appear to be accountable to the inherent difficulties in measuring cadmium ratios and uncertainties in neutron energy spectra (see discussion by Brown (12)).

1. A. P. BAERG, R. M. BARTHOLOMEW, and R. H. BETTS.   Can. J. Chem. 38, 2147 (1960).
2. D. J. HUGHES and R. T. SCHWARTZ.   Brookhaven National Laboratory Report, BNL-325, 2nd ed.
3. R. E. JERVIS.   Atomic Energy of Canada Ltd. Report CRDC-730 (1957).
4. B. D. PATE and L. YAFFE.   Can. J. Chem. 33, 15 (1955).
5. R. M. BARTHOLOMEW and A. P. BAERG.   Can. J. Chem. 34, 201 (1956).
6. P. J. CAMPION.   Intern. J. Appl. Radiation and Isotopes, 4, 232 (1959).
7. T. A. EASTWOOD.   Private communication.
8. C. H. WESTCOTT, W. H. WALKER, and T. K. ALEXANDER.   Intern. Conf. on the Peaceful Uses of Atomic Energy. 2nd Conf. Geneva, 1958. Paper P/202.
9. T. A. EASTWOOD, A. P. BAERG, C. B. BIGHAM, F. BROWN, M. S. CABELL, W. E. GRUMMITT, J. C. ROY, L. P. ROY, and R. P. SCHUMAN.   Intern. Conf. on the Peaceful Uses of Atomic Energy. 2nd Conf. Geneva, 1958. Paper P/203.
10. W. F. MERRITT, P. J. CAMPION, and R. C. HAWKINGS.   Can. J. Phys. 35, 16 (1957).
11. D. R. BIDINOSTI, H. R. FICKEL, and R. H. TOMLINSON.   Intern. Conf. on the Peaceful Uses of Atomic Energy. 2nd Conf. Geneva, 1958. Paper P/201.
12. F. BROWN, P. J. CAMPION, and B. H. OLIVER.   Can. J. Phys. 1960.
13. F. J. JOHNSTON, J. HALPERIN, and R. W. STOUGHTON.   Reactor Science, 11, 95 (1960).

ISOLATION OF HYPERIN FROM RED-OSIER DOGWOOD (CORNUS STOLONIFERA MICHX.)*

G. V. NAIR AND E. VON RUDLOFF

In continuation of a systematic search for flavonoid and phenolic compounds in Prairie plants, red-osier dogwood (*Cornus stolonifera* Michx.) was investigated. The members of the *Cornus* family vary from herbs to fairly large trees. *C. stolonifera*, also known as *Svida stolonifera* (Michx.) Rydb., is a medium-sized shrub with characteristic bright red

twigs and branches. It is common throughout the Prairie provinces. Wall *et al.* (1), in a general survey of steroids, flavones, and tannins in plants, report that an extract of the whole plant gave a positive test only for tannins. In the current study, the leaves and stems of plants from the Saskatoon district were found to be devoid of flavonoid compounds, but a positive color reaction was obtained with an alcoholic extract of the red stem bark.

About 10% of the air-dried stem bark was ethanol-soluble. This extract was solvent fractionated and the chloroform-insoluble portion was chromatographed on a cellulose powder column. One of the products obtained (0.075% yield, based on the weight of bark) was a flavone glycoside, m.p. 238° C, $[\alpha]_D$ −19.7°, identified as hyperin (quercetin-3-galactoside) by mixed melting point. Hyperin was isolated for the first time by Jerzmanowska (2) from the herb *Hypericum perforatum* L.

In addition to hyperin, the alcohol extract contained fumaric acid, tannins, and a mixture of long-chain fatty acids. The latter mixture was resolved by gas–liquid chromatography (3) and found to consist of n-C_{24}- (66.7%), n-C_{26}- (22.8%), and n-C_{28}-carboxylic acids. In one experiment, when fresh bark was extracted at once, these fatty acids were obtained only after saponification, showing that hydrolysis may occur during storage of the plant.

EXPERIMENTAL

Melting points were determined on a Leitz hot-stage microscope, and infrared spectra were recorded with a Perkin–Elmer Model 21 double-beam spectrophotometer. Gas–liquid chromatography was carried out on a Beckman GC-2 chromatograph, using the technique previously described (4).

Air-dried stem bark (1000 g) of dogwood was extracted with ethanol (5 l.) in the cold. The solvent was evaporated, leaving a brownish-red sirupy residue (102 g). This material was extracted with chloroform to remove chlorophyll, waxes, etc. (22 g). An aliquot (16.5 g) of the chloroform-insoluble residue was chromatographed on a 60×7 cm cellulose powder column, using 15% acetic acid as solvent. Aliquots of 20 ml were collected and fractions 33 to 40 on evaporation gave a solid material (150 mg) which gave a pink color reaction when treated with magnesium and dilute hydrochloric acid. The material was crystallized from dilute alcohol, m.p. 238° C, $[\alpha]_D$ −19.7° (c, 3.9 H_2O–acetone 1:1). Found: C, 51.87%; H, 4.70%. Calculated for $C_{21}H_{20}O_{12} \cdot 2H_2O$: C, 52.43%; H, 4.87%. The infrared absorption spectrum corresponded to that of a flavone glycoside. The glycoside (20 mg) was hydrolyzed with dilute sulphuric acid and the aglycone and sugar portions were worked up in the usual manner. Paper chromatography showed these to correspond to quercetin and galactose respectively. The glycoside had the same R_f value (0.32, using 15% acetic acid) as hyperin, and its melting point was undepressed in admixture with an authentic specimen of hyperin.

Fractions 41–43 in the cellulose powder fractionation contained the bulk of the material (12.5 g) and appeared to be mainly tannin-like. On rechromatographing on cellulose powder, using ethyl acetate:ethanol:acetic acid (41:2:1 v/v) as eluent, a small amount of fumaric acid (characterized by mixed melting point and its infrared spectrum) was obtained.

The chloroform-soluble portion was dried and chlorophyll was removed by extraction with petrol (b.p. 40–60° C) in the cold. The insoluble residue was chromatographed on a silicic acid column, using petrol:benzene (1:1) as eluent. The only crystalline material isolated was a mixture of fatty acids, m.p. 78–79° C. Similar material was also found in

the petrol-soluble portion. The mixture was methylated with diazomethane and small aliquots (1 μl) were analyzed by gas–liquid chromatography on a silicone column (18×1/4 in.) at 240° C (3, 4). Three peaks corresponding to n-C_{24}, n-C_{26}, and n-C_{28} methyl ester were recorded in the proportion of 6.7:2.3:1.

1. M. E. WALL, C. S. FENSKE, J. W. GARVIN, J. J. WILLAMAN, Q. JONES, B. G. SCHUBERT, and H. S. GENTRY. J. Am. Pharm. Assoc. 48, 695 (1959).
2. Z. JERZMANOWSKA. Wiadomości farm. 64, 527 (1937); cf. Chem. Abstr. 33, 7299⁸ (1939).
3. B. M. CRAIG and N. L. MURTY. Can. J. Chem. 36, 1297 (1958).
4. G. V. NAIR and E. VON RUDLOFF. Can. J. Chem. 37, 1608 (1959).

CONTENTS OF VOLUME 38

Barclay, L. R. C., Hilchie, J. W., Gray, A. H., and (*in part*) **Hall, N. D.**   Cyclialkylations of alkyl benzenes with olefins and alkyl halides, 94.

Bardwell, J.   See Cherneskey, M., 482.

Barrette, J. P.   See Lemieux, R. U., 656.

Barth, C. A.   See Kaplan, J., 1688.

Bartholomew, R. M.   See Baerg, A. P., 2147, 2528.

Bartlet, J. C. and **Smith, D. M.**   The determination of the areas of resolved and partially resolved chromatography peaks, 2057.

Basco, N. and **Norrish, R. G. W.**   Vibrational disequilibrium in reactions between atoms and molecules, 1769.

Basmadjian, D.   Adsorption equilibria of hydrogen, deuterium, and their mixtures. Part I, 141.
Adsorption equilibria of hydrogen, deuterium, and their mixtures. Part II, 149.

Bavin, P. M. G.   Aliphatic chemistry of fluorene. Part II. An unusual Grignard reaction, 882.
Aliphatic chemistry of fluorene. Part III. Some derivatives of fluorene and phenanthrene, 911.
Aliphatic chemistry of fluorene. Part IV. Preparation and alkylation of some sulphides and sulphones, 917.
Molecular complexes derived from 1,3,6,8-tetranitropyrene, 1017.
Aliphatic chemistry of fluorene. Part V. Spiro-ketones, 1099.
Aliphatic chemistry of fluorene. Part VI. 3,4-Benzofluorene-9-spiro-cyclohexane, 1148.
A note on the cyclization of 3-(2'-naphthyl)-butyric acid, 1227.
See also Anet, F. A. L., 240.

Baxter, J. N. and **Perlin, A. S.**   2,3-O-Isopropylidene-L-*erythro*tetruronic acid and -L-erythrose, and the methyl D-*erythro*- and D-*threo*-tetrofuranosides, 2217.

Bayley, C. H.   See Gingras, B. A., 712.

Beech, J. A.   See Sandler, S., 1455.

Beg, M. A. A. and **Clark, H. C.**   Chemistry of the trifluoromethyl group. Part I. Complex formation by phosphines containing the trifluoromethyl group, 119.

Bell, G. M.   See Levine, S., 1346.

Bennett, R. M. and **Holmes, O. G.**   Electronic states of hydrated vanadium (II) ion, 2319.

Bent, H. A.   A mechanism for the inductive effect, 1235.

Berlinguet, L.   See Laliberté, R., 1933.

Berse, C., Piché, L., and **Uchiyama, A.**   The preparation of L-arginyl dipeptides of asparagine, glutamine, and some basic amino acids, 1946.

Betts, R. H.   See Baerg, A. P., 2147.

Biermann, W. J.   The relative enthalpies of concentrated potassium hydroxide solutions, 57.

Biermann, W. J. and **Heinrichs, M.**   The attack of chromite by sulphuric acid, 1449.

Bishop, C. T.   Crystalline O-methyl ethers of D-galactitol, 1636.
See also Adams, G. A., 2380.

Bishop, C. T., Blank, F., and **Gardner, P. E.**   The cell wall polysaccharides of *Candida albicans*: glucan, mannan, and chitin, 869.

Bishop, C. T. and **Cooper, F. P.**   Separation of carbohydrate derivatives by gas–liquid partition chromatography, 388.
Constitution of a glucomannan from jack pine (*Pinus banksiana*, Lamb), 793.

Blackwell, R. Q.   See Needleman, S. B., 477.

Blades, A. T. and **Gilderson, P. W.**   The hydrogen isotope effect in the pyrolysis of ethyl-1,1,2,2-d_4 acetate, 1401.
The secondary hydrogen isotope effects in the pyrolysis of ethyl-d_5 acetate and ethyl acetate-d_3, 1407.
Kinetics of the thermal decomposition of ethyl propionate, 1412.

Blank, F.   See Bishop, C. T., 869.

Bloom, M.   See Sandhu, H. S., 493.

Blumenthal, J. L., Sourirajan, S., and **Nobe, K.**   Effect of mean pore size on the low-temperature adsorption of nitrogen on alumina, 783.

Boddy, P. J. and **Steacie, E. W. R.**   Hydrogen atom abstraction by ethyl-d_5 radicals. Part I, 1576.

Boivin, J.-L.   See Gagnon, P. E., 1472.

Boos, W. R.   See Manske, R. H., 620.

Bounsall, E. J. and **McBryde, W. A. E.**   Determination of trace amounts of silver in galena ores, 1488.

Bourgault, P. L. and **Conway, B. E.**   The electrochemical behavior of the nickel oxide electrode. Part II. Quasi-equilibrium behavior, 1557.

Bourns, A. N.   See Buncel, E., 2457; Stothers, J. B., 923.

Bowering, W. D. S. and **Timell, T. E.**   A chemical synthesis of 4-O-methyl-D-glucuronic acid, 311.

Breitman, L.   See Orr, R. J., 668.

Bressesti, M. and **Roy, J. C.**   Half-lives of the nuclides Au[195], Pt[195m], and Pt[197], 194.

Brinton, R. K.   The abstraction of hydrogen atoms from amines and related compounds, 1339.

Brissette, C. and **Sandorfy, C.**   Hydrogen bonding in the amine hydrohalides. II. The infrared spectrum from 4000 to 2200 cm⁻¹, 34.

Broida, H. P. and **Golden, S.**   Pressure dependence of rotationally perturbed lines in the ultraviolet band spectrum of CN, 1666.

Brown, R. K.   See Leggetter, B. E., 1467, 2363; Scherf, G. W. H., 697, 2450.

Brown, R. K. and **Eastham, A. M.**   The chemistry of ethylene oxide. VI. The acid-catalyzed reaction of ethylene oxide with ethanol–water mixtures, 2039.

Brownell, H. H.   See Casselman, A. A., 1277.

Reeves, L. W. and **Strømme, K. O.** Studies of rates of conversion and populations of various conformations of saturated ring compounds by N.M.R. I. Chlorocyclohexane and bromocyclohexane, 1241.

Reeves, R. R. See Harteck, P., 1648.

Reid, P. E. See Jones, J. K. N., 944.

Riem, R. H. and **Kutschke, K. O.** Photolysis of azoisopropane, 2332.

Rinfret, M. See Watters, C., 1087.

Rivest, R. See Archambault, J., 1331.

Robertson, A. V. and **Marion, L.** The biogenesis of alkaloids. XXIV. The role of citric acid in the biogenesis of hyoscyamine, 294.
The biogenesis of alkaloids. XXV. The role of hygric acid in the biogenesis of stachydrine, 396.

Robertson, R. E. See Hartman, S., 2033; Leffek, K. T., 1505, 2171; Llewellyn, J. A., 222.

Robertson, R. F. See Gupta, P. R., 259; Rabinovitch, W., 1881.

Robinson, E. A. See Flowers, R. H., 1363.

Robinson, J. R. Diphenylcyanamide derivatives. IV. 1,1-Bis(4-chlorophenyl)-urea, 1396.

Robson, J. H. and **Wright, G. F.** The mechanism of organomercurial oxidation by mercuric salts, 1.
The autooxidation of organomercuric salts, 21.

Rodger, M. N. See Edwards, O. E., 663.

Rosenblum, P. See Lister, M. W., 1827.

Rosenthal, A. The reaction of the O- and N-methyl derivatives of aromatic ketoximes with carbon monoxide and hydrogen, 2025.

Rosenthal, A. and **O'Donnell, J. P.** Reaction of syn-benzaldoxime with carbon monoxide and hydrogen to yield substituted ureas, 457.

Rosenthal, A. and **Zaionchkovsky, A.** The condensation of glyoxal with p-cresol, 2277.

Rowland, F. S. See Lee, J. K., 1756.

Rowlands, J. R. See McDowell, C. A., 503.

Roy, J. C. See Bresesti, M., 194.

von Rudloff, E. The separation of some terpenoid compounds by gas–liquid chromatography, 631.
See also Nair, G. V., 177, 2531.

Russell, K. E. The preparation of cyclic peroxides and their decomposition in solution, 1600.

Ruzicka, D. J. See Bryce, W. A., 835.

Ruzicka, D. J. and **Bryce, W. A.** The pyrolysis of diallyl (1,5-hexadiene), 827.

Ryan, D. E. The determination of zirconium with benzoylphenylhydroxylamine, 2488.

Sakamoto, K. See Yamaguchi, G., 1395.

Sandhu, H. S., Lees, J., and **Bloom, M.** Removal of oxygen from methane and the use of nuclear spin relaxation to measure oxygen concentration, 493.

Sandler, S. and **Beech, J. A.** Quantitative analysis of combustion products by gas chromatography. The oxidation of a rich n-pentane–air mixture in a flow system, 1455.

Sandorfy, C. See Brissette, C., 34; Chevalier, P., 2524; Sauvageau, P., 1901.

Santiago, P. J. See de Maine, P. A. D., 157.

Santry, D. C. and **Yaffe, L.** Absolute thermal neutron fission yields of U^{233}, 421.
The yield of Ba^{140} in the thermal neutron fission of U^{235}, 464.

Sauvageau, P. and **Sandorfy, C.** Hydrogen bonding in the amine hydrohalides. III. Near-infrared spectra of aliphatic amine hydrohalides, 1901.

Savoie, R. See Giguère, P. A., 2467.

Schade, W. J. See Kaplan, J., 1688.

Schaefer, T. and **Schneider, W. G.** Solvent effects as an aid in the analysis of the proton magnetic resonance spectrum of vinyl bromide, 2066.

Scherf, G. W. H. and **Brown, R. K.** Potassium derivatives of fluorene as intermediates in the preparation of C_9-substituted fluorenes. I. The preparation of 9-fluorenyl potassium and the infrared spectra of fluorene and some C_9-substituted fluorenes, 697.
Potassium derivatives of fluorene as intermediates in the preparation of C_9-substituted fluorenes. II. Comparative reactivities of the alkali metals, lithium, sodium, and potassium, with fluorene in glycol dimethyl ether, glycol diethyl ether, tetrahydrofuran, and dioxane, 2450.

Schiff, H. I. See Elias, L., 1657.

Schneider, W. G. See Schaefer, T., 2066; Sunners, B., 681; Taurins, A., 1237.

Scott, B. D. See Heacock, R. A., 508, 516.

Scott, J. M. W. The Orton rearrangement in aprotic solvents. Some observations on the reactions of p-substituted N-bromoacylanilides in chlorobenzene and trichloroacetic acid, 2441.
See also Llewellyn, J. A., 222.

Seaton, J. C., Nair, M. D., Edwards, O. E., and **Marion, L.** The structure and stereoisomerism of three mitragyna alkaloids, 1035.

Secco, E. A. Decomposition of zinc oxide, 596.

Sehon, A. H. See Back, M. H., 1076, 1261, 1271.

Seng, G. C. See Abramovitch, R. A., 624, 761.

Sepall, O. and **Mason, S. G.** Vapor/liquid partition of tritium in tritiated water, 2024.

Sephton, H. H. See Jones, J. K. N., 753.

Sherlock, E. See Reesor, J. B., 1416.

Sherwood, A. G. and **Gunning, H. E.** The primary process in the mercury-6($^3P_1$)-photosensitized polymerization of acetylene, 466.

Siddiqueullah, M. See Pepper, J. M., 2324.

Siddiqui, I. R. and **Adams, G. A.** 3,5-Di-O-methyl-D-galactose, a new methylated sugar from a fully methylated polysaccharide of *Gibberella fujikuroi* (*Fusarium moniliforme*), 2029.

Contents

(*Concluded inside*)